Antarctic Research Vessel (ARV)

Engineering Report: Model Test Report (Open Water and Ice)

Document No.: 5E1-098-R101

Revision: P2

Prepared by the Antarctic Support Contractor
for the
National Science Foundation Office of Polar Programs

Revision History

Revision #	Date	Section (if applicable)	Author/Editor	Change Details
P0	October 11, 2022	All	J. Lee	Initial draft for ASC peer review
P1	December 23,2022	All	J. Cross-Whiter	Revised with 3A test results
P2	July 28, 2023	All	J. Cross-Whiter	Revised with Hull Variant 11 test results

Prepared by:

John Cross-Whiter	John Cross-Whiter	July 25, 2023
Signature		

John Cross-Whiter, Senior Principal Naval Architect, Leidos / Gibbs & Cox

Checked by:

Sean Sweeney	Sean Sweeney	July 26, 2023
Signature	*Print Name*	*Date*

Principal Naval Architect, Leidos / Gibbs & Cox

Engineered/Managed by:

Justin Klag	Justin Klag	July 27, 2023
Signature	*Print Name*	*Date*

Justin Klag, Dept Manager, Leidos / Gibbs & Cox

Approved by:

David Rosenthal	David Rosenthal	July 28, 2023
Signature	*Print Name*	*Date*

David Rosenthal, Assistant Vice President, EG, Leidos / Gibbs & Cox

Table of Contents

List of Tables

List of Figures

1. Executive Summary

During several test sessions, spanning the period from March to July, 2023, a 1:24.384 scale model of the ARV, Hull Variant 11, was tested in the Hamburgische Schiffbau-Versuchsanstalt (HSVA) model testing facility, in Hamburg, Germany. This model test campaign defines the performance of the updated Design Review 5 (DR5) design baseline for the ARV.

The tests included thruster open-water, bubble sweepdown, open-water resistance and propulsion, wake survey, ice resistance and propulsion, ice maneuvering, ice management, open-water maneuvering and seakeeping tests. All propelled tests were conducted with HSVA stock ice-capable propellers on azimuthing thrusters. These tests were conducted to assess compliance with requirements in the ARV Performance Specification and Science Mission Requirements, References (1) and (2), respectively.

The tests are reported in HSVA's bubble sweepdown report, resistance and propulsion test report, wake survey report, ice testing report and open-water maneuvering report, References (4) through (8), respectively. Previous model tests, on the ARV Hull Variant 6, were reported in an earlier revision of this report, Reference (3).

The test measurements were analyzed and scaled according to HSVA's standard methodologies, as described in their test reports. Analysis of the open-water tests followed the ITTC guidance in Reference (10) and related documents. Icebreaking tests were conducted and analyzed according to the basin's best practices for icebreaking tests, developed from their history of researching and designing icebreakers.

Bubble sweepdown tests showed that Hull Variant 11 reduces the sweepdown coverage of the transverse receive array by approximately 50%, relative to Variant 6. All other underwater sensors are free of bubble sweepdown risk.

Calm-water powering tests showed that the objective maximum open-water speed of 14 knots is easily achievable with the installed propulsion power of 19,000 kW. The delivered power required at a transit speed of 11 knots in calm water, with no power margins, is 2298 kW (3082 HP).

The wake survey indicated a relatively smooth variation of velocity across the propeller plane, but with an axial velocity deficit in the inboard upper quadrant. The nominal wake fraction computed from the wake survey is 0.104.

The model tests demonstrate that the installed propulsion power of 19,000 kW provides adequate power to maintain a speed of 3 knots in 1.37m (4.5 ft) thick ice with 0.305m (1 ft) snow coverage, running ahead and astern, resulting in a power margin of approximately 1,600 kW running ahead and 600 kW running astern, at 3 knots.

Good clearance of ice from broken ice channels and brash ice fields was achieved using a range of thruster azimuthing strategies, particularly toe-in.

Maneuvering tests showed that the ARV meets the maneuverability standards in IMO Resolution MSC.137(76), Reference (11). It also meets the Performance Specification of a tactical diameter less than 3 times the vessel length.

At a speed of 12 knots the ARV is not directionally stable for thruster azimuth angles near the neutral angle of 0 deg. The width of the instability loop, i.e. the range of rudder angles over which the vessel is unstable, is 2.1 deg. This width is acceptable, according to the Explanatory Notes to Resolution MSC.137(76), thus fulfilling the Performance Specification of sufficient directional stability via a combination of hull design and control system design. The ARV does not meet the average overshoot angle requirement in the Performance Specification. However, with the high power and consequent control authority afforded by the azimuth thrusters, along with the narrow width of the instability loop, the relatively large overshoot angles in the zig-zag tests do not indicate controllability problems during maneuvering.

There are several tests which were undertaken, but not reported by HSVA, prior to issuance of this report. Once completed, reporting of these tests will further define the performance characteristics of the ARV Hull Variant 11. The additional test reports and analyses include:

a. Results from the maneuvering tests in ice

b. Final reporting of results from open-water maneuvering tests

c. Results from open-water seakeeping tests

d. Further analysis of yaw overshoot angles during open-water zig-zag maneuvers and analysis of yaw-checking capability sensitivity to thruster azimuth angle

These additional results and analyses will be reported in a future revision of this report.

1.1. Acronyms

1D	One Dimensional
ARV	Antarctic Research Vessel
ASC	Antarctic Support Contractor
BWL	Beam at Waterline
CFD	Computational Fluid Dynamics
CPMC	Computerized Planar Motion Carriage
DR	Design Review
DWL	Design Waterline
HP	Horsepower
HSVA	Hamburgische Schiffbau-Versuchsanstalt GmbH
IMO	International Maritime Organization
ITTC	International Towing Tank Conference
kW	Kilowatt
LPP	Length Between Perpendiculars
LT	Long Ton
MCR	Maximum Continuous Rating
NSF	National Science Foundation
SS	Sea State

2. Introduction

During several test sessions, spanning a period from March to July, 2023, a 1:24.384 scale model of the ARV, Hull Variant 11, was tested in the Hamburgische Schiffbau-Versuchsanstalt (HSVA) model testing facility, in Hamburg, Germany. This model test campaign defines the performance of the updated Design Review 5 (DR5) design baseline for the ARV.

The tests included thruster open-water, bubble sweepdown, open-water resistance and propulsion, wake survey, ice resistance and propulsion, ice maneuvering, ice channel clearing, open-water maneuvering and seakeeping tests. The tests are reported in HSVA's bubble sweepdown report, resistance and propulsion test report, wake survey report, ice testing report and open-water maneuvering report, References (4) through (8), respectively. References (4) through (7) are attached as Attachments 1 through 4. At the time of issuance of this report the final maneuvering and seakeeping test reports were not available, and the ice testing report, Reference (7), did not include reporting on some of the maneuvering tests in ice.

The requirements for bubble sweepdown, open-water performance and icebreaking performance are specified in the ARV Performance Specification and Science Mission Requirements, References (1) and (2), respectively. The model testing was conducted to assess compliance with these requirements.

Earlier tests, on Hull Variant 6 of ARV, were reported in the previous revision of this report, Reference (3). HSVA's testing and data analysis methodologies for the thruster open-water, bubble sweepdown, open-water resistance and propulsion, wake survey, ice resistance and ice powering tests are summarized therein.

3. Requirements

The vessel requirements pertaining to the tests conducted in the test campaign are listed in Table 1 through Table 3.

The vessel is designed to minimize the risk of air bubble sweepdown from the free surface affecting the performance of the underwater sensors on the flat of bottom. Quantitatively, the bubble sweepdown requirement is expressed as given in Table 1.

Table 1: Bubble Sweepdown Requirement

Capability	Threshold Requirement
Bubble Sweepdown	Computational fluid dynamics (CFD) flow streamlines originating at the ship's stem shall pass no closer than 13.0 ft, measured transversely, from the centerline of the widest sonar transducer receive array area at sustained speed of 8 kt at the full load condition.

The open-water speed and endurance requirements are listed in Table 2.

Table 2: Open Water Speed and Endurance Requirements

Capability	Threshold Requirement	Objective Requirement
Range	17,000 nm, at 11 kts	Objective = Threshold
Endurance	90 days, in Design Reference Mission	Objective = Threshold
Speed, maximum, calm water	14 knots	Objective = Threshold
Speed, cruising, calm water	1[illegible] knots, at ≤ 80% MCR	12 knots, at ≤ 80% MCR
Speed, survey (quiet mode)	8 knots	Objective = Threshold
Speed, cavitation inception	8 knots	9 knots

The icebreaking requirements are listed in Table 3.

Table 3: Icebreaking Requirements

Capability	Threshold Requirement	Objective Requirement
Transit ahead	4.5 ft ice, at speed ≥ 3 kts	4.5 ft ice, with 1 ft snow cover, at speed ≥ 3 kts
Transit ahead	1.6 ft ice, plus 1.0 ft snow cover, at speed of 5 to 6 kts	Objective = Threshold
Transit astern	4.5 ft ice, with 1 ft snow cover, at speed ≥ 3 kts	Objective = Threshold
Turning, ahead and astern	3.5 ft ice, with 1 ft snow cover, turn 180 deg with 5 ship lengths	Objective = Threshold
Star Maneuver	4.5 ft ice, with 1 ft snow cover, turn 180 deg within 400 ft wide reach	Objective = Threshold
Break out of channel, ahead and astern	4.5 ft ice, plus 1.0 ft snow, achieve 90 deg turn within 300 sec	Objective = Threshold

All icebreaking requirements are to be met in multi-year level ice with 100 psi flexural strength.

The maneuvering requirements are listed in Table 4.

Table 4: Open-Water Maneuvering Requirements

Capability	Threshold Requirement	Objective Requirement
Turning circle	Tactical turning diameter < 3 ship lengths in either direction at 12 knots, full load condition, calm water. No bow thruster.	Objective = Threshold
Directional stability	Stable at all speeds in all loading conditions via a combination of hull design and control system design. Sufficient directional stability to meet maneuverability requirements while maximizing fuel economy.	Objective = Threshold
Yaw overshoot	Average yaw overshoot angle from the second overshoot onwards ≤ 10° for 10/10 zig-zag maneuver, all speeds, full load.	Objective = Threshold

The seakeeping requirements are listed in Table 5

Table 5: Seakeeping Requirements

Capability	Threshold Requirement	Objective Requirement
Operability	SS4: Fully operable SS5: Operable for most routine operations SS6: Shipboard personnel can safely work SS7: Shipboard personnel can safely work for safe operation of the vessel	Objective = Threshold
Maximum motions at key locations	SS5: maximum vertical accelerations <0.15g maximum lateral accelerations , 0.05g at lab deck level Maximum roll < 3° Maximum pitch < 2°	Objective = Threshold

4. Test and Analysis Methodology

4.1. Test Facilities

The tests were carried out in the Hamburgische Schiffbau-Versuchsanstalt (HSVA) model testing facility, in Hamburg, Germany. This facility has a number of test basins, including a Large Towing Tank, an Ice Tank and a large cavitation tunnel (HyKat). The tests reported herein were conducted in the Large Towing Tank and Ice Tank facilities.

4.1.1. Towing Tank

The HSVA Large Towing Tank is described in Appendix Z of Reference (5). As described therein the towing tank is a 300 meter long, 18 meter wide, 5.6 meter deep test basin with a towing carriage running on rails along the long axis. Models are attached to the carriage via a thin wire which transmits the towing force to a force gauge mounted to the model. Model motions are guided by vertical steel guide posts fixed to the carriage, which allow free movement longitudinally and vertically, but restrain lateral motions.

The Large Towing Tank is equipped with a secondary towing carriage, the Computerized Planar Motion Carriage (CPMC), to conduct maneuvering tests. When operating, this carriage is towed by the main towing carriage via tie rods. The CPMC has three sub-carriages, each of which is driven along one degree of freedom relative to the main carriage: X translation, Y translation and yaw rotation. When combined with the forward speed of the main carriage, motions along these three degrees of freedom describe vessel maneuvering trajectories. The CPMC can operate in two modes: captive, in which the subcarriage motions are pre-programmed to force the model along a prescribed trajectory; and tracking, in which the model is controlled by its own control appendages and the subcarriages are forced to follow the model trajectory.

The Large Towing Tank is equipped with two wavemakers: A duplex flap wavemaker at one end, for generating long-crested waves along the axis of the towing tank, and a 40m long snake-type wavemaker along one side wall, for generating oblique waves.

4.1.2. Ice Tank

The HSVA ice testing tank is described in Attachment 5 of Reference (3). As described therein the ice tank is a 78 meter long, 10 meter wide, 2.5 meter deep test basin with an air forced cooling system that can generate air temperatures as low as -20°C. The tank has a towing carriage with two axis motion capabilities, for conducting straight-line and maneuvering tests in ice.

4.2. Model Construction

HSVA Model 5626, a 1:24.384 scale model of ARV Hull Variant 11, was used for all model testing. Model 5626 was constructed of wood, using industry-standard construction techniques and CNC milling of the outer surface.

The hull model was constructed according to the ARV 3D hull model, Reference (9). The full scale and model particulars, at the tested load condition and with the tested propeller, are presented in Table 6.

Table 6: Model 5626 Characteristics

Description	Value (Full Scale)	Value (Model Scale)
Length overall	111.25 m (365.0 ft)	4,562m (14.967 ft)
Length between perpendiculars	108.72 m (356.69 ft)	4.458 m (14.626 ft)
Beam, DWL	24.40 m (80.05 ft)	1.001 m (3.284 ft)
Design draft	9.906 m (32.50 ft)	0.406 m (1.332 ft)
Displacement	13,733 MT (13,516 LT)	947.2 kg (2088 lb)
Propeller diameter	4.877 m (16.00 ft)	0.200m (0.656 ft)

The model scale was established by the availability of stock propellers at the model basin with characteristics matching the full-scale ice-capable propellers as closely as possible. The propellers selected were numbered 2288 and 2289. For tests with podded thrusters, HSVA has stock thruster housings with similar characteristics to ABB Azipod units. These housings were modified to model the design of the ARV thrusters. The base pod models were pod numbers 222-5500 and 223–5500 (Reference (5)).

Further details of the hull, propeller and pod models are provided in References (5), (7) and (8).

The model was marked with vertical stations from 1 to 20 (transom to bow), and waterlines at one-meter intervals above the design waterline, to facilitate observation of the wave and ice profiles in the resistance and propulsion test photographs.

Views of the model, completed and outfitted, are shown in Figure 1, taken from Reference (5).

Figure 1: HSVA Model 5626 (from Reference (5))

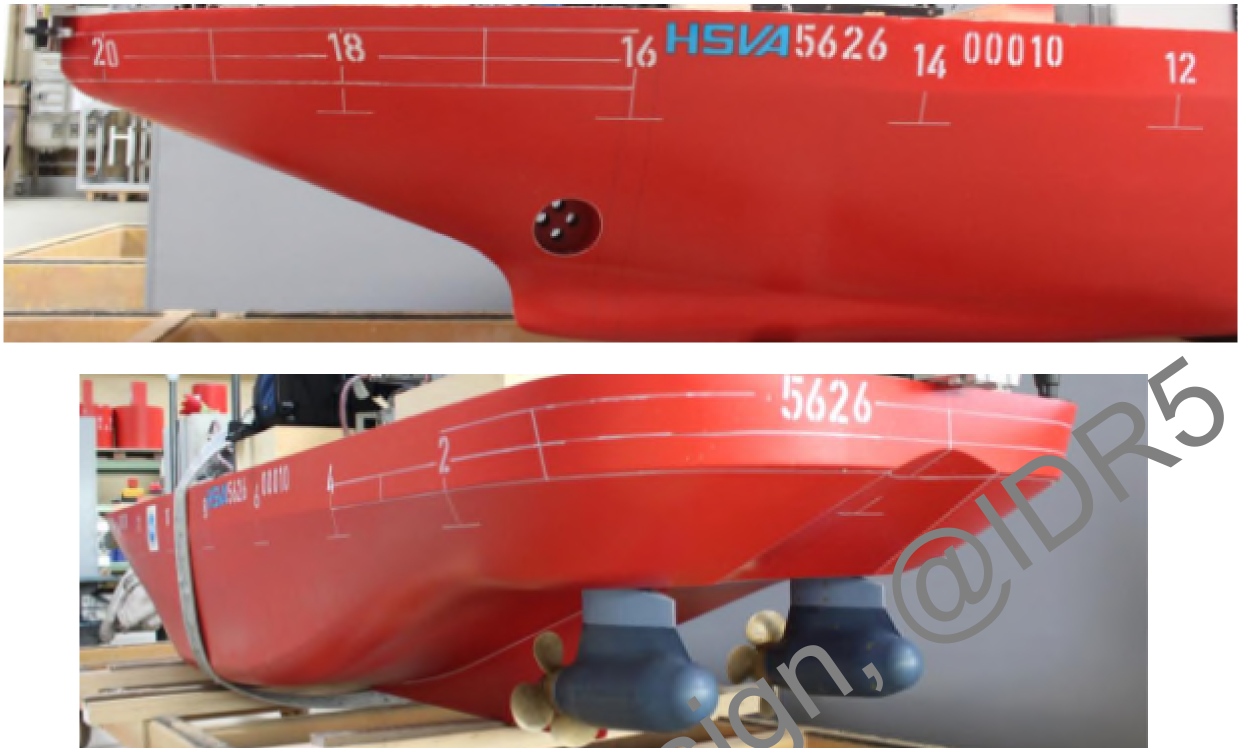

4.3. Model Test Series

To provide data for assessment against the requirements of Table 1 through Table 5, ten types of test were conducted at HSVA:

1. Thruster open-water tests
2. Bubble sweepdown tests
3. Open-water resistance tests
4. Open-water propulsion tests
5. Wake survey tests
6. Towed icebreaking tests
7. Free-running icebreaking tests
8. Ice Channel Clearing Tests
9. Open-water maneuvering tests
10. Seakeeping tests

4.3.1. Thruster Open-Water Tests

Prior to the open-water resistance and propulsion tests, thruster open-water tests were conducted to measure the performance of the thruster units in open water, without the influence of the hull. These tests were conducted in the Large Towing Tank. The results of these tests were used to guide the conduct and analyze the results of the open-water propulsion tests (Section 4.3.4) and icebreaking tests (Sections 4.3.6 and 4.3.7).

The test methodology and data analysis for the thruster open-water tests are reported in Reference (3).

4.3.2. Bubble Sweepdown Tests

Bubble sweepdown tests were conducted to assess the likelihood of entrained air bubbles near the water free surface being drawn down across the underwater sensors on the keel. These tests were conducted in the Large Towing Tank facility.

In these tests a dye/water mix was ejected from an array of dye ejection ports protruding from the hull surface. The ejected dye mix followed the local streamlines at the ejection ports, indicating the trajectories of the flow streamlines from the ports.

The locations of the dye ports corresponded to streamline origination points specified in Reference (1) and used in previous CFD studies of bubble sweepdown. Dye ports were arranged along the centerline at the stem, in full-scale positions shown in Table 7.

Table 7: Bubble Sweep-down Dye Ejection Points

Port	X m aft of FP	Y m port of Centerline	Z m below Waterline
1	0.00	0.00	0.00
2	1.57	0.00	0.58
3	3.15	0.00	1.15
4	3.69	0.00	1.35

The port locations are shown on the hull profile in Figure 2, taken from Reference (4).

Figure 2: Dye Port Locations on HSVA Model 5626 (from Reference (4))

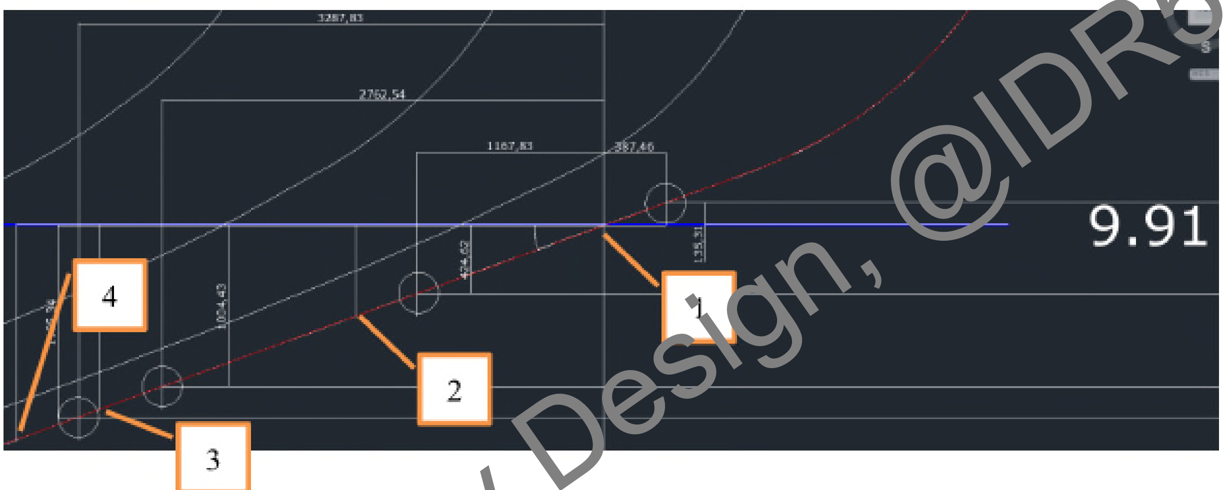

The test methodology and data analysis for these tests are reported in References (3) and (4). Further details of the test set-up and run matrix are reported in Reference (4).

4.3.3. Hull Resistance Tests

Hull resistance tests were conducted to measure the resistance of the model hull, without the influence of the thrusters. These tests were conducted in the Large Towing Tank. The results of these tests were used to guide the conduct and analyze the results of the propulsion tests (Section 4.3.4).

In the resistance tests the hull model was attached to the carriage via the towing wire/guide system described in Section 4.1.1. Resistance was measured by the 1D towing force gauge.

Tests were conducted with the bow thruster tunnel open and closed, to measure the sensitivity of resistance to this design feature.

The test methodology and data analysis for these tests are reported in References (3) and (5). The test matrix is reported in Reference (5).

4.3.4. Propulsion Tests

Propulsion tests were conducted to assess the power requirements of the ARV through its operational speed range. These tests were conducted in the Large Towing Tank, using the resistance dynamometer to measure resistance forces. The resistance, propeller rotation rate, propeller shaft torque and thruster force measurements were used to find the ship self-propulsion points.

Propulsion tests were conducted with the bow thruster tunnel open, as that is the operating condition of the ARV.

The test methodology and data analysis for these tests are reported in References (3) and (5). The test matrix is reported in Reference (5).

4.3.5. Wake Survey Tests

Wake survey tests were conducted to measure the flow velocity vectors at the thruster propeller plane, to provide data for wake-adapted propeller design. These tests were conducted in the Large Towing Tank.

The wake survey tests used 5-hole pitot tubes to measure the axial, radial and tangential velocity vectors, relative to the propeller disk. The wake survey was carried out at a single speed, 9 knots.

The test methodology and data analysis for these tests are reported in References (3) and (6).

4.3.6. Towed Icebreaking Tests

Towed icebreaking tests were conducted to assess the straight-ahead resistance in ice thickness of 1.37m (4.5 ft), with a 0.305m (1 ft) snow cover, at speeds of 6 and 3 knots. These tests were conducted in the Ice Tank facility.

In the towed tests, the model was towed by a moving carriage, and the resistance measured by a force dynamometer between the carriage and model. Above-water and underwater videos were recorded to assess icebreaking behavior. Tests were conducted in level ice, in the ahead and astern directions.

The test methodology and data analysis for these tests are reported in References (3) and (7). The ice characteristics and test matrix are reported in Reference (7).

4.3.7. Free-running Icebreaking Tests

Free-running icebreaking tests were conducted to assess the powering requirements in ice thickness of 1.37m (4.5 ft) with a 0.305m (1 ft) snow cover, and to assess channel break-out and ice maneuvering performance. These tests were conducted in the Ice Tank facility.

Four types of free-running test were conducted:

- Straight trackline in level ice
- Breaking out of channel
- Maneuvering

The straight trackline tests, to measure powering requirements, and break-out tests, to assess channel break-out performance, were conducted in scaled 1.37 m (4.5 ft) ice thickness with 0.305m (1ft) snow cover.

The test methodology and data analysis for these tests are reported in References (3) and (7). The test matrix is reported in Reference (7).

4.3.8. Ice Management Performance

Additional free-running tests were conducted with an additional ice sheet to determine the ability to manage the ice surrounding and trailing the ARV after breaking through it. These tests were to demonstrate the ARV can safely support towed operations in ice. During model testing, three scenarios were tested to demonstrate the ice management abilities of the ARV:

- Maintenance of clear channel during unbroken ice transit
- Execution of the "side step maneuver"
- Channel widening and maintenance of clear channel during brash ice transit

The first set of ice management tests investigated how well the ARV hull can maintain a clear ice channel in an unbroken 1m (3.3 ft) thick ice sheet, while orientating the Azipods at opposing azimuth angles of 60 degrees toe-in and 60 degrees toe-out, and then alternating the pods in parallel from one side to another. The second test was to create an open pool adjacent to the working deck to support overboard science mission in unbroken ice. The third type of ice management test investigated widening of a broken channel and maintaining a channel in a brash ice field, using varying thruster toe-in angles.

4.3.9. Open-Water Maneuvering Tests

Maneuvering tests were conducted to assess compliance with the turning, yaw-checking and course-keeping requirements in Table 4. The maneuvering tests were carried out in the Large Towing Tank, using the CPMC, described in Section 4.1.1. For the maneuvering tests the model was propelled by its model thruster units and controlled to execute a series of zig-zag maneuvers. The CPMC was run in tracking mode to follow the model trajectories and measure the maneuvering motions.

Tests were conducted at speeds of 4 and 12 knots, with a rudder rate of 9 deg/sec (full scale).

As reported in Reference (8), the maneuvering performance of the ARV was determined from a combination of directly measured results and simulated maneuvers. The tested maneuvers were zig-zag maneuvers, using rudder angles ranging from 5 deg to 35 deg and yaw switching angles ranging from 5 deg to 20 deg. These tests were used to derive hydrodynamic coefficients, for use in HSVA's maneuvering simulator. The simulator was used to compute directional stability and to simulate turning circles, zig-zags, spirals and Williamson turns.

The test methodology, test matrix and data analysis for these tests are reported in Reference (8).

4.3.10. Seakeeping Tests

Seakeeping tests were conducted to assess compliance with the seakeeping requirements of Table 5. The seakeeping tests were carried out in the Large Towing Tank, with a free-running model.

At the time of reporting, the HSVA report on the seakeeping tests was not available. The test methodology, test matrix and data analysis for these tests will be reported in a future revision of this report.

5. Results

5.1. Thruster Open-Water Tests

The results of the thruster open-water tests are presented in Figure 3, taken from Reference (5).

Figure 3: Thruster Open-Water Curves (from Reference (5))

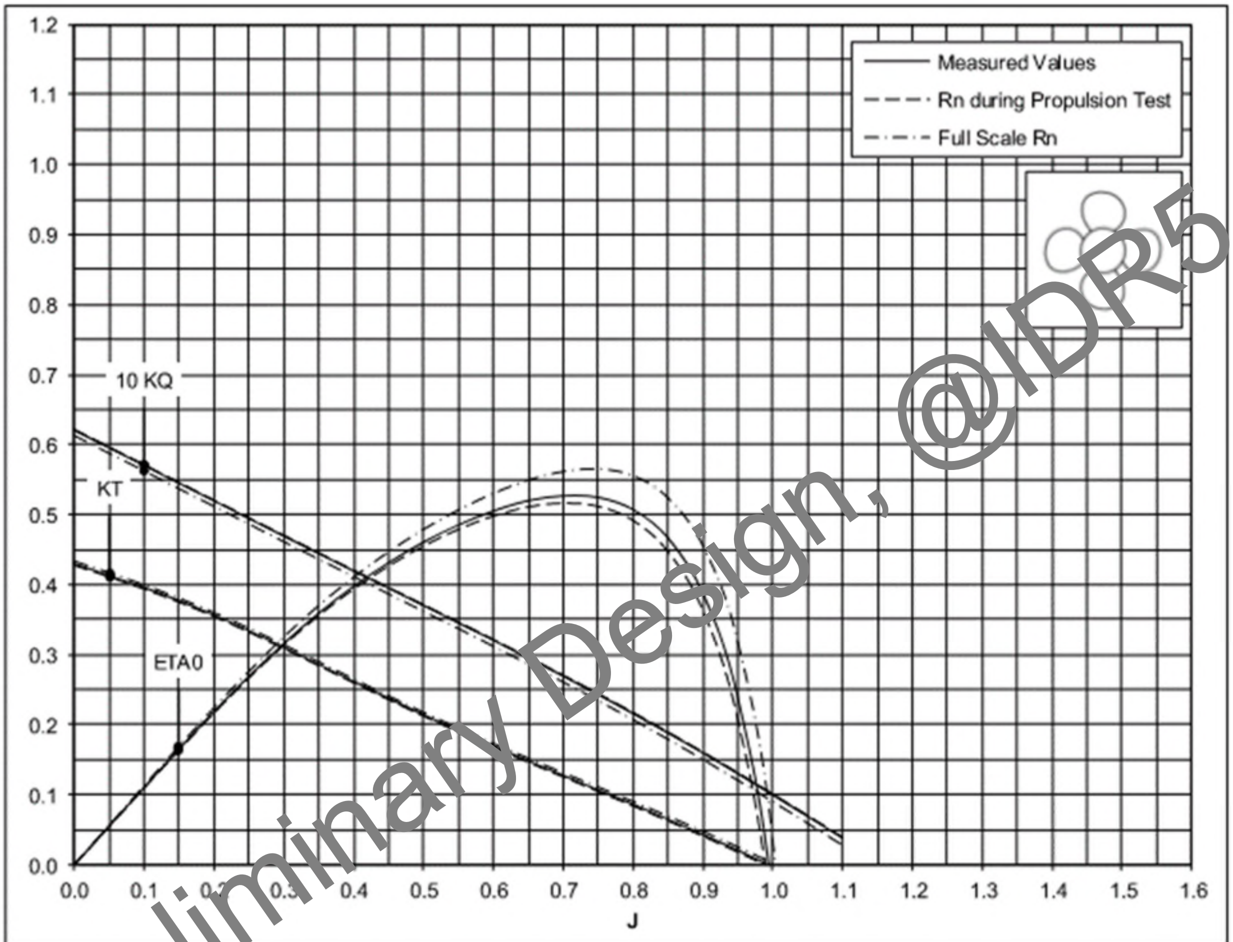

Figure 3 shows the effect of the Reynolds number corrections (model scale to full scale) on the open water curves.

5.2. Bubble Sweepdown Tests

The results of the bubble sweepdown tests are the underwater videos recorded during the runs. These videos have been delivered to Leidos. The video file names and test conditions are indexed in Table 8.

Table 8: Bubble Sweep-down Video File Index

Run	Trim	Speed (kts)	Video File Name (.mp4)
m03	Even keel	6	Leidos_ARV_BSD_6kts
m04	Even keel	8	Leidos_ARV_BSD_8kts
m05	Even keel	4	Leidos_ARV_BSD_4kts
m06	Even keel	10	Leidos_ARV_BSD_10kts
m07	1° Bow Down	8	Leidos_ARV_BSD_8kts _1degTrimBow

The speeds and positions in Table 8 refer to the full-scale ship. The video files all have extension .mp4.

A complete discussion of the bubble sweepdown results is included in Reference (4).

As reported therein, air bubbles originating along the stem centerline travel downwards along the stem to the ice knife, which diverts the flow outboard. At a location between Station 14 and Station 16, depending on speed, the bubble stream is transported below the keel by the keel edge vortex and flows across part of the transverse receive array.

At the lowest tested speed, 4 knots, approximately 2/3 of the transverse receive array is covered by bubbles, reducing to approximately 10% of the sensor area at 8 knots. The sweepdown behavior at 10 knots is very similar to that at 8 knots.

One degree of bow-down trim has little influence on the sweepdown behavior.

The longitudinal transducer arrays and smaller sensors forward of them are free of bubbles at all speeds.

Reference (4) includes comparative photographs of the boundaries of the bubble sweepdown region on the bottom of the keel, on the Hull Variant 6 (as reported in Reference (3)) and Hull Variant 11 hulls. These photographs are reproduced in Figure 4.

Hull Variant 11 reduces the sweepdown coverage of the transverse receive array by approximately 50%, relative to Hull Variant 6.

Figure 4: Bubble Sweepdown Boundaries on Variants 6 and 11 at 6 and 8 Knots

6 knots

Variant 6 Variant 11

8 knots

Variant 6 Variant 11

5.3. Resistance Tests

The results of the resistance tests are reported in Reference (5). These results are summarized in Figure 5, taken from Reference (5).

Figure 5: Resistance Test Results (from Reference (5))

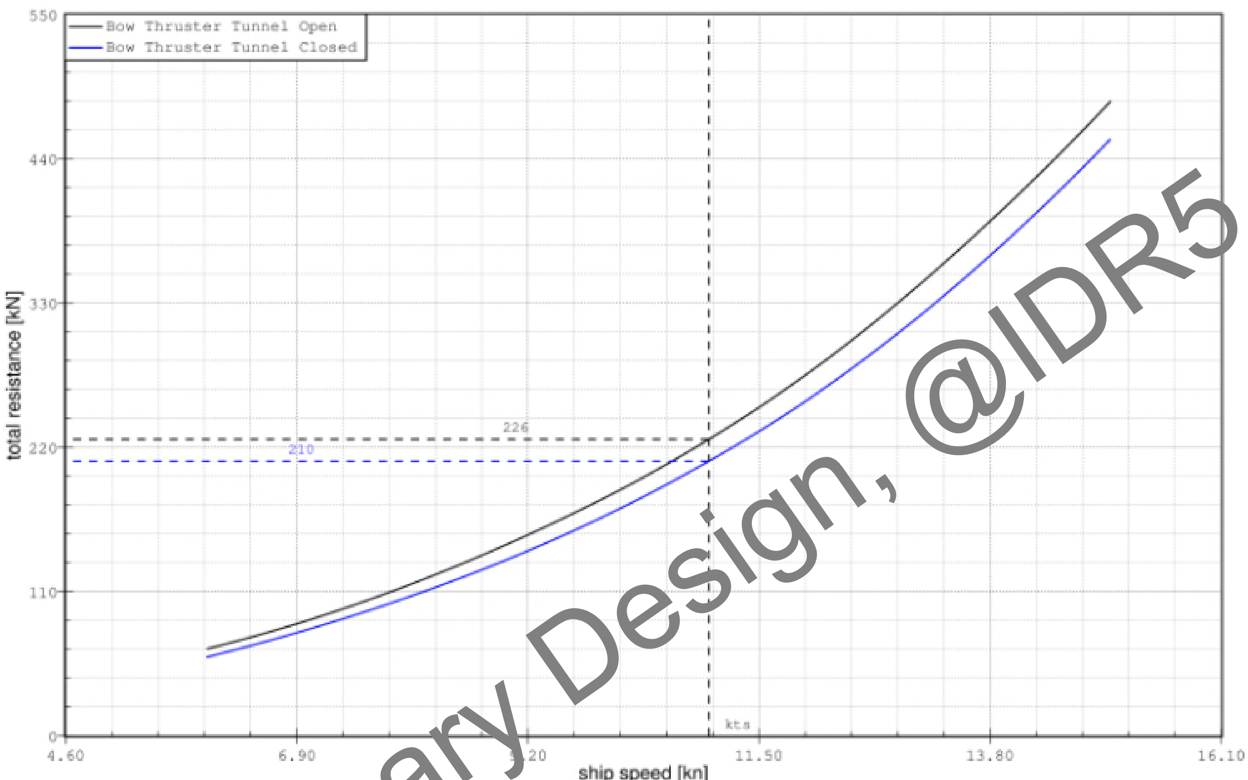

The open bow thruster adds approximately 7% to the resistance over the tested speed range.

5.4. Powering Tests

The results of the powering tests are reported in Reference (5). The full scale powering results, in calm water and zero wind, are presented in Figure 6, taken from Reference (5). Figure 6 shows the delivered power with the tested propeller in blue, and with the propeller used in the previous tests (reported in Reference (3)) in black. As shown in Figure 6 the 19,000 kW installed propulsion power is more than sufficient to achieve the objective top speed of 14 knots. Figure 6 highlights the delivered power at 11 knots, 2298 kW (3082 HP). This delivered power is the calm water propulsion power, as scaled from the model tests, with no power margins applied.

Figure 6: ARV Power Requirements in Calm Water, Zero Wind (from Reference (5))

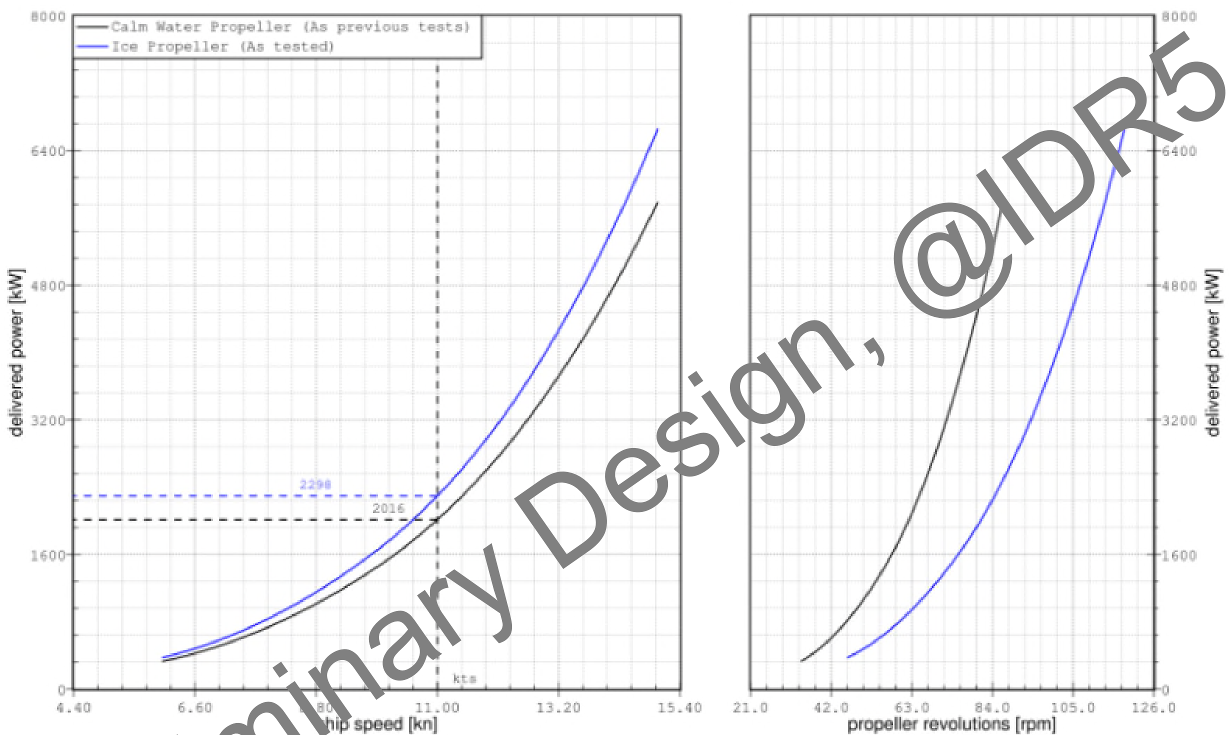

Complete powering results are provided in Reference (5).

5.5. Wake Survey Tests

The wake survey results are reported in Reference (6). The reported results consist of contour and vector plots of axial, radial and circumferential velocities, plots of circumferential variations of the three velocity components and tabulated harmonics of the velocity Fourier series.

The contour plot of axial velocity, overlaid with the vector plot of circumferential and radial velocities, is presented in Figure 7, taken from Reference (6).

Figure 7: Axial, Radial and Circumferential Velocities in Propeller Plane

(From Reference (6))

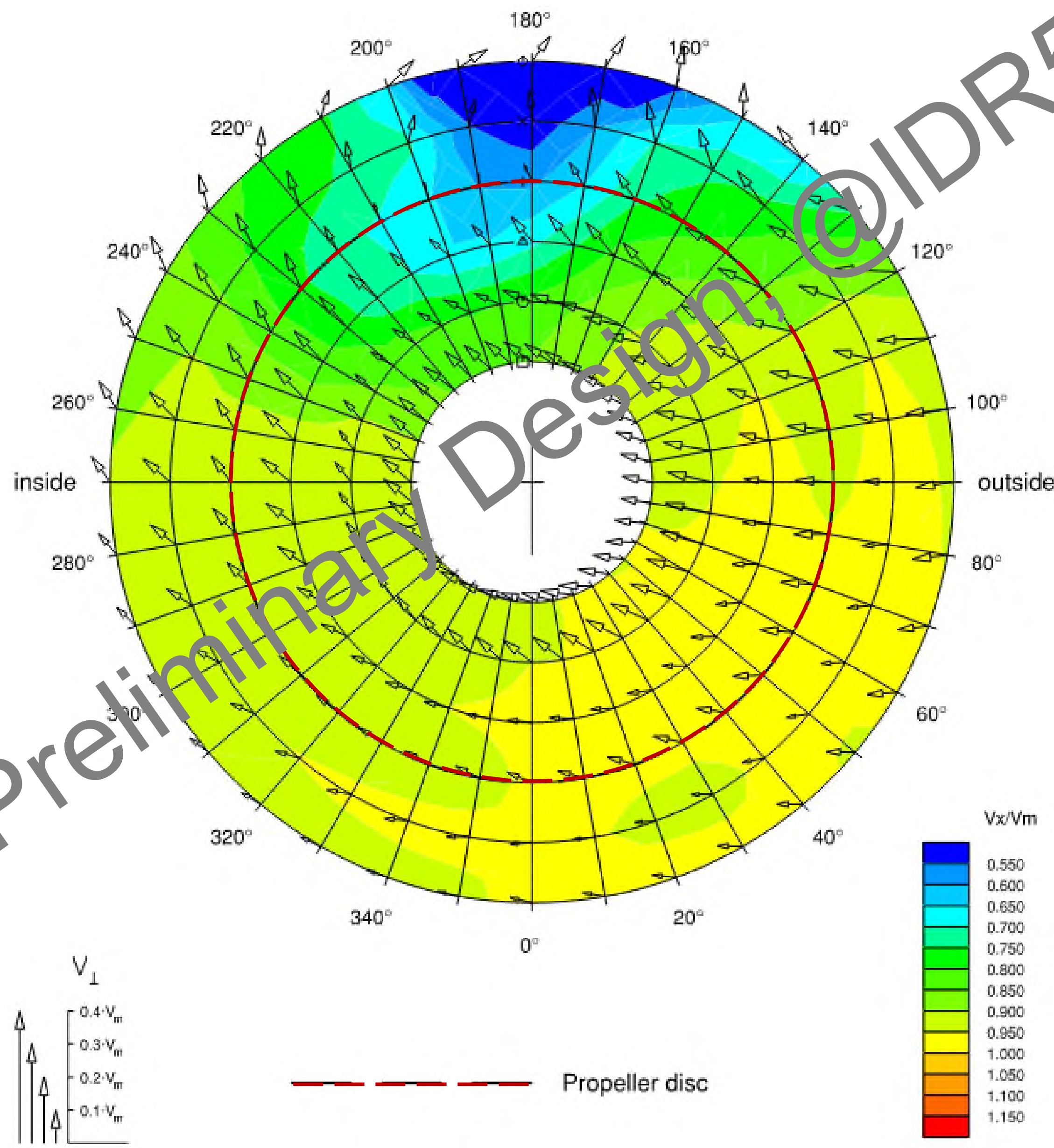

The wake survey plotted in Figure 7 include radii out to 1.4 times the propeller radius. The propeller disk is highlighted in red. Within the propeller disk area, the axial velocities are fairly uniform throughout the propeller plane, which is typical of twin-propeller installations with a centerline skeg. A wake deficit is observed in the upper inner quadrant of the propeller plane, near the hull surface, but within the propeller disk (highlighted in Figure 7) the effects on propeller inflow are modest. Its position in the propeller plane, and increasing width with increasing radius, indicate a primary influence from the decelerated flow in the hull boundary layer.

Inward-directed flow is evident throughout the propeller plane.

The nominal wake fraction, computed from the axial velocities integrated over the propeller plane, is 0.104, an improvement from Hull Variant 6 results and a typical value for this type of hullform.

5.6. Towed Resistance and Propulsion Tests in Ice

The results of the towed resistance and propulsion tests consist of full-scale resistance and powering estimates, together with observations, videos and photographs of model behavior during the tests. These results are reported in Reference (7).

The towed resistance and powering requirements, at 3 knots, in 1.37m (4.5 ft) ice thickness with 0.305m (1 ft) snow cover, are presented in Table 9.

Table 9: Towed Resistance and Powering in 1.37m Ice

Ice Thickness (m)	Direction	Speed (kts)	Resistance (kN)	Delivered Power (kW)
1.37	Ahead	3	1,538	17,392
1.37	Astern	3	1,620	18,416

The observations of the towed ice tests are reported in Reference (7). As noted therein, the model exhibited typical icebreaking behavior in the towed tests ahead. The ice sheet cracked at centerline, forward of the ice knife, and the crack was fully developed prior to ice contact with the ice knife. The ice knife in the Variant 11 hull was more effective in pushing ice pieces outboard, away from the underwater sensors near the keel centerline, than the narrower ice knife on the Variant 6 hull. The areas of underwater sensors were generally ice free. Most broken ice pieces passed above the propellers. There was some ice contact at the upper propeller tip, but these contacts were with small ice pieces, and are not of concern for propeller damage.

Going astern, the model showed good ice breaking and clearing, similar to the Hull Variant 6 design. Rectangular ice floes are broken and then split at the aft skeg. Small broken ice pieces along the outer hull are cleared by the propeller wash, with the hull mostly remaining ice free. Some crushing of broken ice pieces occurred at the thruster struts, which is to be expected.

Propeller-ice interaction was observed to be less than that observed with the Hull Variant 6 design.

5.7. Free-Running Tests in Ice

Figure 8 presents the speeds attained in the free-running tests ahead in 1.37m (4.5 ft) ice with 0.305m (1 ft) snow cover, at power levels ranging from 84% to 104% of full power. Figure 9 presents the speeds attained in the free-running tests astern head in 1.37m (4.5 ft) ice, at power levels ranging from 61% to 114% of full power.

Figure 8: Free-running Power Ahead in 1.37m Ice

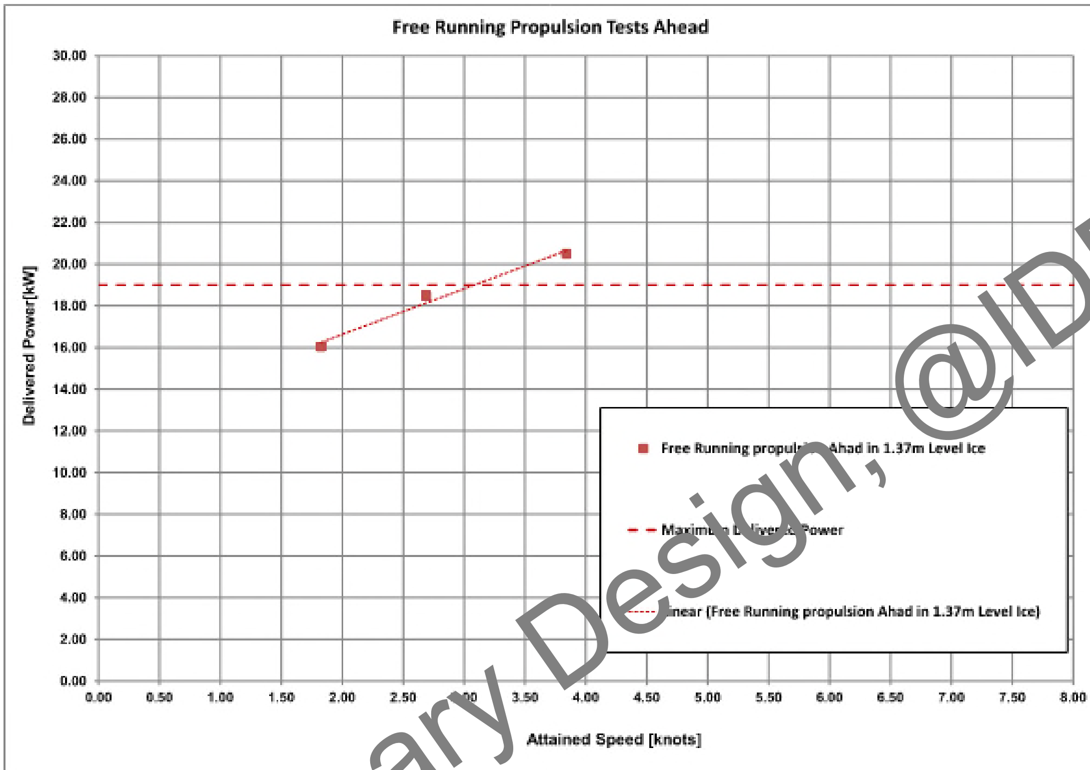

Figure 9: Free-running Power Astern in 1.37m Ice

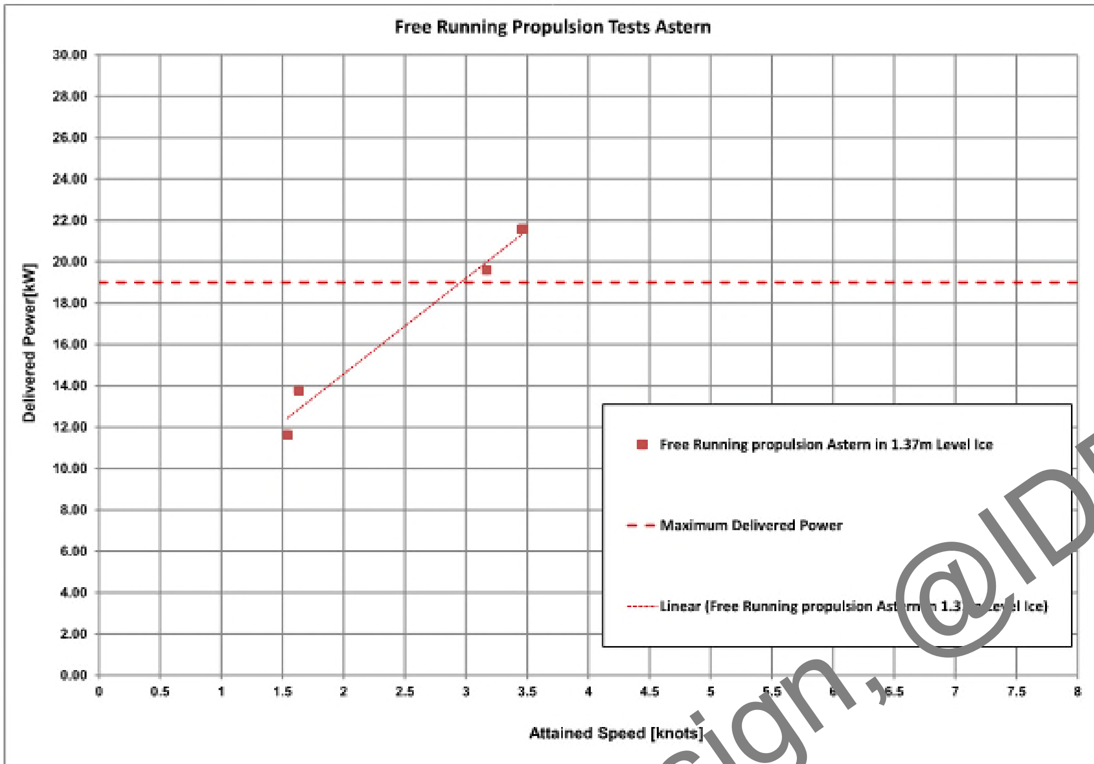

These tests showed attainable speeds of 3.1 knots and 3.0 knots in 1.37m ice, ahead and astern, respectively with the 19,000 kW propulsion power available in the ARV design.

Test observations of the free-running tests are reported in Reference (7). As reported therein, the icebreaking and clearing behavior in the free-running tests was similar to that observed in the towed tests, with slightly less ice coverage on the underside of the hull and less propeller-ice interaction.

Underwater views of the hull while icebreaking in scaled 1.37m thick ice are shown in Figure 10 and Figure 11.

Figure 10: Icebreaking Ahead in 1.37m Ice Thickness

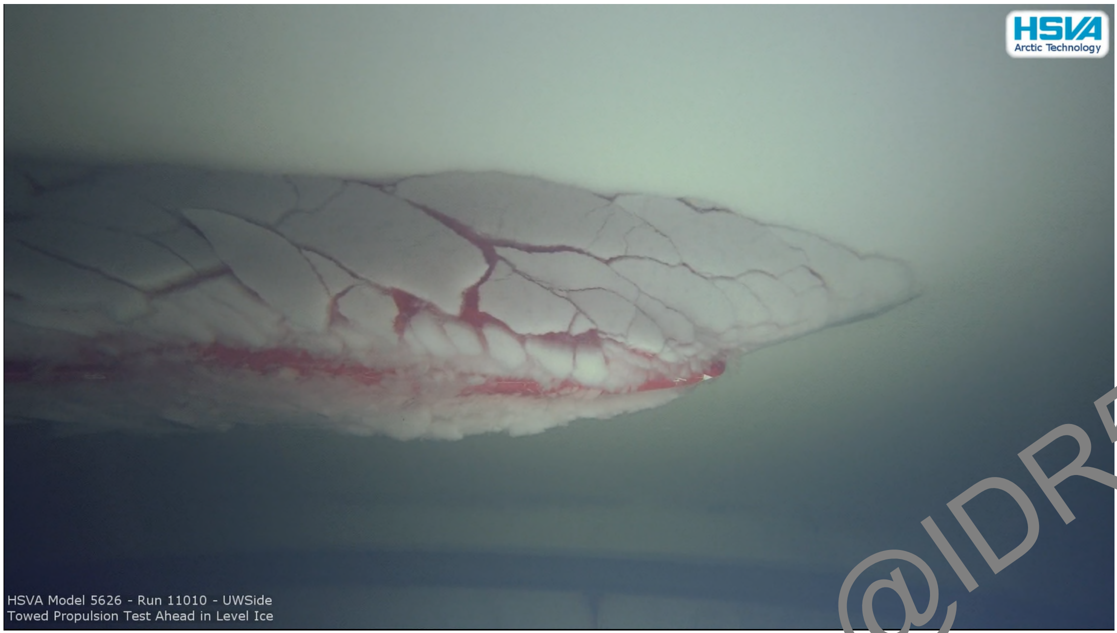

Figure 11: Icebreaking Astern in 1.37m Ice Thickness

5.8. Ice Maneuvering

5.8.1. Breaking out of the Channel

Vessel trajectories, measured quantities and observations of the break-out tests are reported in Reference (7). Break-out was successful in scaled 1.37m ice, both ahead and astern. Break-out ahead was achieved in 2-3 ship lengths, and break-out astern was achieved in a little more than 1 ship length. Break-out was achieved in less than 300 seconds, in both directions, satisfying the break-out requirement in Table 3.

5.8.2. Star Maneuver

At the time of reporting the portion of Reference (7) that reports on the star maneuver tests was not available. These results will be included in a future revision of this report. The Icebreaking Performance Report in Reference (12) discusses observed behavior during these tests.

5.8.3. Turning Circle

At the time of reporting the portion of Reference (7) that reports on the turning circle tests in ice was not available. These results will be included in a future revision of this report. The Icebreaking Performance Report in Reference (12) discusses observed behavior during these tests.

5.9. Ice Management Performance

The results of the ice clearing tests in scaled 1m (3.3ft) thick ice are reported in Reference (7).

Tests for breaking the ice sheet and clearing the broken channel with thruster wash were run with the thrusters at zero degree azimuth, 60 degrees toe-in and 60 degrees toe-out. The toe-in strategy was successful in clearing the channel aft of the ARV of all but small ice pieces. The toe-out strategy pulled ice in from the channel edges, leaving larger ice pieces in the channel.

Tests with the thrusters azimuthing in parallel, alternating from side to side, left a widened channel aft of the ARV, using the aft end of the hull to break the ice along alternating sides of the channel and the thruster wash to clear the broken ice.

A side-step maneuver was used to force the aft end of the hull against one side of the channel, with zero ahead or astern speed, using the thruster wash to clear ice from the opposite side. This maneuver was successful in creating a wide pool of clear water at the ARV position.

Underwater photographs of the 60 degree toe-in, 60 degree toe-out and parallel azimuthing tests are shown in Figure 12 through Figure 14, taken from Reference (7).

Figure 12: Ice breaking, Clearing with 60 degree Thruster Toe-In

Figure 13: Ice breaking, Clearing with 60 degree Thruster Toe-Out

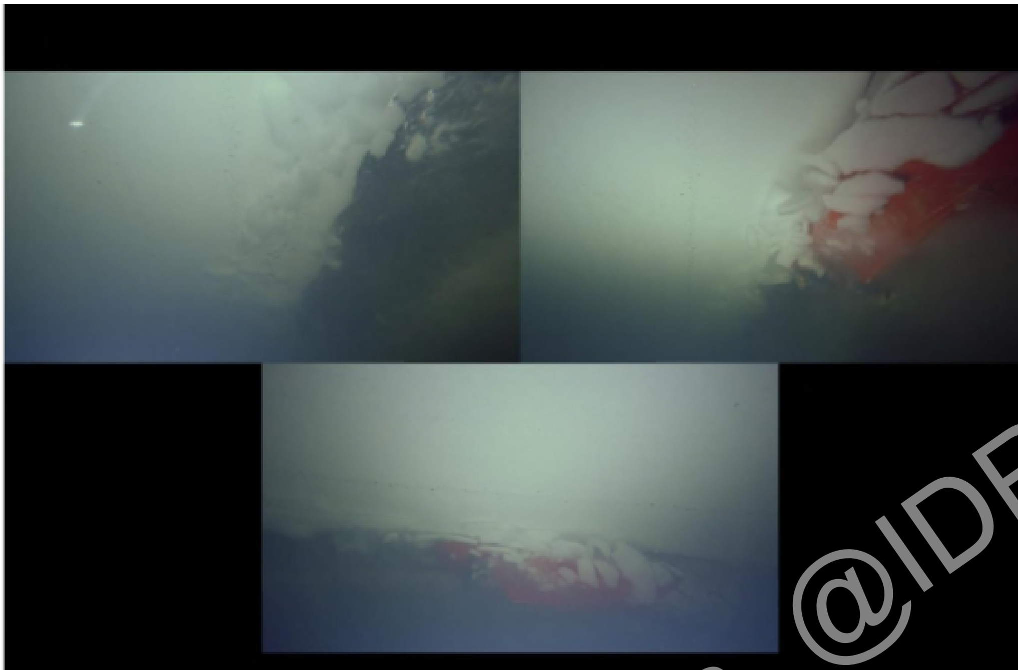

Figure 14: Ice Breaking, Clearing with Parallel Thrusters

Running the model through a broken channel, created in the thruster azimuth tests above, showed that a thruster toe-in angle of 60 degrees was effective in widening a broken channel and clearing the channel of large ice pieces.

Thruster toe-in angles of 30, 60 and 85 degrees were all effective at clearing a channel through a brash ice field, with forward speed and width of channel dependent on the thruster angle. Figure 15 shows brash ice clearing with 60 degree thruster angle.

Figure 15: Channel Clearing in Brash Ice Field with 60 degree Thrusters

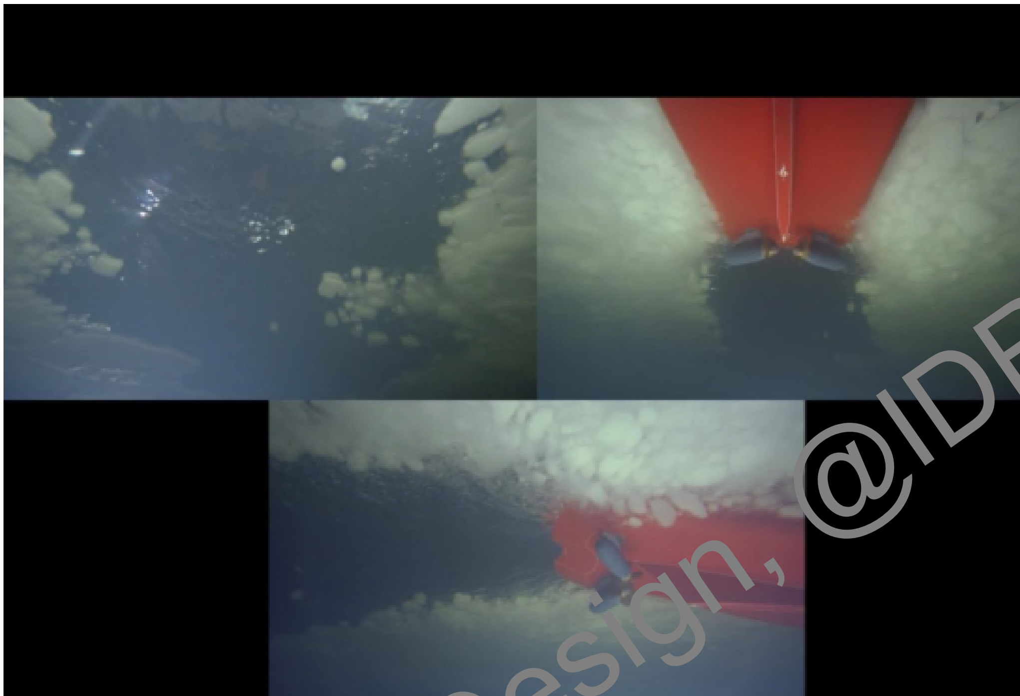

Additional photographs of ice breaking and clearing are provided in References (7) and (12).

5.10. Open-Water Maneuvering Tests

The results of the open-water maneuvering tests are reported in Reference (8). The results are summarized in Table 10. For reference, Table 10 lists maneuvering criteria from IMO Resolution MSC.137(76) (Reference (11)) with the ARV achieved results compared to the IMO threshold values.

Table 10: Open-Water Maneuvering Results

Criterion	4 Knots		12 knots	
	Achieved	IMO Standard	Achieved	IMO Standard
10/10 zig-zag 1st overshoot angle (deg)	8.4	20.0	9.9	13.8
10/10 zig-zag 2nd overshoot angle (deg)	25.0	40.0	24.4	30.7
20/20 zig-zag 1st overshoot angle (deg)	15.6	25.0	22.6	25.0
Distance travelled for 10 deg change of heading with 10 deg thruster angle (/LPP)	1.07	2.5	1.12	2.5
Tactical Diameter, with 35 deg thruster angle (/LPP)	1.20	5.0	1.62	5.0
Turning Circle Advance at 35 deg thruster angle (/LPP)	1.47	4.5	1.55	4.5

As shown in Table 10, the ARV exceeds the IMO maneuverability standards.

The ARV also meets the turning circle requirement in Table 4.

At a speed of 12 knots the ARV is not directionally stable for thruster azimuth angles between -1.1 deg and +1.1 deg. The total instability loop width, i.e. the range of rudder angles over which the vessel is unstable, is 2.1 deg. Some degree of yaw instability is not unusual for vessels with azimuthing stern thrusters, particularly with the lateral area of the ice knife at the bow. As reported in Reference (8), the Explanatory Notes for Reference (11) recognize that yaw instability at low rudder angles is acceptable, provided that the width of the instability loop is within a specified range. The maximum acceptable instability loop width is 2.9 deg for the length/speed ratio of the ARV at 12 knots, so its degree of instability is acceptable by IMO standards. The maneuvering requirements of Table 4 require the ARV to be stable via a combination of hull design and control system design, with sufficient directional stability to meet maneuverability requirements. The narrow width of the ARV instability loop fulfills these requirements.
The average yaw overshoots from the 10/10 zig-zags are not reported in Reference (8), but it is apparent from the 2nd overshoot angles that the ARV does not meet the average overshoot angle requirement in Table 4. With the high power and consequent control authority afforded by the azimuthing thrusters (less than 20% utilization at 12 kts), together with the narrow width of the instability loop, the relatively large overshoot angles in the zig-zag tests do not indicate controllability problems during maneuvering.

At the time of reporting the final version of Reference (8) was not available. A future revision of this report will include the final report, further analysis of the zig-zag yaw overshoot angles and analysis of yaw-checking capability.

5.11. Seakeeping Tests

At the time of reporting the HSVA report on seakeeping tests was not available. These results will be included in a future revision of this report.

6. Conclusions

Bubble sweepdown, open-water resistance and propulsion, wake survey, ice resistance and propulsion, ice maneuvering, ice management, open-water maneuvering and seakeeping tests were successfully carried out on a 1:24.384 scale model of the ARV, Hull Variant 11, at the HSVA model testing facility. This model testing provides definition of the performance of the DR5 design baseline for the ARV. Earlier tests, on ARV Hull Variant 6, were reported in an earlier revision of this report (Reference (3)).

During the bubble sweepdown tests, at 4 knots approximately 2/3 of the transverse receive array is covered by bubbles, reducing to approximately 10% of the sensor area at 8 and 10 knots. Hull trim makes little difference to the sweepdown behavior. Hull Variant 11 reduces the sweepdown coverage of the transverse received array by approximately 50%, relative to Hull Variant 6.

The maximum power required by the ARV is governed by icebreaking, not open-water performance, so the objective maximum open-water speed of 14 knots is easily achievable with the installed propulsion power of 19,000 kW. The delivered power required at a transit speed of 11 knots is 2298 kW (3082 HP).

The wake survey indicated a relatively smooth variation of velocity across the propeller plane, but with an axial velocity deficit in the inboard upper quadrant. The nominal wake fraction computed from the wake survey is 0.104.

The installed propulsion power of 19,000 kW provides adequate power to maintain speeds of over 3 knots in 1.37m (4.5 ft) thick ice with 0.305m (1 ft) snow cover, running ahead and astern. The power margin to maintain a 3 knot speed is approximately 1600 kW running ahead and 600 kW running astern. The power required to maintain a speed of 3 knots in 1.37 m ice with 0.305m snow cover is reduced by 200kW (19,400 to 17,400) relative to Hull Variant 6.

Observations of the icebreaking behavior during the resistance and powering tests in ice demonstrated similar, or slightly better icebreaking performance compared to Hull Variant 6. These observations are supported by the reduction in power required to maintain speed in 1.37m ice.

Break out from a cleared channel was achieved in less than 300 seconds, ahead and astern, in 1.37m (4.5 ft) ice thickness with 0.305m (1 ft) snow cover.

Good clearance of ice from broken channels during icebreaking was achieved, using a range of toe-in, toe-out and parallel thruster strategies. Good clearance of channels through brash ice fields was achieved with thruster toe-in angles of 30, 60 and 85 degrees.

The ARV meets the IMO maneuverability standards in IMO Resolution MSC.137(76). It also meets the Performance Specification of a tactical diameter less than 3 times the vessel length.

At a speed of 12 knots, the ARV is not directionally stable for thruster azimuth angles near the neutral angle of 0 deg. The width of the instability loop is 2.1 deg, which is acceptable according to the Explanatory Notes to Resolution MSC.137(76), thus fulfilling the Performance Specification of sufficient directional stability via a combination of hull design and control system design. The ARV does not meet the average overshoot angle requirement in the Performance Specification. However, with the high power and consequent control authority afforded by the azimuthing thrusters, together with the narrow width of the instability loop, the relatively large overshoot angles in the zig-zag tests do not indicate controllability problems during maneuvering.

There are several tests which were undertaken, but not reported by HSVA, prior to issuance of this report. Once completed, reporting of these tests will further define the performance characteristics of the ARV Hull Variant 11. The additional test reports and analyses include:

a. Results from the maneuvering tests in ice
b. Final reporting of results from open-water maneuvering tests
c. Results from open-water seakeeping tests
d. Further analysis of yaw overshoot angles during open-water zig-zag maneuvers and analysis of yaw-checking capability sensitivity to thruster azimuth angle

These additional results and analyses will be reported in a future revision of this report.

7. References

1) *ARV Performance Specification*, Rev. A, Change 05, 23 July 2023

2) *ARV Pep Appendix 01: ARV Science Mission Requirements*, Rev 3, 2022

3) *Antarctic Research Vessel: Model Test Report (Stage 3A)*, 5E1-098-R101, Rev P1, December, 2022

4) *Bubble Sweep Down Model Test for an Revised ARV – Hull Variant 11*, Report RP-2023-028, HSVA, June, 2023

5) *Calm Water Model Tests for Leidos of a Revised ARV Hullform – Stock Propeller – Hull Variant 11*, Report RP-2023-029, HSVA, May, 2023

6) *3-D Wake Measurement for an Antarctic Research Vessel (ARV)*, Report WM-2023-009, HSVA, June, 2023

7) *Ice Model Tests for Antarctic Research Vessel (ARV) – Addendum 5 Post-PDR Hull Variant Testing*, Report AT-2023-006, HSVA, July, 2023

8) *Model Tests on the Manoeuvring and Course Keeping Performance of the Arctic Research Vessel*, Report MAN-2023-005, HSVA, July, 2023.

9) *ARV_Variant 11_Model Test_Hullform.3dm*, March, 2023

10) *ITTC Quality System Manual: Recommended Procedures and Guidelines: 1978 ITTC Performance Prediction Method*, 7.5-02-03-01.4, ITTC, 2017

11) *Resolution MSC.137(76): Standards for Ship Manoeuverability*, IMO, 2002.

12) *Antarctic Research Vessel (ARV): Icebreaking Performance Report*, 5E1-050-R201, Rev P2, June, 2023

8. Attachment 1 ─ HSVA Bubble Sweepdown Test Report (Reference 4)

HAMBURGISCHE SCHIFFBAU-VERSUCHSANSTALT GMBH

THE HAMBURG SHIP MODEL BASIN

Report RP-2023-028

Bubble Sweep Down Model Test for an revised ARV - Hull Variant 11 -

HSVA Model No. 5626

Customer:
Leidos

HSVA

Document Control Sheet

Customer	**:** Leidos
Project	**:** ARV
Contract No.	**:** 617456
Report No.	**:** RP-2023-028
Report Title	**:** Additional Bubble Sweep Down Model Test for an ARV
File	**:** RP-2023-028_RevA.pdf

Rev. No.	**Date**	**Reason for Issue**	**Prepared by**	**Checked by**	**Approved by**
.	21-Apr-2023	Customer Review	CS	NR	
A	21-June-2023	Final Revision	CS	NR	NR

Summary: On behalf of *Leidos* bubble sweep down model tests were performed for an Antarctic Research Vessel (ARV) with a revised hull variant (Hull Variant 11) at the draught of 9.91 m using a model towing test setup in calm water at the speeds of 4, 6, 8 and 10 kts.

The aim of these tests was to visualize the bubble flow characteristics while these are being transported downwards from the water surface along the stem to below the hull. Special attention was paid to the interaction with the sonar array. Initial tests were conducted before with an initial hull form in 2 test phases documented in HSVA Report RP-2023-009 and RP-2022-086.

Four underwater cameras were taking video footage of dark coloured dye flowing out of various outlets located on the bow.

Conclusions:

(1) Air bubbles in the water near the bow close to the centre line were found to travel downwards along the stem to the forefoot of the keel. Here the flow is deflected sideways, but later transported below the keel by an edge vortex.

(2) The lowest speed (4 kts) showed the highest coverage of marked streamlines on the transversal transducer. Improvements can be indicated until 8 kts as 10 kts tests showed a similar behaviour. The streamline covers about 2/3 of the cross beam transducer area at 4 kts speed while at 8 kts only about 10% are covered.

(3) The longitudinal beam sonar sensor was free from marked streamlines.

(4) The additional, smaller sonar transducers, forward of the longitudinal beam sonar, were free from any air bubble flow.

(5) Comparisons of the initial tests with Mo5601 and Mo5626 showed a reduction of about 50% coverage on the transversal sonar transducer.

Keywords: Bubble Sweep Down, ARV

Report RP-2023-028

Bubble Sweep Down Model Test
for an revised ARV
- Hull Variant 11 -

Leidos
Antarctic Support Contract
11951 Freedom Drive
20190 Reston
USA

HSVA Model No. 5626

Hamburg, June 2023

HAMBURGISCHE SCHIFFBAU-
VERSUCHSANSTALT GmbH

M.Sc. Christian Schröder
- Senior Project Manager -

i.V.
Dipl.-Ing. Nils Reimer
- Division Manager Arctic Technology -

Contents

1.1 Introduction and Description of the Model

On behalf of Leidos bubble sweep down model tests were performed for an Antarctic Research Vessel (ARV) with a revised hull variant (Hull Variant 11) at the draught of 9.91 m using a model towing test setup in calm water at the speeds of 4, 6, 8 and 10 kts.

The aim of these tests was to visualize the bubble flow characteristics while these are being transported downwards from the water surface along the stem to below the hull. Special attention was paid to the interaction with the sonar array. Initial tests were conducted before with an initial hull form in 2 test phases documented in HSVA Report RP-2023-009 and RP-2022-086.

Air bubbles may occur in the water due to

- breaking bow wave
- outgassing in flow regions of lower pressure / higher flow speed
- naturally present in the upper layer close to the water surface (e.g. from breaking wind waves)
- trapped air in e.g. thruster tunnels due to pitch and heave motion of the vessel in waves

Bubbles due to the breaking bow wave and due to breaking wind waves are expected to be present only in the water column between the surface and a depth of approx. 1.5 meter.

The HSVA Model 5626 is built from wood to a scale ratio of 1: 24.384. The principal dimensions of ship and model are as follows:

	Ship	Model
Number	—	5626
Index	—	00010
L_{PP}	108.72 m	4458.7 mm
B_{WL}	24.4 m	1000.7 mm
T_{Design}	9.906 m	406.3 mm
$C_{B,Design}$	0.5094	
∇_{Design} (excl. appendages)	13385,4 m^3	0.923 m^3

In order to stimulate turbulent flow around the model it was equipped with two sand stripes. One 50 mm wide sand stripe is running from the intersection of station 18 with a horizontal line on 11.91 m above base line diagonal to the fore foot. A second 30 mm wide sand strip was fitted vertically aft of frame 19.5.

The hull geometry of the model is displayed in figures F1. 3D view of the models are given by figures F2. For the bubble sweep down tests no propulsion aft arrangement was fitted.

Four underwater cameras with different view angles were taking video footage of dark coloured ink flowing out of various outlets located on the hull in the bow region. The markings of the sonar array were provided by the customer and are shown in figure F3. A sketch of the underwater camera rig is depicted in figure F4.

Based on previously performed CFD calculations, fixed positions for ink outlets were installed. The positions of the outlets are given in the following table:

Outlet No	X [mm] aft of FP	Y [mm] port of CL	Z [mm] below WL	Comment
1	0	0	0	
2	1570	0	580	
3	3150	0	1150	
4	3690	0	1350	

The designated number for each outlet is shown in figure F5. Numbering increases in the direction from bow to stern and centre line to port.
The following two figures show the locations marked in extracts of the hull lines.

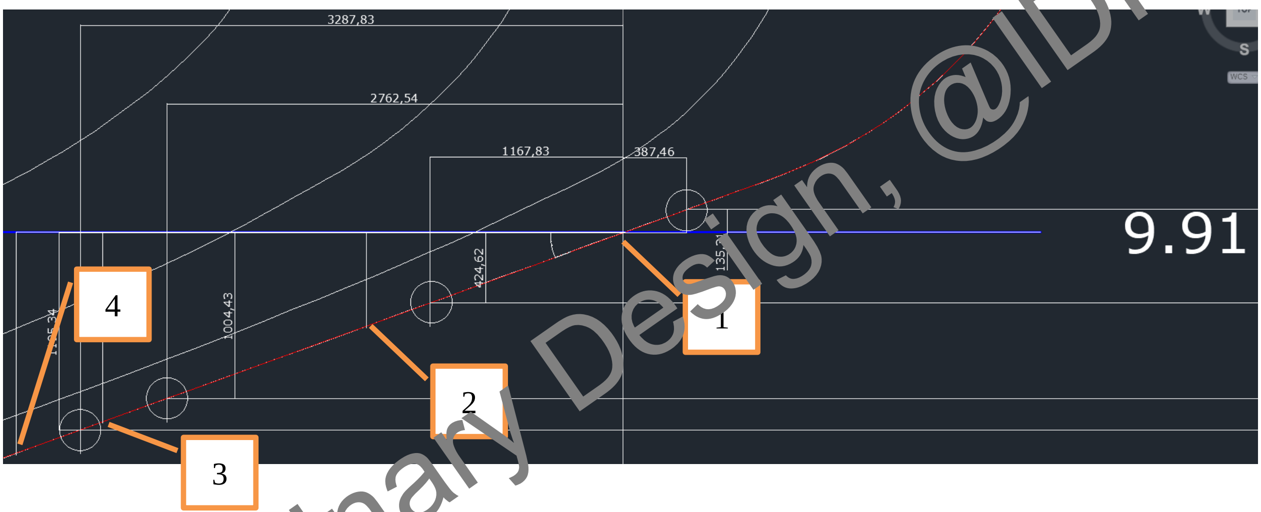

1.2 Test Methodology

Tests were carried out in HSVA's large towing tank with a usable test length of approximately 200 m. The model was towed underneath the test carriage and was free to trim and heave. A biodegradable dye was used as ink. Each outlet on the hull could be opened individually.

The following tests were carried out on 14th of April 2023:

Test No.	Draught	Trim	Outlets	Speeds	Outlet Distance hull
m03	9.906 m	Even keel	1-4 / all together	6 kts	10 mm
m04	9.906 m	Even keel	1-4 / all together	8 kts	10 mm
m05	9.906 m	Even keel	1-4 / all together	4 kts	10 mm
m06	9.906 m	Even keel	1-4 / all together	10 kts	10 mm
M07	9.906 m	Trimmed 1° to the bow	1-4 / all together	8 kts	10 mm

Each listed test runs was recorded on video and provided to the customer in digital MP4 format (codec: H.264 MPEG-4 AVC, resolution: 1920x1080 pixels, frame rate: 30 fps).

1.3 Test Results

Video snapshots of the first test run (m03) on even keel and at the speed of 4.0 kts are shown in figures F6; F7; F8 and F9, each opened outlet separately with an outlet distance of 10mm to the model hull. Please note, that judging the flow of the dye is far easier from watching the video than from the snapshots.
The air bubbles, following the flow from outlet 1, travel down the stem and pass outlet 2/3 which are located on the same streamline. The flow stays above and aside the box keel until approximately frame 16 where the keel edge vortex takes the flow below and right across the sensor area of the cross beam sonar (frame #12.3), see page F6, F7. The data from the tests with opened outlets 2/3 and 4 give a very similar impression to the opened outlet 1 as they are located downstream on approximately the same/ close flowline. About 50% of the area of the transversal transducers is covered by the coloured streamlines.
Video snapshots of the second test run (m04) on even keel and at the speed of 6.0 kts are shown in figures F10; F11; F12 and F13. The flow stays above and aside the box keel until approximately frame 15.5 where the keel edge vortex takes the flow below and right across the sensor area of the cross beam sonar (frame #12.3), see page F10, F11. The data from the tests with opened outlets 2/3 and 4 give a very similar impression. About 25% of the area of the transversal transducers is covered by the coloured streamlines.
Video snapshots of the third test run (m05) on even keel and at the speed of 8.0 kts are shown in figures F14; F15; F16 and F17. The flow stays above and aside the box keel until approximately frame 15 where the keel edge vortex takes the flow below and right across the sensor area of the cross beam sonar (frame #12.3), see page F14, F15. The data from the tests with opened outlets 2/3 and 4 give a very similar impression. About 10% of the area of the transversal transducers is covered by the coloured streamlines.

Video snapshots of the fourth test run (m03) on even keel and at the speed of 10.0 kts are shown in figures F18; F19; F20 and F21. The figures show, that no significant changes can be noted compared to the 8kts tests. The flow stays above and aside the box keel until approximately frame 14.5 where the keel edge vortex takes the flow below and right across the sensor area of the cross beam sonar (frame #12.3), see page F18, F19. The data from the tests with opened outlets 2/3 and 4 give a very similar impression. About 10% of the area of the transversal transducers is covered by the coloured streamlines.
Video snapshots of the last test run (m03) trimmed 1° to the bow and at the speed of 8.0 kts are shown in figures F22; F23; F24 and F25. The figures shows, that no significant changes can be noted compared to the even keel condition.

1.4 Comparison to Initial ARV Bubble Sweep Down Tests

The actual tests presented in this report are compared to the previous bubble sweep down tests in January with the initial tested hull form (Mo5602). Below the conditions wich are tested during both test campaigns (6/ 8 kts) are compared directly. Exemplary opening 2 is choses as the results of both tests showed very comparable conditions for opening 1-3. The figures below clearly show an improvement in between the tests of hull form Mo5601 and Mo5626. The covered are of the marked streamlines on the transversal transducers are reduced by about 50% judged by the team of HSVA based in the videos and snapshots.

……………………….6kts………………………. ……….…..8kts…………………….

Mo 5602 Mo 5626 Mo 5602 Mo 5626

1.5 Conclusions

The following conclusions can be drawn from the bubble sweep down mode tests:

(1) Air bubbles in the water near the bow close to the centre line were found to travel downwards along the stem to the forefoot of the keel. Here the flow is deflected sideways, but later transported below the keel by an edge vortex.

(2) The lowest speed (4 kts) showed the highest coverage of marked streamlines on the transversal transducer. Improvements can be indicated until 8 kts as 10 kts tests showed a similar behaviour. The streamline covers about 2/3 of the cross beam transducer area at 4 kts speed while at 8 kts only about 10% are covered.

(3) The longitudinal beam sonar sensor was free from marked streamlines.

(4) The additional, smaller sonar transducers, forward of the longitudinal beam sonar, were free from any air bubble flow.

(5) Comparisons of the initial tests with Mo5601 and Mo5626 showed a reduction of about 50% coverage on the transversal sonar transducer.

(6) Compared to research ships designed for a similar operational profiles the bubble sweep down test observation of the ARV (Hull Variant 11) is showing less potential sonar areas covered with flowlines orientating from the bow centre-line origin.

2.1 Hull Form Characteristics - HSVA Modell 5626-00000

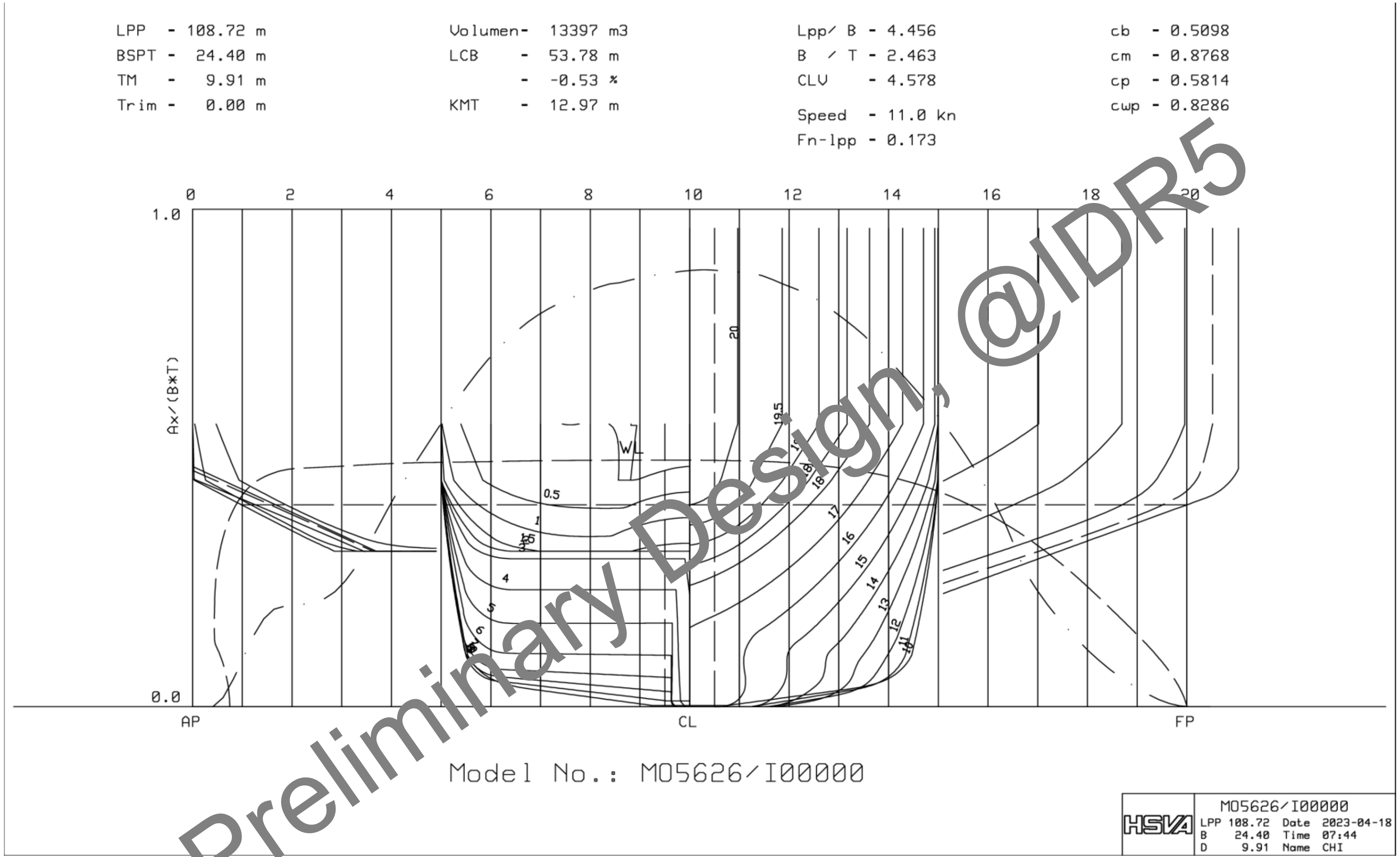

2.2 3D View of the Fore Body – HSVA Modell 5626-00000

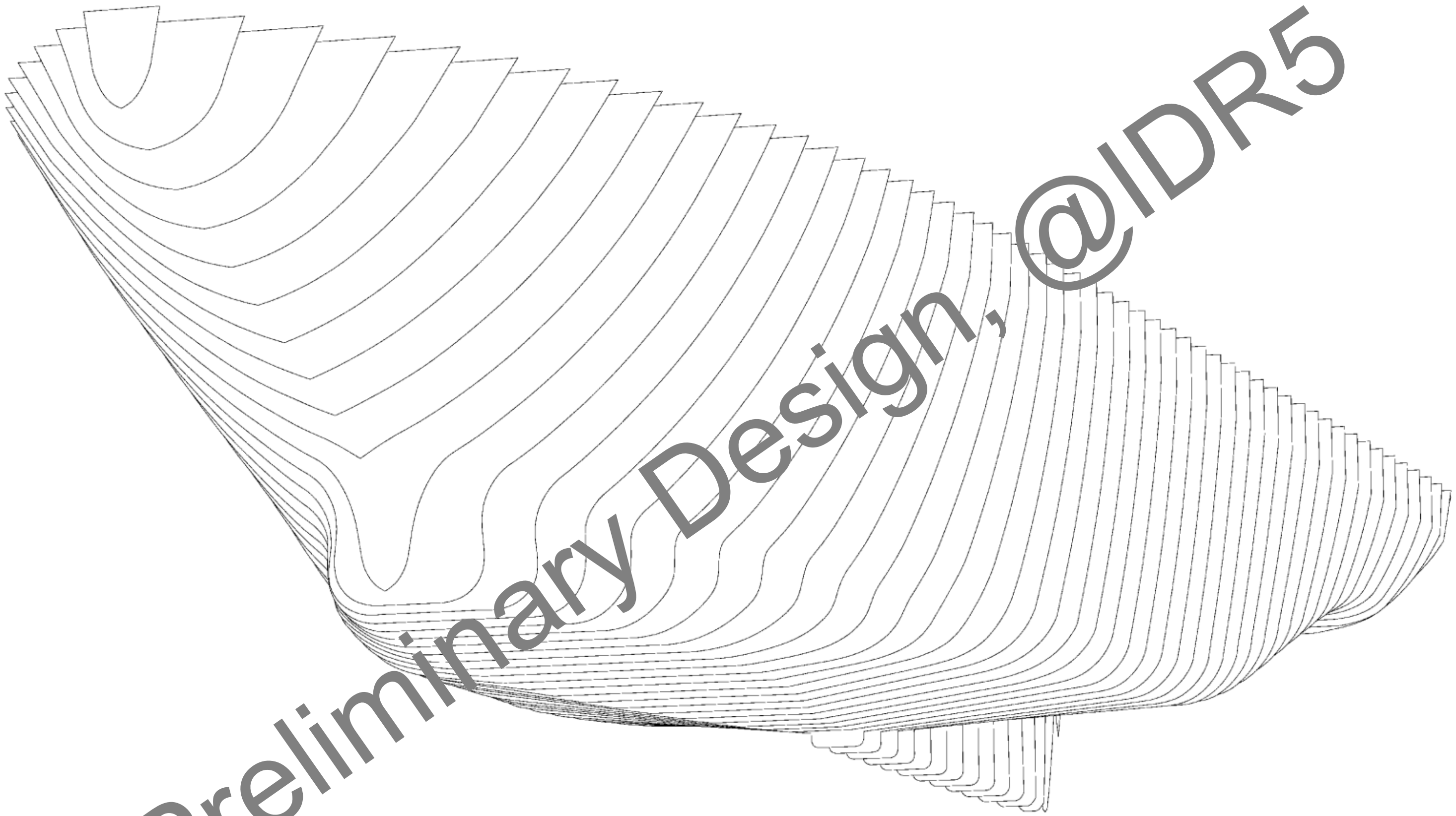

2.3 Markings on the Box Keel – HSVA Modell 5601-00010

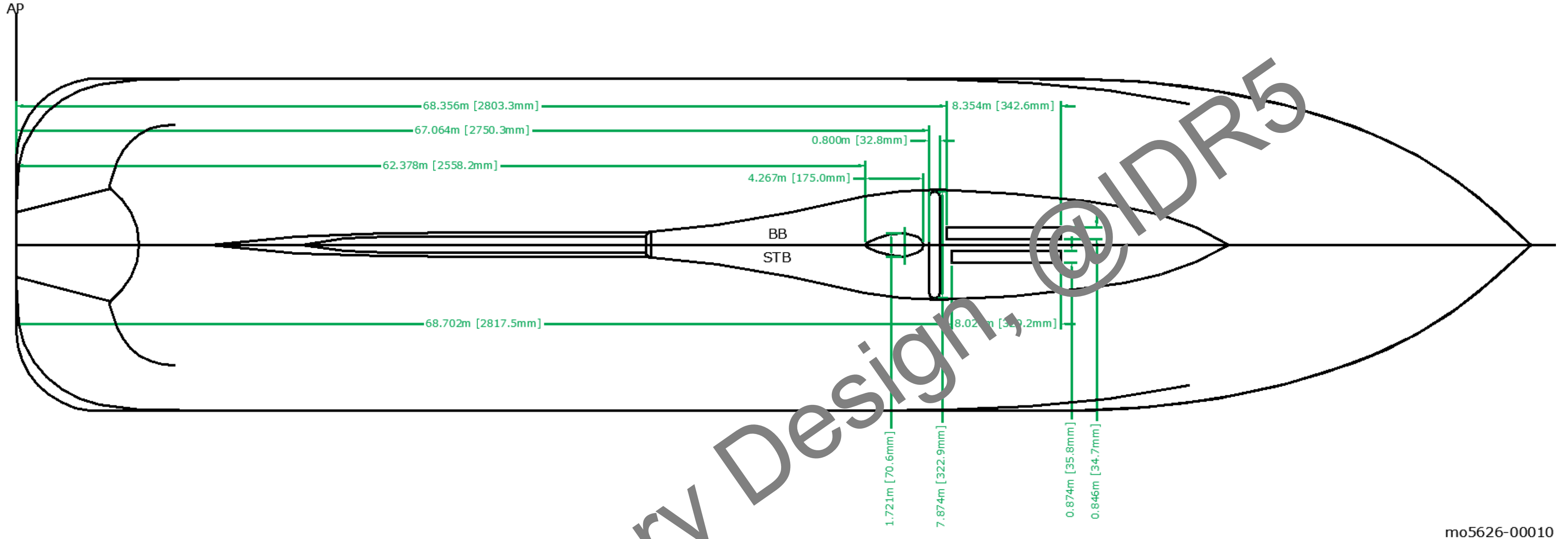

2.4 Underwater Camera Rig (Example)

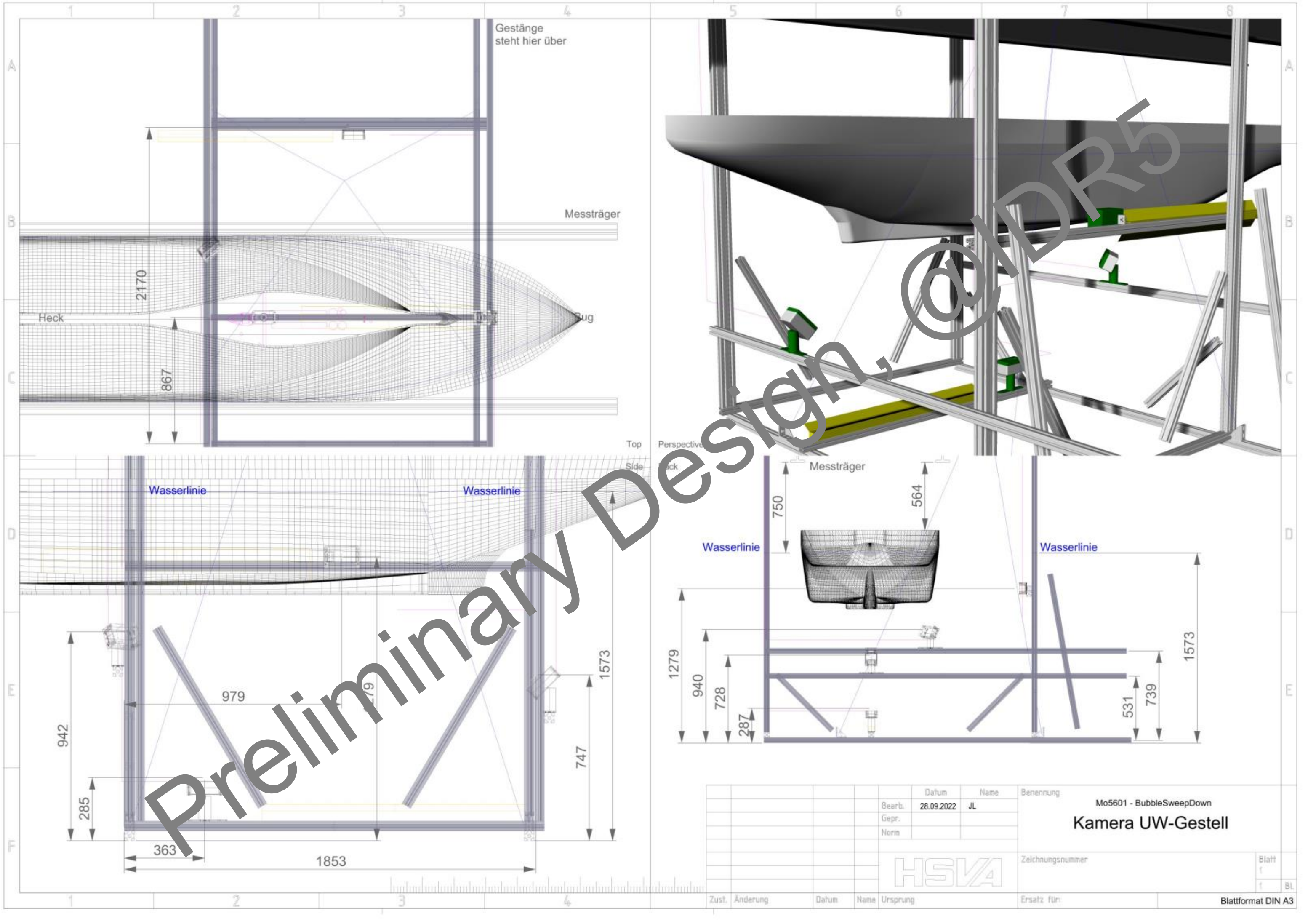

2.5 Camera Angles and Outlet Numbering – HSVA Modell 5626-00010

2.6 Video Snapshot, Even Keel, 4.0 kts, Outlet 1

2.7 Video Snapshot, Even Keel, 4.0 kts, Outlet 2

2.8 Video Snapshot, Even Keel, 4.0 kts, Outlet 3

2.9 Video Snapshot, Even Keel, 4.0 kts, Outlet 4

2.10 Video Snapshot, Even Keel, 6.0 kts, Outlet 1

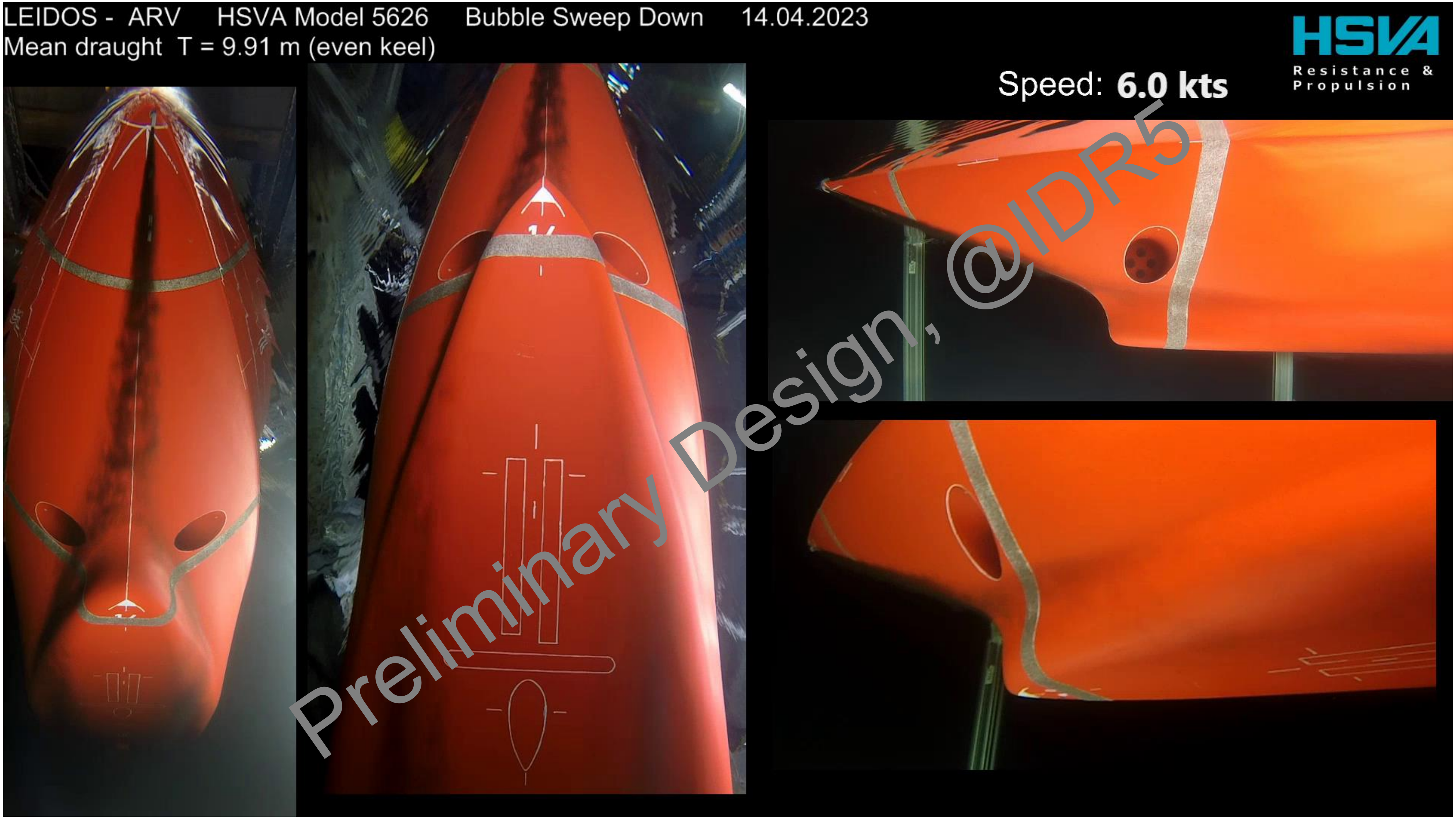

2.11 Video Snapshot, Even Keel, 6.0 kts, Outlet 2

2.12 Video Snapshot, Even Keel, 6.0 kts, Outlet 3

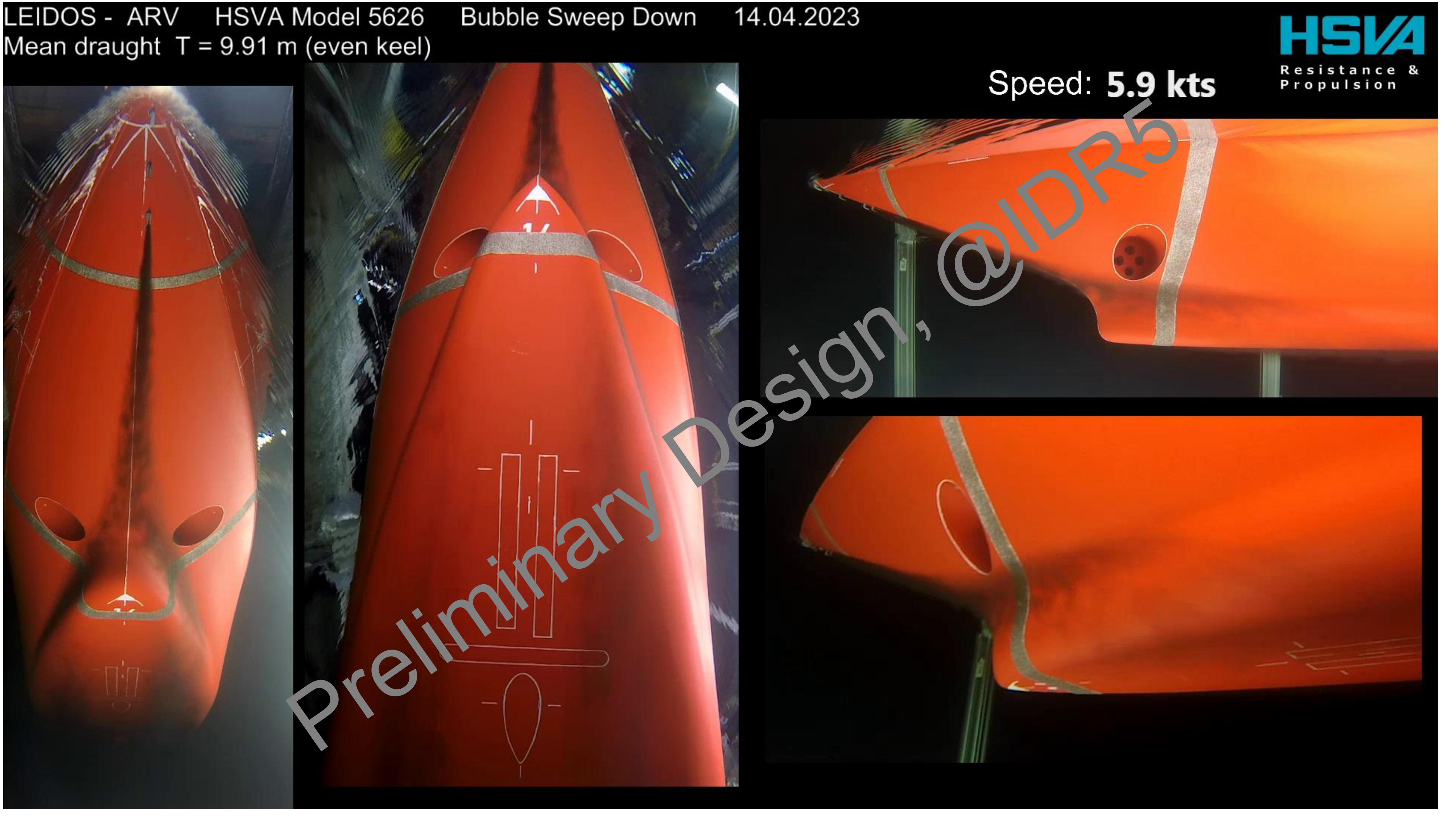

2.13 Video Snapshot, Even Keel, 6.0 kts, Outlet 4

2.14 Video Snapshot, Even Keel, 8.0 kts, Outlet 1

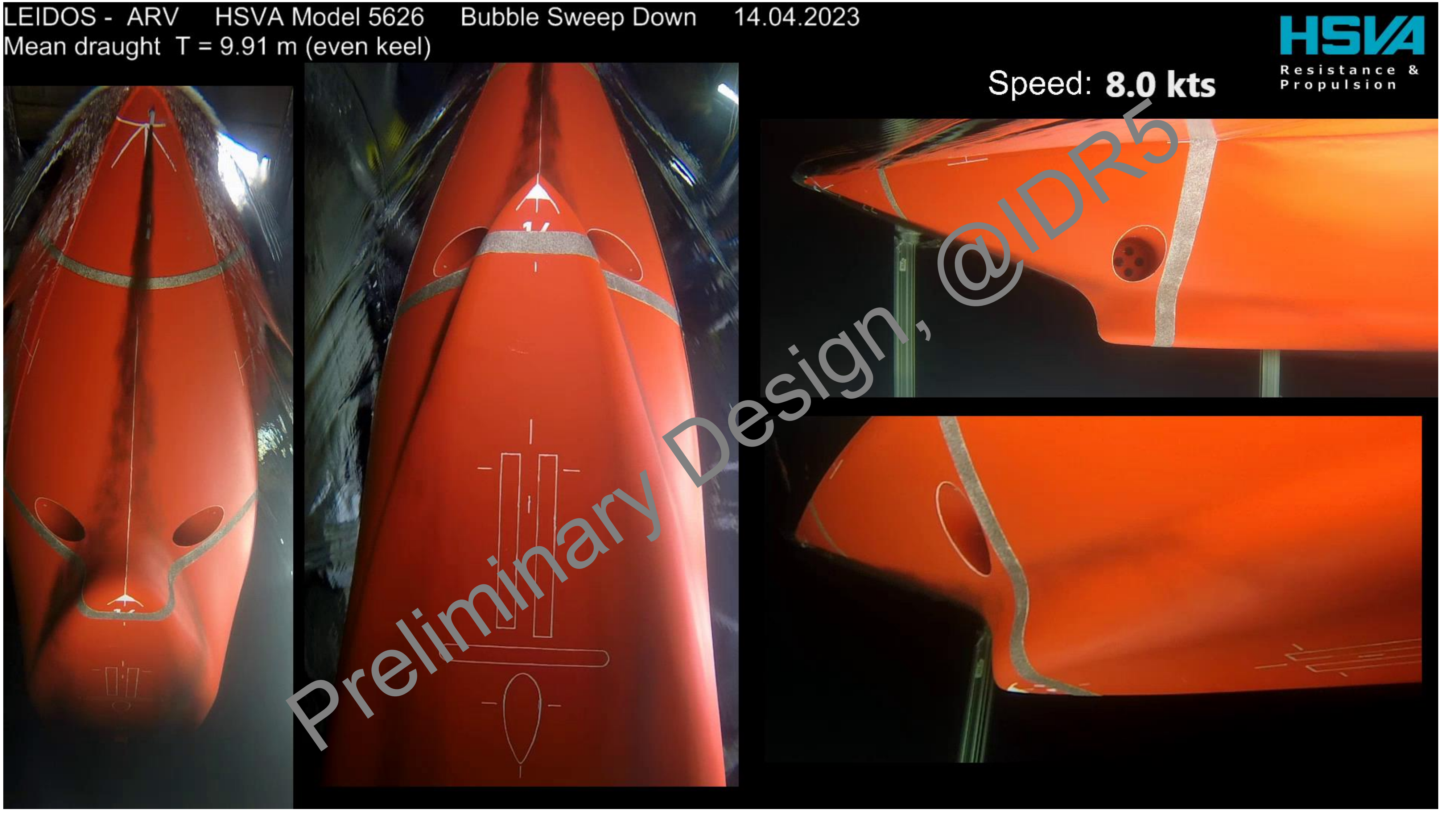

2.15 Video Snapshot, Even Keel, 8.0 kts, Outlet 2

2.16 Video Snapshot, Even Keel, 8.0 kts, Outlet 3

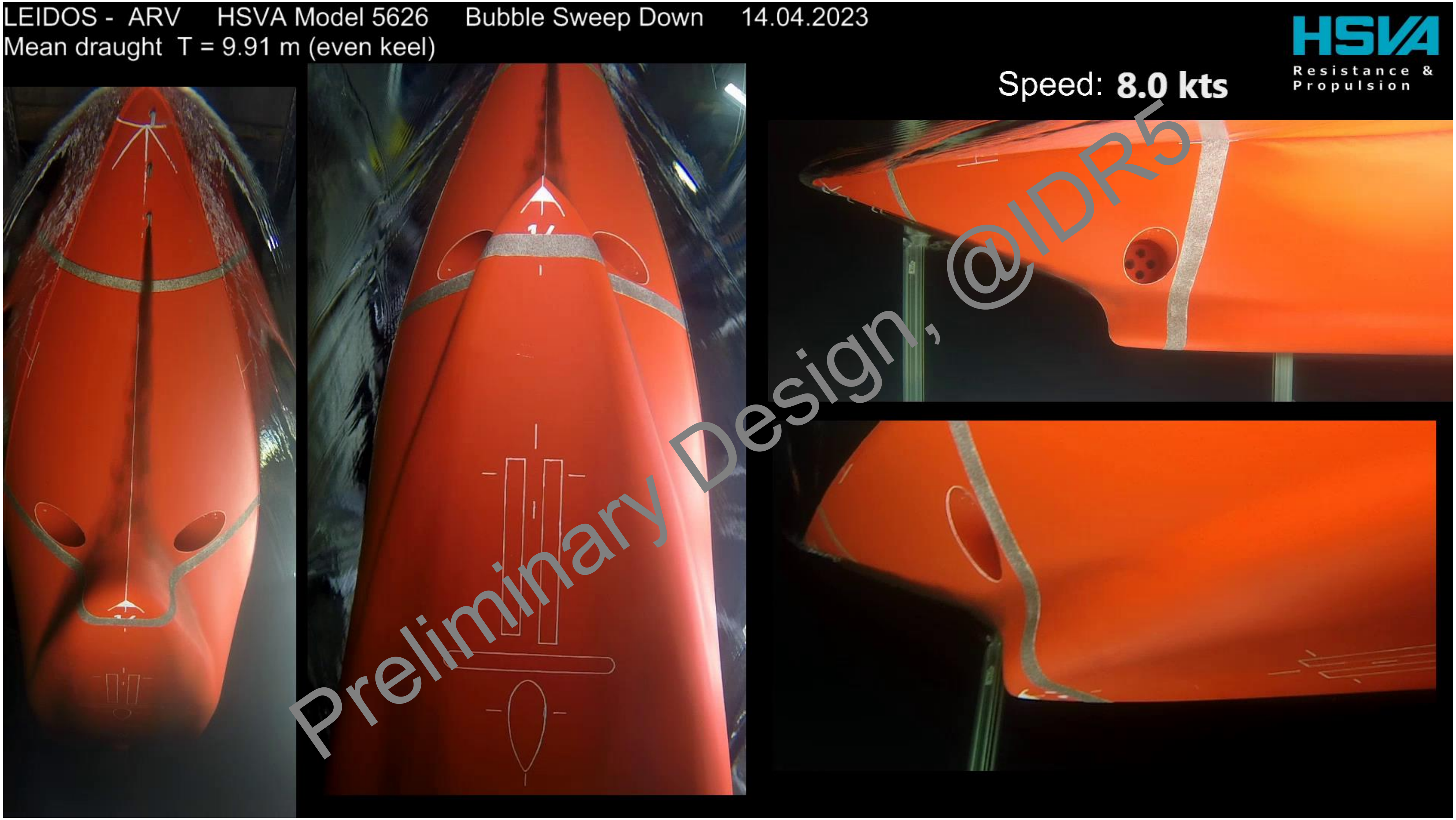

2.17 Video Snapshot, Even Keel, 8.0 kts, Outlet 4

2.18 Video Snapshot, Even Keel, 10 kts, Outlet 1

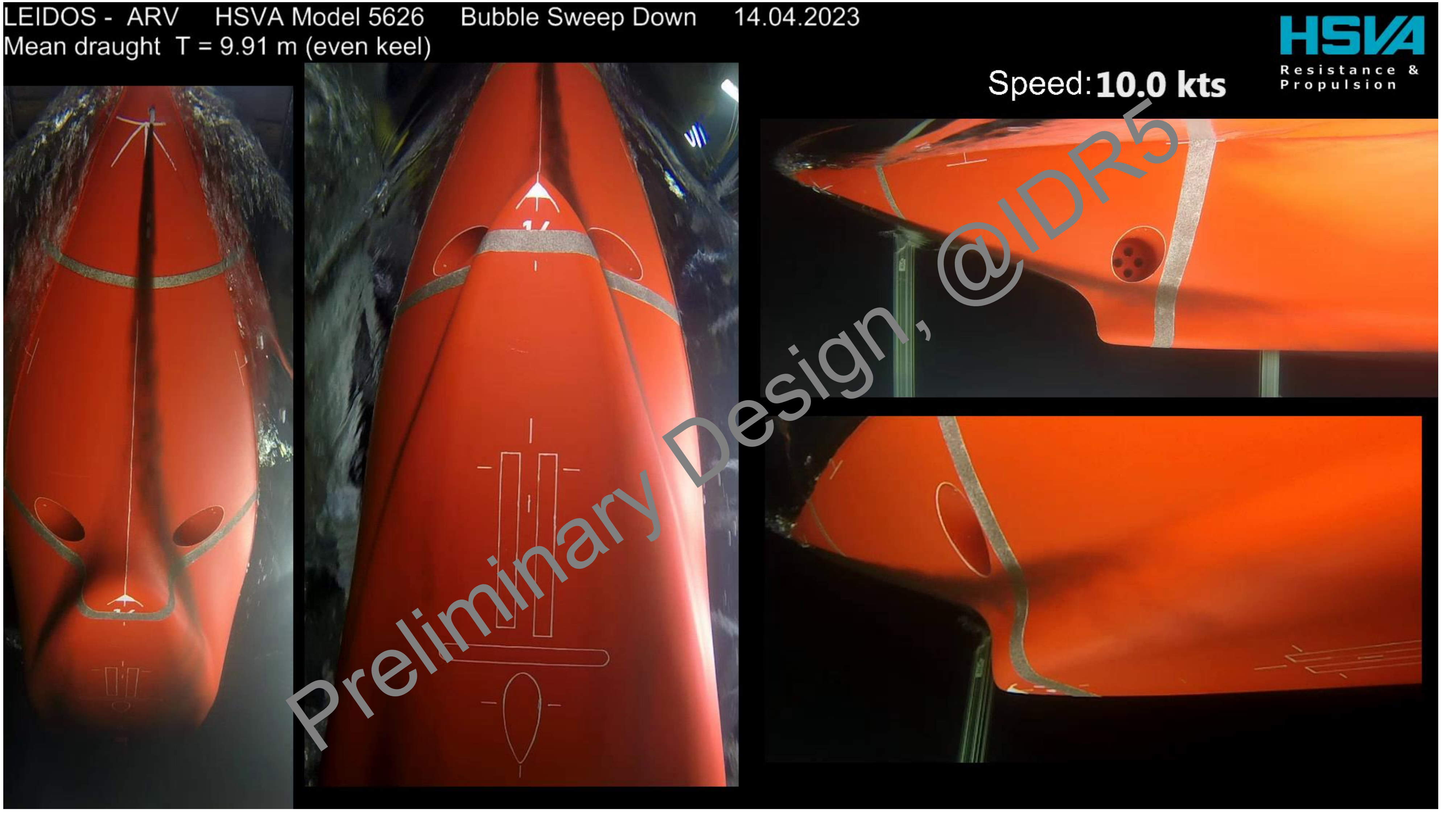

2.19 Video Snapshot, Even Keel, 10 kts, Outlet 2

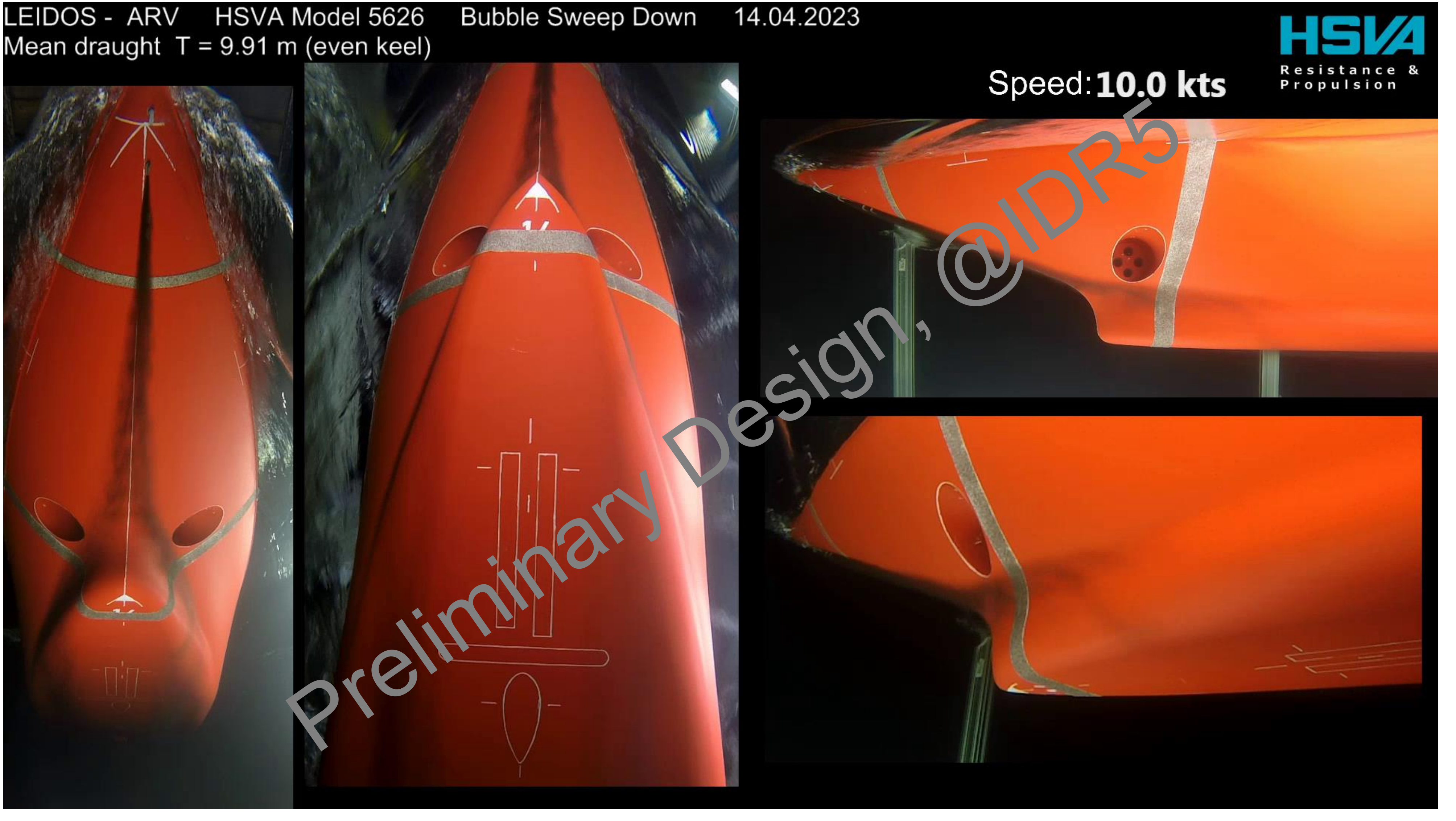

2.20 Video Snapshot, Even Keel, 10 kts, Outlet 3

2.21 Video Snapshot, Even Keel, 10 kts, Outlet 4

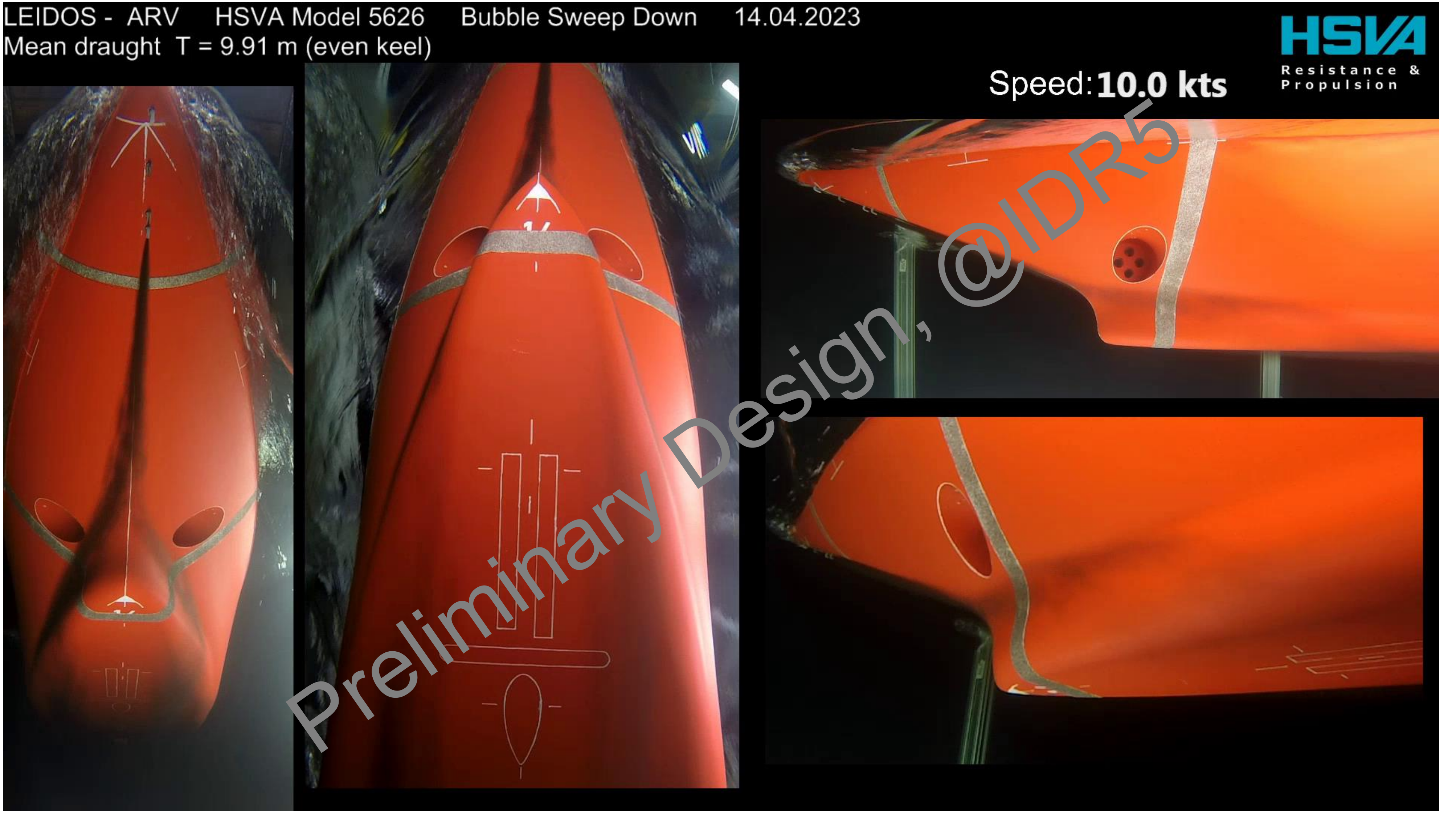

2.22 Video Snapshot, 1° trim to bow, 8 kts, Outlet 1

2.23 Video Snapshot, 1° trim to bow, 8 kts, Outlet 2

2.24 Video Snapshot, 1° trim to bow, 8 kts, Outlet 3

2.25 Video Snapshot, 1° trim to bow, 8 kts, Outlet 4

9. Attachment 2 ─ HSVA Resistance and Propulsion Test Report (Reference 5)

HAMBURGISCHE SCHIFFBAU-VERSUCHSANSTALT GMBH

THE HAMBURG SHIP MODEL BASIN

Report RP-2023-029

Calm Water Model Tests for Leidos of a Revised ARV Hullform

- Stock Propeller -
- Hull Variant 11 -

HSVA Model No. 5626

Customer:
Leidos

HSVA

Document Control Sheet

Customer	**:** Leidos
Project	**:** Model Tests for an ARV
Contract No.	**:** 617456
Report No.	**:** RP-2023-029
Report Title	**:** Calm Water Model Tests for Leidos of a revised ARV Hullform - Stock Propeller - Hull Varinat 11 -
File	**:** RP-2023-029.pdf

Rev. No.	Date	Reason for Issue	Prepared by	Checked by	Approved by
.	12-May-2023	Final report	CS	SBR	NR
.					

Summary:

On behalf of *Leidos* calm water model tests were performed for a revised Antarctic Research Vessel (ARV). The actual tested hullform is hull variant 11. The vessel´s propulsion system consists of two azipod units in pulling condition (HSVA no. 222/223-5500) with controllable pitch propeller (HSVA no. 2288/2289).
This report presents the results of self-propulsion and resistance tests performed at one draught with the model equipped with all appendages on a speed range from 6 knots to 15 knots. Furthermore the influence of the condition with closed bow thruster tunnel was tested from 6 knots to 15 knots. The results of the 3D-wake measurement at the location of the propeller plane are documented in the separate HSVA report WM-2023-009.

Conclusions:

(1) The wave pattern of the vessel showed a typical picture. From 12 knots and higher speeds a breaking bow wave can be observed. Starting at 13.5 knots a pronounced bow wave and stern wave system can be seen. This is probably forced by the hull shape optimised for ice breaking.

(2) At the 9.906 m draught a delivered power of 2298 kW is predicted at a ship speed of 11 knots for the trial condition without head wind (force Bft. 0) based on the used high class ice propeller. The recalculation for the previous used stock propellers for the same conditions results in a required power of 2016 kW.

(3) At the 9.906 m draught a delivered power of 2642 kW is predicted at a ship speed of 11 knots for the service condition with 15 % added on PD and without head wind (force Bft. 0) based on the used high class ice propeller. The recalculation for the previous used stock propellers for the same conditions results in a required power of 2318 kW.

(4) The difference in the effective power between the condition with bow thruster tunnel open and closed is in average over the whole speed range about 3 %.

Keywords: Self-propulsion test, Resistance test

Report RP-2023-029

Calm Water Model Tests for Leidos of a Revised ARV Hullform

- Stock Propeller -
- Hull Variant 11 -

Leidos
Antarctic Support Contract
11951 Freedom Drive
20190 Reston
USA

HSVA Model No. 5626

Hamburg, May 2023

HAMBURGISCHE SCHIFFBAU-VERSUCHSANSTALT GmbH

i.A. Christian Schröder
- Senior Project Manager -

i.V. Nils Reimer
- Division Manager Arctic Technology -

Contents

1.1 Introduction and Description of the Model

On behalf of *Leidos* calm water model tests were performed for a revised Antarctic Research Vessel (ARV). The actual tested hullform is hull variant 11. The vessel´s propulsion system consists of two azipod units in pulling condition (HSVA no. 222/223-4400) with controllable pitch propeller (HSVA no. 2288/2289).
This report presents the results of self-propulsion and resistance tests performed at one draught with the model equipped with all appendages on a speed range from 6 knots to 15 knots. Furthermore the influence of the condition with closed bow thruster tunnel was tested from 6 knots to 15 knots. The results of the 3D-wake measurement at the location of the propeller plane are documented in the separate HSVA report WM-2023-009.

The HSVA model 5626 is built from wood to a scale ratio of 1:24.384. The principal dimensions ofthe ship and model are as follows:

	Ship		Model
Number	—		5626
Index	—		00000
L_{PP}	108.72 m		4458.7 mm
B_{WL}	24.40 m		1000.7 mm
$T_{Design\ Draught}$	9.91 m		406.3 mm
$C_{B,Design\ Draught}$		0.5094	
$\nabla_{Design\ Draught}$ (excl. appendages)	13385 m^3		0.9232 m^3

In order to stimulate turbulent flow around the model it was equipped with two sand stripes. One50 mm wide sand stripe is running from the intersection of station 18 with a horizontal line on11.91 m above base line diagonal to the fore foot. A second 30 mm wide sand strip was fitted vertically aft of frame 19.5. These are not shown on the model pictures as these were done during ice model tests.
A photo grid with 41 mm spacing (corresponding to 1 m in full scale) is applied at the 9.906 m design waterline for judging the wave system generated by the vessel.
The hull geometry of the model is displayed in figures F1. 3D views of the models are given by figures F2 and F3. The pod-propeller arrangement is shown on figure F4. Photographs of the model are given on pages P5 through P6.

For the self-propulsion tests the stock propeller HSVA nos. 2288/2289 on POD nos. 222/223-5500 were used. The open water characteristics of the propulsion system are shown in diagram D4 and table T23. The propellers have the following principal particulars:

	Ship	**Model**
Propeller No.	—	2288 / 2289
Diameter	4.877 m	200 mm
Hub diameter ratio	0.381	
Mean pitch ratio	0.985	
Disk area ratio	0.553	
Material	—	Brass
Sense of rotation	Right	
Number of blades	4	
Type	Controllable pitch	

For the previous self-propulsion tests the stock propeller HSVA nos. 2621/2622 on POD nos. 222/223-4400 were used. This open water characteristics of the propulsion system are shown in diagram D5 and table T24. The results of this test campaign are recalculated for the previous used stock propellers to gain a good comparison of the two hull variants.

The propeller plane was located 597.2 mm [14.563 m in full scale] in front of the aft perpendicular. The propeller shaft was inclined by 4°. The POD azimuth axis is located 450.2 mm [10.977 m in full scale] in front of the aft perpendicular and orthogonal towards the base line. The PODs are mounted 225.0 mm [5.486 m in full scale] to each side. The propeller turning direction was set to turning inside over the top when going ahead. The arrangement drawing can be seen on page F4.

1.2 Test Program

The following tests were carried out in HSVA's large towing tank in week 16 / 2023:

Test No.	Draught	Kind of Test	Speeds	Remark
23-0252	9.91 m	Resistance	6.0 – 15.0 kts	bow thrutser tunnel closed
23-0253	9.91 m	Resistance	6.0 – 15.0 kts	bow thrutser tunnel open
23-0254	9.91 m	Self propulsion	6.0 – 15.0 kts	bow thrutser tunnel open
23-245	9.91 m	3D- Wake	9 kts	bow thrutser tunnel open
9373/9374	---	Propeller Open Water Test	---	System test of pod and propeller

1.3 Test Analysis

The test results were analysed according to the HSVA Standard Correlation Method which is described in Appendix A. The resistance coefficient was calculated using HSVA's method with the following correlation allowance:

$$C_A = 0.189E\text{-}3$$

For comparison reasons and consistency with other projects a virtual length of L_{PP} = 97.727 m was taken as input for the calculation of C_A. That length reflects the distance between perpendiculars if the aft perpendicular is placed in the rudder shaft / azimuth turning centre.
The resistance of the appendages and openings such as bilge keels, bow thruster tunnels etc., which are not fitted on the model, is considered theoretically by adding an additional frictional resistance component for the trial and service predictions (see DRT-Values in the footnotes of the data tables). In this case all relevant appendages were fitted on the model during the tests, thus DRT-value is set to 0

1.4 Test Results

The tables T1 to T9 summarise the model test results as well as the trial and service predictions for wind from ahead of Bft. 0. For the service predictions a sea margin of 15 % on P_D is taken into account. The information is additionally visualised in diagrams D1 and D2 (trial and service condition) in which the delivered power is plotted in function of both ship speed and propeller revolutions. These diagrams show as well the recalculated results for the previous used stock propellers which are also shown in tables T10 to T18. In these diagrams, the power demand at a ship speeds of 11 knots is marked For trial and service condition the following power demands are predicted at a ship speed of 11 knots:

M5626-00020 with stock propeller HSVA nos. 2288/2289 on POD nos. 222/223 5500

Draught	**Trial Condition** **Head wind Bft. 0** v_S **= 11 kts**	**Service Condition (15 % sea margin)** **Head wind Bft. 0** v_S **= 11 kts**
T = 9.906 m	P_D = 2298 kW	P_D = 2642 kW

M5626-00020 with stock propeller HSVA nos. 2288/2289 on POD nos. 222/223 5500
recalculated to propeller HSVA nos. 2621/2622 on POD nos. 222/223 4400

Draught	**Trial Condition** **Head wind Bft. 0** v_S **= 11 kts**	**Service Condition (15 % sea margin)** **Head wind Bft. 0** v_S **= 11 kts**
T = 9.906 m	P_D = 2016 kW	P_D = 2318 kW

The wave patterns generated by the model are visualised on pages P1 through P4.
The difference in the effective power between the condition with bow thruster tunnel open and closed is about 3 % in average over the whole speed range and is displayed in diagram D3.

1.5 Conclusions

2 The following conclusions can be drawn from the model tests conducted:

(1) The wave pattern of the vessel showed a typical picture. From 12 knots and higher speeds a breaking bow wave can be observed. Starting at 13.5 knots a pronounced bow wave and stern wave system can be seen. This is probably forced by the hull shape optimised for ice breaking.

(2) At the 9.906 m draught a delivered power of 2298 kW is predicted at a ship speed of 11 knots for the trial condition without head wind (force Bft. 0) based on the used high class ice propeller. The recalculation for the previous used stock propellers for the same conditions results in a required power of 2016 kW.

(3) At the 9.906 m draught a delivered power of 2642 kW is predicted at a ship speed of 11 knots for the service condition with 15 % added on PD and without head wind (force Bft. 0) based on the used high class ice propeller. The recalculation for the previous used stock propellers for the same conditions results in a required power of 2318 kW.

(4) The difference in the effective power between the condition with bow thruster tunnel open and closed is in average over the whole speed range about 3 %.

2.1 Trial Prediction - Headwind Bft. 0

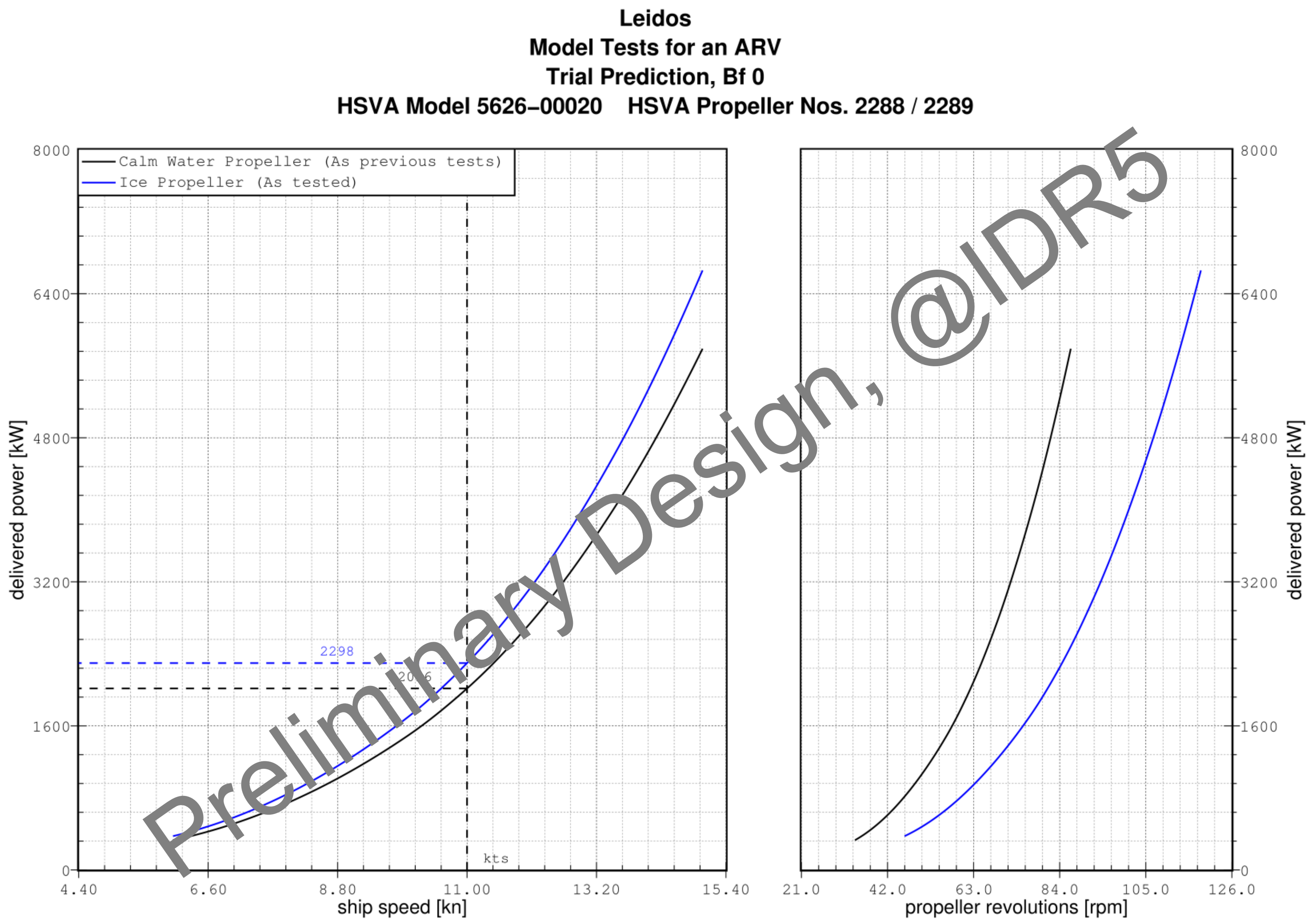

2.2 Service Prediction - 15% Sea Margin on PD, Headwind Bft 0

Leidos
Model Tests for an ARV
Service, 15% PD, Bf 0
HSVA Model 5626–00020 HSVA Propeller Nos. 2288 / 2289

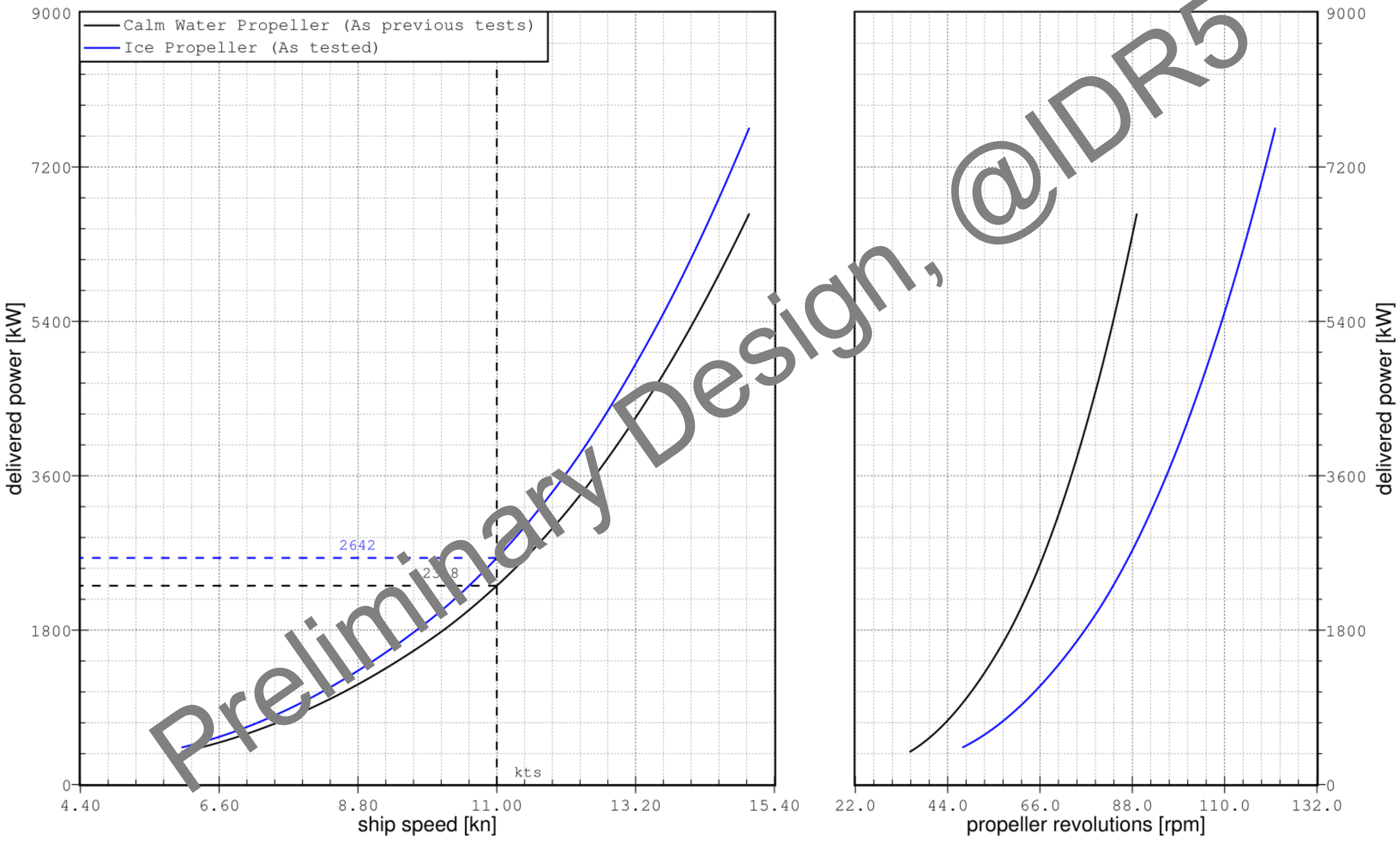

2.3 Resistance Comparison - Bow Thurster Tunnel Impact

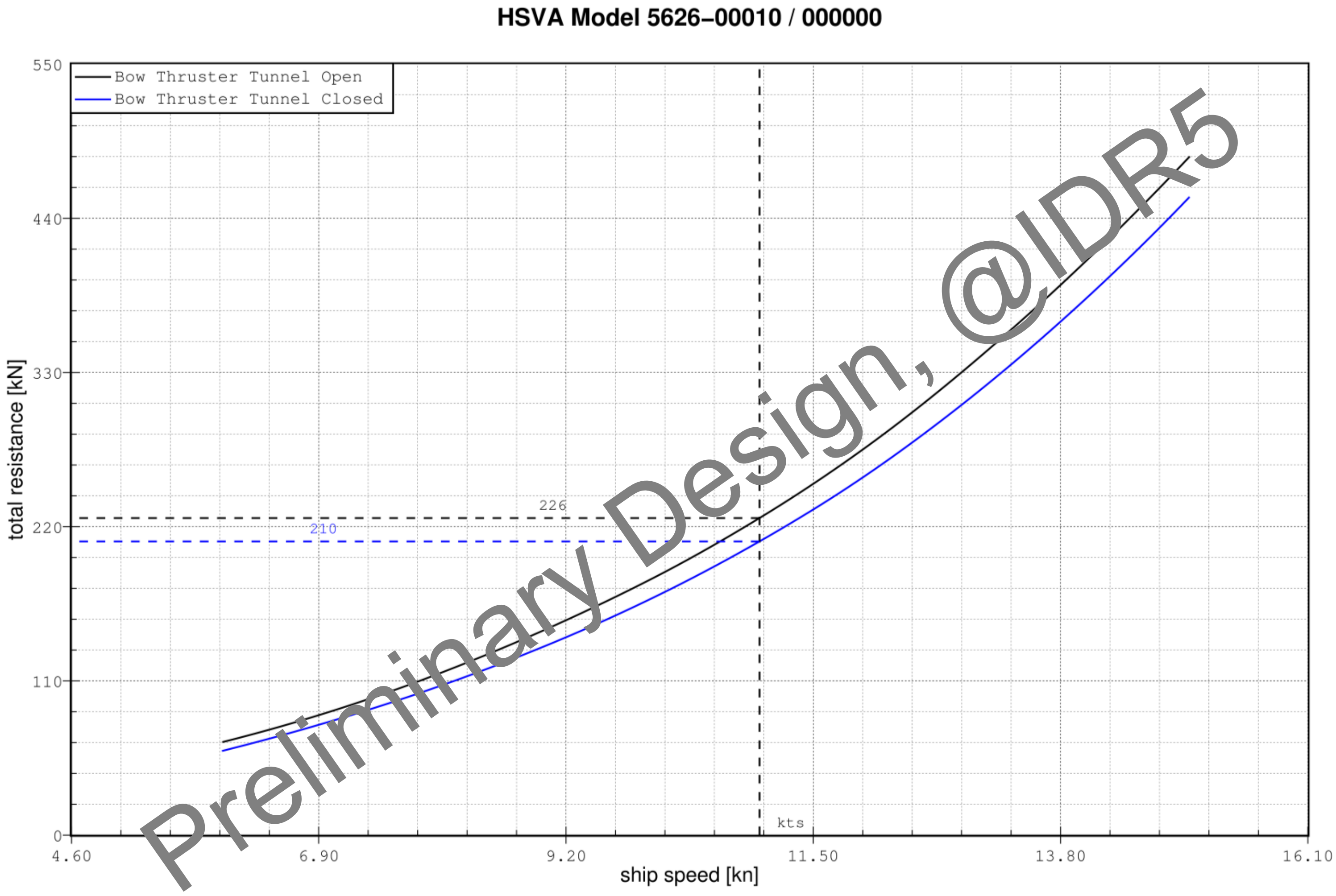

2.4 System Open Water Characteristic of Propeller 2288/89 and Pod 222/223

Open Water Test Result

Customer:		Leidos	Model Propeller No.:		2288/2289
Test No.:		9373/9374	Ship Model No.:		5626
Test Date:		18.04.2023	Diameter	D =	200.00 mm
Reynolds No.	$Rn_{0.7R}$ =	8.64E+05	Hub Diameter	d_H =	76.20 mm
Water Temperature		15.30 °C	Pitch-Dia.-Ratio	P_m/D =	0.985
No. of Prop. Rev.		24.99 1/s	Blade Area Ratio	A_E/A_0 =	0.553
Model Scale		24.384	No. of Blades	Z =	4

STR1315

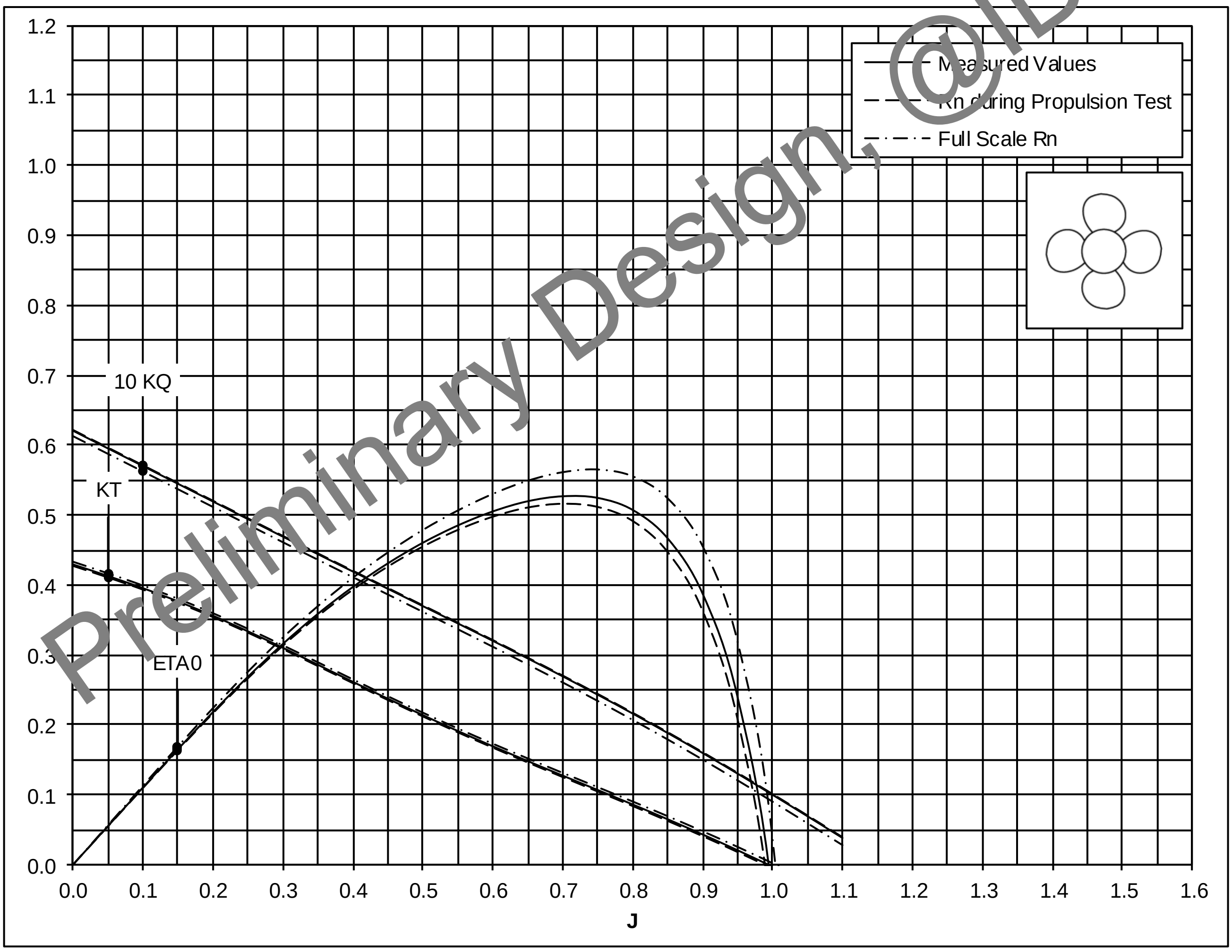

2.5 System Open Water Characteristic of Propeller 2621/22 and Pod 222/223

Open Water Test Result

Customer:		Leidos	Model Propeller No.:		2621/2622
Test No.:		9184/9183	Ship Model No.:		5626
Test Date:		10.10.2022	Diameter	D =	228.98 mm
Reynolds No.	$Rn_{0.7R}$ =	9.05E+05	Hub Diameter	d_H =	56.48 mm
Water Temperature		19.60 °C	Pitch-Dia.-Ratio	P_m/D =	1.012
No. of Prop. Rev.		17.00 1/s	Blade Area Ratio	A_E/A_0 =	0.686
Model Scale		24.384	No. of Blades	Z =	4

STR1290

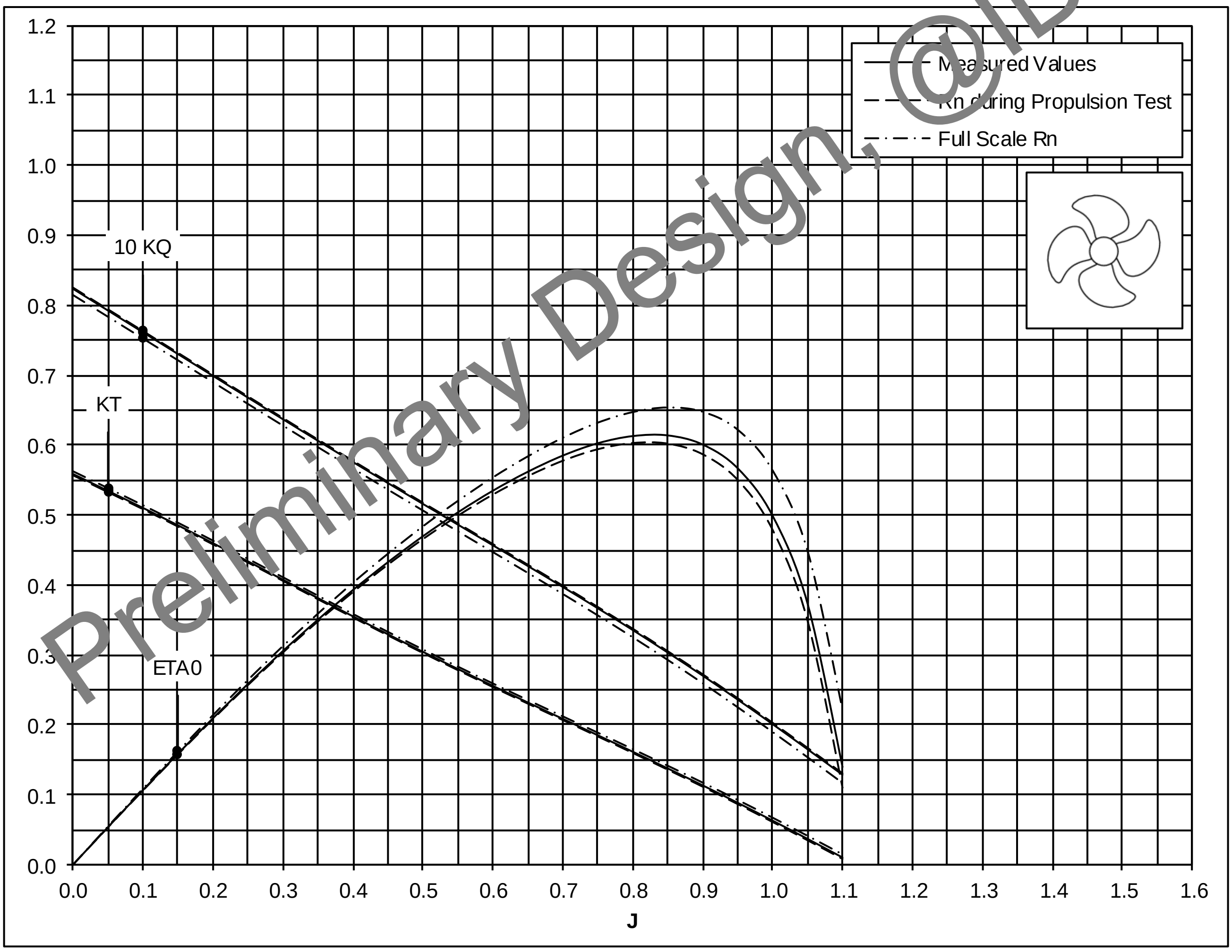

3.1 Hull Form Characteristics - HSVA Model 5626-00000

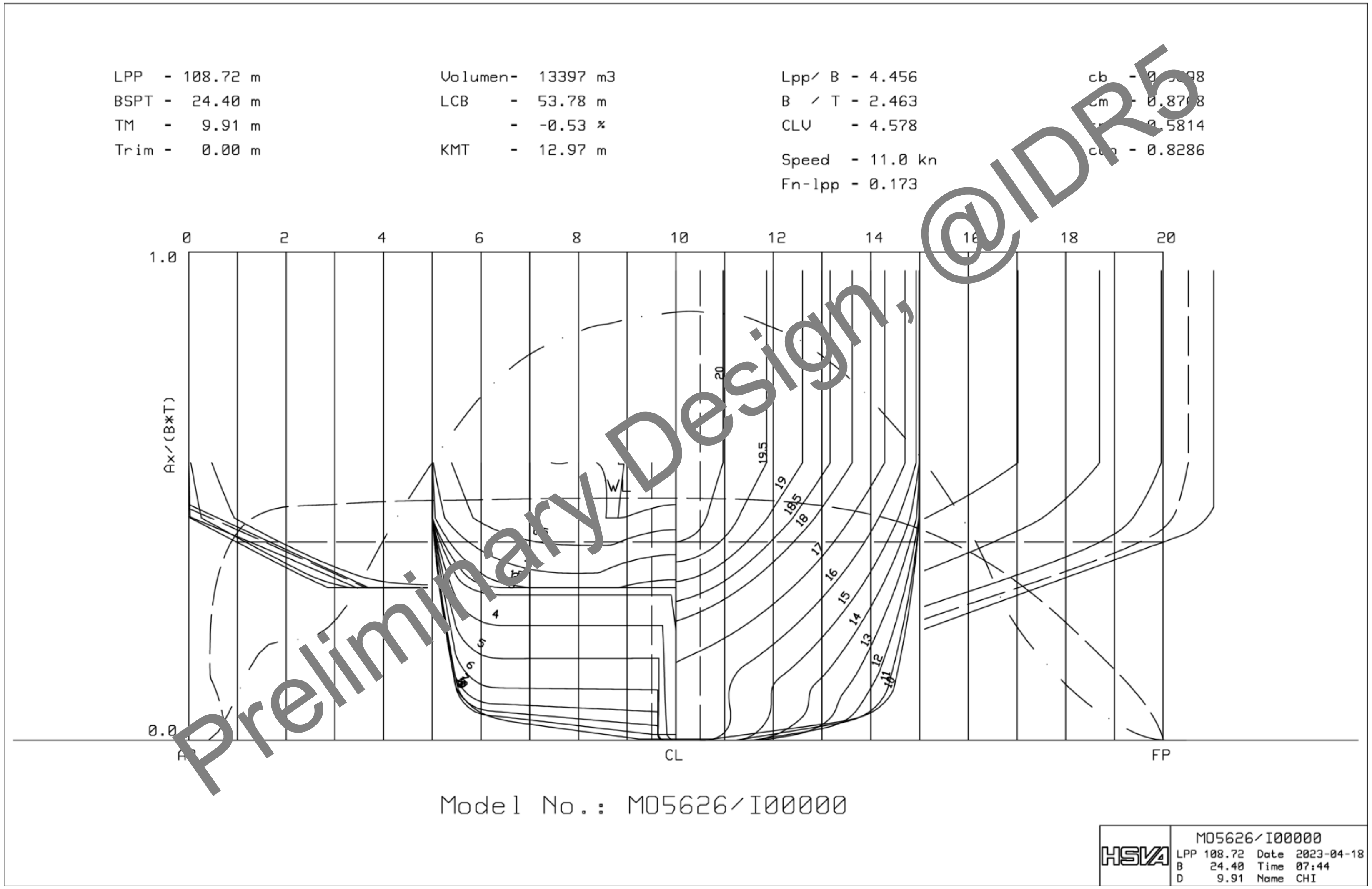

3.2 3D View of the Fore Body - HSVA Model 5626-00000

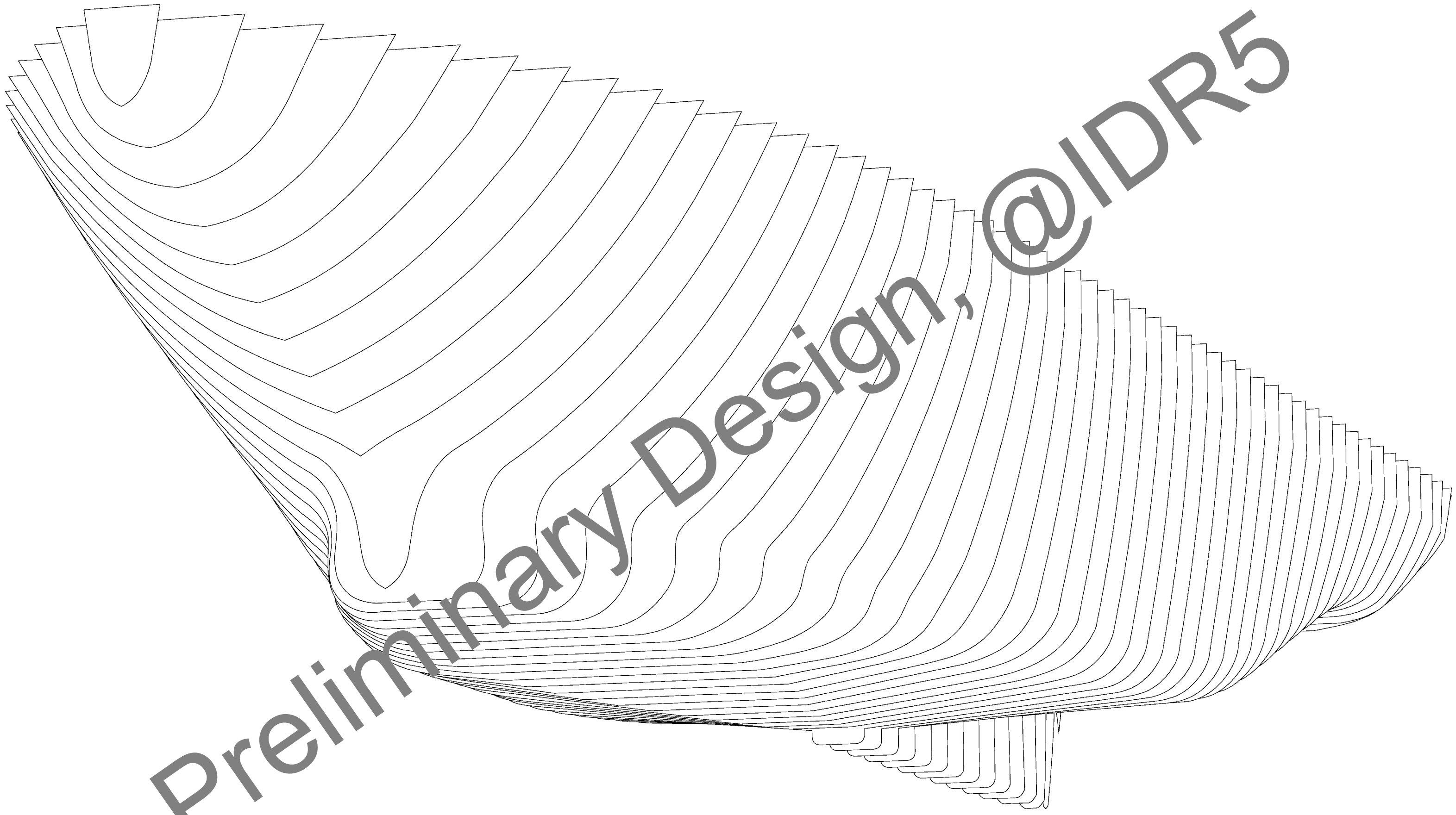

3.3 3D View of the Aft Body - HSVA Model 5626-00000

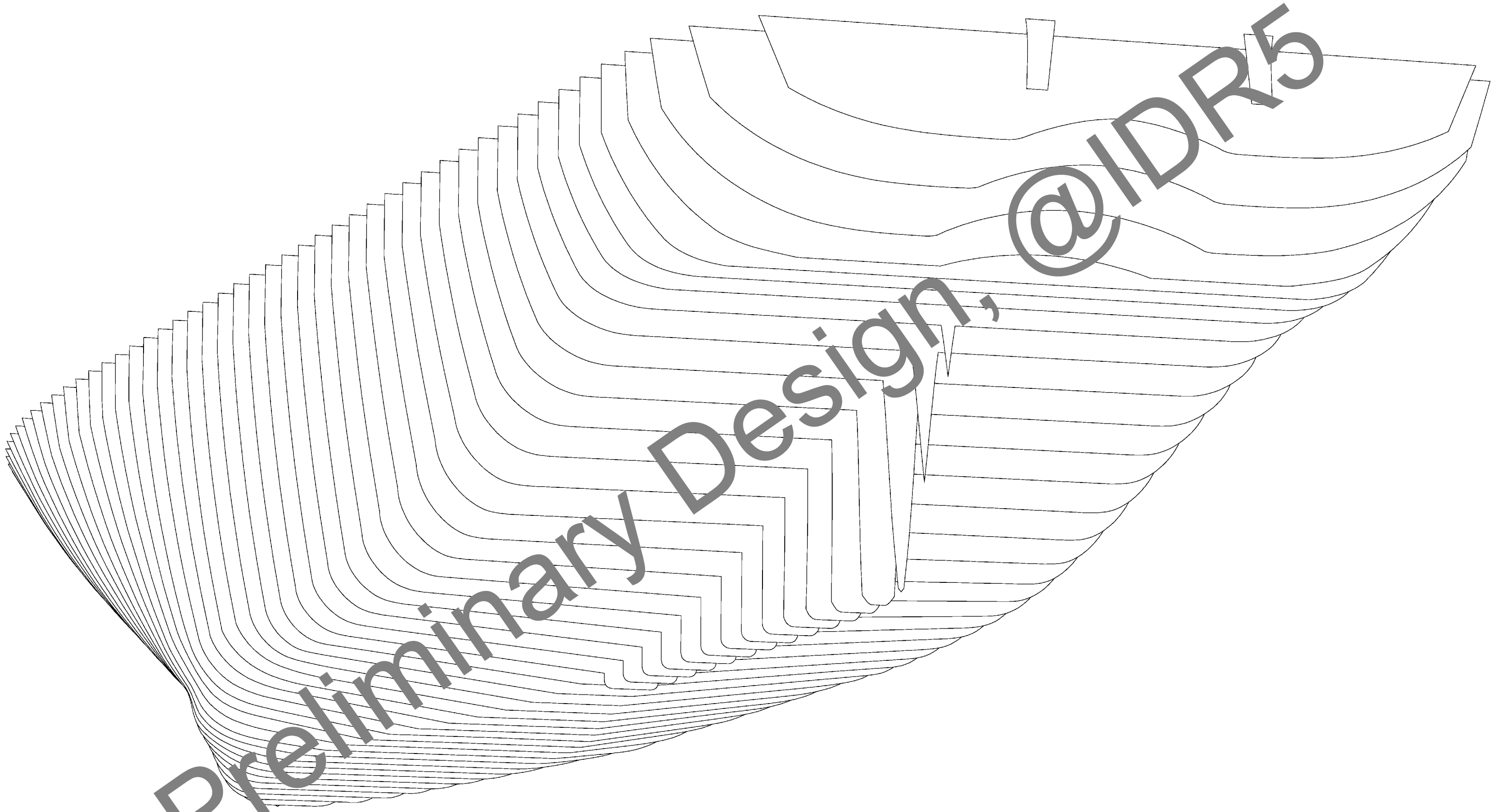

3.4 Propulsion Arrangement

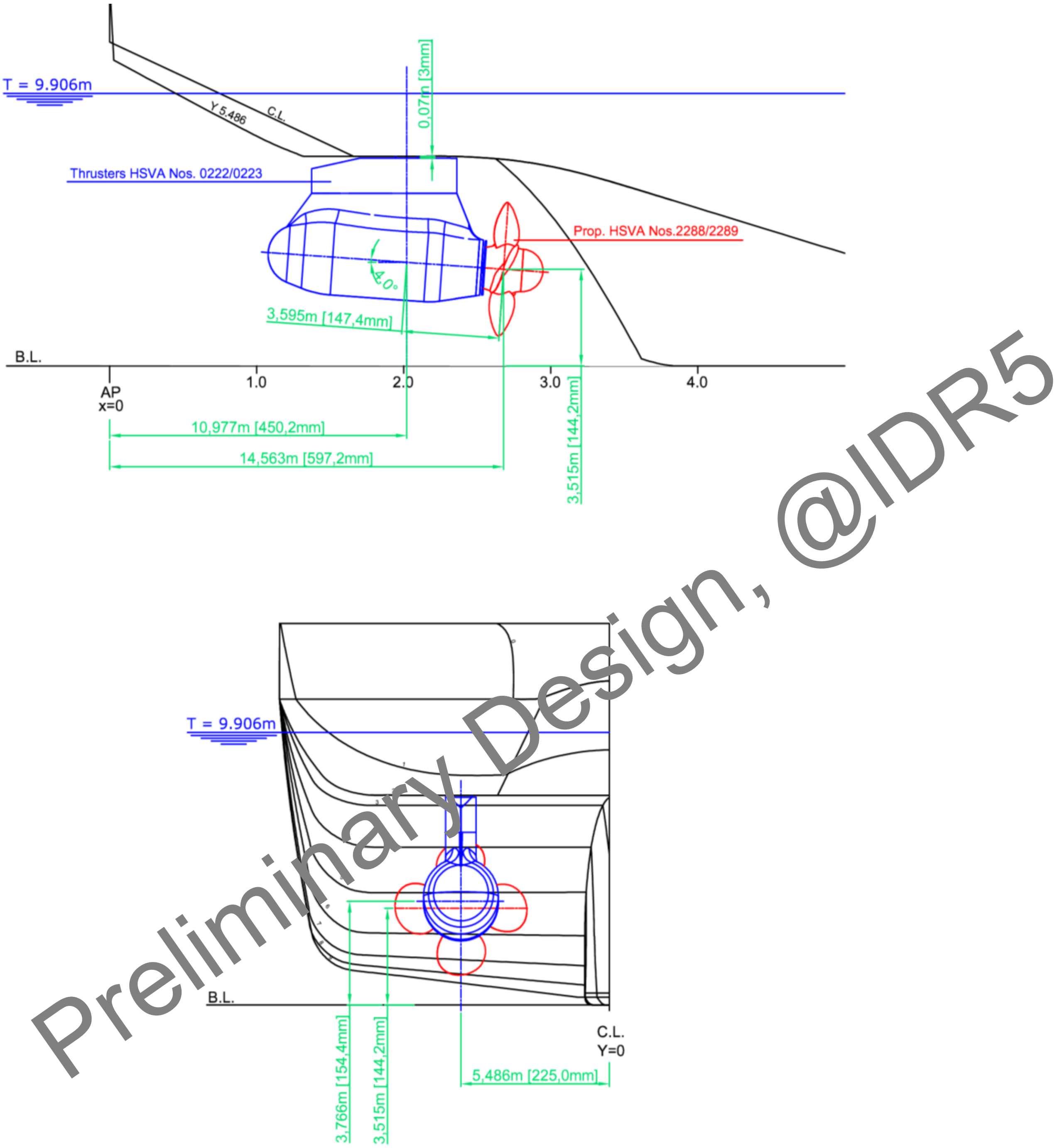

HSVA
Hamburg Ship Model Basin | Bramfelder Strasse 164 | 22305 Hamburg, Germany
Phone.: +49 (0) 40 / 69 203 -0 | Fax: +49 (0) 40 / 69 203 -345 | www.hsva.de

HSVA Model 5626-00010
Leidos
Arrangement of the Thruster and Propeller
Lambda 24.384

Dwg no. 45-23 Date: 17.03.2023 -ka-

4.1 Formation of Waves – Model 5626-00020, T = 9.91 m

V = 6.00 kts / F_N = 0.0956

V = 8.00 kts / F_N = 0.1274

V = 10.00 kts / F_N = 0.1593

V = 11.00 kts / F_N = 0.1752

V = 12.00 kts / F_N = 0.1911

V = 13.50 kts / F_N = 0.2150

V = 15.00 kts / F_N = 0.2389

4.2 Photographs of Model 5626-00010


4
2


5626
2
4
HSVA 5626
00010


5626

5.1 Result Tables - T= 9.906 m - Resistance and Propulsion

Hamburgische Schiffbau-Versuchs-Anstalt GmbH	Leidos Prepared by cs Date 20.04.2023	Report WP T1

Model Tests for an ARV

Model 5626-00020 Propeller 2288 / 2289 Scale 24.384

MAIN DIMENSIONS OF SHIP

Length betw. perpendiculars	LPP =	108.720	m
" waterline	LWL =	106.360	m
" submerged	LOS =	106.360	m
Breadth, waterline	BWL =	24.400	m
Draught, fore	TF =		m
" mean	TM =	9.906	m
" aft	TA =		m
Displacement, bare	DISV =	13385	m3
" , appended	DISV =	13406	m3
Wetted surface, bare	S =	3315	m2
" , with appendages ...	S =	3296	m2
Block coefficient	CB =	0.509	(based on LPP)
Prismatic coefficient	CP =	0.581	(" " ")
Waterline coefficient	CWP =	0.826	(" " ")
Centre of buoyancy	XB =	0.53% LPP aft of LPP/2	

DIMENSIONS OF PROPELLER

		Port	Stb
Diameter	DP =	4.877 m	4.877 m
Pitch ratio ... (mean) ...	PP/DP =	0.985	0.985
Hub diameter ratio	DH/DP =	0.381	0.381
Disc area ratio	AE/A0 =	0.553	0.553
Number of blades	NPB =	4	4
Sense of rotation		right	left

RATED POWER MCR: 19,000 kW (2x 9,500 kW)

MODEL CONDITION with POD nos. 222/223-5500
propeller turning inward over the top when going ahead
bow thruster tunnel open

TURBULENCE INDUCTION 2 sandstripe

FILES
WP230254_P.D
Str1316

Model Tests for an ARV

Model 5626-00020 Propeller 2288 / 2289 Scale 24.384

Test No. 23-0254/23-0253 Draught = 9.906 m
Test Date 19.04.2023 Displacement = 13406 m3

Model condition: with POD nos. 222/223-5500
propeller turning inward over the top when going ahead
bow thruster tunnel open

FAIRED MODEL DATA

V [m/s]	FN [-]	RN*E-6 [-]	RTM [N]	N [1/s]	T [N]	Q [NM]	FD [N]
.625	.0956	2.414	6.31	3.78	2.13	.1126	2.07
.833	.1274	3.216	10.71	5.00	3.72	.1949	3.39
1.042	.1593	4.022	16.69	6.27	6.03	.3066	4.99
1.146	.1753	4.425	20.38	6.92	7.49	.3752	5.88
1.250	.1911	4.824	24.60	7.59	9.22	.4557	6.83
1.406	.2150	5.428	32.26	8.63	12.45	.6017	8.39
1.563	.2390	6.033	41.27	9.70	15.42	.7740	10.07

Conversion with values for model

Length for calcul. LOS = 4.362 m Tankw.-temp. = 15.3 deg C
CF acc. to ITTC, CA = 0.189E-3 NY .... = 1.1300E-6 m2/s
1+k .... = 1.000 RHO .... = 999.0 kg/m3
Wetted surface .... = 5.54 m2

Hamburgische Schiffbau-Versuchs-Anstalt GmbH	Leidos Prepared by cs Date 20.04.2023	Report WP T3

Model Tests for an ARV

Model 5626-00020 Propeller 2288 / 2289   Scale 24.384

Test No.   23-0254/23-0253   Draught = 9.906 m
Test Date 19.04.2023   Displacement = 13406 m3

Model condition: with POD nos. 222/223-5500
---------------- propeller turning inward over the top when going ahead
bow thruster tunnel open

RESISTANCE AND PROPULSION COEFFICIENTS

Full scale ship without correction of wake and propeller efficiency

V [KTS]	FN [-]	RN*E-8 [-]	CR*E3 [-]	CF*E3 [-]	CT*E3 [-]	ADVCV [-]	KT [-]	KQ [-]
6.00	.0956	2.764	1.922	1.808	3.918	.8274	.0932	.02466
8.00	.1274	3.683	1.881	1.740	3.809	.8331	.0931	.02438
10.00	.1593	4.605	2.015	1.689	3.894	.8307	.0959	.02439
11.00	.1753	5.067	2.125	1.668	3.983	.8278	.0978	.02449
12.00	.1911	5.524	2.268	1.650	4.107	.8235	.1002	.02476
13.50	.2150	6.216	2.545	1.625	4.359	.8146	.1046	.02526
15.00	.2390	6.908	2.820	1.603	4.612	.8057	.1092	.02574

Conversion with

Length for calcul. LOS =	106.360 m	Seaw.-temp. = 15.0	deg C
CF acc. to ITTC, CA =	0.189E-3	NY .... = 1.1882E-6	m2/s
1+k .... =	1.000	RHO .... = 1025.9	kg/m3

Model Tests for an ARV

Model 5626-00020 Propeller 2288 / 2289 Scale 24.384

Test No. 23-0254/23-0253 Draught = 9.906 m
Test Date 19.04.2023 Displacement = 13406 m3

Model condition: with POD nos. 222/223-5500
propeller turning inward over the top when going ahead
bow thruster tunnel open

POWER AND PROPELLER REVOLUTIONS

Full scale ship without correction of wake and propeller efficiency

V [KTS]	PE [KW]	PD [KW]	N [RPM]	FN [-]	RF/RT [-]	CTVOL [-]	CDVOL [-]	ETAD [-]	TETP [MIN]	ZV [M]
6.00	195	393	45.9	.0956	.4613	.02289	.04611	.496	0	.024
8.00	449	900	60.8	.1274	.4566	.02225	.04466	.498	0	.054
10.00	897	1777	76.2	.1593	.4338	.02274	.04507	.505	0	.107
11.00	1221	2400	84.1	.1753	.4189	.02326	.04572	.509	0	.132
12.00	1632	3194	92.2	.1911	.4017	.02399	.04696	.511	0	.166
13.50	2468	4799	104.9	.2150	.3728	.02546	.04950	.514	0	.212
15.00	3585	6936	117.8	.2390	.3476	.02694	.05212	.517	0	.278

Conversion with

Length for calcul. LOS = 106.360 m   Seaw.-temp. = 15.0 deg C
CF acc. to ITTC, CA = 0.189E-3   NY .... = 1.1882E-6 m2/s
1+k .... = 1.000   RHO .... = 1025.9 kg/m3

NOTE: Trim (TETP) positive down by the stern
----- Sinkage (ZV) positive parallel immersion

Model Tests for an ARV

Model 5626-00020 Propeller 2288 / 2289 Scale 24.384

Test No. 23-0254/23-0253 Draught = 9.906 m
Test Date 19.04.2023 Displacement = 13406 m3

Model condition: with POD nos. 222/223-5500
propeller turning inward over the top when going ahead
bow thruster tunnel open

HULL EFFICIENCY ELEMENTS

Full scale ship without correction of wake and propeller efficiency

V [KTS]	FN [-]	ADVC [-]	THDF [-]	WFT [-]	ETAH [-]	ETAO [-]	ETAR [-]	ETAD [-]	CTH [-]
6.00	.0956	.777	.003	.060	1.061	.503	.930	.496	.393
8.00	.1274	.778	.016	.066	1.054	.503	.940	.498	.392
10.00	.1593	.771	.029	.072	1.046	.505	.954	.505	.410
11.00	.1753	.766	.033	.074	1.044	.507	.961	.509	.424
12.00	.1911	.761	.037	.076	1.043	.509	.963	.511	.441
13.50	.2150	.750	.042	.079	1.04[illegible]	.512	.966	.514	.473
15.00	.2390	.739	.050	.083	1.036	.514	.971	.517	.509

REMARK: The coefficients are valid for identity of KT.

Model Tests for an ARV

Model 5626-00020 Propeller 2288 / 2289 Scale 24.384

Test No. 23-0254/23-0253 Draught = 9.906 m
Test Date 19.04.2023 Displacement = 13406 m3

Model condition: with POD nos. 222/223-5500
propeller turning inward over the top when going ahead
bow thruster tunnel open

TRIAL PREDICTION

Head wind 0.000 m/s ^ BF 0

V [KTS]	FN [-]	RT [KN]	T [KN]	PE [KW]	PD [KW]	ETAD [-]	N [RPM]
6.00	.0956	66	66.5	205	375	.545	46.2
8.00	.1274	115	116.4	471	861	.548	61.1
10.00	.1593	183	188.4	941	1701	.55[illegible]	76.6
11.00	.1753	226	234.0	1281	2300	.557	84.6
12.00	.1911	277	287.6	170[illegible]	3063	.558	92.7
13.50	.2150	371	387.4	2579	4604	.560	105.4
15.00	.2390	484	50[illegible].4	3736	6662	.561	118.4

Conversion with

DRT, related to RF ... = 0.0 % RHO air.... = 1.2255 kg/m3
AV .... = 632 m2 CAA .... = 0.85

TRIAL CONDITIONS: Clean smooth hull, deep calm water, no current

Hamburgische Schiffbau-Versuchs-Anstalt GmbH	Leidos Prepared by cs Date 20.04.2023	Report WP T7

Model Tests for an ARV

Model 5626-00020 Propeller 2288 / 2289 Scale 24.384

Test No. 23-0254/23-0253 Draught = 9.906 m
Test Date 19.04.2023 Displacement = 13406 m3

Model condition: with POD nos. 222/223-5500
propeller turning inward over the top when going ahead
bow thruster tunnel open

HULL EFFICIENCY ELEMENTS

Trial conditions, Head wind 0.000 m/s ^ BF 0

V [KTS]	FN [-]	ADVC [-]	THDF [-]	WFT [-]	ETAH [-]	ETAO [-]	ETAR [-]	ETAD [-]	CTH [-]
6.00	.0956	.784	.003	.047	1.046	.560	.930	.545	.401
8.00	.1274	.784	.016	.053	1.040	.560	.940	.548	.401
10.00	.1593	.778	.029	.059	1.032	.562	.954	.553	.419
11.00	.1753	.773	.033	.061	1.030	.563	.961	.557	.432
12.00	.1911	.767	.037	.063	1.028	.564	.963	.558	.449
13.50	.2150	.757	.042	.066	1.026	.565	.966	.560	.481
15.00	.2390	.746	.050	.070	1.022	.565	.971	.561	.516

REMARK: The coefficients are valid for identity of KT.

Corrections: (1-WFTS)/(1-WFTM) = 1.014

Hamburgische Schiffbau-Versuchs-Anstalt GmbH	Leidos Prepared by cs Date 20.04.2023	Report WP T8

Model Tests for an ARV

Model 5626-00020 Propeller 2288 / 2289 Scale 24.384

Test No. 23-0254/23-0253 Draught = 9.906 m
Test Date 19.04.2023 Displacement = 13406 m3

Model condition: with POD nos. 222/223-5500
propeller turning inward over the top when going ahead
bow thruster tunnel open

SERVICE PREDICTION

Allowance = 15.0 % on PD-trial (Head wind 0.000 m/s ^ BF 0)

V [KTS]	FN [-]	RT [KN]	T [KN]	PE [KW]	PD [KW]	ETAD [-]	N [RPM]
6.00	.0956	77	77.0	237	432	.549	47.5
8.00	.1274	133	134.8	546	990	.551	62.9
10.00	.1593	212	217.8	1088	1957	.556	78.9
11.00	.1753	261	270.3	1479	2645	.559	87.1
12.00	.1911	319	331.7	1972	3522	.560	95.5
13.50	.2150	427	445.9	2968	5295	.561	108.6
15.00	.2390	556	585.1	4291	7661	.560	122.1

Hamburgische Schiffbau-Versuchs-Anstalt GmbH	Leidos Prepared by cs Date 20.04.2023	Report WP T9

Model Tests for an ARV

Model 5626-00020 Propeller 2288 / 2289 Scale 24.384

Test No. 23-0254/23-0253 Draught = 9.906 m
Test Date 19.04.2023 Displacement = 13406 m3

Model condition: with POD nos. 222/223-5500
propeller turning inward over the top when going ahead
bow thruster tunnel open

HULL EFFICIENCY ELEMENTS UNDER SERVICE CONDITIONS

Allowance = 15.0 % on PD-trial (Head wind 0.000 m/s ^ BF 0)

V [KTS]	FN [-]	ADVC [-]	THDF [-]	WFT [-]	ETAH [-]	ETAO [-]	ETAR [-]	ETAD [-]	CTH [-]
6.00	.0956	.762	.003	.047	1.046	.564	.930	.549	.464
8.00	.1274	.762	.016	.053	1.040	.564	.940	.551	.464
10.00	.1593	.755	.029	.059	1.032	.565	.954	.556	.485
11.00	.1753	.751	.033	.061	1.030	.565	.961	.559	.499
12.00	.1911	.745	.037	.063	1.028	.565	.963	.560	.518
13.50	.2150	.734	.042	.066	1.026	.565	.966	.561	.553
15.00	.2390	.723	.050	.070	1.022	.565	.971	.560	.593

REMARK: The coefficients are valid for identity of KT.

Corrections: (1-WFTS)/(1-WFTM) = 1.014

5.2 Result Tables - T= 9.906 m - Resistance and Propulsion (Recalculation P2621/2622

```
Hamburgische   |                   Leidos                        | Report
Schiffbau-     |                                                 | WP-2023-029
Versuchs-      |      Prepared by cs  Date  12.05.2023           | T10
Anstalt GmbH   |                                                 |

                         Model Tests for an ARV


  Model  5626-00020  Full Scale Propeller 2621 / 2622          Scale 24.384
                     Model Test Propeller 2288 / 2289

MAIN DIMENSIONS OF SHIP
-----------------------
  Length betw. perpendiculars  LPP =   108.720 m
     "   waterline ........... LWL =   106.360 m
     "   submerged ........... LOS =   106.360 m
  Breadth, waterline ......... BWL =    24.400 m
  Draught, fore ............... TF =           m
     "    mean ................ TM =     9.906 m
     "    aft ................. TA =           m
  Displacement, bare .......  DISV =     13385 m3
       "    , appended .....  DISV =     13406 m3
  Wetted surface, bare ......... S =      3315 m2
       "   , with appendages ... S =      3296 m2
  Block coefficient ........... CB =     0.509 (based on LPP)
  Prismatic coefficient ....... CP =     0.581 (  "   "  " )
  Waterline coefficient ...... CWP =     0.826 (  "   "  " )
  Centre of buoyancy .......... XB =  0.53% LPP aft of LPP/2

DIMENSIONS OF PROPELLER                    P             Stb
-----------------------
  Diameter .................... DP =     5.583 m       5.583 m
  Pitch ratio ... (mean) ... PP/DP =     1.012         1.012
  Hub diameter ratio ...... DH/DP =     0.247         0.247
  Disc area ratio ......... AE/A0 =     0.686         0.686
  Number of blades  ......... NPB =         4             4
  Sense of rotation ...........      right          left

RATED POWER  MCR: 19,000 kW (2x 9,500 kW)
-----------


MODEL CONDITION   with POD nos. 222/223-5500
---------------   propeller turning inward over the top when going ahead
                  bow thruster tunnel open

TURBULENCE INDUCTION   2 sandstripe
--------------------

                                                                FILES
                                                                -----
                                                                WP230254.DAT
                                                                Str1316
                                                                Str1290
```

Hamburgische Schiffbau-Versuchs-Anstalt GmbH	Leidos Prepared by cs Date 12.05.2023	Report WP-2023-029 T11

Model Tests for an ARV

Model 5626-00020 Full Scale Propeller 2621 / 2622 Scale 24.384
Model Test Propeller 2288 / 2289

Test No. 23-0254/23-0253 Draught = 9.906 m
Test Date 19.04.2023 Displacement = 13406 m3

Model condition: with POD nos. 222/223-5500
---------------- propeller turning inward over the top when going ahead
bow thruster tunnel open

FAIRED MODEL DATA (PROPELLER 2288)

V [m/s]	FN [-]	RN*E-6 [-]	RTM [N]	N [1/s]	T [N]	Q [NM]	FD [N]
.625	.0956	2.414	6.31	3.78	2.13	.1126	2.07
.833	.1274	3.216	10.71	5.00	3.72	.1949	3.39
1.042	.1593	4.022	16.69	6.27	6.03	.3060	4.99
1.146	.1753	4.425	20.38	6.92	7.49	.3752	5.88
1.250	.1911	4.824	24.60	7.59	9.22	.4557	6.83
1.406	.2150	5.428	32.26	8.63	12.45	.6017	8.39
1.563	.2390	6.033	41.27	9.70	16.42	.7740	10.07

Conversion with values for model

Length for calcul. LOS = 4.362 m Tankw.-temp. = 15.3 deg C
CF acc. to ITTC, CA = 0.189E-3 NY .... = 1.1300E-6 m2/s
1+k .... = 1.000 RHO .... = 999.0 kg/m3
Wetted surface .... = 5.54 m2

Hamburgische Schiffbau-Versuchs-Anstalt GmbH	Leidos Prepared by cs Date 12.05.2023	Report WP-2023-029 T12

Model Tests for an ARV

Model 5626-00020 Full Scale Propeller 2621 / 2622 Scale 24.384
Model Test Propeller 2288 / 2289

Test No.	23-0254/23-0253	Draught	=	9.906	m
Test Date	19.04.2023	Displacement	=	13406	m3

Model condition: with POD nos. 222/223-5500
---------------- propeller turning inward over the top when going ahead
bow thruster tunnel open

RESISTANCE AND PROPULSION COEFFICIENTS (PROPELLER 2288)

Full scale ship without correction of wake and propeller efficiency

V [KTS]	FN [-]	RN*E-8 [-]	CR*E3 [-]	CF*E3 [-]	CT*E3 [-]	ADVCV [-]	KT [-]	KQ [-]
6.00	.0956	2.764	1.922	1.808	3.918	.8274	.0932	.02466
8.00	.1274	3.683	1.881	1.740	3.809	.8331	.0931	.02438
10.00	.1593	4.605	2.015	1.689	3.894	.8307	.0959	.02439
11.00	.1753	5.067	2.125	1.668	3.983	.8278	.0978	.02449
12.00	.1911	5.524	2.268	1.650	4.107	.8235	.1002	.02476
13.50	.2150	6.216	2.545	1.625	4.359	.8146	.1046	.02526
15.00	.2390	6.908	2.820	1.603	4.612	.8057	.1092	.02574

Conversion with

Length for calcul. LOS = 106.360 m	Seaw.-temp. =	15.0	deg C
CF acc. to ITTC, CA = 0.189E-3	NY .... =	1.1882E-6	m2/s
1+k .... = 1.000	RHO .... =	1025.9	kg/m3

Hamburgische Schiffbau-Versuchs-Anstalt GmbH	Leidos Prepared by cs Date 12.05.2023	Report WP-2023-029 T13

Model Tests for an ARV

Model 5626-00020 Full Scale Propeller 2621 / 2622 Scale 24.384
Model Test Propeller 2288 / 2289

Test No. 23-0254/23-0253 Draught = 9.906 m
Test Date 19.04.2023 Displacement = 13406 m3

Model condition: with POD nos. 222/223-5500
propeller turning inward over the top when going ahead
bow thruster tunnel open

POWER AND PROPELLER REVOLUTIONS (PROPELLER 2288)

Full scale ship without correction of wake and propeller efficiency

V [KTS]	PE [KW]	PD [KW]	N [RPM]	FN [-]	RF/RT [-]	CTVOL [-]	CDVOL [-]	ETAD [-]	TETP [MIN]	ZV [M]
6.00	195	393	45.9	.0956	.4613	.02289	.04611	.496	0	.024
8.00	449	900	60.8	.1274	.4566	.02225	.04466	.498	0	.054
10.00	897	1777	76.2	.1593	.4338	.02274	.04507	.505	0	.107
11.00	1221	2400	84.1	.1753	.4189	.02326	.04572	.509	0	.132
12.00	1632	3194	92.2	.1911	.4017	.02399	.04696	.511	0	.166
13.50	2468	4799	104.9	.2150	.3728	.02546	.04950	.514	0	.212
15.00	3585	6936	117.8	.2390	.3476	.02694	.05212	.517	0	.278

Conversion with

Length for calcul. LOS = 106.360 m Seaw.-temp. = 15.0 deg C
CF acc. to ITTC, CA = 0.189E-3 NY .... = 1.1882E-6 m2/s
1+k .... = 1.000 RHO .... = 1025.9 kg/m3

NOTE: Trim (TETP) positive down by the stern
----- Sinkage (ZV) positive parallel immersion

Model Tests for an ARV

Model 5626-00020 Full Scale Propeller 2621 / 2622 Scale 24.384
Model Test Propeller 2288 / 2289

Test No. 23-0254/23-0253 Draught = 9.906 m
Test Date 19.04.2023 Displacement = 13406 m3

Model condition: with POD nos. 222/223-5500
propeller turning inward over the top when going ahead
bow thruster tunnel open

HULL EFFICIENCY ELEMENTS (PROPELLER 2288)

Full scale ship without correction of wake and propeller efficiency

V [KTS]	FN [-]	ADVC [-]	THDF [-]	WFT [-]	ETAH [-]	ETAO [-]	ETAR [-]	ETAD [-]	CTH [-]
6.00	.0956	.777	.003	.060	1.061	.503	.930	.496	.393
8.00	.1274	.778	.016	.066	1.054	.503	.940	.498	.392
10.00	.1593	.771	.029	.072	1.046	.505	.954	.505	.410
11.00	.1753	.766	.033	.074	1.044	.507	.961	.509	.424
12.00	.1911	.761	.037	.076	1.043	.509	.963	.511	.441
13.50	.2150	.750	.042	.079	1.041	.512	.966	.514	.473
15.00	.2390	.739	.050	.083	1.036	.514	.971	.517	.509

REMARK: The coefficients are valid for identity of KT.

Hamburgische Schiffbau-Versuchs-Anstalt GmbH	Leidos Prepared by cs Date 12.05.2023	Report WP-2023-029 T15

Model Tests for an ARV

Model 5626-00020 Full Scale Propeller 2621 / 2622 Scale 24.384
Model Test Propeller 2288 / 2289

Test No. 23-0254/23-0253 Draught = 9.906 m
Test Date 19.04.2023 Displacement = 13406 m3

Model condition: with POD nos. 222/223-5500
propeller turning inward over the top when going ahead
bow thruster tunnel open

TRIAL PREDICTION (PROPELLER 2621)

Head wind 0.000 m/s ^ BF 0

V [KTS]	FN [-]	RT [KN]	T [KN]	PE [KW]	PD [KW]	ETAD [-]	N [RPM]
6.00	.0956	66	66.5	205	331	.619	34.1
8.00	.1274	115	116.4	471	758	.622	45.1
10.00	.1593	183	188.4	941	1495	.630	56.5
11.00	.1753	226	234.0	1281	2018	.635	62.3
12.00	.1911	277	287.6	1709	2681	.638	68.2
13.50	.2150	371	387.4	2579	4016	.642	77.3
15.00	.2390	484	500.4	3736	5791	.645	86.7

Conversion with

DRT, related to RF ... = 0.0 % RHO air.... = 1.2255 kg/m3
AV .... = 632 m2 CAA .... = 0.85

TRIAL CONDITIONS: Clean smooth hull, deep calm water,
no current

Hamburgische Schiffbau-Versuchs-Anstalt GmbH	Leidos Prepared by cs Date 12.05.2023	Report WP-2023-029 T16

Model Tests for an ARV

Model 5626-00020 Full Scale Propeller 2621 / 2622 Scale 24.384
Model Test Propeller 2288 / 2289

Test No.	23-0254/23-0253	Draught	=	9.906	m
Test Date	19.04.2023	Displacement	=	13406	m3

Model condition: with POD nos. 222/223-5500
propeller turning inward over the top when going ahead
bow thruster tunnel open

HULL EFFICIENCY ELEMENTS (PROPELLER 2621)

Trial conditions, Head wind 0.000 m/s ^ BF 0

V [KTS]	FN [-]	ADVC [-]	THDF [-]	WFT [-]	ETAH [-]	ETAO [-]	ETAR [-]	ETAD [-]	CTH [-]
6.00	.0956	.928	.003	.047	1.046	.636	.930	.619	.306
8.00	.1274	.928	.016	.053	1.040	.636	.940	.622	.306
10.00	.1593	.922	.029	.059	1.032	.639	.954	.630	.320
11.00	.1753	.917	.033	.061	1.030	.642	.961	.635	.330
12.00	.1911	.911	.037	.063	1.028	.644	.963	.638	.343
13.50	.2150	.901	.042	.066	1.026	.647	.966	.642	.367
15.00	.2390	.890	.050	.070	1.022	.650	.971	.645	.394

REMARK: The coefficients are valid for identity of KT.

Corrections: (1-WFTS)/(1-WFTM) = 1.014

Model Tests for an ARV

Model 5626-00020 Full Scale Propeller 2621 / 2622 Scale 24.384
Model Test Propeller 2288 / 2289

Test No. 23-0254/23-0253 Draught = 9.906 m
Test Date 19.04.2023 Displacement = 13406 m3

Model condition: with POD nos. 222/223-5500
---------------- propeller turning inward over the top when going ahead
bow thruster tunnel open

SERVICE PREDICTION (PROPELLER 2621)

Allowance = 15.0 % on PD-trial (Head wind 0.000 m/s ^ BF 0)

V [KTS]	FN [-]	RT [KN]	T [KN]	PE [KW]	PD [KW]	ETAD [-]	N [RPM]
6.00	.0956	77	77.7	239	380	.629	34.9
8.00	.1274	134	136.0	551	872	.631	46.2
10.00	.1593	213	219.6	1097	1719	.638	57.9
11.00	.1753	263	272.4	1491	2320	.643	63.9
12.00	.1911	322	334.2	1987	3083	.644	70.0
13.50	.2150	430	449.0	2988	4619	.647	79.4
15.00	.2390	560	588.8	4319	6661	.648	89.1

Model Tests for an ARV

Model 5626-00020 Full Scale Propeller 2621 / 2622 Scale 24.384
Model Test Propeller 2288 / 2289

Test No. 23-0254/23-0253 Draught = 9.906 m
Test Date 19.04.2023 Displacement = 13406 m3

Model condition: with POD nos. 222/223-5500
propeller turning inward over the top when going ahead
bow thruster tunnel open

HULL EFFICIENCY ELEMENTS UNDER SERVICE CONDITIONS (PROPELLER 2621)

Allowance = 15.0 % on PD-trial (Head wind 0.000 m/s ^ BF 0)

V [KTS]	FN [-]	ADVC [-]	THDF [-]	WFT [-]	ETAH [-]	ETAO [-]	ETAR [-]	ETAD [-]	CTH [-]
6.00	.0956	.905	.003	.047	1.046	.646	.930	.629	.357
8.00	.1274	.905	.016	.053	1.040	.646	.940	.631	.357
10.00	.1593	.898	.029	.059	1.032	.648	.954	.638	.373
11.00	.1753	.894	.033	.061	1.030	.649	.961	.643	.384
12.00	.1911	.888	.037	.063	1.028	.651	.963	.644	.398
13.50	.2150	.877	.042	.066	1.026	.652	.966	.647	.425
15.00	.2390	.866	.050	.070	1.022	.654	.971	.648	.455

REMARK: The coefficients are valid for identity of KT.

Corrections: (1-WFTS)/(1-WFTM) = 1.014

5.3 Result Tables - T= 9.906 m - Resistance - Bare Hull

Hamburgische Schiffbau-Versuchs-Anstalt GmbH	Leidos Prepared by cs Date 12.05.2023	Report WP T19

Model Tests for an ARV

Model 5626-00000 Scale 24.384

MAIN DIMENSIONS OF SHIP

Length betw. perpendiculars	LPP =	108.720	m
" waterline	LWL =	106.360	m
" submerged	LOS =	106.360	m
Breadth, waterline	BWL =	24.400	m
Draught, fore	TF =		m
" mean	TM =	9.906	m
" aft	TA =		m
Displacement, bare	DISV =	13385	m3
" , appended	DISV =		m3
Wetted surface, bare	S =	3315	m2
" , with appendages ...	S =		m2
Block coefficient	CB =	0.509	(based on LPP)
Prismatic coefficient	CP =	0.581	(" " ")
Waterline coefficient	CWP =	0.826	(" " ")
Centre of buoyancy	XB =	0.53% LPP aft of LPP/2	

RATED POWER MCR: 19,000 kW (2x 9,500 kW)

MODEL CONDITION Bare Hull - Bow thruster tunnel closed

TURBULENCE INDUCTION 2 sandstripe

FILES

WP230252.DAT

Hamburgische Schiffbau-Versuchs-Anstalt GmbH	Leidos Prepared by cs Date 12.05.2023	Report WP T20

Model Tests for an ARV

Model 5626-00000 Scale 24.384

Test No. 23-0252 Draught = 9.906 m
Test Date 19.04.2023 Displacement = 13385 m3

Model condition: Bare Hull - Bow thruster tunnel closed

FAIRED MODEL DATA				RESISTANCE COEFFICIENTS Model values				
V [m/s]	FN [-]	RN*E-6 [-]	RTM [N]	CR*E3 [-]	CF*E3 [-]	CT*E3 [-]	CT/CF [-]	FN4/CF [-]
.625	.0956	2.413	6.10	1.697	3.905	5.601	1.434	.021
.833	.1274	3.217	10.49	1.729	3.691	5.420	1.468	.071
1.042	.1593	4.021	16.33	1.867	3.538	5.404	1.528	.182
1.146	.1752	4.423	19.95	1.981	3.475	5.456	1.570	.271
1.250	.1911	4.826	24.11	2.121	3.419	5.540	1.620	.390
1.406	.2150	5.429	31.63	2.397	3.346	5.743	1.716	.639
1.563	.2389	6.032	40.65	2.695	3.282	5.977	1.821	.993

Conversion with values for model

Length for calcul. LOS = 4.362 m Tankw.-temp. = 15.3 deg C
CF acc. to ITTC, CA = 0.189E-3 NY .... = 1.1300E-6 m2/s
1+k .... = 1.000 RHO .... = 999.0 kg/m3
Wetted surface .... = 5.58 m2

Hamburgische Schiffbau-Versuchs-Anstalt GmbH	Leidos Prepared by cs Date 12.05.2023	Report WP T21

Model Tests for an ARV

Model 5626-00000 Scale 24.384

Test No. 23-0252 Draught = 9.906 m
Test Date 19.04.2023 Displacement = 13385 m3

Model condition: Bare Hull - Bow thruster tunnel closed

TEST RESULTS

Full scale ship

V [KTS]	FN [-]	RT [KN]	PE [KW]	CTVOL [-]	TETP [MIN]	ZV [M]
6.00	.0956	60	185	.02172	0	.017
8.00	.1274	105	434	.02151	-1	.063
10.00	.1593	169	867	.02202	-2	.095
11.00	.1752	209	1183	.02257	-2	.132
12.00	.1911	257	1584	.02329	-2	.151
13.50	.2150	345	2399	.02476	-3	.207
15.00	.2389	454	3506	.02689	-3	.273

Conversion with

Length for calcul. LOS = 106.360 m Seaw.-temp. = 15.0 deg C
CF acc. to ITTC, CA = 0.189E-3 NY .... = 1.1882E-6 m2/s
1+k .... = 1.000 RHO .... = 1025.9 kg/m3

NOTE: Trim (TETP) positive down by the stern
----- Sinkage (ZV) positive parallel immersion

Hamburgische Schiffbau-Versuchs-Anstalt GmbH	Leidos Prepared by cs Date 12.05.2023	Report WP T22

Model Tests for an ARV

Model 5626-00000 Scale 24.384

Test No. 23-0252 Draught = 9.906 m
Test Date 19.04.2023 Displacement = 13385 m3

Model condition: Bare Hull - Bow thruster tunnel closed

TRIAL PREDICTION

Head wind 0.000 m/s ^ BF 0

V [KTS]	FN [-]	RT [KN]	PE [KW]	CTVOL [-]
6.00	.0956	63	194	.02286
8.00	.1274	111	456	.02264
10.00	.1593	177	912	.02316
11.00	.1752	220	1242	.02371
12.00	.1911	269	1662	.02442
13.50	.2150	361	2509	.02590
15.00	.2389	474	3657	.02753

Conversion with

DRT, related to RF ... = 0.0 % RHO air.... = 1.2255 kg/m3
AV .... = 632 m2 CAA .... = 0.85

TRIAL CONDITIONS: Clean smooth hull, deep calm water, no current

5.4 System Open Water Characteristic of Propeller 2288/89 and Pod 222/223

Propeller number	2288/2289
Propeller file	STR1316
Diameter in m	4.877
Pitch ratio (mean)	0.985
Hub diameter ratio	0.381
Disc area ratio	0.553
Number of blades	4

Open Water Test Values				Open Water Test Values corrected for the Rn of the Propulsion Test of mo. 5626				Open Water Test Values corrected for full scale			
J	KT	10KQ	ETA	J	KT	10KQ	ETA	J	KT	10KQ	ETA
0.00	0.4294	0.6206	0.000	0.00	0.4273	0.6217	0.000	0.00	0.4332	0.6128	0.000
0.05	0.4128	0.5953	0.055	0.05	0.4107	0.5964	0.055	0.05	0.4167	0.5875	0.056
0.10	0.3954	0.5700	0.110	0.10	0.3934	0.5711	0.110	0.10	0.3992	0.5622	0.113
0.15	0.3766	0.5447	0.165	0.15	0.3746	0.5458	0.164	0.15	0.3803	0.5369	0.169
0.20	0.3560	0.5194	0.218	0.20	0.3541	0.5205	0.217	0.20	0.3597	0.5116	0.224
0.25	0.3337	0.4942	0.269	0.25	0.3318	0.4953	0.267	0.25	0.3373	0.4863	0.276
0.30	0.3102	0.4691	0.316	0.30	0.3083	0.4702	0.313	0.30	0.3137	0.4611	0.325
0.35	0.2859	0.4441	0.359	0.35	0.2840	0.4452	0.355	0.35	0.2894	0.4361	0.370
0.40	0.2615	0.4193	0.397	0.40	0.2597	0.4204	0.393	0.40	0.2650	0.4112	0.410
0.45	0.2374	0.3946	0.431	0.45	0.2355	0.3957	0.426	0.45	0.2409	0.3864	0.446
0.50	0.2139	0.3698	0.460	0.50	0.2120	0.3709	0.455	0.50	0.2175	0.3616	0.479
0.55	0.1912	0.3451	0.486	0.55	0.1893	0.3462	0.479	0.55	0.1948	0.3367	0.506
0.60	0.1694	0.3202	0.505	0.60	0.1674	0.3213	0.498	0.60	0.1730	0.3117	0.530
0.65	0.1482	0.2949	0.520	0.65	0.1462	0.2960	0.511	0.65	0.1520	0.2863	0.549
0.70	0.1274	0.2693	0.527	0.70	0.1253	0.2704	0.516	0.70	0.1313	0.2606	0.561
0.75	0.1068	0.2431	0.525	0.75	0.1047	0.2442	0.512	0.75	0.1109	0.2342	0.565
0.80	0.0861	0.2161	0.507	0.80	0.0839	0.2172	0.492	0.80	0.0903	0.2071	0.555
0.85	0.0650	0.1883	0.467	0.85	0.0626	0.1894	0.447	0.85	0.0694	0.1791	0.524
0.90	0.0432	0.1597	0.387	0.90	0.0408	0.1608	0.363	0.90	0.0478	0.1503	0.455
0.95	0.0206	0.1302	0.239	0.95	0.0180	0.1313	0.208	0.95	0.0254	0.1206	0.319
1.00	-.0030	0.0999	-	1.00	-.0056	0.1010	-	1.00	0.0021	0.0901	0.036
1.05	-.0273	0.0692	-	1.05	-.0301	0.0703	-	1.05	-.0221	0.0591	-
1.10	-.0521	0.0382	-	1.10	-.0551	0.0393	-	1.10	-.0466	0.0279	-

5.5 System Open Water Characteristic of Propeller 2621/22 and Pod 222/223

Propeller number	2621/2622
Propeller file	STR1290
Diameter in m	5.583
Pitch ratio (mean)	1.012
Hub diameter ratio	0.247
Disc area ratio	0.686
Number of blades	4

Open Water Test Values				Open Water Test Values corrected for the Rn of the Propulsion Test of mo. 5601				Open Water Test Values corrected for full scale			
J	KT	10KQ	ETA	J	KT	10KQ	ETA	J	KT	10KQ	ETA
0.00	0.5587	0.8235	0.000	0.00	0.5568	0.8252	0.000	0.00	0.5626	0.8146	0.000
0.05	0.5346	0.7925	0.054	0.05	0.5327	0.7942	0.053	0.05	0.5385	0.7835	0.055
0.10	0.5102	0.7614	0.107	0.10	0.5084	0.7631	0.106	0.10	0.5140	0.7524	0.109
0.15	0.4853	0.7303	0.159	0.15	0.4835	0.7320	0.158	0.15	0.4890	0.7213	0.162
0.20	0.4598	0.6991	0.209	0.20	0.4581	0.7008	0.208	0.20	0.4634	0.6901	0.214
0.25	0.4338	0.6680	0.258	0.25	0.4321	0.6697	0.257	0.25	0.4374	0.6589	0.264
0.30	0.4076	0.6371	0.305	0.30	0.4059	0.6388	0.303	0.30	0.4111	0.6280	0.313
0.35	0.3813	0.6063	0.350	0.35	0.3796	0.6081	0.348	0.35	0.3847	0.5971	0.359
0.40	0.3552	0.5759	0.393	0.40	0.3536	0.5777	0.390	0.40	0.3586	0.5666	0.403
0.45	0.3296	0.5458	0.432	0.45	0.3280	0.5476	0.429	0.45	0.3330	0.5364	0.445
0.50	0.3045	0.5160	0.470	0.50	0.3029	0.5178	0.465	0.50	0.3079	0.5065	0.484
0.55	0.2799	0.4864	0.504	0.55	0.2782	0.4882	0.499	0.55	0.2833	0.4768	0.520
0.60	0.2558	0.4568	0.535	0.60	0.2541	0.4586	0.529	0.60	0.2592	0.4471	0.554
0.65	0.2320	0.4272	0.562	0.65	0.2304	0.4290	0.555	0.65	0.2355	0.4173	0.584
0.70	0.2086	0.3972	0.585	0.70	0.2069	0.3991	0.578	0.70	0.2122	0.3872	0.610
0.75	0.1852	0.3668	0.603	0.75	0.1835	0.3686	0.594	0.75	0.1888	0.3566	0.632
0.80	0.1616	0.3356	0.613	0.80	0.1598	0.3375	0.603	0.80	0.1653	0.3252	0.647
0.85	0.1377	0.3035	0.614	0.85	0.1359	0.3054	0.602	0.85	0.1416	0.2929	0.654
0.90	0.1134	0.2704	0.601	0.90	0.1116	0.2723	0.587	0.90	0.1174	0.2596	0.648
0.95	0.0886	0.2362	0.567	0.95	0.0867	0.2381	0.550	0.95	0.0927	0.2252	0.622
1.00	0.0630	0.2010	0.499	1.00	0.0611	0.2029	0.479	1.00	0.0672	0.1898	0.564
1.05	0.0369	0.1650	0.373	1.05	0.0349	0.1670	0.349	1.05	0.0412	0.1536	0.449
1.10	0.0103	0.1285	0.140	1.10	0.0082	0.1306	0.110	1.10	0.0148	0.1168	0.222

Appendix A

Performance and Analysis of Ship Powering Tests

(HSVA Standard Correlation Method)

1. Correlation Factors and Physical Properties
2. Test Procedure
3. Measured Model Values in Non-dimensional Form
4. Elementary Test Analysis (Without Consideration of Scale Effects)
5. Trial Prediction including Consideration of Scale Effects
6. List of Symbols

1. Correlation Factors and Physical Properties

The tests and their analysis (which will be briefly described in the following sections) are carried out in accordance with Froude's method, i.e. the total resistance is split up into a frictional and a residual component.

The overall submerged length is used as the reference length for both the Reynolds and Froude numbers. The frictional coefficient is calculated according to the 1957 ITTC-Line:

Frictional Resistance Coefficient (Model):

$$C_{Fm} = \frac{0.075}{(\log R_{nm} - 2)^2} \quad \textbf{(1)}$$

Frictional Resistance Coefficient (Ship):

$$C_F = \frac{0.075}{(\log R_n - 2)^2} \quad \textbf{(2)}$$

Moreover, the analysis is based on the following physical properties:

acceleration due to gravity: $g = 9.80665$ m/s^2
density of seawater (15 deg C): $\rho = 1025.9$ kg/m^3
kinematic viscosity of seawater: $v = 1.1882 \cdot 10^{-6}$ m^2/s
density of air: $\rho_A = 1.2255$ kg/m^3

The density and kinematic viscosity of the tank water are calculated based on the actual water temperature measured during the tests.

2. Test Procedure

The model tests relevant to ship powering are carried out in HSVA's large towing tank, which has a length of 300 m, a breadth of 18 m and a depth of 6 m.

The towing carriage is electronically controlled so that, following a short acceleration phase, the selected carriage speed is kept constant during the actual measuring period before decelerating and stopping. The towing carriage is equipped with a computerized data recording and processing system.
During resistance tests the ship model is towed by means of a thin wire which is connected to a load cell mounted inside the model. The tow force measured at the load cell is identical to the resistance of the model. A guide system keeps the model on a straight course while allowing free trim and sinkage.

During the propulsion tests the ship model is driven by its own propeller(s) powered by an electric motor. In order to compensate for the model's increased surface friction (compared with that of the ship) it is additionally towed by a thin wire during the propulsion test. The towing force which is applied is calculated as a function of the model's speed according to:

$$F_D = \rho_m / 2 \cdot V_m^2 \cdot S_m \cdot (C_{Fm} - C_F - C_A) \qquad \textbf{(3)}$$

The correlation allowance C_A is a function of the vessel's length and its block coefficient. The C_A value used is stated at the bottom of the relevant tables of results.

Prior to starting the measurements of thrust and torque in the propeller shaft(s), the propeller revolutions are adjusted so that the speed of the self propelled model matches the pre-selected carriage speed.

The recording of the propulsion test data is done with electronic counters and dynamometers with strain gauges.

For both the resistance and the propulsion tests the individual test runs are carried out for different speeds spaced narrowly enough to provide sufficient accuracy over the requested speed range.

The trim angle θ and the sinkage z_V are recorded to better understand the vessel's resistance and propulsion behaviour.

3. Measured Model Values in Non dimensional Form

The following coefficients are calculated from the data acquired during the model tests.

Froude Number:

$$F_n = \frac{V}{(g \cdot L_{OS})^{0.5}} \tag{4}$$

Reynolds Number:

$$R_n = \frac{V \cdot L_{OS}}{\nu} \tag{5}$$

Residual Resistance Coefficient:

$$C_R = C_{Tm} - C_{Fm} \tag{6}$$

Frictional Resistance Coefficient: C_F (See equations (1) and (2))

Total Resistance Coefficient:

$$C_T = \frac{R_T}{\rho / 2 \cdot V^2 \cdot S} = C_R + C_F + C_A \tag{7}$$

Ship Speed Advance Coefficient:

$$J_V = \frac{V}{n \cdot D} \tag{8}$$

Thrust Coefficient:

$$K_T = \frac{T}{\rho \cdot n^2 \cdot D^4} \tag{9}$$

Torque Coefficient:

$$K_Q = \frac{Q}{\rho \cdot n^2 \cdot D^5} \tag{10}$$

4. Elementary Test Analysis (Without Consideration of Scale Effects)

The conversion of the measured model values to those of the full scale ship is first performed without corrections according to the following equations (Froude scaling):

Speed:

$$V = V_m \cdot \lambda^{0.5} \tag{11}$$

Thrust:

$$T = T_m \cdot \lambda^3 \cdot \rho / \rho_m \tag{12}$$

Torque:

$$Q = Q_m \cdot \lambda^4 \cdot \rho / \rho_m \tag{13}$$

Effective Power:

$$P_E = R_T \cdot V = (R_{Tm} - F_D) \cdot V_m \cdot \lambda^{3.5} \cdot \rho / \rho_m \tag{14}$$

Power delivered at Propeller:

$$P_D = 2\pi \cdot n \cdot Q = 2\pi \cdot n_m \cdot Q_m \cdot \lambda^{3.5} \cdot \rho / \rho_m \tag{15}$$

Revolutions:

$$n = n_m \cdot \lambda^{-0.5} \tag{16}$$

Blockage is accounted for by applying the equation of continuity without considering the deformation of the free water surface. Due to the large cross section of HSVA's towing tank, this method is sufficiently accurate.

The speed, power and propeller revolutions thus determined are compiled in the tables of results separately for each test condition. In these tables the Froude number F_n and the ratio of frictional resistance to total resistance R_F / R_T are given as well as:

Resistance Displacement Coefficient:

$$C_{T\nabla} = \frac{R_T}{\rho / 2 \cdot V^2 \cdot \nabla^{2/3}} \tag{17}$$

Power Displacement Coefficient:

$$C_{D\nabla} = \frac{P_D}{\rho / 2 \cdot V^3 \cdot \nabla^{2/3}} \quad \textbf{(18)}$$

Propulsive Efficiency:

$$\eta_D = P_E / P_D \quad \textbf{(19)}$$

In a following table all hull efficiency elements are listed for the same Froude numbers and under the same conditions, i.e. without any further corrections. These are:

Advance Coefficient:

$$J = \frac{V_A}{n \cdot D} \quad \textbf{(20)}$$

Thrust Deduction Fraction:

$$t = \frac{T - R_T}{T} \quad \textbf{(21)}$$

Taylor Wake Fraction:

$$w = \frac{V - V_A}{V} \quad \textbf{(22)}$$

Hull Efficiency:

$$\eta_H = \frac{1 - t}{1 - w} \quad \textbf{(23)}$$

Propeller Efficiency in Open Water:

$$\eta_O = \frac{T \cdot V_A}{2\pi \cdot n \cdot Q_O} \quad \textbf{(24)}$$

Relative Rotative Efficiency:

$$\eta_R = \frac{K_{Q\,(\text{open water test})}}{K_{Q\,(\text{propulsion test})}} \qquad \textbf{(25)}$$

and also

Thrust Loading Coefficient:

$$C_{Th} = \frac{T}{\rho / 2 \cdot V_A^{\,2} \cdot D^2 \cdot \pi / 4} \qquad \textbf{(26)}$$

In the elementary analysis the wake fraction and the propeller efficiency are determined assuming thrust identity. The propeller open water characteristics are corrected for the friction under fully turbulent flow conditions at the Reynolds number of the model propeller during the propulsion test. This correction takes into account that the propeller influx has a higher degree of turbulence in the "behind" condition than in "open water"

5. Trial Prediction including Consideration of Scale Effects

The added resistance of the zinc anodes, hull roughness and small openings (which are typical of real ships but which are not modelled) are accounted for in the correlation allowance C_A. For larger appendages and/or hull openings not present on the model, an allowance ΔR_T (related to the frictional resistance R_F) is made. Its value is stated at the bottom of the relevant table for the trial prediction. Furthermore, the air resistance of the superstructure and hull R_{AA} is estimated based on the relative velocity of the wind V_R and the area A_V exposed to it.

Air Resistance:

$$R_{AA} = \rho_A / 2 \cdot V_R^2 \cdot A_V \cdot C_{AA} \tag{27}$$

The effective power under trial conditions is:

$$P_E = (R_T + \Delta R_T + R_{AA}) \cdot V \tag{28}$$

The next step in the analysis considers Reynolds number scale effects on the wake as well as on the propeller efficiency. The respective corrections are based on the following assumptions:

(a) The thrust deduction fraction *t* determined for the model is the same as for the full scale ship.

(b) The relative rotative efficiency η_R will not differ between model and full scale propeller.

(c) The wake fraction (being lower for the ship due to the higher Reynolds number) can be determined by a constant correction factor (1-w / 1-w_m), kept constant over the whole speed range. (This factor is stated at the bottom of the respective tables).

(d) The open water efficiency η_O of the full scale propeller is greater than that of the model propeller because of scale effect on the viscous drag of the blades. The respective correlation is done by means of the Strip method according to Streckwall, which has been described in brief in the 2/2012 issue of HSVA's newsletter NewsWave.

See also: Streckwall, H. Greitsch, L. and Bugalski, T.: 'Development of a Strip Method Proposed to Serve as a New Standard for Propeller Performance Scaling', Ship Technology Research Vol. 60, Nr.2, 2013

The propeller revolutions of the ship differ from those calculated by equation (16) due to the relatively lower wake the higher propeller loading as well as the higher efficiency of the full scale propeller compared to that of the model. The correct number of revolutions is determined using the following procedure:

The dimensionless ratio $[K_T / J^2]_B$, which does not include the unknown number of revolutions, is calculated from the data derived from the propulsion test, i.e. from the "behind" condition according to:

$$\left[\frac{K_T}{J^2}\right]_B = \frac{T}{\rho \cdot V_A^2 \cdot D^2} = \frac{T_m}{\rho_m \cdot V_{Am}^2 \cdot D_m^2} \cdot \left[\frac{1 - w_m}{1 - w}\right]^2 \cdot \frac{R_T + \Delta R_T + R_{AA}}{R_T} \qquad \textbf{(29)}$$

The factor $[(1-w_m) / (1-w)]^2$ accounts for the relative smaller wake of the full scale ship compared with that of the model and the factor $[(R_T + \Delta R_T + R_{AA}) / R_T]$ for the higher propeller loading under trial conditions. The equation implies the identity of the thrust deduction factors for model and ship.

The actual advance ratio J is determined by interpolating in the $(K_T / J^2)_O$ versus J curve using the $(K_T / J^2)_B$ value. For this step the full scale open water characteristic including corrections is used. Subsequently the actual number of revolutions and power to be delivered at the propeller are calculated from the following expressions:

$$n = \frac{V \cdot (1 - w)}{D \cdot J} \qquad \textbf{(30)}$$

$$K_{QB} = K_{Q0} / \eta_R \qquad \textbf{(31)}$$

$$P_D = 2\pi \cdot n \cdot Q = 2\pi \cdot \rho \cdot n^3 \cdot D^5 \cdot K_{QB} \qquad \textbf{(32)}$$

K_{QB} is the torque coefficient of the full size propeller(s) for the behind condition.

In the standard HSVA extrapolation method a hull roughness of 150 microns is taken into account. For hull roughness values other than 150 microns the propulsion data for the full scale ship is calculated to include a difference in frictional resistance ΔC_{F_R} in addition to the standard ITTC friction coefficient equation (2).

$$\Delta C_{F_R} = C_{F_R} - C_{F_{R,KR=150}} \qquad \textbf{(33)}$$

The modified frictional resistance coefficients used in equation (33) are calculated according to the following empirical HSVA formula:

$$C_{F_R} = 0.075 / [\log(Rn/(1 + 0.0011 \frac{K_R}{L} Rn)) - 2]^2 \qquad \textbf{(34)}$$

with

K_R average hull roughness [m]
L ship length [m]

6. List of Symbols

The following list shows some relevant ITTC standard symbols and their computer variable names.

Symbol in Report	**Computer Symbols**	**Symbol Name**
A_V	AV	Area Exposed to Wind
C_A	CA	Correlation Allowance Coefficient
C_{AA}	CAA	Air Resistance Coefficient
$C_{D\nabla}$	CDVOL	Power-Displacement Coefficient
C_F	CF	Frictional Resistance Coefficient
C_R	CR	Residuary Resistance Coefficient
C_T	CT	Total Resistance Coefficient
C_{Th}	CTH	Thrust Loading Coefficient
$C_{T\nabla}$	CTVOL	Resistance-Displacement Coefficient
∇	DISV	Displacement Volume
D	DP	Propeller Diameter
F_D	FD	Towing Force in Propulsion Test
F_n	FN	Froude Number
g	G	Acceleration due to Gravity
J	ADVC	Propeller Advance Coefficient
J_v	ADVCV	Ship Advance Coefficient
K_Q	KQ	Torque Coefficient
K_T	KT	Thrust Coefficient
L_{OS}	LOS	Overall Submerged Length
n	N	Propeller Revolutions per Minute
P_D	PD	Delivered Power at Propeller
P_E	PE	Effective Power
Q	Q	Torque
R_{AA}	RAA	Wind Resistance
R_F	RF	Frictional Resistance
R_n	RN	Reynolds Number
R_T	RT	Total Resistance
ΔR_T	DRT	Additional Resistance
S	S	Wetted Surface
T	T	Thrust
t	THDF	Thrust Deduction Fraction

Symbol in Report	**Computer Symbols**	**Symbol Name**
V	V	Speed
V_A	VA	Speed of Advance of Propeller
V_R	VR	Relative Wind Velocity
w	WFT	Taylor Wake Fraction
z_V	ZV	Sinkage of Ship
η_D	ETAD	Propulsive Efficiency
η_H	ETAH	Hull Efficiency
η_O	ETAO	Open-Water Propeller Efficiency
η_R	ETAR	Relative Rotative Efficiency
θ	TETP	Angle of Trim
λ	SCALE	Ship-Model Scale Ratio
ν	NU	Kinematic Viscosity
ρ	RHO	Mass Density
ρ_A	RHOA	Mass Density of Air

Notes:

1. All symbols followed with a subscript of either "O" or "B" are open-water or "behind" condition values respectively.
2. All symbols followed by a subscript "m" are Model values. Ship values are written without subscripts.

Appendix B

Model Tests with Azimuthing Drives

Procedure of Evaluation

In addition to the self-propulsion test itself, open water tests with the propeller only and also with the propeller/pod unit are used for the evaluation of Azimuth propulsion. During both the propulsion tests and the open water test with the propeller/pod unit the following quantities are measured:

- model speed
- propeller speed
- propeller torque
- system thrust

The test results are analysed according to the HSVA Standard Method, which is described in **Appendix A**, however with the following modifications:

(a) The model appendage resistance (Azimuth drive resistance) is converted to full scale as described in section (e.3) below. The wetted surface of the pod housing is not taken into account when determining the towing force during the propulsion test.

(b) As only the system thrust T_{sy} of the propeller/pod unit is measured, the hull efficiency elements are valid for the system thrust and not for the propeller thrust.

(c) The thrust deduction fraction t is calculated using the system thrust and the bare hull resistance according to:

$$t = \frac{T_{sy} - R_{T_{barehull}}}{T_{sy}}$$

(d) The wake fraction w_T and the efficiencies η_R and η_O are determined using KT-identity (based on system thrust T_{sy}). In addition to this w_Q is also determined based on KQ-identity.

(e) The propeller/pod unit open water efficiency is corrected as follows:

(e.1) ΔKT_1 and ΔKQ_1 values corresponding to the propeller are determined by the strip method acc. to Streckwall (HSVA standard procedure).

(e.2) The open water test results are corrected for Reynold's number of the propulsion test using the corresponding ΔKT_1 and ΔKQ_1 values as determined under (e.1) above. A further correction, ΔKT_2 is made to account for scale effects on the pod housing drag. This correction is done using a simplified strip method (Mewis/Praefke, 2003). The resulting open water values are used to account for the difference in Reynold's number between the open water test and the propulsion test. These corrected data are used for the determination of w_T and w_Q and η_R.

(e.3) The open water test results for the propeller/pod units are corrected also for full scale using the corresponding ΔKT_1 and ΔKQ_1 values as determined under (e.1) above. A further correction, ΔKT_2 is made to account for scale effects on the pod housing drag. The resulting open water characteristic is used for the full scale ship.

Appendix I

Load Variation Coefficients for Ship Speed Trials

(HSVA Standard Method)

7. General

According to revision 1.1 of the ITTC recommended procedures and guidelines 7.5-04-01-01.2 dated 2014, propulsive efficiency and shaft rate of speed and power trials are corrected based on the coefficients ξ_p, ξ_n and ξ_v obtained from load variation tests according to the following equations:

$$P_{DC} = P_{DM} - \frac{\Delta R_M \cdot v_{SM}}{\eta_{D0}} \cdot \left(1 - \frac{P_{DM}}{P_{DC}} \cdot \xi_p\right) \qquad \textbf{(1)}$$

$$n_C = \frac{n_M}{\xi_n \cdot \frac{P_{DM} - P_{DC}}{P_{DC}} + \xi_v \cdot \frac{\Delta v}{v_{SM}} + 1} \qquad \textbf{(2)}$$

8. Model test setup

The load variation model tests are carried out at the same draught as the planned sea trial draught and at one speed similar to the predicted EEDI (75 % MCR) speed. The tested speed should also be included in the standard resistance and self-propulsion test sequence. The load variation test consists of four self-propulsion test runs, each one at a different rate of revolution. The rates of revolution are selected such that:

$$\Delta R \approx [-0.1; 0; +0.1; +0.2] \cdot (F_D - F_X) \cdot \lambda^3 \cdot \frac{\rho_s}{\rho_m} \qquad \textbf{(3)}$$

9. Dependency of propulsion efficiency with resistance increase

The fraction between the propulsion efficiency from the load variation test to the normal self-propulsion test is plotted as a function of the added resistance fraction. The slope of the linear least squares fit curve corresponds to the factor ξ_p.

10. Dependency of shaft rate with power increase

The fraction between the change in shaft speed from the load variation test to the normal self-propulsion test is plotted as a function of the added delivered power fraction. The slope of the linear least squares fit curve corresponds to the factor ξ_n.

11. Dependency of shaft rate with speed change

The shaft rate from the load variation is plotted as a function of the corresponding resistance. For other speeds, this trend is assumed to be parallel to that line and pass through the point determined in self-propulsion tests. The slope of the $\Delta n/n - \Delta v/v$ linear least squares fit curve corresponds to the factor ξ_v.

12. List of Symbols

The list of symbols used by the HSVA Standard Method is given as follows:

Symbol in Report	**Symbol Name**
F_D	Skin friction correction force as in self-propulsion test
F_X	External tow force measured during load variation test
n_C	Corrected rpm of the sea trial
n_M	Measured rpm during sea trial
P_{DC}	Delivered power corrected to ideal condition
P_{DM}	Measured delivered power during sea trial
v_{SM}	Ship speed
ΔR	Difference in (full scale) resistance
ΔR_M	Resistance increase from external factors
Δv	Difference in ship speed
η_{D0}	Propulsion efficiency coefficient in ideal condition
λ	Scale factor
ξ_n	Revolution overload factor
ξ_p	Power overload factor
ξ_v	Speed overload factor
ρ_m	Water density during model test
ρ_s	Full scale water density

December, 2015

Appendix Z

Specification
Of Large Towing Tank

(HSVA Facilities)

1. General
2. Towing Carriage
3. Computerized Planar Motion Carriage (CPMC)
4. Wavemaker

1. General

The following tests can be performed in the large towing tank:

- resistance tests,
- self-propulsion tests (Continental or British method, bollard pull, hawser, …),
- horizontal planar motion testing (Towing and tracking, CPMC),
- flow observation (paint and underwater TV),
- wake measurements,
- propeller open water tests,
- seakeeping tests (in regular or irregular waves),
- measurement of forces and pressures acting on hulls or offshore structures,
- rolling tests,
- mooring tests,
- static submarine tests,
- non-stationary submarine tests.

The dimensions of the tank are:

Length	**300.00 m**
Breadth	**18.00 m**
Depth	**5.60 m**

A general overview of the tank is given below:

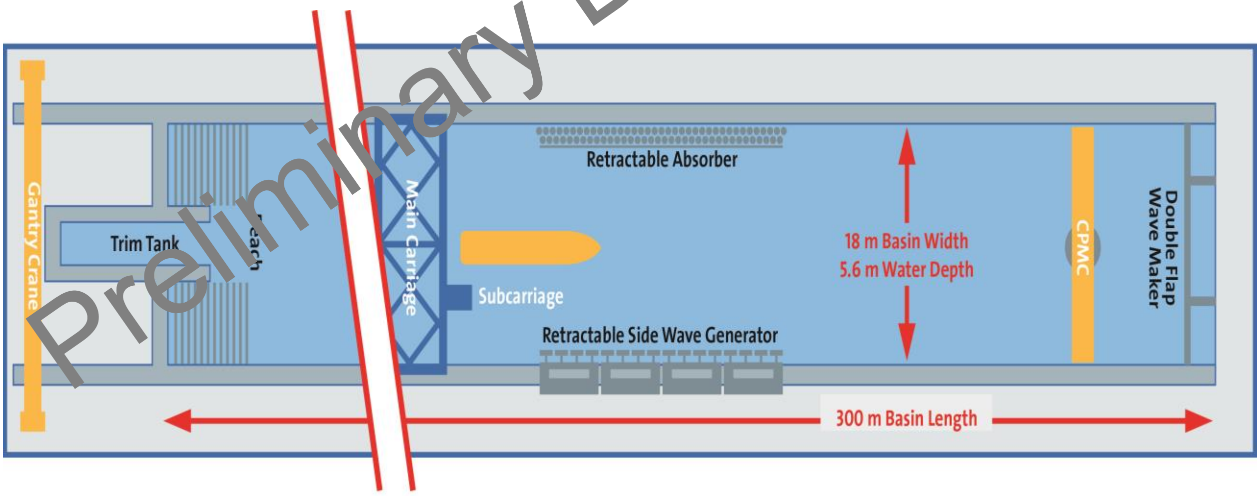

Accordingly model size ranges of **2 - 12 m** can be tested.

The Models are either controlled by human operators or fully automatic by process control computers. The model tests and test results are digitally monitored and stored.

2. Towing Carriage

The main carriage moves in longitudinal direction with four wheels over two rails at the edge of the large towing tank. Accordingly, the width of the main carriage is **18 m**. To ease operability and improve accessibility, the main carriage is supported by a sub carriage, moving in transverse direction.

With a total power of 560 kW, provided by 8 servo drives with 70 kW each, the towing carriage reaches a maximum speed of 10 m/s. The maximum acceleration is 0.80 m/s² and the maximum deceleration is 1.40 m/s².

Towing Carriage max. speed	**10.00 m/s**
Towing Carriage max. acceleration:	**0.80 m/s²**
Towing Carriage max. deceleration	**1.40 m/s²**

3. Computerized Planar Motion Carriage (CPMC)

The CMPC operates in conjunction with the towing carriage. It reaches a maximum longitudinal speed of 4.00 m/s and a maximum transverse speed of 1.9 m/s. Additional the CMPC can reach a maximum yaw rate of 23 °/s.

CMPC max. speed, longitudinal	**4.00 m/s**
CMPC max. speed, transverse	**1.90 m/s**
CMPC max. yaw rate	**23 °/s**

4. Wavemaker

The large towing tank is equipped with two wave generators: an 18 meter wide hydraulic duplex flap type wave generator at the end of the basin and a side wave generator with the appropriate absorber in the middle of the basin. To absorb the longitudinal waves, sparred wood gratings are installed at the trimming tank side.

The side wave generator is a Snake type wavemaker consisting of 80 flaps each of 0.5m in width, for beam and oblique waves in the range from 20° to 160° wave direction. Regular waves, irregular long- and short-crested seas, wave packets, user-defined wave trains and spectra can be generated. Various methods for wave generation are possible:

- regular waves, computer generated wave trains with chosen spectra,
- regular waves, wave packets and reproduction of measured wave trains,
- irregular waves, spectra composed of at least 100 single components (electro-mechanical).

The maximum wave height is **0.5 m**.

10. Attachment 3 ─ HSVA Wake Survey Test Report (Reference 6)

HAMBURGISCHE SCHIFFBAU-VERSUCHSANSTALT GMBH

THE HAMBURG SHIP MODEL BASIN

Report
WM-2023-009

3-D-Wake Measurement for an Antarctic Research Vessel (ARV)

HSVA Model No. 5626-00010

Customer:
Leidos

HSVA

Document Control Sheet

Customer:	Leidos
Project:	Antarctic Research Vessel (ARV)
Contract No.:	617456
Report No.:	WM-2023-009
Title:	3-D-Wake Measurement for an Antarctic Research Vessel (ARV)
File:	617456-WM-2023-009.pdf

Rev.	Date	Reason for Issue	prepared	checked	approved
-	22-06-2023	Final report	KLa	CS	NR

Summary: A three-dimensional wake measurement was performed for an Antarctic Research Vessel. The measurement was performed with HSVA model No. 5626-00010 - hull variant 11. A wake fraction of $w_{nom} = 0.104$ was obtained which is lower than the value of the initial hull (WM-2022-018) and a more common value for a vessel with this propulsion concept and block coefficient.
The axial velocity distribution shows a relatively wide zone of slightly decelerated flow in the upper inner quadrant of the propeller plane. In addition, a second wake peak occurs, but only at the outer radii; it has to be noticed that the two outermost radii are larger than the propeller disc itself. The flow is generally directed inwards. The wake field is essentially relatively smooth and nearly undisturbed.

Keywords: Three-dimensional wake measurement, Antarctic Research Vessel

Report
WM-2023-009

3-D-Wake Measurement for an Antarctic Research Vessel (ARV)

Leidos
11951 Freedom Drive
20190 Reston
USA

HSVA Model No. 5626-00010

Hamburg, June 2023

HAMBURGISCHE SCHIFFBAU-
VERSUCHSANSTALT GmbH

Katrin Lassen
- Project Manager -

i.V.
Nils Reimer
- Division Manager AT -

Table of Contents

1 Introduction

On behalf of Leidos a three-dimensional wake measurement was carried out at HSVA for an Antarctic Research Vessel (ARV). The test was performed with HSVA model No. 5626-00010 - hull variant 11. The wake measurement for the initial hull was documented in report WM-2022-018.

2 Test Procedure and Test Conditions

The wake measurement was carried out in the large towing tank of the HSVA behind the ship model No. 5626-00010, which was built to a scale of 1 : 24.384. The three-dimensional velocity vectors were determined by means of 6 five-hole pitot tubes, that were mounted on a two-armed holder at 6 different radii.
In opposite to the normal procedure for conventional hull forms, this holder was mounted on a temporary support from behind the ship model. The support was adjusted to maintain the longitudinal position and the inclination angle of the propeller plane of the azimuth drive. The latter was not installed during the measurement. The result of the measurement describes the *nominal* wake field of the ship model.
During the test runs the holder was rotated over one complete revolution. A sketch of the arrangement is given in Fig. 1.

The local dynamic pressure values at the holes of the probes were led to a set of electronic pressure transducers by water-filled, flexible plastic tubes. The transformation of the pressure differences into the components of the local velocity vectors was performed with the help of calibration arrays for each probe. The calibration arrays of the five-hole pitot tubes allow a reliable evaluation up to a flow angle of 30° against the direction of the shaft center line. Whenever the velocity vector at a measuring point was outside of this calibration range, a simplified axial evaluation was used to get additional input for the further analysis of the axial velocity components. In this case the average pressure level at the side holes of the probe was compared to the front hole pressure by use of Bernoulli's law.

The measurement was carried out at a draught of 9.906 m and at a model speed corresponding to 9.00 kts. The complete test conditions are summarized in Tab. 1.

3 Evaluation and Manner of Presentation

The velocity values v_0, v_x, v_t and v_r at the individual measuring points were made non-dimensional with the ship model speed v_m. They are given in Tabs. 2 to 7 for the 6 measuring radii and are plotted against the angle of circumference ϕ in Figs. 2 to 4. The definition of ϕ as well as the sign convention for the velocity components is given in Fig. 1. The non-dimensional radii denoted in Figs. 2 to 4 were calculated with an assumed propeller diameter given in Tab. 1. In Figs. 2 to 4 the radii are marked by different symbols. Those points, which could be determined by the simplified axial evaluation method only, are marked in Fig. 2 by a X-symbol. In case that even this method has failed the missing symbols were replaced by smooth dotted lines between the adjoining data points. This also holds for Figs. 3 and 4.

Fig. 5 shows the sum $\vec{v_t} + \vec{v_r}$ as a vector diagram. In Fig. 6 the curves of constant axial velocity v_x are given. A combination of both is shown in the color plot in Fig. 7.

For each radius the mean velocity v_A^* was obtained by Simpson-integration over the circumference, using the data points shown in Fig. 2:

$$\frac{v_A^*}{v_m} = \frac{1}{2\pi} \cdot \int_0^{2\pi} \frac{v_x}{v_m} d\phi \tag{1}$$

These values are plotted in Fig. 8 as a function of the non-dimensional radius x. A secondary Simpson-integration of the v_A^*-values in the radial direction from $x_0 = R_0/R$ to $x_1 = 1$ led to the mean inflow velocity v_A, averaged over the whole propeller disc:

$$\frac{v_A}{v_m} = \frac{2}{x_1^2 - x_0^2} \cdot \int_{x_0}^{x_1} \frac{v_A^*}{v_m} x dx \tag{2}$$

For $x = 0$ no measurement result was available to serve as a supporting point for this integration. Instead, the mean speed over all measuring radii was assumed at this position. The variation of the mean value v_A with the upper integration limit x_1 is given in Tab. 10 and is plotted in Fig. 9. The mean values $v_{t,mean}$ of the tangential components were determined accordingly to v_A and are given in Tab. 10 as well.

Furthermore, a harmonic analysis of the axial velocity field was carried out based on the data points given in Fig. 2. The results are summarized in Tab. 9, where the Fourier-coefficients a_n and b_n up to the 9^{th} order are listed for each radius:

$$\frac{v}{v_m} = \sum_{n=0}^{9} (a_n cos(n\phi) + b_n sin(n\phi)) \tag{3}$$

4 Result and Conclusion

HSVA was contracted by Leidos to carry out a three-dimensional wake measurement for an Antarctic Research Vessel (ARV). The measurement was performed at 9.906 m draught and at the speed of 9.00 kts with HSVA model No. 5626-00010 - hull variant 11. The wake measurement for the initial hull was documented in report WM-2022-018.

From equation (2) a nominal wake fraction of $w_{nom} = 0.104$ was obtained which is lower than the value of the initial hull (WM-2022-018) and a more common value for a vessel with this propulsion concept and block coefficient.

The axial velocity distribution (Fig. 2) shows a relatively wide zone of slightly decelerated flow in the upper inner quadrant of the propeller plane. In addition, a second wake peak occurs, but only at the outer radii; it has to be noticed that the two outermost radii are larger than the propeller disc itself. The flow is generally directed inwards. The wake field is essentially relatively smooth and nearly undisturbed.

5 List of Symbols

a_n, b_n	Fourier-coefficients
r	Radius under consideration
R	Assumed propeller radius
R_0	Assumed propeller hub radius
v_0	Local flow velocity in direction of the flow
v_x	Local axial velocity component
v_t	Local tangential velocity component
v_r	Local radial velocity component
v_m	Model speed
v_A^*	Inflow velocity, averaged over the circumference at a certain radius
v_A	Inflow velocity, averaged over the whole propeller disc
w_{nom}	Taylor wake fraction $(1 - v_A/v_m)$
x	Non-dimensional radius r/R
x_0, x_1	Integration limits for calculation of v_A
ϕ	Angle of circumference

6 List of Tables

7 List of Figures

Tables

Report No.	WM-2023-009	
Test No.	23-0245	
Type of Ship	Antarctic Research Vessel	
Ship Model No.	5626-00010	
Scale	24.384	
Ship Speed	9.00	kts
Length Between Perpendiculars	108.720	m
Breadth in the Waterline	24.400	m
Draught AP	9.906	m
Draught FP	9.906	m
Displacement	13385	m^3
Block Coefficient	0.509	
Distance Measuring Plane - Frame 0	14.563	m
Tilt Angle α	4°	
Water Temperature	15.3	°C
kinematic Viscosity of Water (acc. ITTC 63)	0.1130E-05	m^2/s
Evaluation Based on Propeller No.	2288	
Diameter	4.88	m

Table 1: Test Conditions.

3D Wake Survey

Table of the Velocity Components

HSVA Model No. 5626-00010

Leidos

Model Tests for an ARV

Test No. WM-2023-009

Radius r = 140.0 mm   r/R = 1.400

Phi/deg	Vo/Vm	Vx/Vm	Vr/Vm	Vt/Vm
0	0.965	0.962	0.016	-0.067
10	0.964	0.962	0.023	-0.065
20	0.965	0.962	0.031	-0.066
30	0.967	0.964	0.040	-0.066
40	0.963	0.960	0.052	-0.061
50	0.947	0.943	0.068	-0.05[illegible]
60	0.961	0.957	0.076	-0.052
70	0.960	0.955	0.084	-0.043
80	0.954	0.948	0.102	-0.031
90	0.955	0.948	0.114	-0.017
100	0.951	0.942	0.128	0.007
110	0.948	0.936	0.148	0.047
120	0.899	0.880	0.158	0.101
130	0.767	0.748	0.089	0.141
140	0.652	0.639	-0.028	0.124
150	0.655	0.647	-0.092	0.049
160	0.553	0.538	-0.125	0.022
170	0.331	0.313	-0.102	-0.041
180	0.267	0.251	-0.076	-0.055
190	0.360	0.346	-0.040	-0.094
200	0.666	0.657	-0.048	-0.101
210	0.761	0.756	-0.061	-0.061
220	0.792	0.785	-0.075	-0.064
230	0.831	0.823	-0.095	-0.066
240	0.885	0.877	-0.096	-0.070
250	0.884	0.878	-0.081	-0.068
260	0.897	0.891	-0.066	-0.073
270	0.914	0.909	-0.056	-0.077
280	0.905	0.901	-0.041	-0.073
290	0.920	0.916	-0.034	-0.073
300	0.927	0.924	-0.024	-0.073
310	0.934	0.931	-0.016	-0.070
320	0.935	0.932	-0.011	-0.068
330	0.938	0.936	-0.007	-0.068
340	0.943	0.940	-0.001	-0.067
350	0.944	0.941	0.005	-0.066

Table 2: Table of the Velocity Components, r/R = 1.400

3D Wake Survey

Table of the Velocity Components

HSVA Model No. 5626-00010

Leidos

Model Tests for an ARV

Test No. WM-2023-009

Radius r = 120.0 mm   r/R = 1.200

Phi/deg	Vo/Vm	Vx/Vm	Vr/Vm	Vt/Vm
0	0.955	0.952	-0.004	-0.066
10	0.956	0.954	0.004	-0.066
20	0.945	0.943	0.017	-0.061
30	0.936	0.934	0.032	-0.056
40	0.962	0.960	0.033	-0.059
50	0.962	0.960	0.044	-0.05[illegible]
60	0.952	0.949	0.061	-0.039
70	0.963	0.960	0.066	-0.032
80	0.963	0.960	0.076	-0.017
90	0.963	0.959	0.090	0.003
100	0.963	0.958	0.099	0.029
110	0.963	0.955	0.101	0.063
120	0.923	0.911	0.097	0.111
130	0.840	0.827	0.046	0.136
140	0.776	0.764	-0.030	0.131
150	0.750	0.738	-0.088	0.099
160	0.720	0.708	-0.112	0.067
170	0.608	0.595	-0.118	0.030
180	0.521	0.512	-0.093	0.006
190	0.556	0.550	-0.078	-0.030
200	0.724	0.719	-0.075	-0.046
210	0.740	0.735	-0.082	-0.030
220	0.779	0.771	-0.106	-0.040
230	0.795	0.785	-0.116	-0.049
240	0.873	0.862	-0.122	-0.064
250	0.914	0.905	-0.110	-0.068
260	0.919	0.912	-0.093	-0.068
270	0.934	0.928	-0.082	-0.071
280	0.936	0.930	-0.066	-0.073
290	0.944	0.940	-0.055	-0.072
300	0.947	0.943	-0.045	-0.072
310	0.950	0.947	-0.036	-0.072
320	0.954	0.951	-0.030	-0.071
330	0.958	0.955	-0.025	-0.071
340	0.961	0.958	-0.018	-0.070
350	0.962	0.959	-0.011	-0.068

Table 3: Table of the Velocity Components, r/R = 1.200

3D Wake Survey

Table of the Velocity Components

HSVA Model No. 5626-00010

Leidos

Model Tests for an ARV

Test No. WM-2023-009

Radius r = 100.0 mm r/R = 1.000

Phi/deg	Vo/Vm	Vx/Vm	Vr/Vm	Vt/Vm
0	0.963	0.959	0.031	-0.075
10	0.963	0.959	0.035	-0.075
20	0.960	0.956	0.049	-0.071
30	0.961	0.957	0.059	-0.067
40	0.966	0.961	0.067	-0.061
50	0.979	0.975	0.067	[illegible]
60	0.961	0.956	0.091	-0.043
70	0.953	0.948	0.101	-0.027
80	0.960	0.954	0.104	-0.019
90	0.951	0.944	0.113	0.006
100	0.944	0.935	0.121	0.033
110	0.937	0.927	0.121	0.068
120	0.914	0.902	0.108	0.104
130	0.866	0.853	0.064	0.135
140	0.827	0.814	0.023	0.142
150	0.787	0.779	-0.034	0.111
160	0.757	0.750	-0.063	0.083
170	0.654	0.649	-0.064	0.057
180	0.592	0.590	-0.052	0.024
190	0.595	0.594	-0.038	-0.003
200	0.657	0.655	-0.054	-0.005
210	0.701	0.698	-0.061	-0.008
220	0.709	0.704	-0.086	-0.017
230	0.773	0.764	-0.109	-0.053
240	0.828	0.820	-0.091	-0.060
250	0.904	0.895	-0.097	-0.080
260	0.919	0.912	-0.074	-0.083
270	0.925	0.919	-0.058	-0.080
280	0.933	0.927	-0.053	-0.089
290	0.935	0.930	-0.039	-0.087
300	0.934	0.930	-0.023	-0.084
310	0.939	0.935	-0.013	-0.086
320	0.935	0.932	-0.003	-0.083
330	0.937	0.934	0.005	-0.083
340	0.939	0.935	0.013	-0.082
350	0.940	0.937	0.023	-0.078

Table 4: Table of the Velocity Components, r/R = 1.000

3D Wake Survey

Table of the Velocity Components

HSVA Model No. 5626-00010

Leidos

Model Tests for an ARV

Test No. WM-2023-009

Radius r = 80.0 mm   r/R = 0.800

Phi/deg	Vo/Vm	Vx/Vm	Vr/Vm	Vt/Vm
0	0.963	0.960	0.007	-0.074
10	0.964	0.961	0.016	-0.072
20	0.979	0.977	0.021	-0.070
30	1.001	0.998	0.029	-0.071
40	0.966	0.963	0.049	-0.057
50	0.966	0.963	0.058	-0.05[illegible]
60	0.985	0.982	0.063	-0.044
70	0.964	0.960	0.075	-0.027
80	0.959	0.956	0.082	-0.010
90	0.963	0.959	0.087	0.010
100	0.962	0.957	0.086	0.035
110	0.959	0.954	0.078	0.063
120	0.945	0.938	0.063	0.094
130	0.919	0.910	0.040	0.121
140	0.880	0.871	0.002	0.128
150	0.853	0.843	-0.037	0.126
160	0.827	0.816	-0.066	0.114
170	0.755	0.745	-0.078	0.092
180	0.694	0.687	-0.076	0.063
190	0.661	0.656	-0.070	0.043
200	0.658	0.653	-0.070	0.041
210	0.712	0.706	-0.089	0.024
220	0.716	0.707	-0.111	0.021
230	0.792	0.782	-0.124	-0.018
240	0.823	0.813	-0.122	-0.037
250	0.883	0.873	-0.119	-0.058
260	0.939	0.930	-0.109	-0.071
270	0.938	0.931	-0.090	-0.071
280	0.946	0.940	-0.075	-0.076
290	0.937	0.932	-0.061	-0.078
300	0.945	0.940	-0.047	-0.079
310	0.945	0.941	-0.036	-0.080
320	0.948	0.944	-0.027	-0.080
330	0.949	0.945	-0.018	-0.081
340	0.954	0.951	-0.008	-0.079
350	0.956	0.953	0.002	-0.078

Table 5: Table of the Velocity Components, r/R = 0.800

3D Wake Survey

Table of the Velocity Components

HSVA Model No. 5626-00010

Leidos

Model Tests for an ARV

Test No. WM-2023-009

Radius r = 60.0 mm r/R = 0.600

Phi/deg	Vo/Vm	Vx/Vm	Vr/Vm	Vt/Vm
0	0.960	0.954	0.068	-0.088
10	0.953	0.946	0.083	-0.079
20	0.964	0.957	0.091	-0.075
30	0.965	0.957	0.103	-0.067
40	0.969	0.961	0.112	-0.055
50	0.971	0.962	0.120	-0.04[illegible]
60	0.970	0.961	0.129	-0.029
70	0.965	0.956	0.131	-0.010
80	0.960	0.950	0.139	0.008
90	0.960	0.950	0.137	0.030
100	0.953	0.943	0.134	0.050
110	0.952	0.941	0.123	0.071
120	0.945	0.934	0.107	0.092
130	0.943	0.933	0.083	0.107
140	0.928	0.918	0.062	0.119
150	0.901	0.892	0.035	0.117
160	0.880	0.872	0.008	0.113
170	0.847	0.840	-0.013	0.105
180	0.816	0.810	-0.035	0.089
190	0.807	0.802	-0.046	0.071
200	0.803	0.798	-0.064	0.062
210	0.807	0.802	-0.071	0.043
220	0.837	0.833	-0.081	0.025
230	0.824	0.820	-0.080	0.011
240	0.860	0.856	-0.080	-0.015
250	0.919	0.915	-0.072	-0.039
260	0.912	0.909	-0.054	-0.053
270	0.930	0.927	-0.050	-0.061
280	0.933	0.930	-0.033	-0.071
290	0.938	0.934	-0.023	-0.078
300	0.945	0.941	-0.008	-0.083
310	0.944	0.940	0.007	-0.088
320	0.945	0.940	0.019	-0.089
330	0.945	0.940	0.031	-0.090
340	0.944	0.939	0.043	-0.087
350	0.947	0.942	0.055	-0.084

Table 6: Table of the Velocity Components, r/R = 0.600

```
3D Wake Survey

Table of the Velocity Components

HSVA Model No. 5626-00010

Leidos

Model Tests for an ARV

Test No. WM-2023-009
```

Radius r = 40.0 mm r/R = 0.400

Phi/deg	Vo/Vm	Vx/Vm	Vr/Vm	Vt/Vm
0	0.946	0.941	0.028	-0.095
10	0.949	0.944	0.039	-0.090
20	0.968	0.963	0.046	-0.089
30	0.994	0.989	0.052	-0.086
40	0.949	0.944	0.072	-0.064
50	0.951	0.946	0.080	-0.05[illegible]
60	0.975	0.970	0.080	-0.044
70	0.948	0.944	0.090	-0.023
80	0.939	0.935	0.092	-0.002
90	0.944	0.940	0.092	0.018
100	0.941	0.936	0.086	0.037
110	0.940	0.935	0.075	0.055
120	0.937	0.933	0.060	0.072
130	0.934	0.929	0.042	0.088
140	0.920	0.914	0.023	0.100
150	0.909	0.903	0.000	0.101
160	0.894	0.888	-0.021	0.102
170	0.878	0.872	-0.044	0.094
180	0.858	0.851	-0.061	0.085
190	0.850	0.844	-0.081	0.066
200	0.834	0.827	-0.095	0.051
210	0.865	0.857	-0.111	0.030
220	0.843	0.835	-0.114	0.028
230	0.891	0.883	-0.113	-0.007
240	0.875	0.867	-0.115	-0.022
250	0.912	0.904	-0.109	-0.043
260	0.935	0.928	-0.101	-0.063
270	0.931	0.923	-0.089	-0.072
280	0.933	0.926	-0.075	-0.087
290	0.937	0.931	-0.062	-0.093
300	0.934	0.928	-0.050	-0.097
310	0.935	0.930	-0.035	-0.099
320	0.938	0.932	-0.023	-0.103
330	0.940	0.934	-0.010	-0.104
340	0.944	0.939	0.002	-0.102
350	0.946	0.941	0.016	-0.098

Table 7: Table of the Velocity Components, r/R = 0.400

3D WAKE SURVEY WM-2023-009

Harmonic Analysis of the Axial Components
List of Fourier-Coefficients

N	r = 40.0 mm, x = 0.400 AN	r = 40.0 mm, x = 0.400 BN	r = 60.0 mm, x = 0.600 AN	r = 60.0 mm, x = 0.600 BN
0	0.9167	0.0000	0.9112	0.0000
1	0.0429	0.0200	0.0588	0.0262
2	-0.0156	-0.0087	-0.0273	-0.0179
3	0.0046	0.0137	0.0060	0.0151
4	-0.0011	-0.0011	-0.0018	-0.0036
5	-0.0019	-0.0003	0.0004	-0.0013
6	-0.0020	0.0009	-0.0012	0.0020
7	-0.0011	0.0020	0.0029	-0.0000
8	-0.0025	-0.0018	-0.0006	-0.0019
9	-0.0033	-0.0016	-0.0007	[illegible]

N	r = 80.0 mm, x = 0.800 AN	r = 80.0 mm, x = 0.800 BN	r = 100.0 mm, x = 1.000 AN	r = 100.0 mm, x = 1.000 BN
0	0.8887	0.0000	0.8662	0.0000
1	0.1138	[illegible]	0.1340	0.0282
2	-0.0577	[illegible]	-0.0732	-0.0164
3	0.0203	0.0286	0.0281	0.0185
4	-0.0014	-0.0079	-0.0067	-0.0052
5	[illegible]	0.0024	0.0033	0.0006
6	[illegible]	-0.0015	-0.0062	0.0006
7	[illegible]	0.0051	0.0119	0.0013
8	-0.0037	-0.0035	-0.0073	-0.0017
9	-0.0007	-0.0010	0.0058	0.0032

N	r = 120.0 mm, x = 1.200 AN	r = 120.0 mm, x = 1.200 BN	r = 140.0 mm, x = 1.400 AN	r = 140.0 mm, x = 1.400 BN
0	0.8679	0.0000	0.8275	0.0000
1	0.1423	0.0140	0.2041	0.0032
2	-0.0878	-0.0065	-0.1300	0.0277
3	0.0409	-0.0067	0.0814	-0.0265
4	-0.0142	0.0018	-0.0441	0.0174
5	0.0086	-0.0018	0.0304	0.0008
6	-0.0123	-0.0042	-0.0286	-0.0046
7	0.0190	0.0036	0.0306	0.0071
8	-0.0160	-0.0038	-0.0274	-0.0021
9	0.0122	0.0039	0.0187	-0.0024

Table 8: Fourier Coefficients, Axial Components

3D WAKE SURVEY WM-2023-009

Harmonic Analysis of the Tangential Components
List of Fourier-Coefficients

N	r = 40.0 mm, x = 0.400 AN	BN	r = 60.0 mm, x = 0.600 AN	BN
0	-0.0169	0.0000	-0.0048	0.0000
1	-0.0916	0.0450	-0.0905	0.0468
2	0.0110	-0.0119	0.0100	-0.0151
3	0.0015	-0.0002	0.0025	0.0008
4	-0.0012	-0.0010	-0.0027	-0.0001
5	0.0011	0.0008	0.0020	0.0002
6	0.0004	-0.0010	-0.0005	-0.0010
7	0.0005	-0.0001	-0.0010	0.0001
8	0.0020	-0.0004	0.0003	-0.0001
9	-0.0001	0.0006	0.0001	[illegible]

N	r = 80.0 mm, x = 0.800 AN	BN	r = 100.0 mm, x = 1.000 AN	BN
0	-0.0108	0.0000	-0.0222	0.0000
1	-0.0817	[illegible]	-0.0679	0.0574
2	0.0150	[illegible]	0.0080	-0.0351
3	0.0061	[illegible]	0.0126	0.0091
4	[illegible]	0.0009	-0.0118	0.0017
5	[illegible]	-0.0003	0.0070	-0.0031
6	[illegible]	-0.0011	-0.0018	0.0015
7	0.0004	0.0015	-0.0006	0.0016
8	0.0008	-0.0011	0.0010	-0.0023
9	0.0006	0.0010	-0.0012	0.0010

N	r = 120.0 mm, x = 1.200 AN	BN	r = 140.0 mm, x = 1.400 AN	BN
0	-0.0225	0.0000	-0.0378	0.0000
1	-0.0524	0.0535	-0.0308	0.0492
2	0.0003	-0.0388	-0.0114	-0.0418
3	0.0165	0.0138	0.0271	0.0159
4	-0.0130	0.0001	-0.0210	-0.0003
5	0.0057	-0.0029	0.0083	-0.0061
6	0.0000	0.0014	0.0013	0.0036
7	-0.0025	0.0019	-0.0040	0.0011
8	0.0019	-0.0027	0.0035	-0.0038
9	-0.0018	0.0014	-0.0015	0.0044

Table 9: Fourier Coefficients, Tangential Components

3D WAKE SURVEY WM-2023-009

Mean Values of Axial and Tangential Velocity (VA/Vm; Vt,mean/Vm)
(in dependence of assumed propeller diameter)

x1	VA/Vm	Vt(mean)/Vm	w=1-VA/Vm
0.600	0.912	-.028	0.088
0.650	0.912	-.024	0.088
0.700	0.911	-.022	0.089
0.750	0.909	-.020	0.091
0.800	0.907	-.019	0.093
0.850	0.904	-.018	0.096
0.900	0.901	-.018	0.099
0.950	0.899	-.018	0.101
1.000	0.896	-.018	0.104
1.050	0.893	-.018	0.107
1.100	0.891	-.019	0.109
1.150	0.889	-.019	0.111
1.200	0.887	-.019	0.113
1.250	0.885	-.020	0.115
1.300	0.883	-.020	0.117
1.350	0.880	-.021	0.120
1.400	0.877	-.022	0.123
1.450	0.874	-.023	0.126

Table 10: Mean Values of Axial and Tangential Velocity (V_A/V_m, $V_{t,mean}/V_m$)

Figures

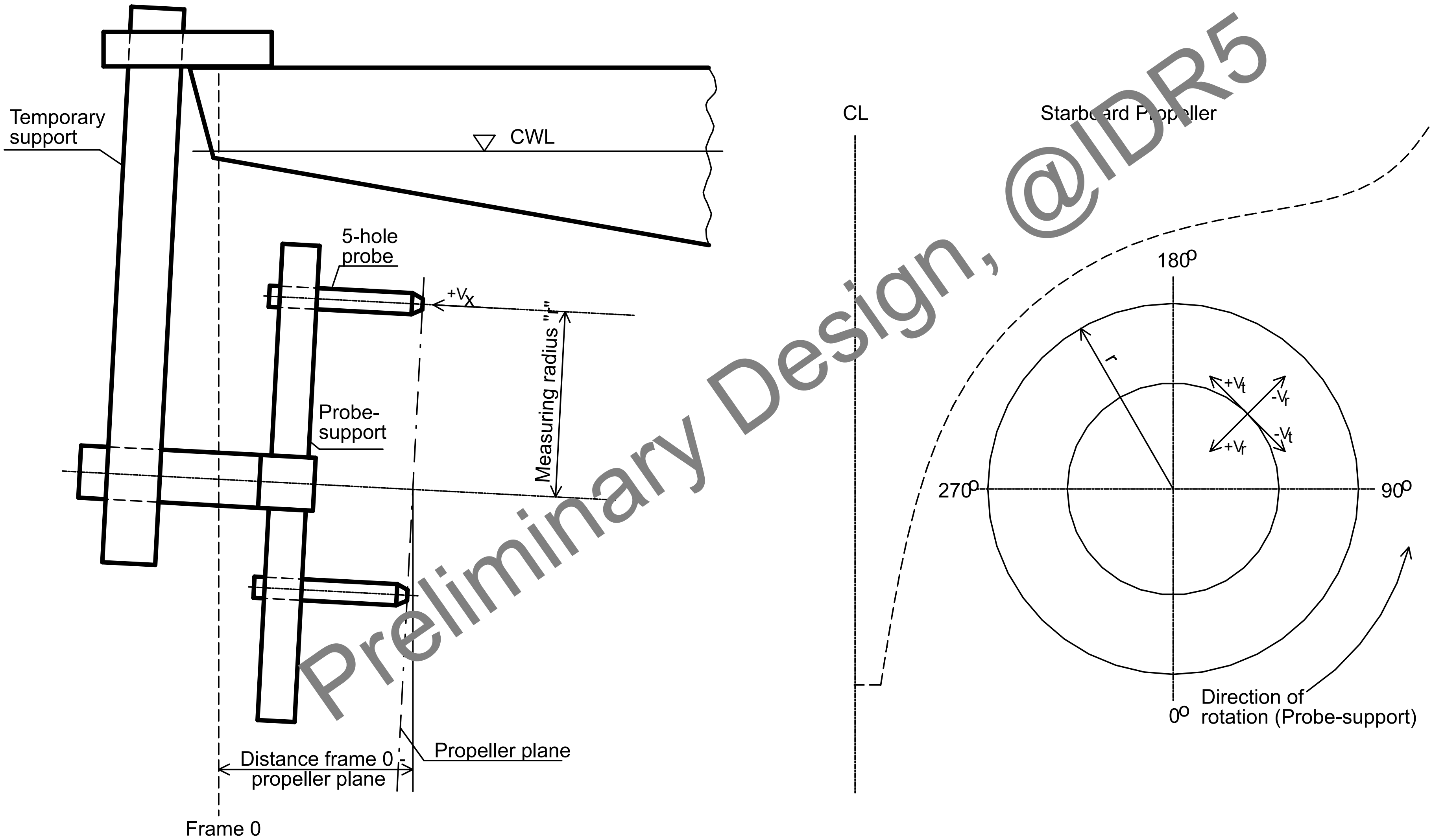

Figure 1: Arrangement of the Test Setup and Assignment of the Velocity Components

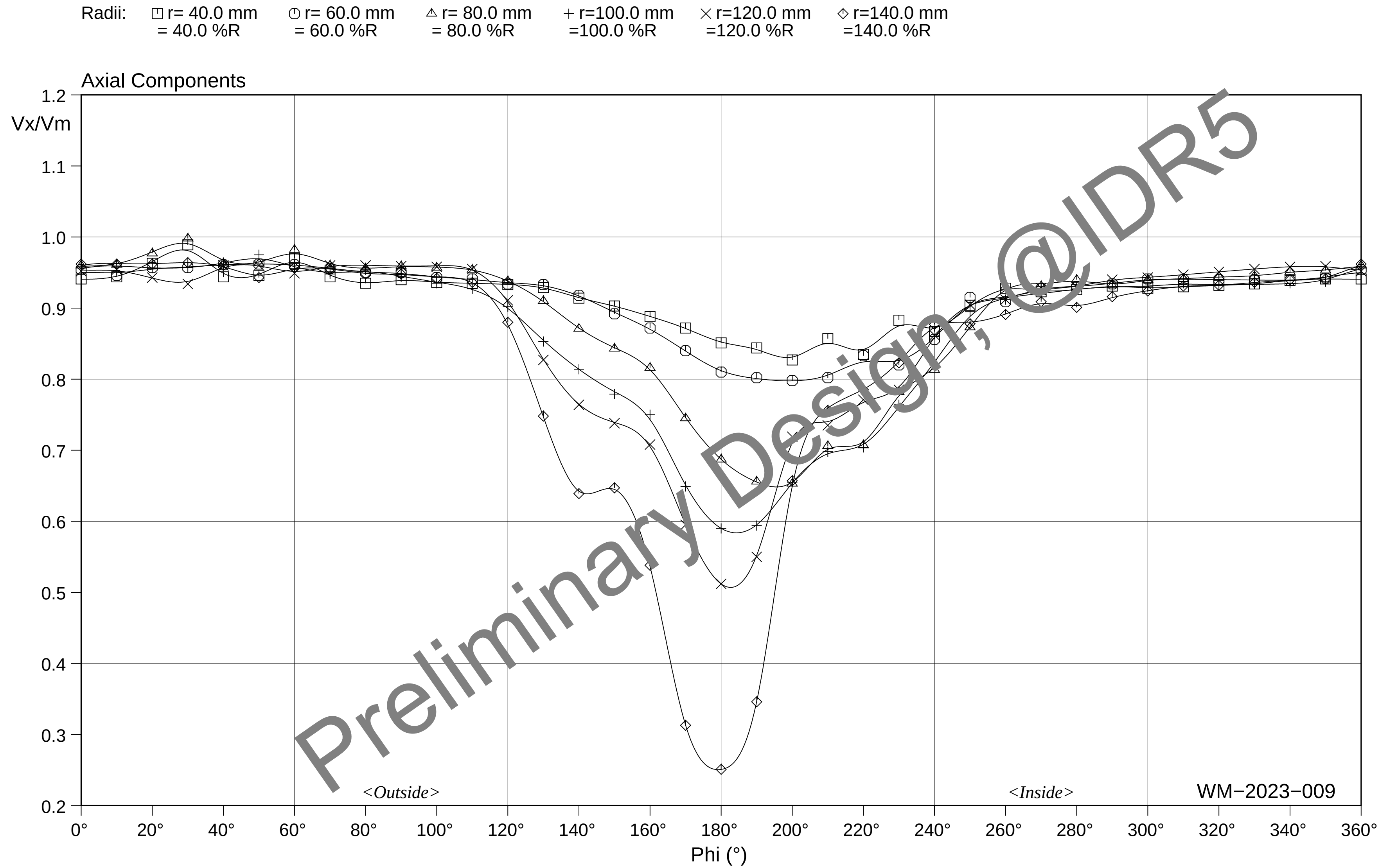

Figure 2: v_x - ϕ - Diagram

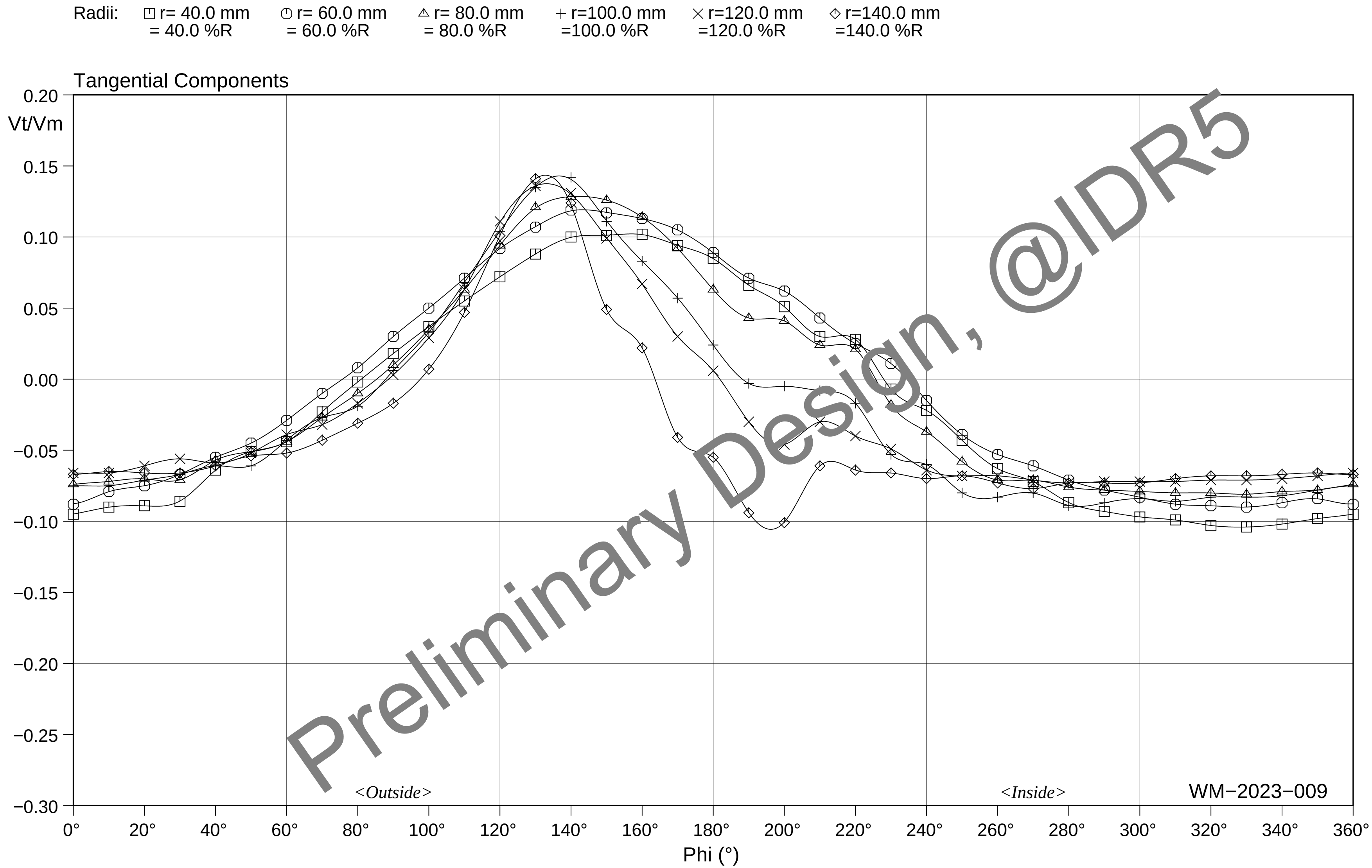

Figure 3: v_t - ϕ - Diagram

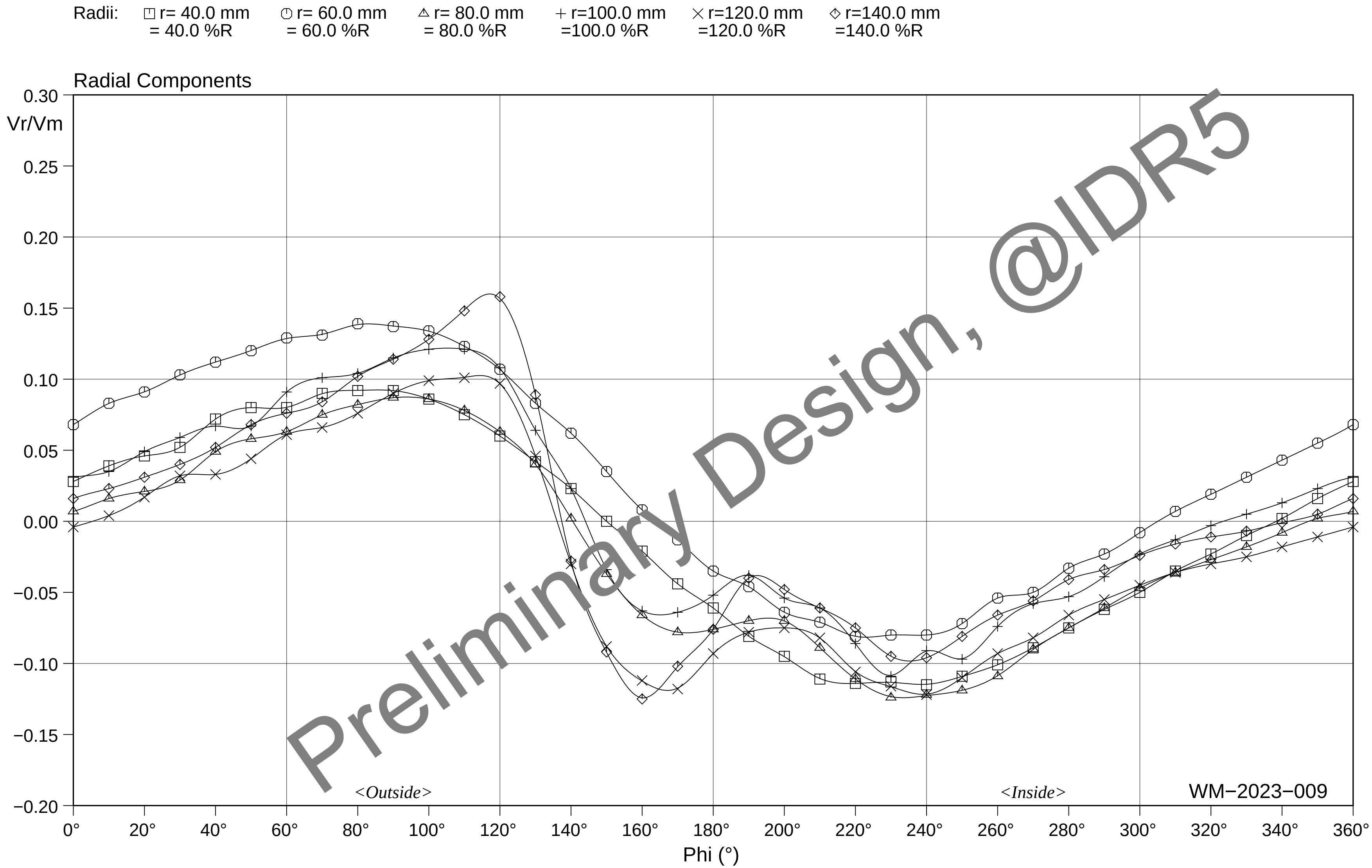

Figure 4: v_r - ϕ - Diagram

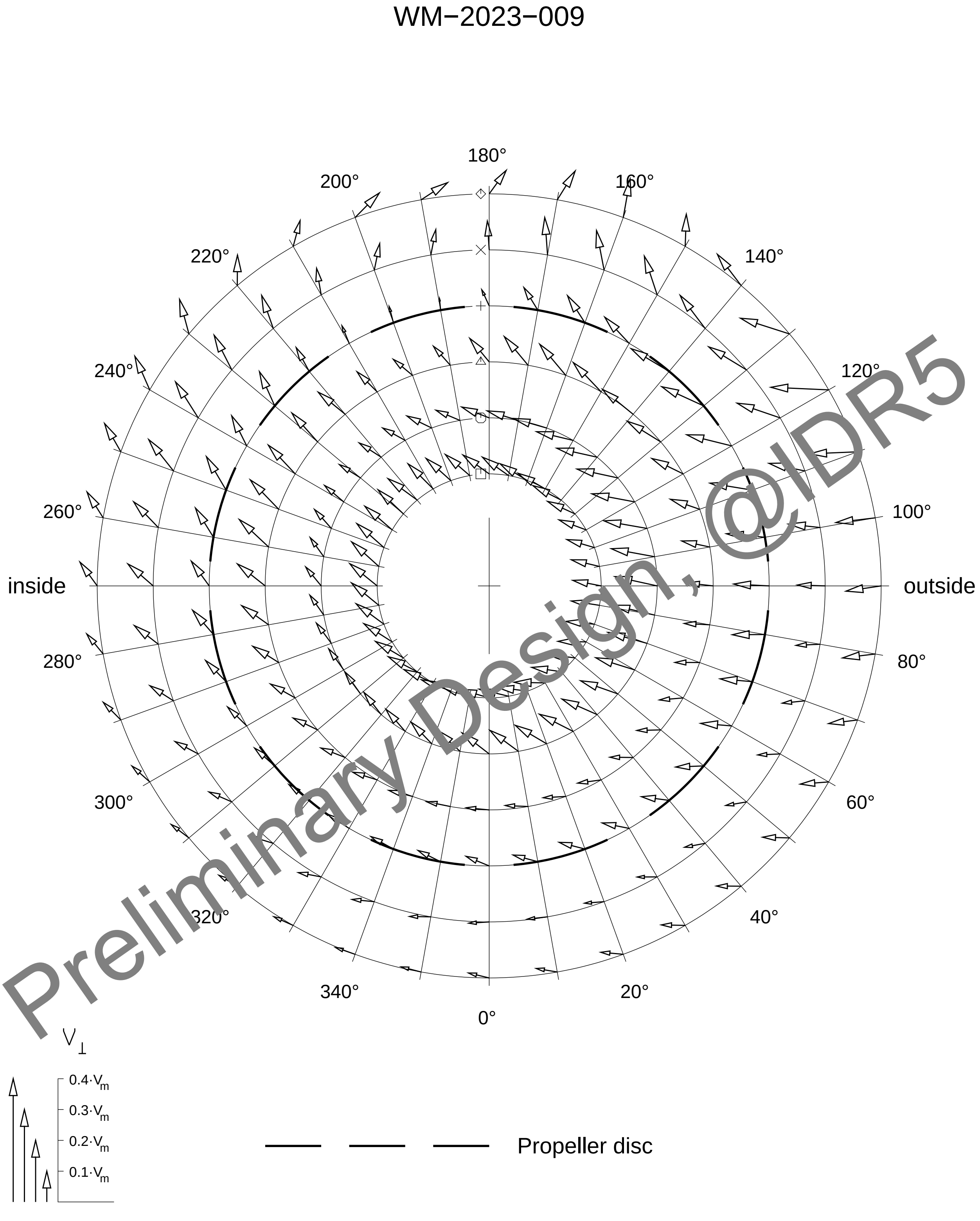

Figure 5: Vector Diagram $v_t + v_r$

WM−2023−009

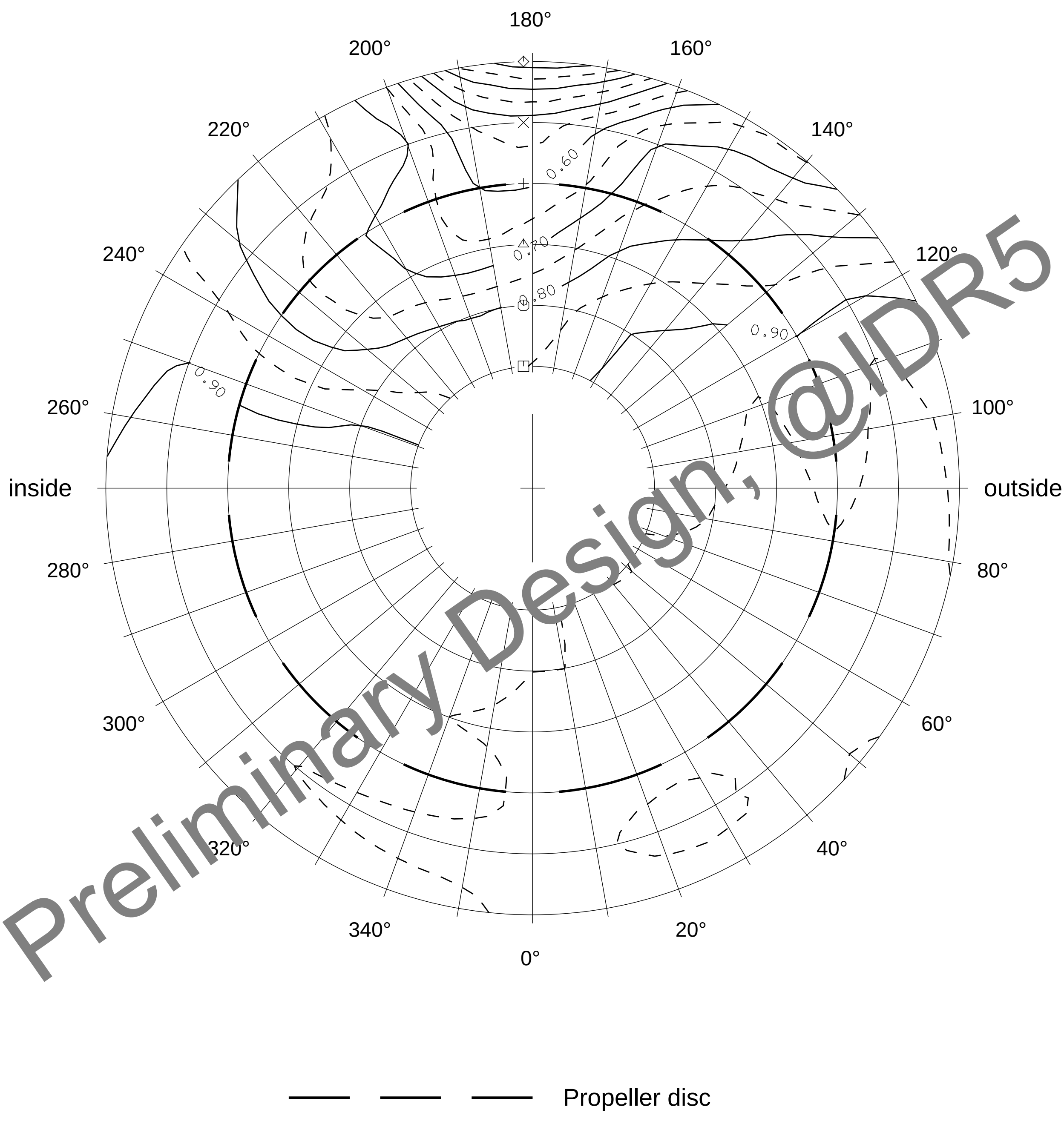

Figure 6: Lines of Constant Axial Velocity

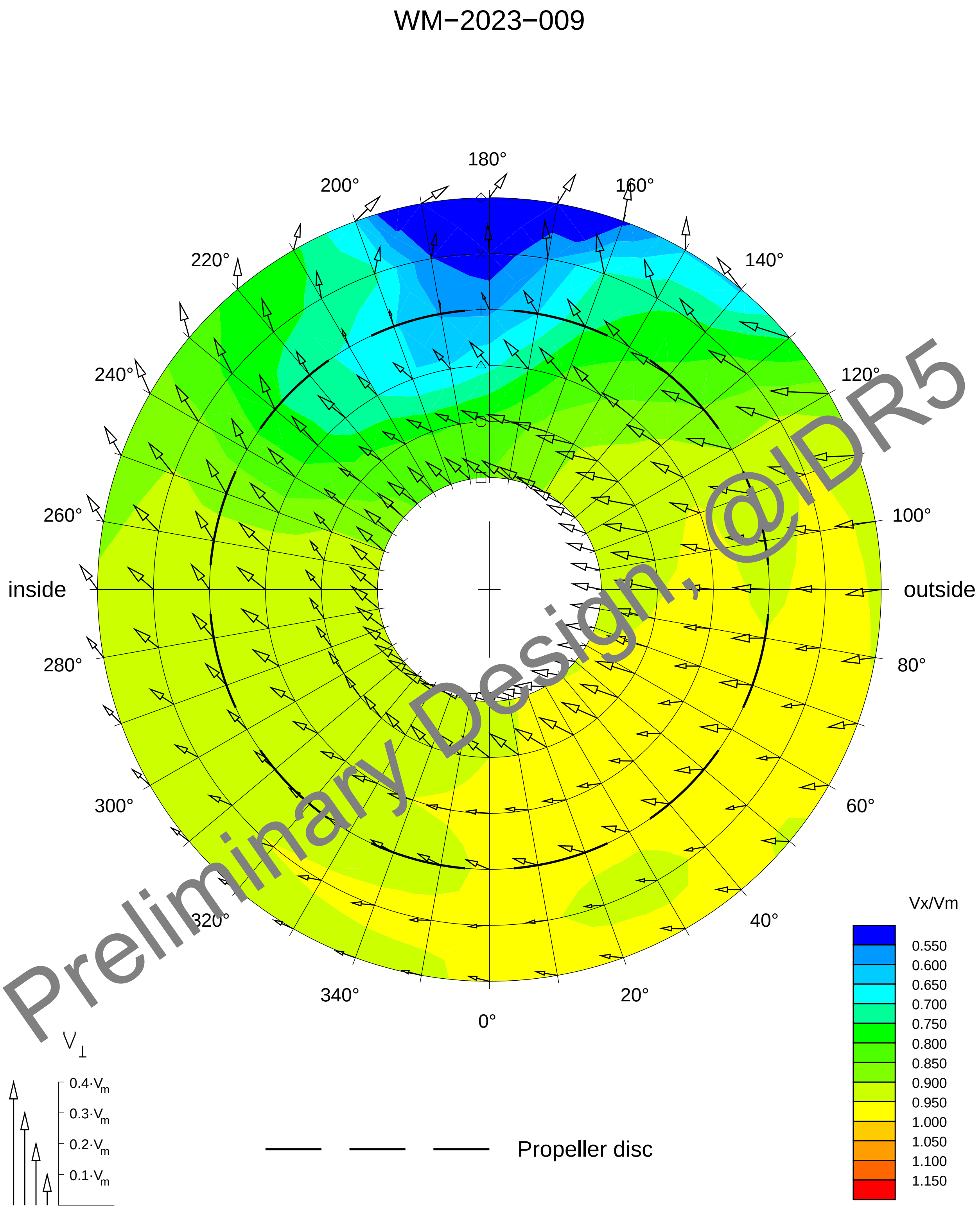

Figure 7: Lines of Constant Axial Velocity Combined with Vector Diagram

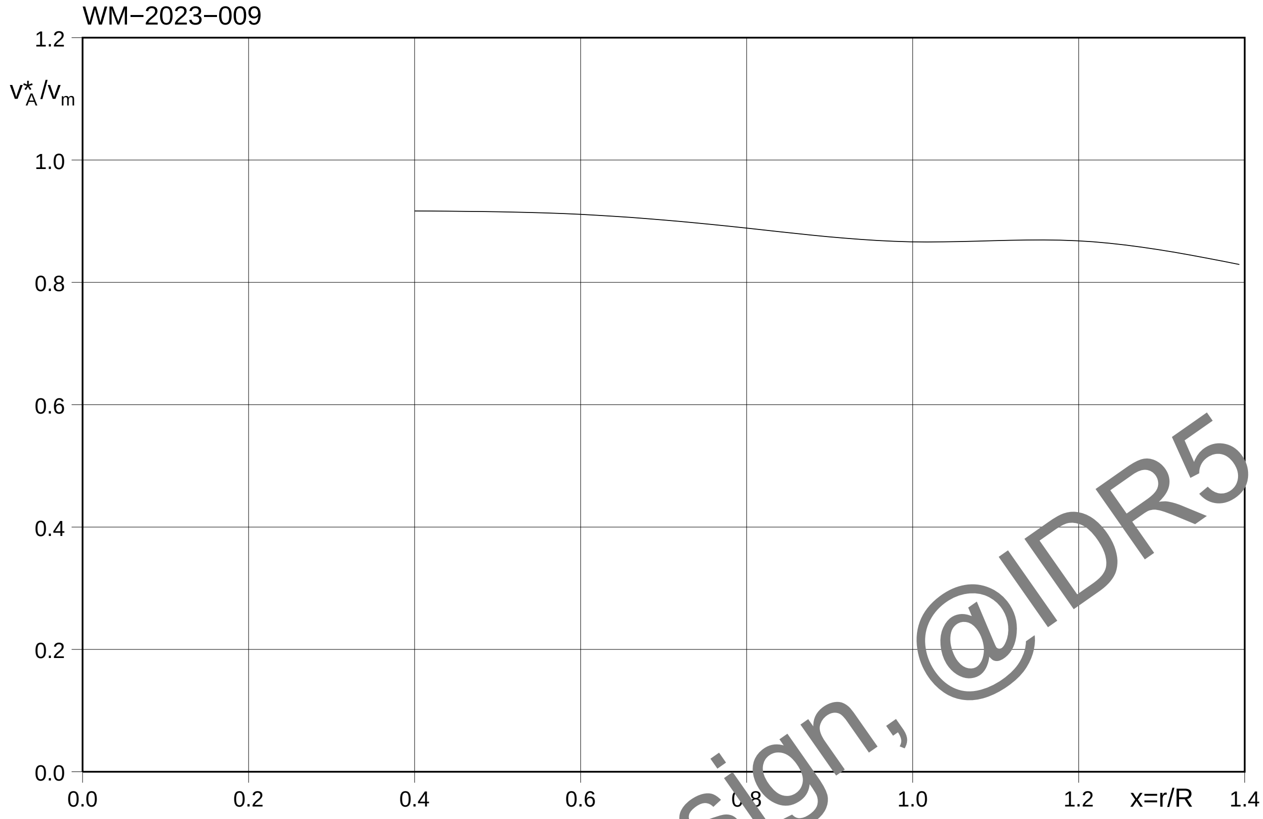

Figure 8: v_A^* - x – Diagram

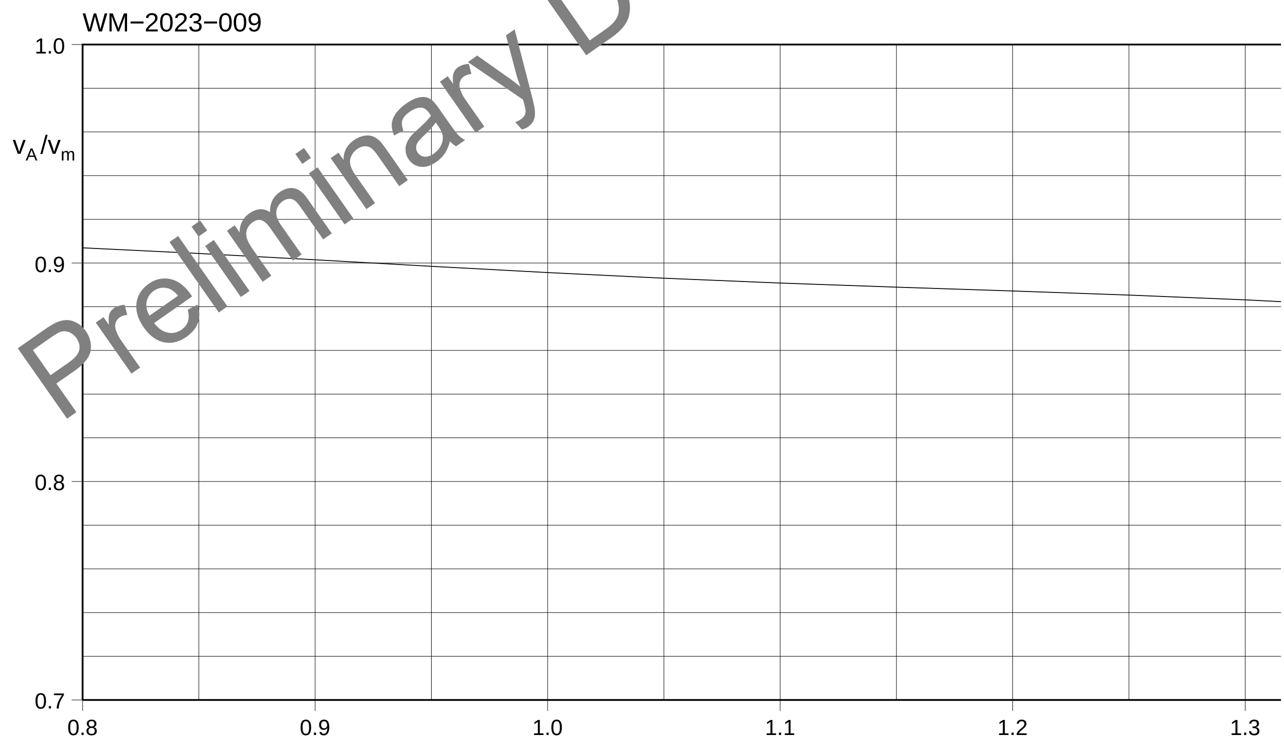

Figure 9: v_A - x_1 – Diagram

11. Attachment 4 ─ HSVA Ice Test Report (Reference 7)

HAMBURGISCHE SCHIFFBAU-VERSUCHSANSTALT GMBH

THE HAMBURG SHIP MODEL BASIN

Report AT-2023-006

Ice Model Tests for Antarctic Research Vessel (ARV) -Addendum 5 Post-PDR Hull Variant Testing

HSVA Model No. 5626-00010

Customer:
Leidos Inc.

HSVA

Document Control Sheet

Customer	**:** Leidos
Project	**:** Antarctic Research Vessel (ARV)
Contract No.	**:** 617456
Report No.	**:** AT-2023-006
Report Title	**:** Ice Model Tests for Antarctic Research Vessel (ARV) -Addendum 5 Post-PDR Hull Variant Testing
File	**:** 617456-AT-2023-006.pdf

Rev. No.	**Date**	**Reason for Issue**	**Prepared by**	**Checked by**	**Approved by**
00	03-07-2023	For Clients Review	NR	OH	

Summary:

In March and April 2023 the performance of a new model that was built according to the design revision of ARV was investigated in three ice model test series. The model was manufactured in HSVA's workshop and equipped with ice type stock propellers and azimuth housings. The test series included tests in level ice and broken channel. First tests focused on the verification of ice performance (attainable speed and maneuvering) after design revision while the last test series was used to determine specific operational capabilities. In all test series the model ice properties were measured and compared to the target specified properties. Corrections were applied to account for deviations in the analysis.

Conclusions:

The test observations and analysis from the additional test series show that the revised design (hull variant 11) achieves either similar or even better ice performance compared to the first design revision (hull variant 6) tested in autumn 2022. In the third test series the model showed good ability to clear the broken channel using the azimuth thrusters at a different angle.

Keywords: Antarctic Research Vessel, Ice Model Tests, Level Ice, Ice Ridges, Towed Propulsion Tests, Free Running Propulsion Tests, Break Out Tests

Report AT-2023-006

Ice Model Tests for Antarctic Research Vessel (ARV) - Addendum 5 Post-PDR Hull Variant Testing

Leidos, Inc.

HSVA Model No. 5626-00010

Hamburg, December 2023

Prepared by:

Nils Reimer

HAMBURGISCHE SCHIFFBAU-
VERSUCHSANSTALT GmbH

Content

List of Figures

List of Tables

1 Background and Objectives of Ice Model Tests

Leidos provides logistical support to the United States Antarctic Program (USAP) for the Antarctic Support Contract (ASC). The specified support includes operation and maintenance of facilities, vehicles, and equipment at all USAP stations, as well as two ice-classed research vessels. Support is also provided to all National Science Foundation (NSF) sponsored research projects in Antarctica, and includes construction and operations at USAP stations as well as the temporary field camps used during the austral summer field season.

NSF is planning for replacement of existing Nathaniel B. Palmer with a future Antarctic Research Vessel (ARV) to provide state of the art research science capabilities, improved open water and icebreaking performance and efficiency. ARV Concept Design studies resulted in an indicative design as proof of concept. Preliminary Design phase efforts have commenced to further project definition by completing whole-ship architecture trade-offs, developing a converged preliminary level design with all necessary technical documentation, and developing an associated Design and Construction cost estimate and schedule. The Preliminary Design phase culminates in a Preliminary Design Review (PDR). Upon successful completion of PDR, the NSF director may approve entry into the Final Design phase which will likely occur 6 to 12 months following PDR.

Development of the ARV hull form to meet open water, icebreaking, and science related missions is crucial to the success of the overall ARV design and mission. Physical model testing in open water and ice is required to validate the approach [1].

Leidos, Inc. contracted HSVA to assess the ice breaking performance of a revised design (hull variant 11) for an Antarctic Research Vessel (ARV). An additional ice model test campaign was carried out for the project in HSVA’s large ice model basin between March and April 2023. For the tests a model at a scale ratio of 1:24.384 was manufactured in HSVA’s model workshop. The test campaign in ice included test in three ice sheets, two ice sheets with a thickness corresponding to 1.37m in full scale and one ice sheets with a thickness corresponding to 1.00m level ice in full scale.. The tests in level ice included towed propulsion tests and free running propulsion tests in ahead and astern direction. In addition break out tests from the channel ahead and astern were carried out in 1.37m hick ice. In 1.00m level ice channel clearing tests with variation of azimuth thruster angles was carried out.

2 Description of Model and Appendages

Table 1 Main particulars of ARV and HSVA model 5626

Main particulars of ARV design and HSVA model no. 5626			
Scale ratio	λ	1:1	1:24.384
Length between perpendiculars[1]	Lpp [m]	108.72	4.459
Length of Waterline	Lwl [m]	106.50	4.368
Maximum Breadth	B [m]	24.38	0.999
Breadth at Waterline	Bcwl [m]	23.81	0.976
Draft[2]	T [m]	9.91	0.406
Displacement	V [m]	13385.4	0.923
Longitudinal Center of Buoyancy	LCB [m]	53.783	2.206
Metacentric Height	GM [m]	1.38	0.057

Table 2 Main particulars of HSVA stock propellers 2288 and 2289

Main particulars of ARV design and HSVA stock propellers 2288 and 2289			
Scale ratio	λ	1:1	1:24.384
Propeller Diameter	D [m]	4.877	0.200
Mean Pitch Ratio	Pm/D [-]	0.98520	0.98520
Area Ratio	A_e/A_0 [-]	0.55290	0.55290
Hub / Diameter Ratio	Dh/D [m]	0.38100	0.38100
Skew	[deg]	4.50000	4.50000
No. of Blades	[-]	4	4

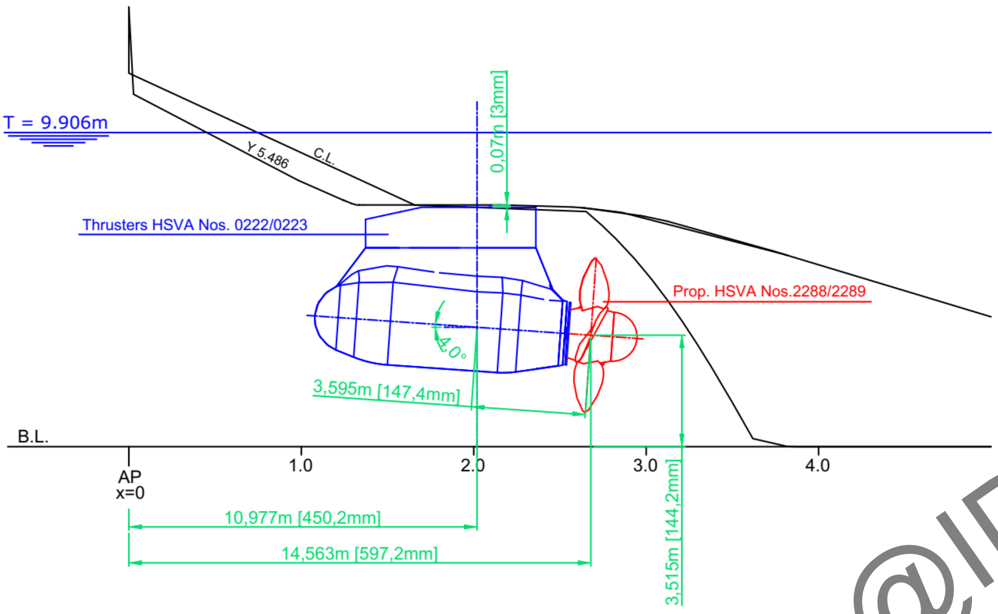

Figure 1 Side view of stock azimuth-propeller arrangement

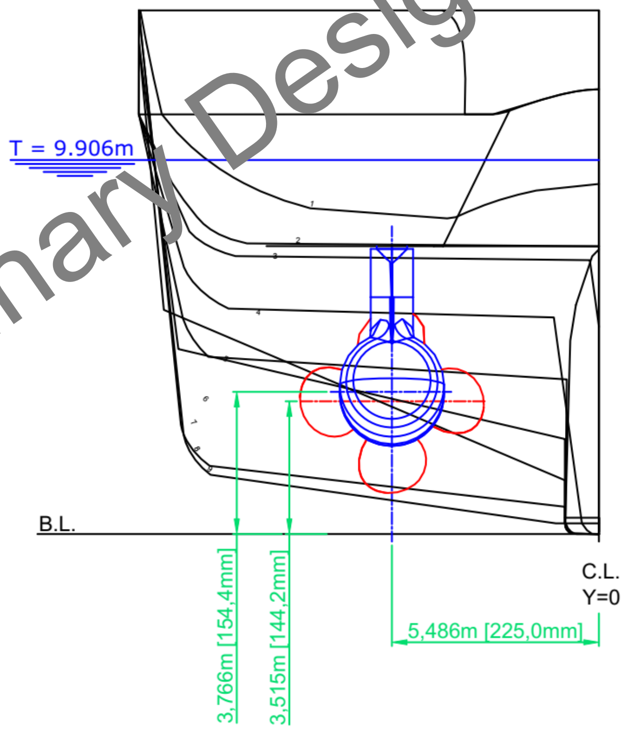

Figure 2 Stern view of stock azimuth-propeller arrangement

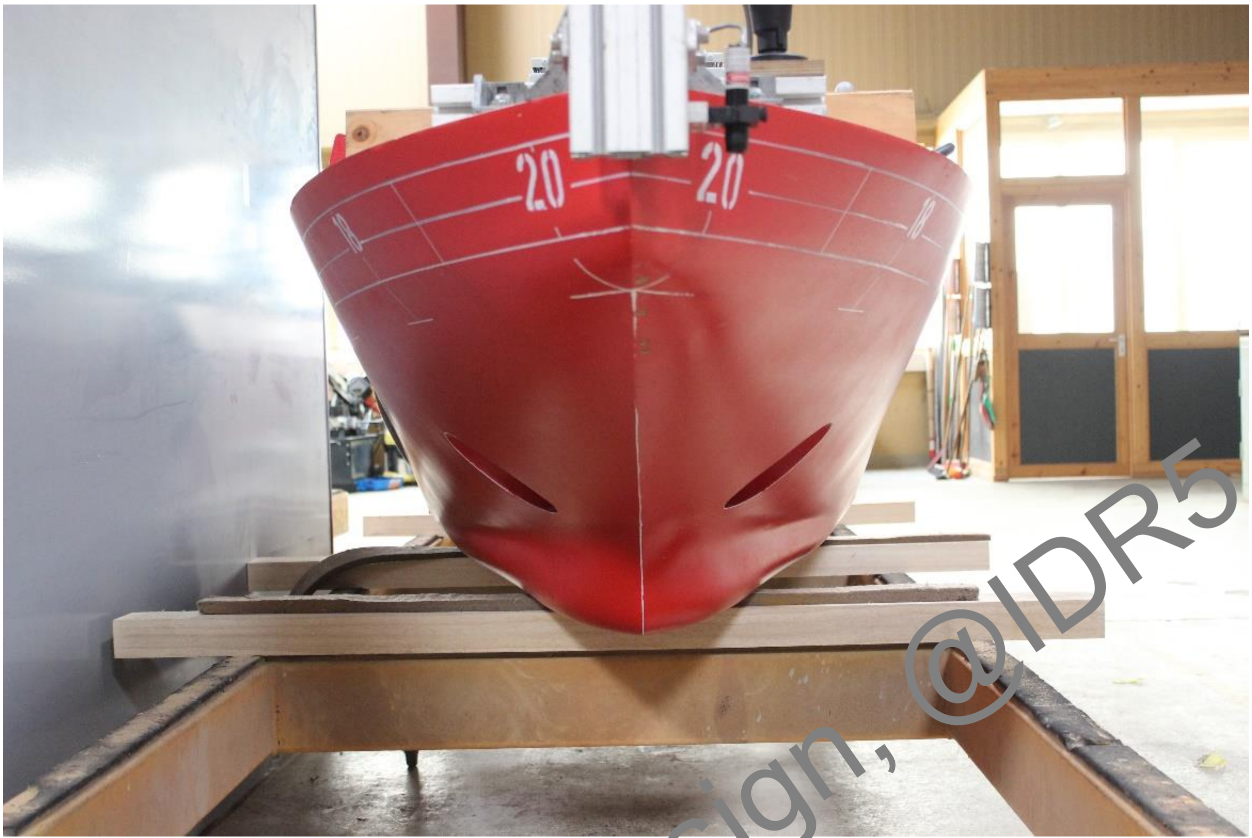

Figure 3 Front view of HSVA model no. 5626

Figure 4 Oblique front view of HSVA model no. 5626

Figure 5 Stern front view of HSVA model no. 5626

Figure 6 Oblique stern view of HSVA model no. 5626

Figure 7 Side view of aftship HSVA model no. 5626

3 Test Programs

Series 10000R – Thu, 30-Mar-2023

Ice conditions: Level ice 1.37 m (MS: 56 mm), 700 kPa flexural strength
Loading: Tcwl (T_a=T_f=9.906 m)

Run 11010R - 12010R – Towed Propulsion Test Ahead in Level Ice

Ship model will be towed through the Level Ice at V_1 = 6.0 kts (MS: 625 mm/s) and V_2 = 3.0 kts (MS: 313 mm/s)

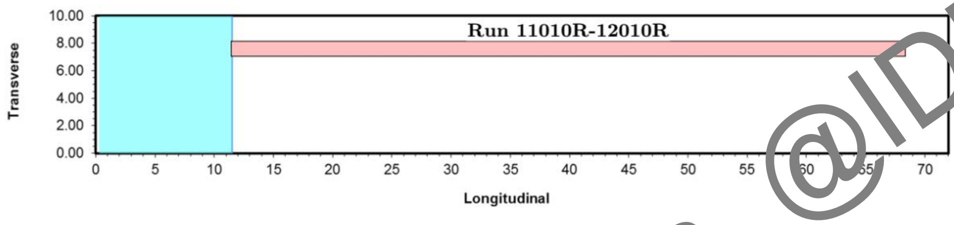

Run 13011R – Towed Propulsion Test Astern in Level Ice

Ship model will be towed through the Level Ice at V = 3.0 kts (MS: 313 mm/s)

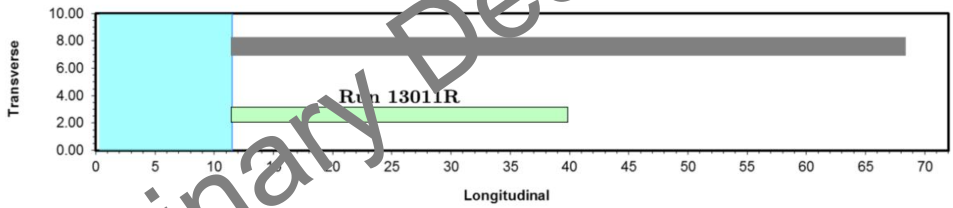

Run 14011R & 15011R – Free Running Tests Astern in Level Ice (70-100pc PD)

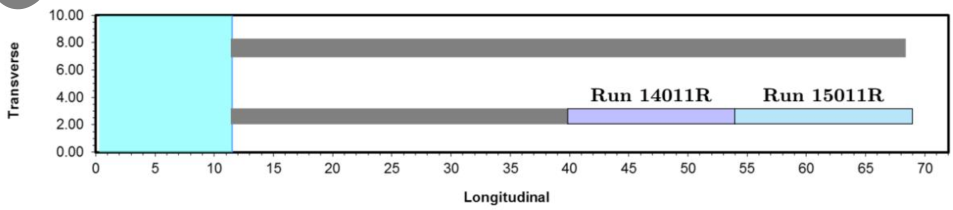

Series 20000 – Mon, 3-Apr-2023

Ice conditions: Level ice 1.37 m (MS: 56 mm), 700 kPa flexural strength
Loading: Tcwl (T_a=T_f=9.906 m)

Run 21010R, 22010R & 23010R – Free Running Tests Ahead in Level Ice (40-70-100pc PB)

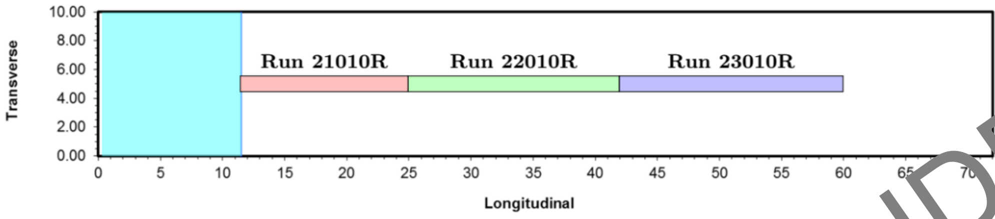

Run 24011R – Free Running Test Astern in Level Ice (40pc PB)

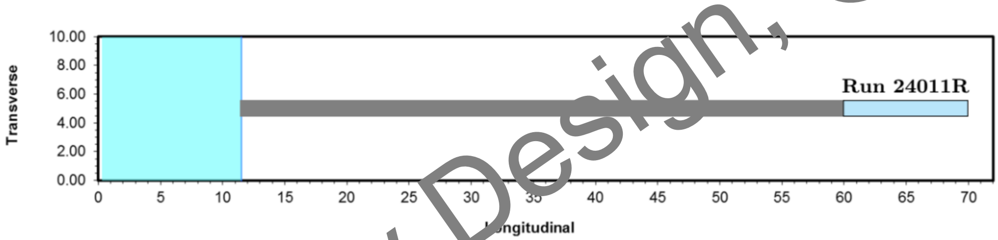

Run 25011R & 26010R – Break out Tests Ahead and Astern in Level Ice

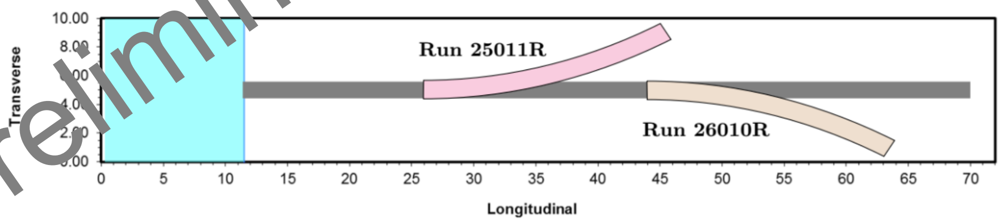

Series 30000 – Thu, 6-Apr-2023

Ice conditions: Level ice 1.00 m (MS: 41 mm), 700 kPa flexural strength
Loading: Tcwl (T_a=T_f=9.906 m)

Run 31010R, 32010R, 33010R & 34010R – Channel Clearing Tests Ahead in Level Ice

Differents configurations to be tested. Forward speed between 4 kts and 8 kts.

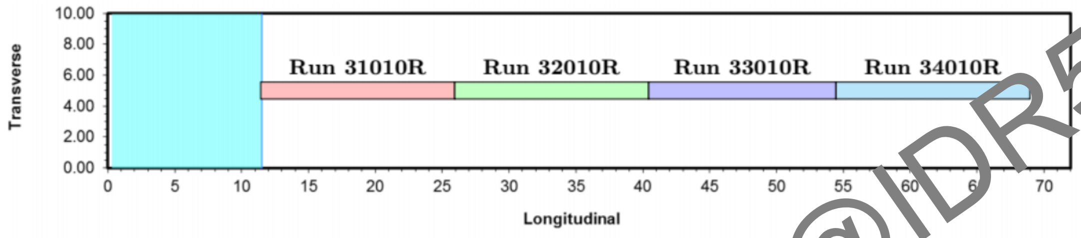

Additional Tests:

35010R

Side Step Test

36010R

Channel clearing running back ahead

37011R

Creation of brash ice field running astern

38010R

Brash Ice clearing with 3 different Pod angels

4 Test Parameter

4.1 Ice Properties

4.1.1 Ser 10000R

Table 3 Model ice thickness in test series 11010R, 12020R

Level Ice Thickness

Pos. Tm.	Port [mm]	Centre [mm]	Stbd. [mm]		Pos. Tm.	Port [mm]	Centre [mm]	Stbd. [mm]	
12					43	62.0		58.0	
13					44	63.0		56.0	
14					45	65.0		58.0	
15					46	60.0		58.0	
16	58.0		56.0		47	63.0		61.0	
17	57.0		55.0		48	60.0		63.0	
18	55.0		56.0		49	65.0		59.0	
19	62.0		59.0		50	63.0		61.0	
20	60.0		63.0		51	60.0		59.0	
21	62.0		58.0		52	60.0		57.0	
22	57.0		57.0		53	62.0		62.0	
23	61.0		45.0		54	65.0		60.0	
24	61.0		59.0		55	61.0		59.0	
25	65.0		55.0		56	59.0		57.0	
26	62.0		57.0		57	57.0		58.0	
27	65.0		60.0		58	62.0		60.0	
28	59.0		52.0		59	63.0		61.0	
29	62.0		58.0		60	65.0		56.0	
30	63.0		61.0		61	62.0		55.0	
31	63.0		62.0		62	62.0		56.0	
32	63.0		59.0		63	63.0		60.0	
33	66.0		64.0		64	65.0		63.0	
34	63.0		62.0		65	65.0		63.0	
35	62.0		61.0		66	66.0		61.0	
36	63.0		64.0		67	62.0		62.0	
37	66.0		61.0		68		62.0		
38	64.0		62.0		69				
39	64.0		60.0		70				
40	63.0		59.0		71				
41	61.0		60.0		72				
42	61.0		62.0		Av.	62.1	62.0	59.0	
					Av. of all		60.6		

Table 4 Model ice thickness in test series 13011R, 14011R, 15011R

Date:	30-Mar-2023	Time:		Test Series:		10000R	
Pos. Tm.	Port [mm]	Centre [mm]	Stbd. [mm]	Pos. Tm.	Port [mm]	Centre [mm]	Stbd. [mm]
12				43	59.0		57.0
13				44	59.0		57.0
14				45	59.0		56.0
15				46	58.0		59.0
16	53.0		56.0	47	60.0		62.0
17	54.0		56.0	48	62.0		64.0
18	54.0		57.0	49	61.0		65.0
19	55.0		57.0	50	59.0		63.0
20	56.0		57.0	51	59.0		62.0
21	58.0		56.0	52	57.0		62.0
22	57.0		58.0	53	58.0		63.0
23	55.0		58.0	54	59.0		59.0
24	55.0		58.0	55	58.0		63.0
25	58.0		59.0	56	57.0		61.0
26	57.0		60.0	57	59.0		60.0
27	55.0		59.0	58	57.0		62.0
28	58.0		57.0	59	58.0		65.0
29	59.0		55.0	60	60.0		64.0
30	57.0		62.0	61	61.0		62.0
31	57.0		59.0	62	57.0		60.0
32	60.0		61.0	63	58.0		64.0
33	59.0		61.0	64	70.0		63.0
34	57.0		59.0	65	62.0		64.0
35	61.0		60.0	66	60.0		65.0
36	60.0		64.0	67	62.0		64.0
37	63.0		61.0	68	64.0		62.0
38	62.0		60.0	69	61.0		62.0
39	59.0		58.0	70	61.0		64.0
40	55.0		56.0	70.5	65.0	Heck	64.0
41	55.0		58.0	72			
42	57.0		54.0	Av.	58.7		60.3

Broken Channel Width

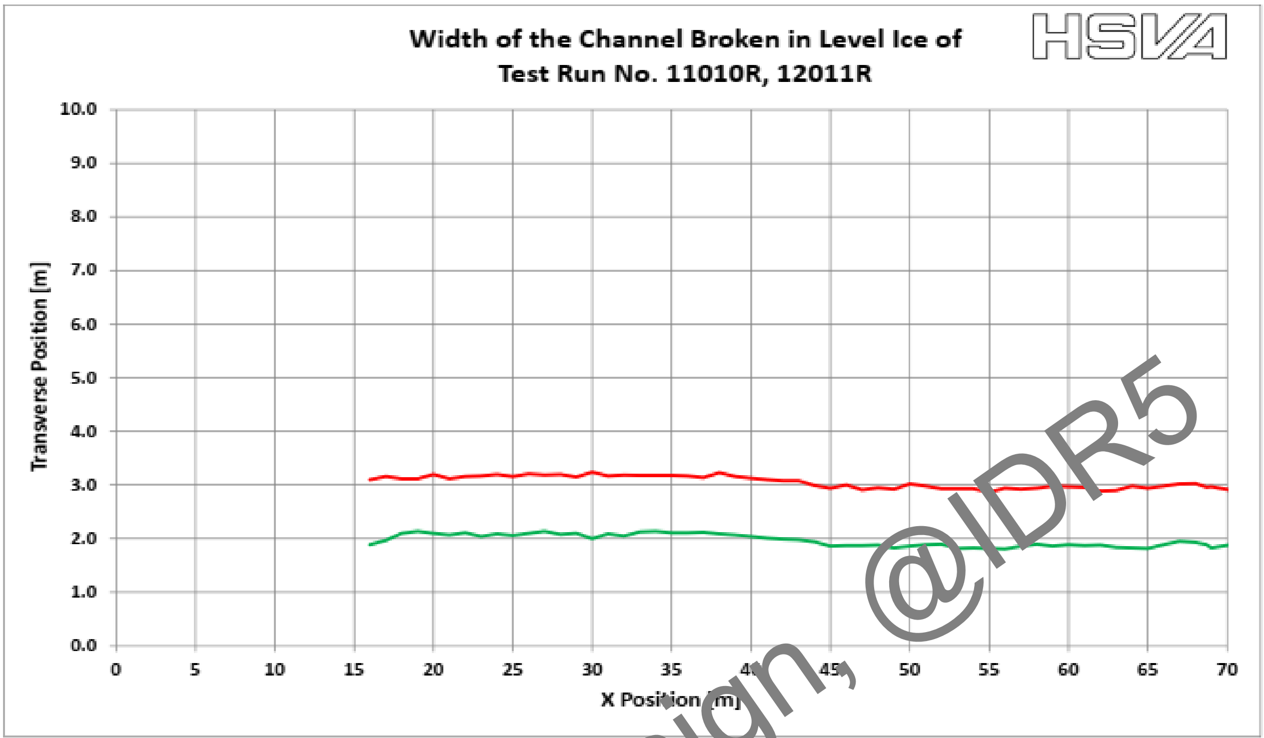

Figure 8 Plot of the broken channel of test run 11010R and 12011R

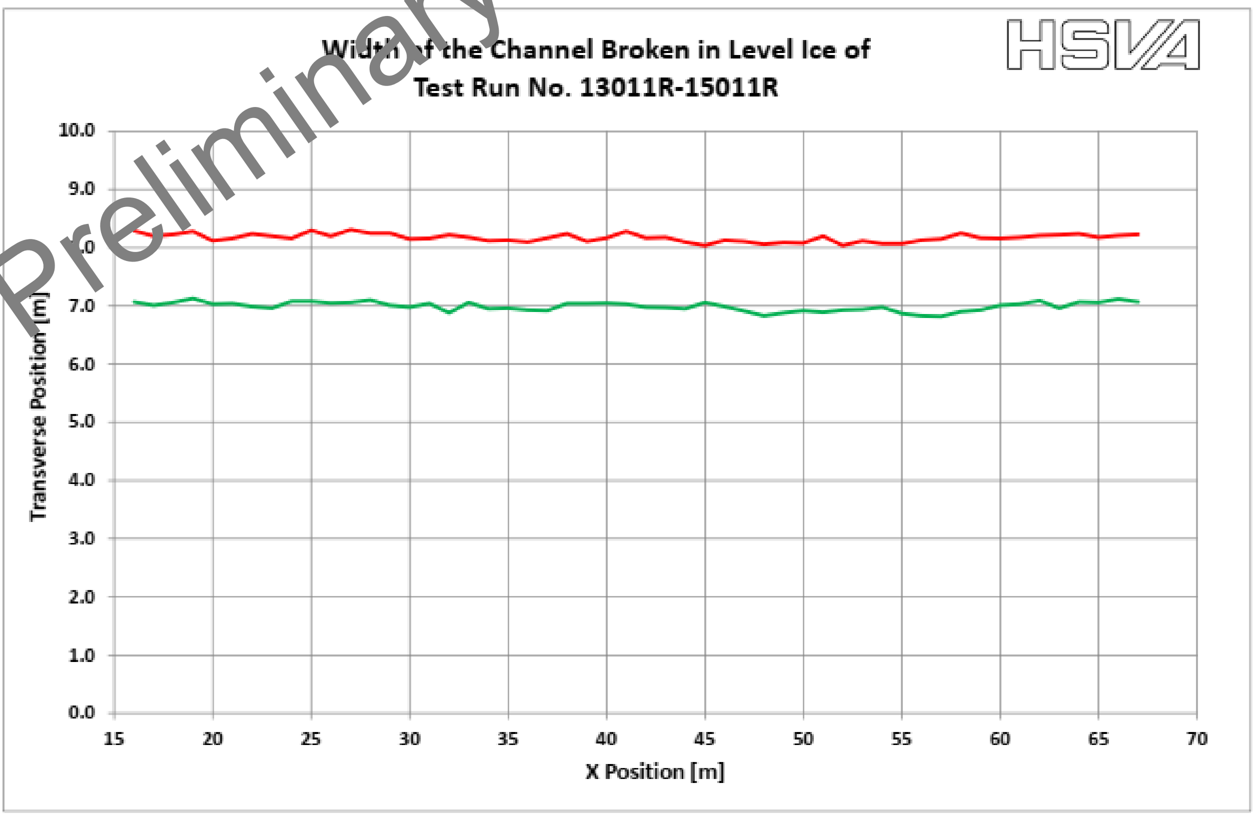

Figure 9 Plot of the broken channel of test run 13011R and 15011R

Average Width of broken channel:
11010R: 1.09m = 1.089 x B
12010R: 1.09m = 1.089 x B
13011R: 1.18m = 1.179 x B
14011R: 1.18m = 1.179 x B
15011R: 1.18m = 1.179 x B

Flexural Strength

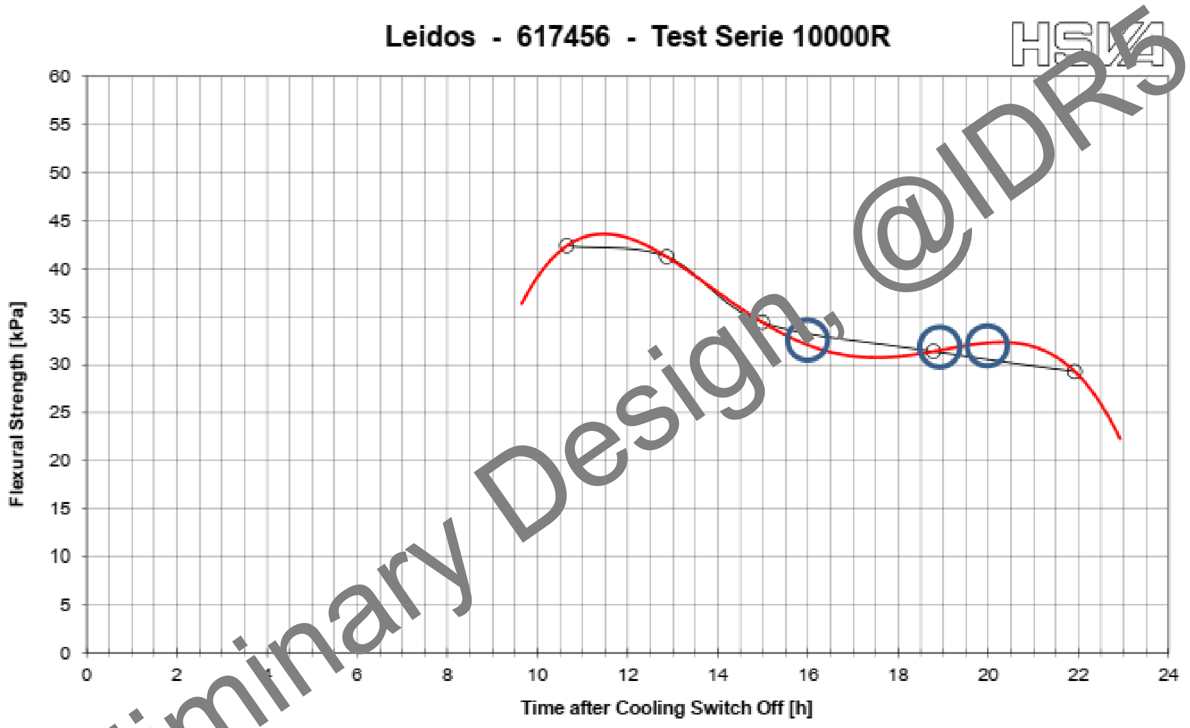

Figure 10 Plot of flexural strength measurements during test series 10000R

Crushing Strength

$\sigma_{cr} = \frac{F_{cr}}{c_i \cdot m \cdot D \cdot k \cdot h} = 143.0$ kPa

F = force (measured)

m = shape factor (round structure 0.9)

k = contact factor (0.4 - 0.7)

h = ice thickness D = diameter of indenter

ci = factor depending on the D/h ratio

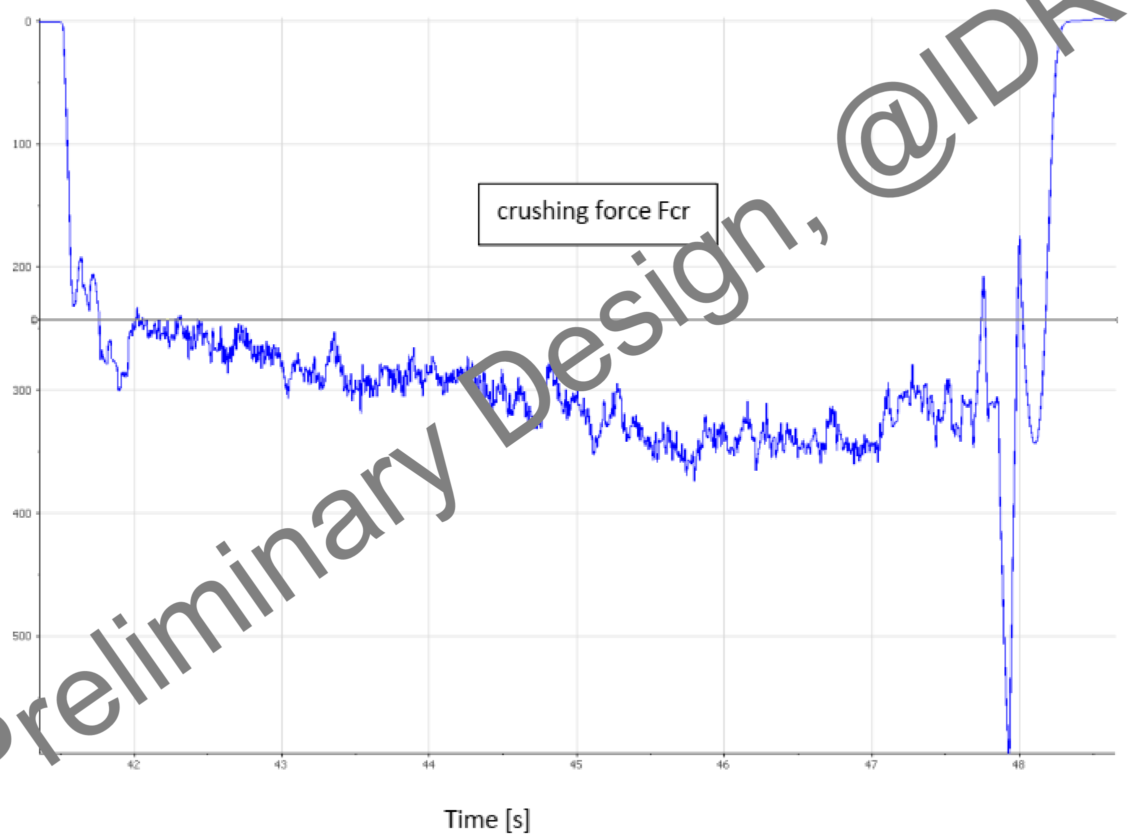

Figure 11 Plot of crushing force time series from indentation test, test series 10000R

Level ice density

Client:	Leidos
Project:	617456
Date:	30-Mar-2023

Test Series:		10000R	
Water Density:	ρ_{water} =	1005.5	[kg/m³]
Water Salinity:	S_w =	7.0	[‰]
Oxygen set value:	O_2 =	18.3	[mg/l]

Ice density ρ_i :

$$\rho_i = \frac{w_2}{w_3} \rho_w$$

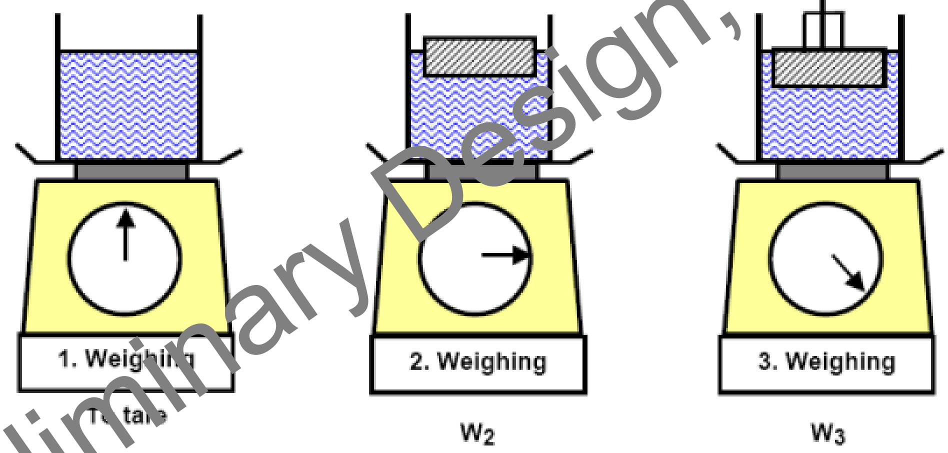

@ev

Specimen No. or x \ y-Tank Pos.	w_2 [g]	w_3 [g]	ρ_{ice} [kg/m³]	Salinity [‰]
21 / 1	828	913	912	
43 / 1	854	953	901	
66 / 1	946	1034	920	
mean >>>	876.0	966.7	911.0	

Figure 12 Level ice density measurements of series 10000R

4.1.2 Ser 20000R

Table 5 Level ice thickness measurements of test series 20000R part 1

Level Ice Thickness

Date:	2023-04-03		Time:		Test Series:		20000R
Pos. Tm.	Port [mm]	Centre [mm]	Stbd. [mm]	Pos. Tm.	Port [mm]	Centre [mm]	Stbd. [mm]
12				43	63.0		57.0
13				44	58.0		58.0
14				45	57.0		56.0
15				46	59.0		58.0
16				47	60.0		60.0
17				48	59.0		59.0
18	52.0		60.0	49	61.0		61.0
19	58.0		58.0	50	60.0		60.0
20	56.0		60.0	51	59.0		59.0
21	58.0		61.0	52	60.0		57.0
22	59.0		61.0	53	62.0		58.0
23	58.0		60.0	54	60.0		59.0
24	57.0		58.0	55	59.0		60.0
25	60.0		57.0	56	57.0		59.0
26	58.0		56.0	57	58.0		58.0
27	59.0		55.0	57.4		58.0	
28	56.0		58.0	59			
29	56.0		59.0	60			
30	60.0		58.0	61			
31	60.0		59.0	62			
32	63.0		56.0	63			
33	62.0		59.0	64			
34	60.0		59.0	65			
35	60.0		59.0	66			
36	63.0		60.0	67			
37	62.0		61.0	68			
38	61.0		59.0	69			
39	62.0		58.0	70			
40	59.0		58.0	71			
41	58.0		58.0	72			
42	58.0		56.0	Av.	59.2	58.0	58.6
				Av. of all		58.9	

Table 6 Level ice thickness measurements of test series 20000R part 1

Date: 2023-04-03			Time:	Test Series: 20000R			
Pos. Tm.	Port [mm]	Centre [mm]	Stbd. [mm]	Pos. Tm.	Port [mm]	Centre [mm]	Stbd. [mm]
12				43	63.0		60.0
13				44	57.0		60.0
14				45	57.0		58.0
15				46	59.0		59.0
16				47	59.0		61.0
17				48	63.0		62.0
18				49	61.0		63.0
19				50	61.0		60.0
20				51	60.0		60.0
21				52	58.0		57.0
22				53	62.0		65.0
23				54	63.0		59.0
24				55	59.0		59.0
25				56	58.0		59.0
26				57	59.0		57.0
27				58	59.0		58.0
31.5				59	61.0		61.0
32	61.0		59.0	60	61.0		58.0
32.5	62.0		62.0	61	57.0		56.0
33	61.0		61.0	62	55.0		55.0
33.5	62.0		60.0	63	58.0		57.0
34	60.0		61.0	64	56.0		65.0
34.5	60.0		68.0	65	59.0		63.0
35	ow		69.0	66	60.0		63.0
35.5	63.0		60.0	67	61.0		61.0
37				68	61.0		60.0
38				69	64.0		62.0
39				70	62.0		62.0
40				71	61.0		58.0
41				71.1	58.0		58.0
42				Av.	60.0		60.4
				Av. of all		60.2	

Broken Channel Width

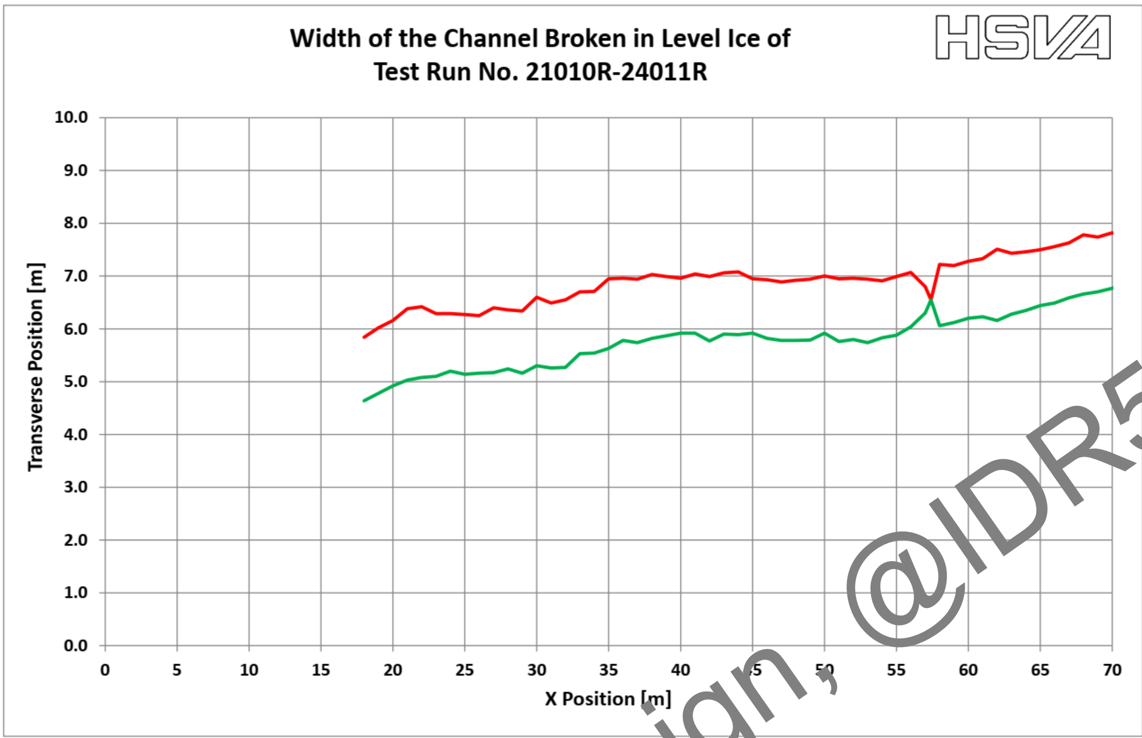

Figure 13 Measurement of broken channel width, test run nos. 21010R-24010R

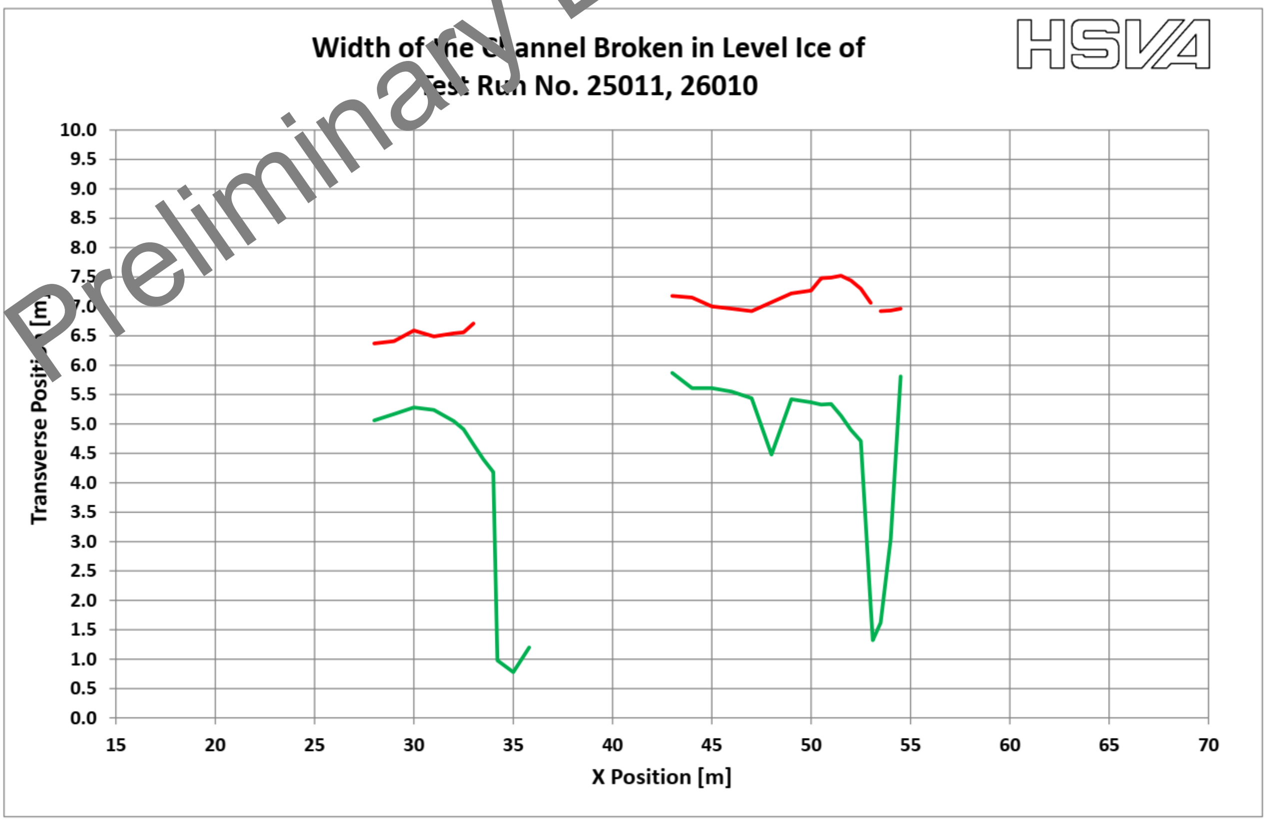

Figure 14 Measurement of broken channel width, test run nos. 25010R-26010R

Flexural Strength

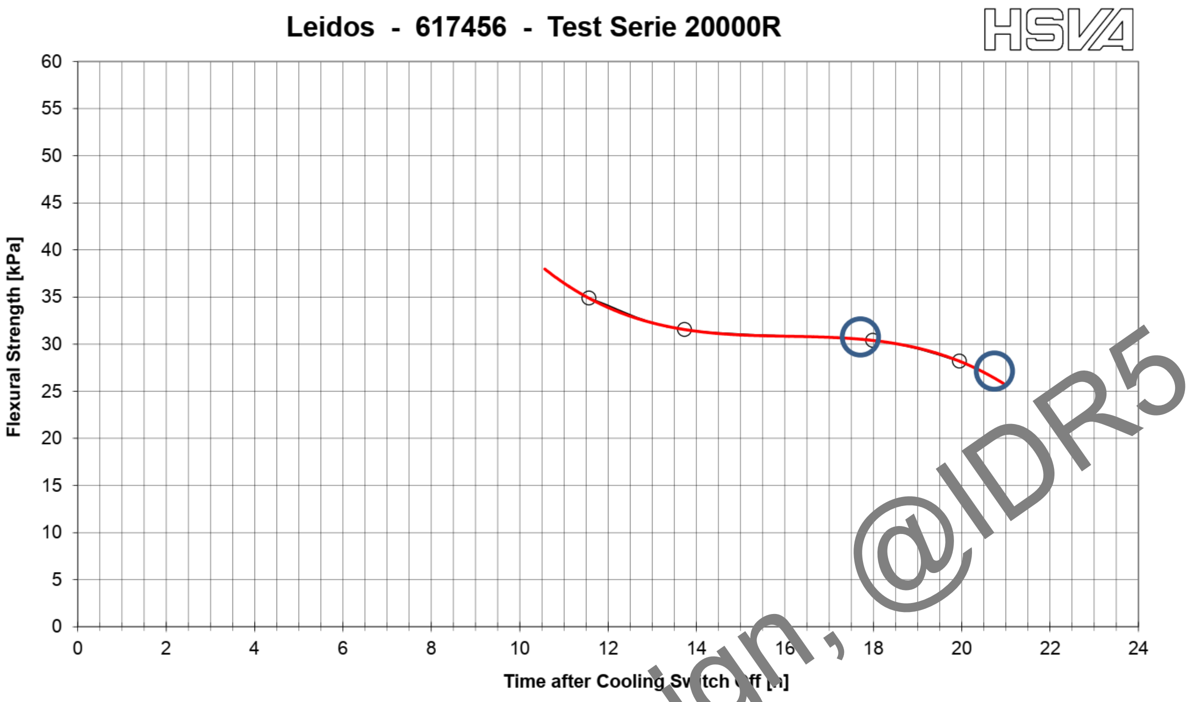

Figure 15 Flexural strength for test series 20000R

Crushing Strength

$\sigma_{cr} = \frac{F_{cr}}{c_i \cdot m \cdot D \cdot k \cdot h} = 155.6$ kPa

F = force (measured)

m = shape factor (round structure 0.9)

k = contact factor (0.4 - 0.7)

h = ice thickness D = diameter of indenter

ci = factor depending on the D/h ratio

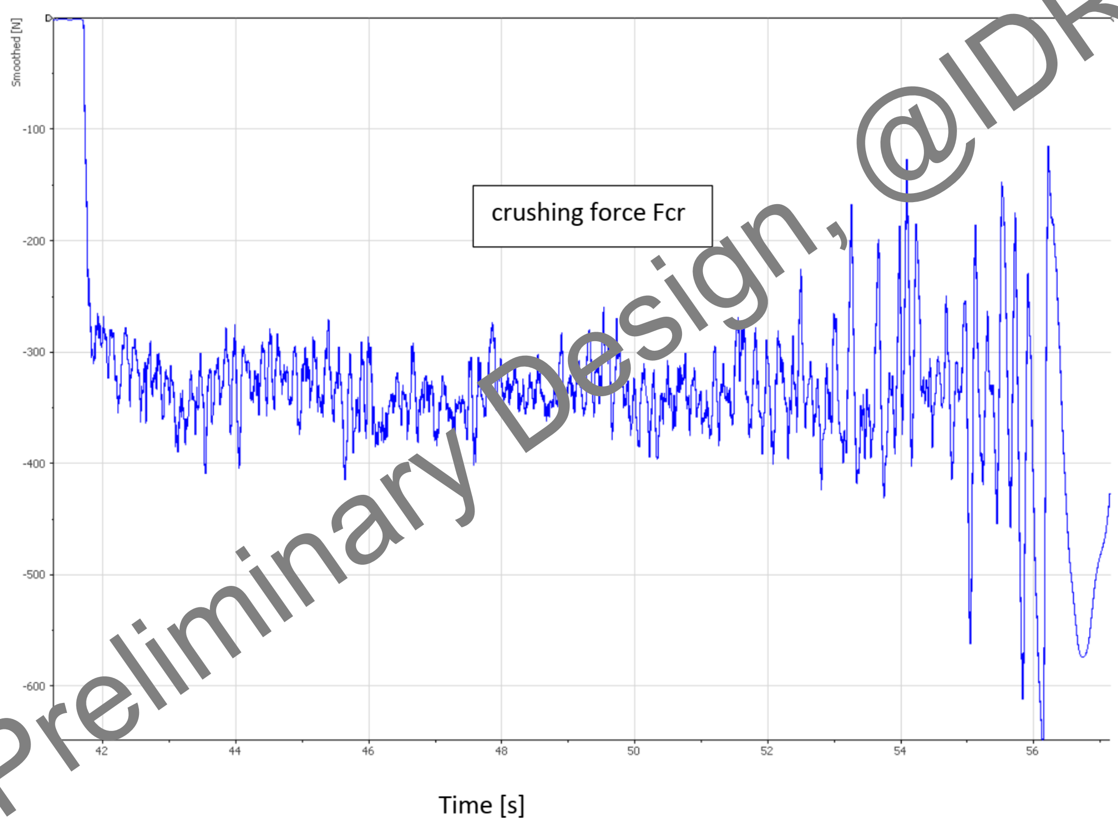

Figure 16 Plot of crushing force time series from indentation test, test series 20000R

Level ice density

Client:	Leidos	HSVA
Project:	617456	
Date:	3.4.2023	

Test Series:		20000R	
Water Density:	ρ_{water} =	1005.5	[kg/m³]
Water Salinity:	S_W =	7.0	[‰]
Oxygen set value:	O_2 =	18.3	[mg/l]

Ice density ρ_i :

$$\rho_i = \frac{W_2}{W_3}\,\rho_w$$

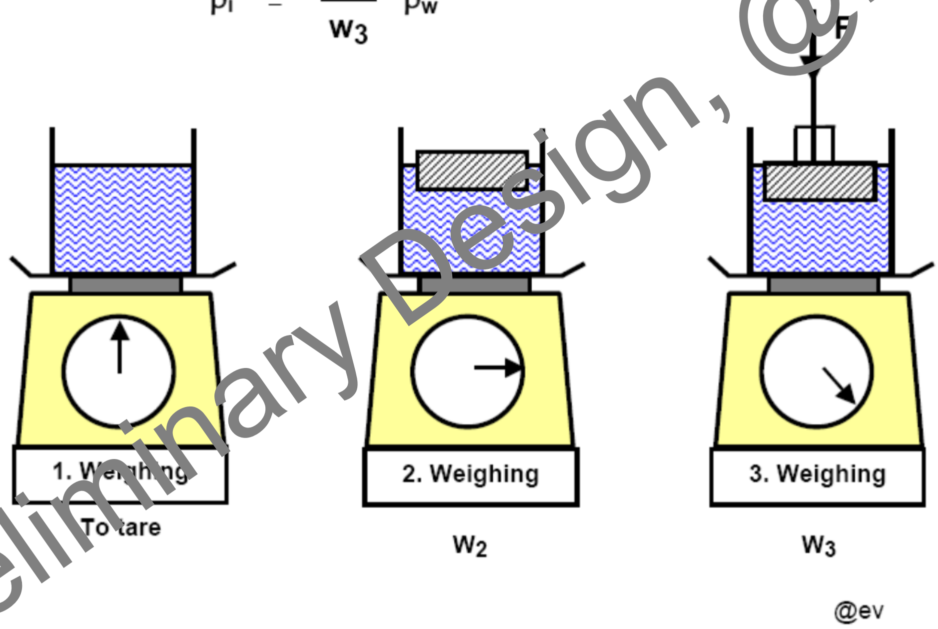

Specimen No. or x \ y-Tank Pos.	W_2 [g]	W_3 [g]	ρ_{ice} [kg/m³]	Salinity [‰]
21 / 1	855	936	918	3.5
43 / 1	853	938	914	3.5
66 / 1	939	1021	925	3.5
mean >>>	882.3	965.0	919.2	3.5

Figure 17 Level ice density measurements of series 20000R

4.2 Ser 30000R

Level Ice Thickness

Date:	2023-04-06		Time:	Test Series:	30000R		
Pos. Tm.	Port [mm]	Centre [mm]	Stbd. [mm]	Pos. Tm.	Port [mm]	Centre [mm]	Stbd. [mm]
12				43	43.0		43.0
13				44	43.0		41.0
14				45	41.0		41.0
15				46	43.0		42.0
16				47	45.0		45.0
17				48	46.0		46.0
18	40.0		44.0	49	46.0		46.0
19	43.0		41.0	50	44.0		44.0
20	43.0		44.0	51	45.0		44.0
21	43.0		44.0	52	43.0		43.0
22	43.0		44.0	53	42.0		44.0
23	44.0		41.0	54	44.0		45.0
24	43.0		45.0	55	44.0		43.0
25	45.0		45.0	56	44.0		43.0
26	43.0		46.0	57	42.0		43.0
27	44.0		45.0	58	45.0		43.0
28	42.0		44.0	59	46.0		45.0
29	42.0		42.0	60	45.0		44.0
30	44.0		45.0	61	47.0		45.0
31	45.0		45.0	62	48.0		44.0
32	46.0		45.0	63	46.0		45.0
33	47.0		45.0	64	48.0		48.0
34	44.0		45.0	65	44.0		47.0
35	45.0		47.0	66	46.0		47.0
36	42.0		44.0	67	44.0		48.0
37	42.0		44.0	68	46.0		45.0
38	44.0		45.0	69	44.0		43.0
39	43.0		44.0	70	47.5		47.0
40	42.0		44.0	70.25		47.0	
41	42.0		42.0	72			
42	42.0		40.0	Av.	44.0	47.0	44.2
				Av. of all		44.2	

Figure 18 Level ice density measurements of series 30000R

Broken Channel Width

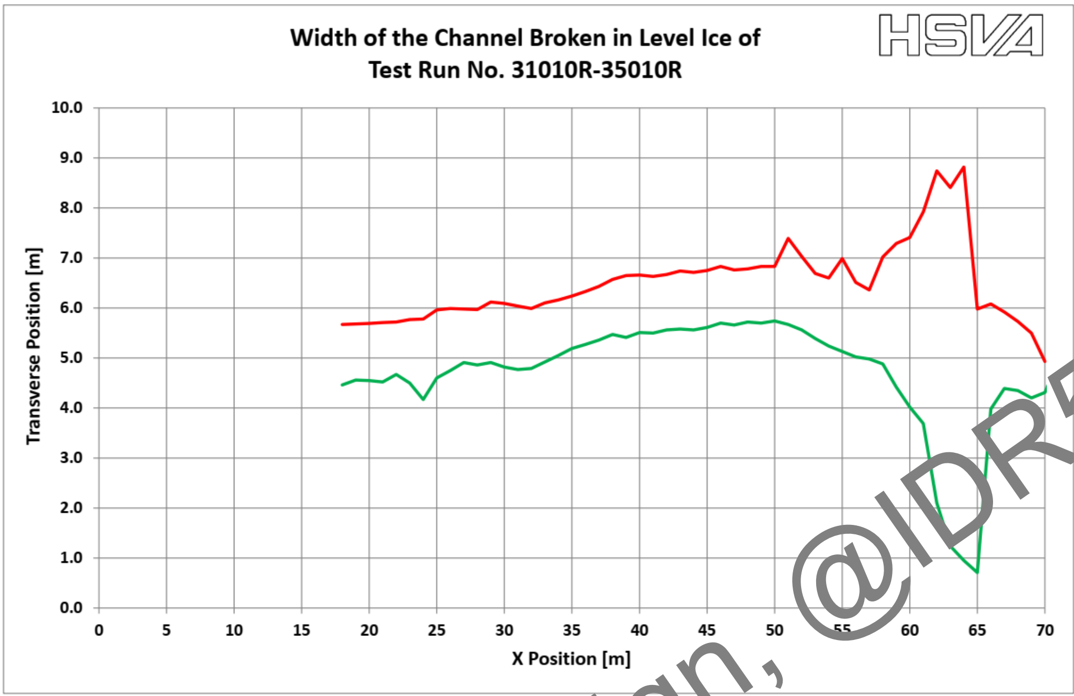

Figure 19 Measurement of broken channel width, test run nos. 31010R-35010R

Average Width of broken channel:
21010R-24011R: 1.17m = 1.17 x B

Flexural Strength

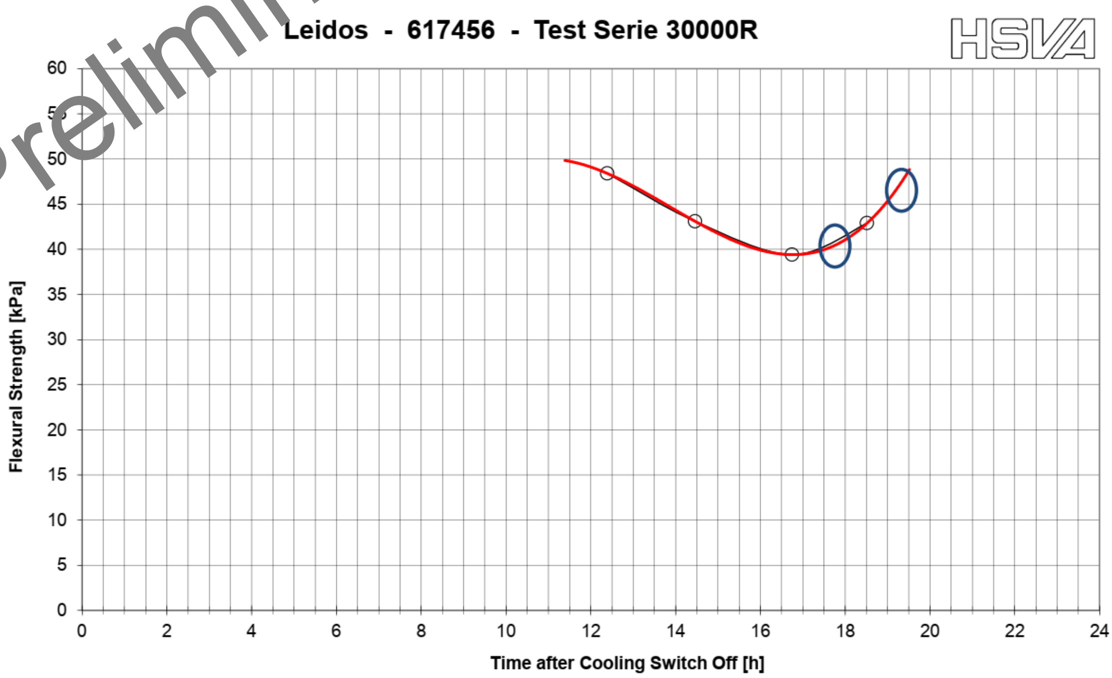

Figure 20 Flexural strength for test series 20000R

Crushing Strength

$\sigma_{cr} = \frac{F_{cr}}{c_i \cdot m \cdot D \cdot k \cdot h} = 77.1$ kPa

F = force (measured)

m = shape factor (round structure 0.9)

k = contact factor (0.4 - 0.7)

h = ice thickness D = diameter of indenter

ci = factor depending on the D/h ratio

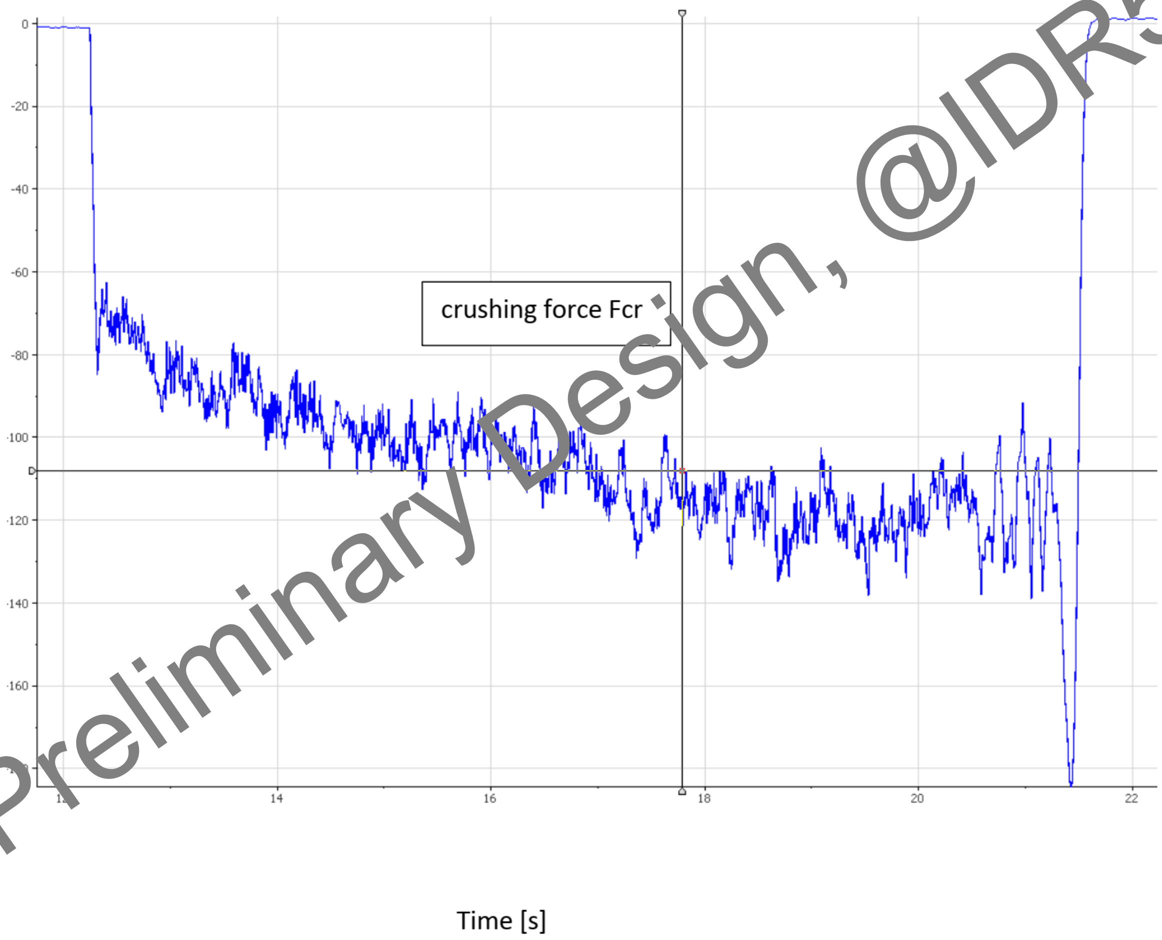

Figure 21 Plot of crushing force time series from indentation test, test series 30000R

Client:	**Leidos**		
Project:	**617456**		
Date:	**2023-04-06**		

Test Series 30000R

General				
Weight per Step	200	[g]	1.9628	[N]
ρ_w:	1005.5	[kg/m^3]		
ny:	0.3	[-]		
g:	9.814	[m/s^2]		

Test No.:	**#001**		**Test No.:**	**#002**	
Time:	06:28	[hh:mm]	Time:	06:36	[hh:mm]
Tank Pos. X:	21.00	[m]	Tank Pos. X:	43.00	[m]
h_ice_1:	44.50	[mm]	h_ice_2:	44.00	[mm]
σ_f_1:	43.10	[kPa]	σ_f_2:	49.20	[kPa]
E_mean:	52	[MPa]	E_mean:	21	[MPa]
E_mean/σ_f:	1205	[-]	E_mean/σ_f:	428	[-]

Test No.:	**#003**		**Test No.:**	**#004**	
Time:	06:44	[hh:mm]	Time:		[hh:mm]
Tank Pos. X:	66.00	[m]	Tank Pos. X:		[m]
h_ice_1:	47.00	[mm]	h_ice_2:		[mm]
σ_f_1:	41.00	[kPa]	σ_f_2:		[kPa]
E_mean:	23	[MPa]	E_mean:		[MPa]
E_mean/σ_f:	559	[-]	E_mean/σ_f:		[-]

Figure 22 Plot of crushing force time series from indentation test, test series 30000R

Level ice density

Client:	**Leidos**	HSVA
Project:	**617456**	
Date:	**6.4.2023**	

Test Series:		**30000R**	
Water Density:	ρ_{water} =	**1005.5**	[kg/m³]
Water Salinity:	S_w =	**7.0**	[‰]
Oxygen set value:	O_2 =	**19.3**	[mg/l]

Ice density ρ_i :

$$\rho_i = \frac{W_2}{W_3} \rho_w$$

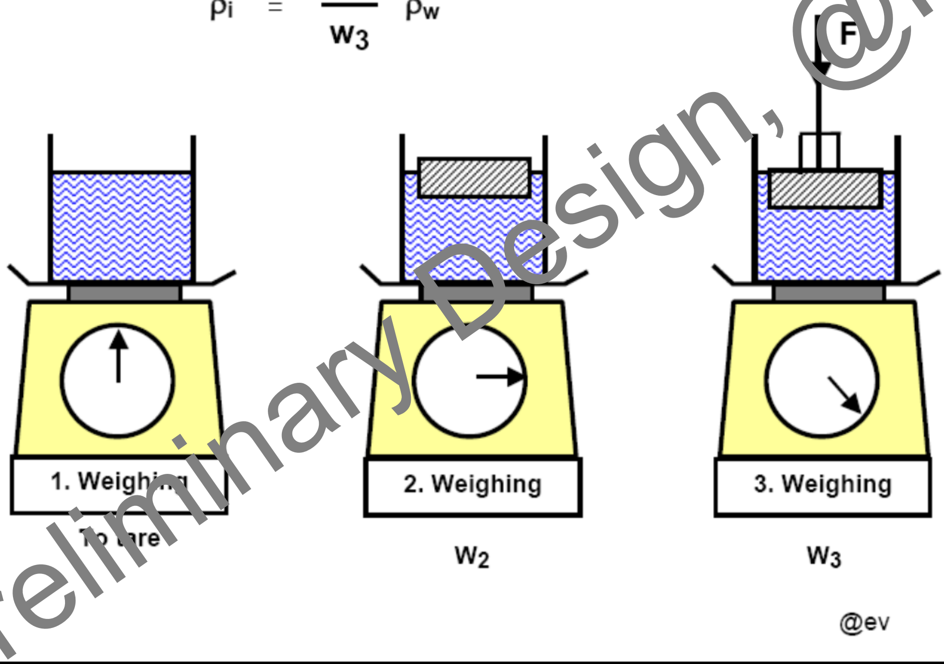

Specimen No. or x \ y-Tank Pos.	W_2 [g]	W_3 [g]	ρ_{ice} [kg/m³]	Salinity [‰]
21 / 1	670	734	918	3.4
43 / 1	628	693	911	3.3
66 / 1	729	791	927	3.5
mean >>>	675.7	739.3	918.6	3.4

Figure 23 Level ice density measurements of series 30000R

5 Test Observations

5.1 Ser 10000R

During towed propulsion test in level ice ahead the model showed typical breaking behaviour at the bow. The center crack is fully developed before the fore skeg (which is now wider) interacts with the ice floes. At the outer lower edges of the skeg some broken ice floes get crushed into smaller pieces. The sides and outer part of flat bottom / box keel are fully covered by ice floes while the inner part (areas of sonar beams) remains mainly ice free. At the aftship some ice floes which are sliding along the bilge radius area are getting sucked into the propellers. Most of the ice floes are attached to the hull and can pass above the propellers but some of them are hitting the upper blade tip (torque increase). Possibility of additional clearance of the propellers to hull should be checked.

Figure 24 Test run no. 11010R underwater ice observations

During towed and free running tests astern the model showed good icebreaking and ice clearing behaviour similar to the behaviour of previous tested version. In the center between the pods rectangular floes are broken and they get split at the aft skeg. At the outer hull area relative small floes get broken which can be easily cleared by the propeller wash. Despite some single smaller floes sliding along the bottom the hull remains mainly ice free. Crushing of ice floes seem to occur at the struts of Pods which is indicated by a streamline of crushed ice in the underwater video.

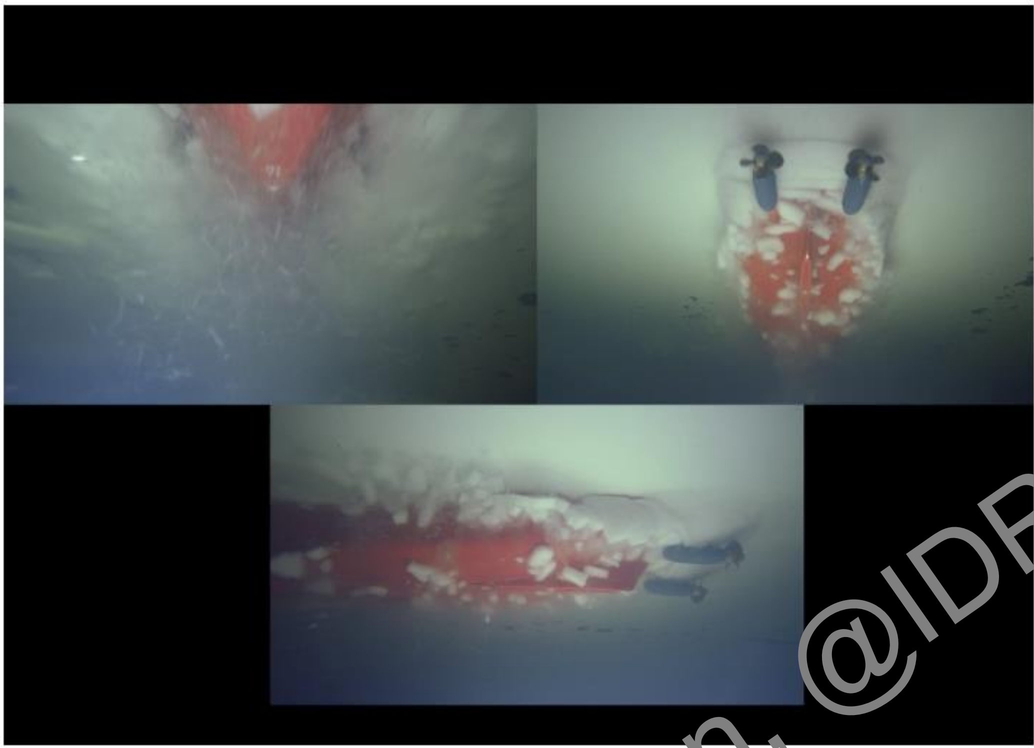

Figure 25 Test run no. 13011R underwater ice observations

Figure 26 Test run no. 14011R underwater ice observations

5.2 Ser 20000R

During free running propulsion test in level ice ahead the model showed typical breaking behaviour at the bow. The center crack is fully developed before the fore skeg (which is now wider) interacts with the ice floes. At the outer lower edges of the skeg some broken ice floes get crushed into smaller pieces. The sides and outer part of flat bottom / box keel are fully covered by ice floes while the inner part (areas of sonar beams) remains mainly ice free. At the aftship some ice floes which are sliding along the bilge radius area are getting sucked into the propellers. Compared to the observations made during towed propulsion tests the ice coverage and propeller-ice interaction seem to be less in free running condition (also due to lower advance speed).

Figure 27 Test run no. 21010R underwater ice observations

The first free running test astern was carried out at 40% power. The model was accelerated in the ice free channel and decelerated immediately after entering the level ice with bow. The model came to full stop and could not be moved with the available thrust. A second test astern at 70% power was added to the program. The model could be started with available thrust and was maintaining a continuous speed. The breaking and clearing behaviour was very similar to the one observed during towed propulsion tests while the ice overage seemed even less.

Figure 28 Test run no. 24011R underwater ice observations

After free running tests astern two break out maneuvers were carried out. The tests were started from previous broken channel (with naturally broken width). First a break out maneuver astern was performed. The model was accelerated in the channel and the thrusters were turned shortly after. The model immediately began to pull into the surrounding ice stern first showing significant heel angle (abt. 8 degree). The break out was completed within small space and the model could be turned to 90 degree and could leave the channel completely within short time. The propellers remained mainly ice free while one of the propellers was occasionally milling single ice floes.

After the break out test astern was completed the model was moved to another position of the channel and a break out test ahead was started. The model was accelerated to a constant speed and the thrusters were turned thereafter. The model began to slide along the edge of the channel breaking off pieces of ice and widening the channel. During this process the model showed significant heel (abt. 7 degree). After a certain distance the model could obtain an efficient angle of attack and could enter the surrounding ice with the bow while the aft ship was pushed into opposite ice next to the channel.

Figure 29 Test run no. 25011R underwater ice observations

Figure 30 Test run no. 26010R underwater ice observations

5.3 Ser 30000R

Test run 31010R was carried out to check the natural breaking behaviour of the model in around 1m level ice (full scale) while the thrusters are aligned in longitudinal direction.

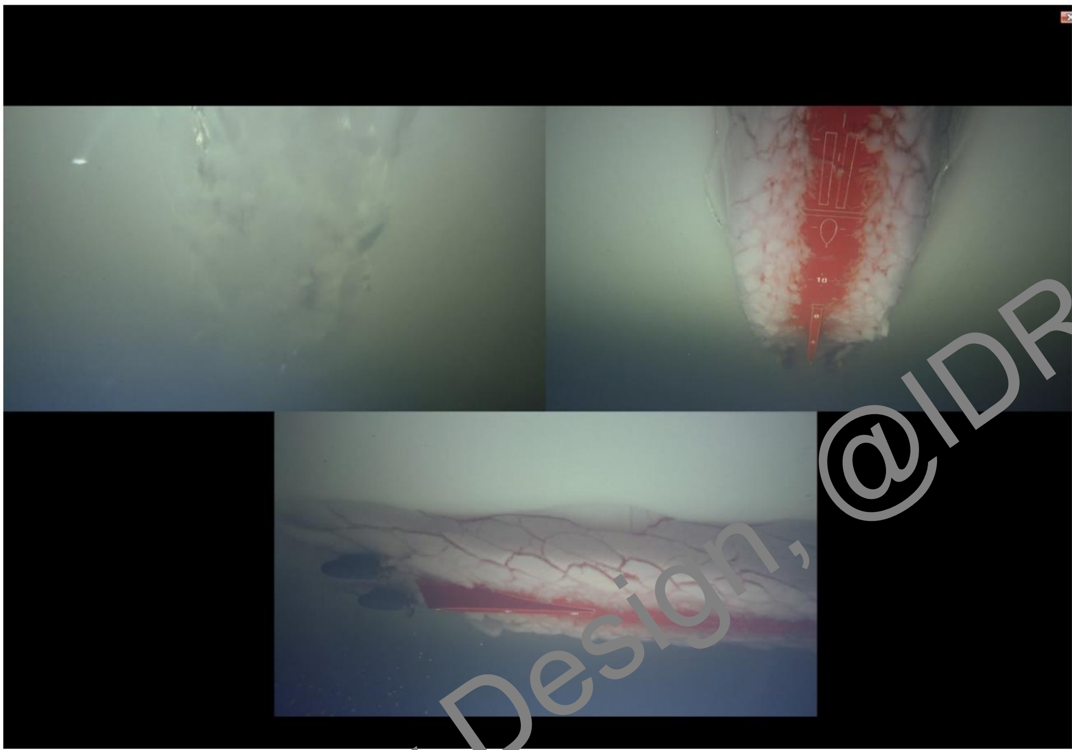

Figure 31 Test run no. 31010R underwater ice observations

In test run no. 32010R both thrusters were set at a toe in angle of around 60 degree. The model was proceeding at low speed and the channel behind the vessel was cleared by the thruster wash. Only single small pieces of ice remained in the wake of the model.

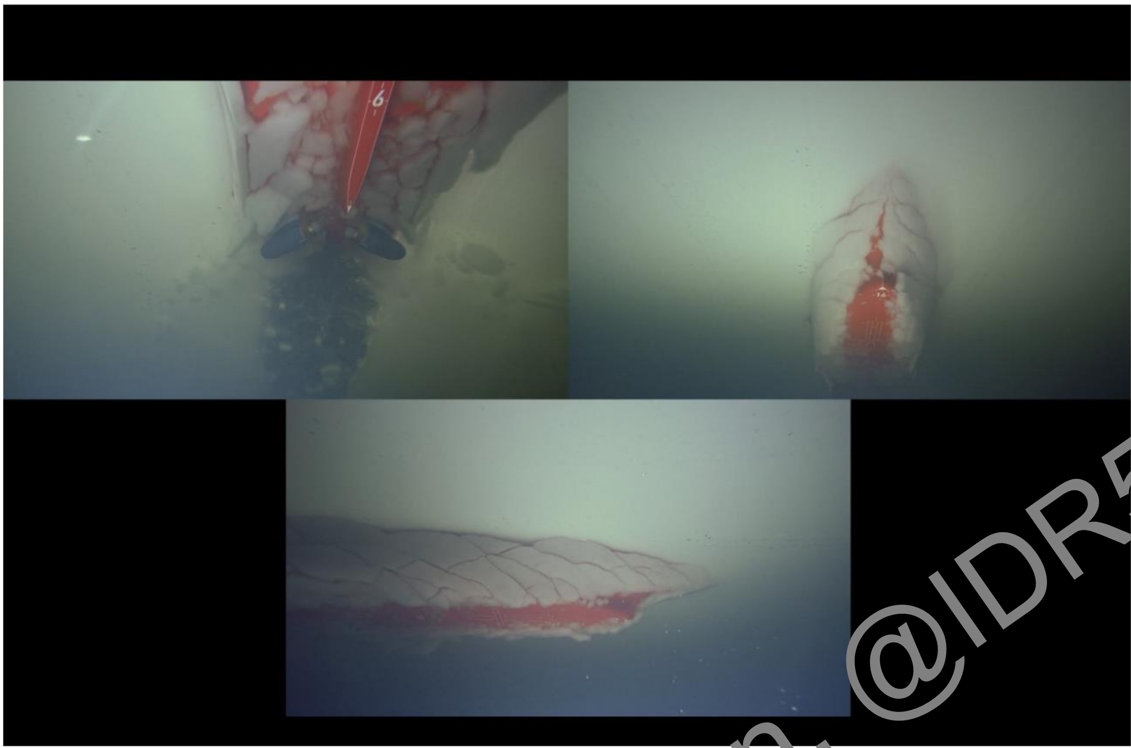

Figure 32 Test run no. 32010R underwater ice observations

In test run no 33010R both thursters were put at an toe out angle of around 60 degree. The propeller wash was now coring and interfering. Larger pieces of ice were observed in the channel behind the model.

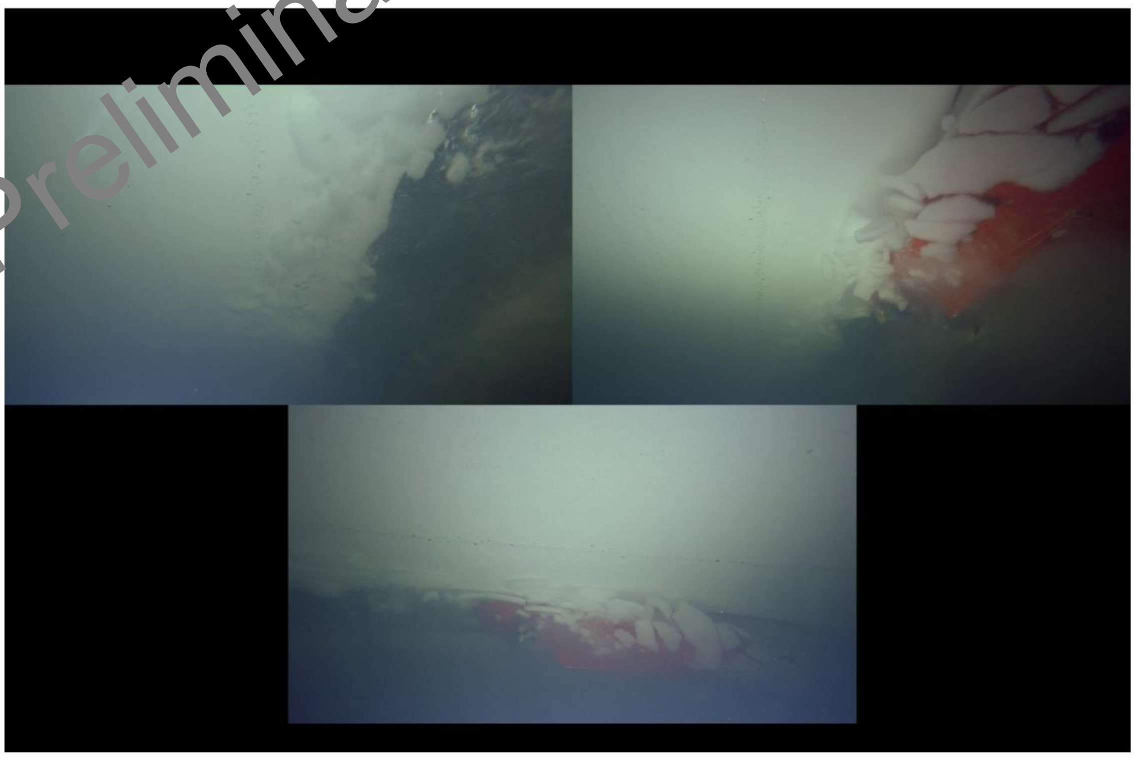

Figure 33 Test run no. 33010R underwater ice observations

In test run no. 34010R the thruster angles were alternating from one side to the other while both thrusters were moved in parallel. The channel behind the vessel was cleared by the thruster wash and the channel was widened by the relative strong motions of the model (roll and yaw motion).

Figure 34 Test run no. 34010R underwater ice observations

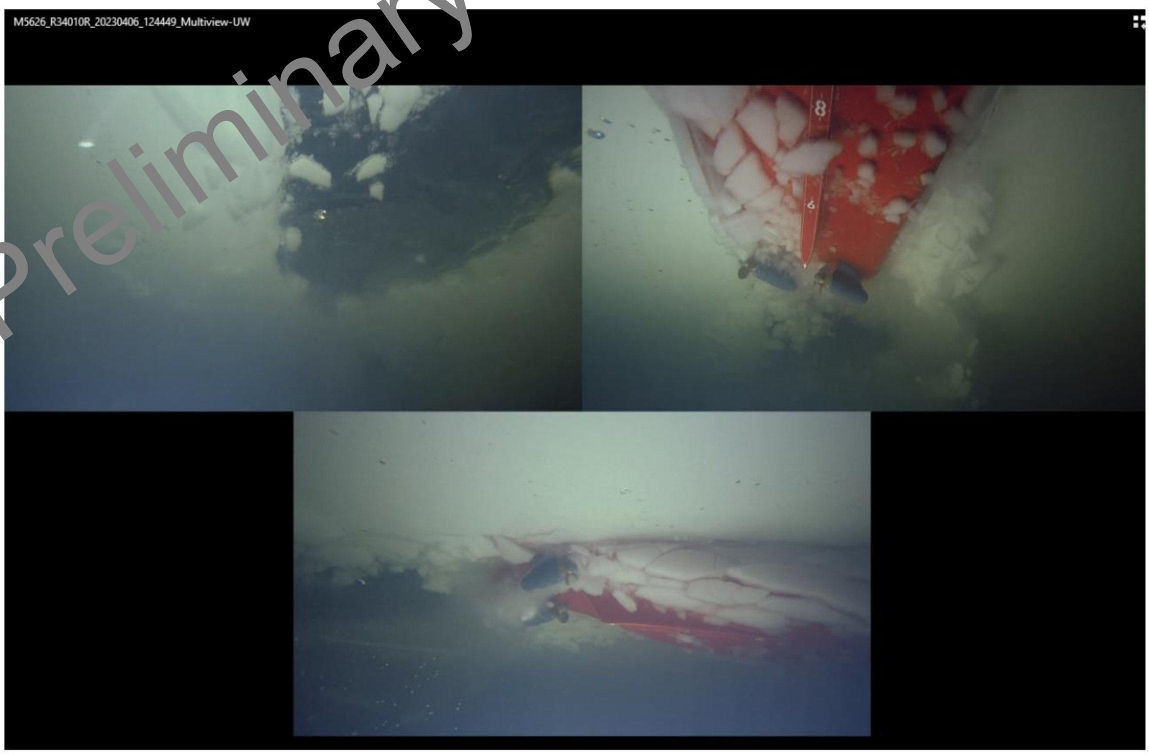

Figure 35 Test run no. 35010R underwater ice observations 1

In test run no 35010R a side step was performed by moving the thrusters such that the model did not make any significant forward or backward moves but the thurster wash was creating an open pool beside the starboard side of the model. It turned out after some attempts that the operator needed to move both thrusters to the same side and push the model against the intact ice on one side to create the open pool on the other side. A pool of sucfficient size could be opened using this strategy.

Figure 36 Test run no. 35010R underwater ice observations 2

During tests run 36010R the model was running back through the previously broken channel (after being turned round in the open pool created in test run 35010R). The model was using the toe in thruster strategy (same as test urn 32010R) during moving back in order to completely clear the channel.

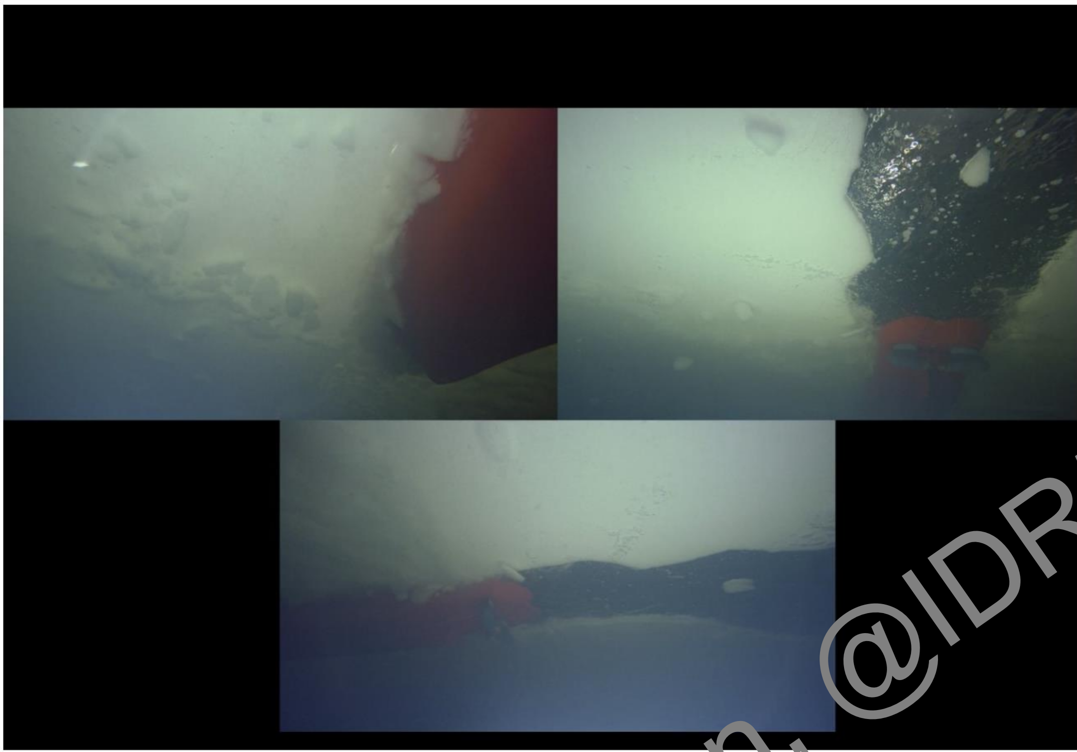

Figure 37 Test run no. 36010R underwater ice observations

Test run 37010R was used to create a wider filed of brahs ice. The model was cutting larger fragments off the intact ice from the sides of the basin and was further breaking this ice into smaller brash ice pieces running astern.

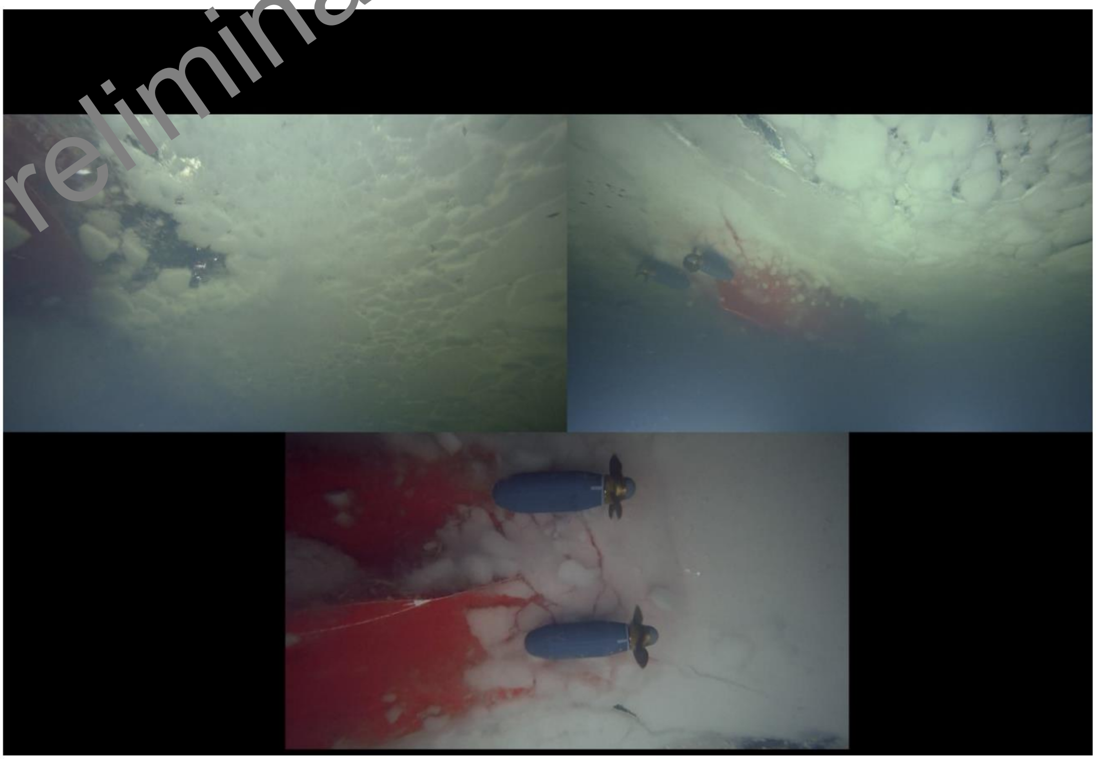

Figure 38 Test run no. 37011R underwater ice observations 1

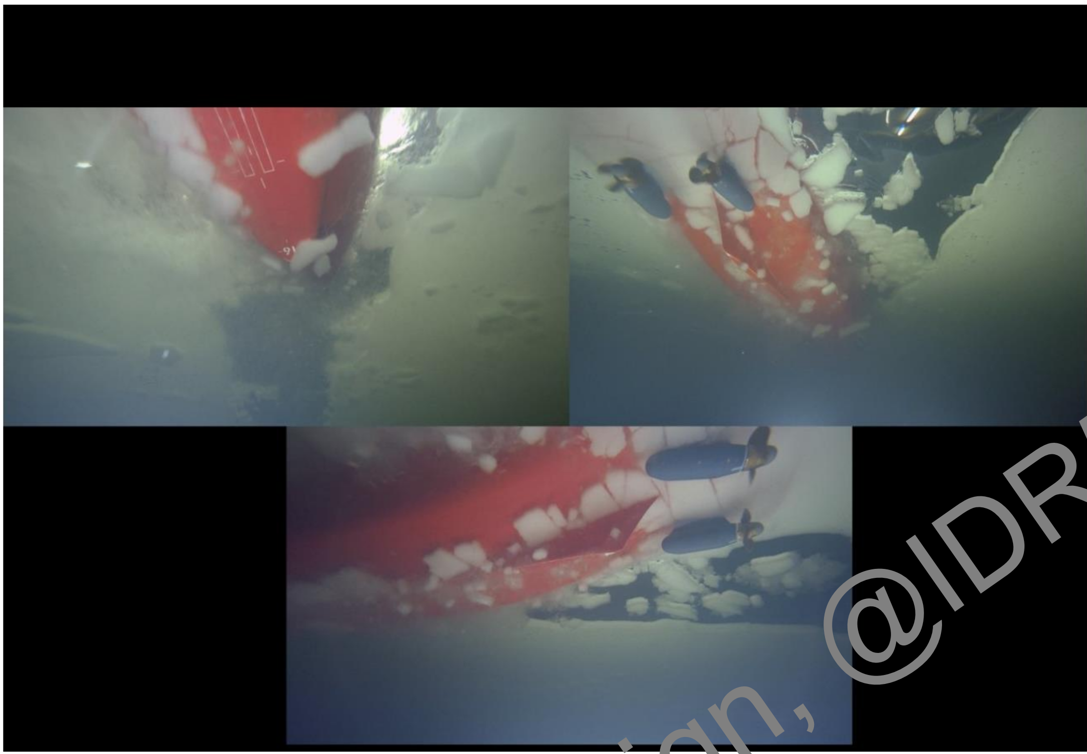

Figure 39 Test run no. 37011R underwater ice observations 2

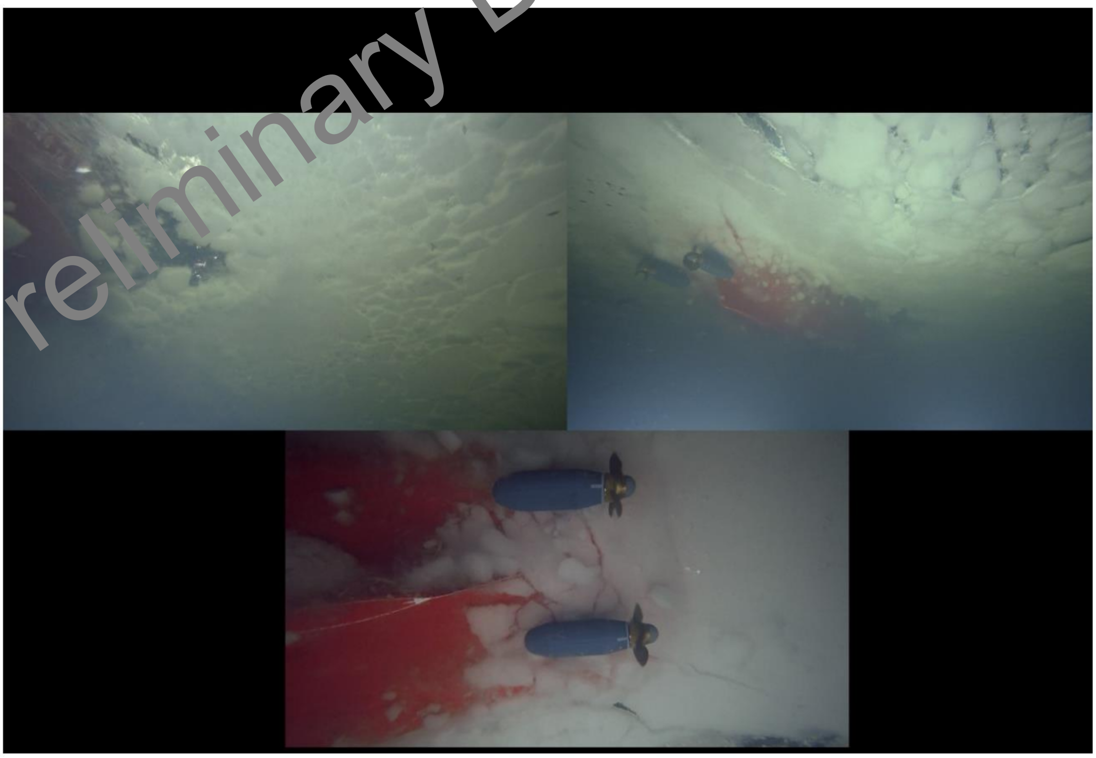

Figure 40 Test run no. 37011R underwater ice observations 3

In test run 38010R the model was moved through the brash ice field and was clearing the brash ice with thruster wash with thruster angles angles 85, 60 and 30 degree toe in. The clearing was very sufficient at all three thruster angles and different resulting speeds.

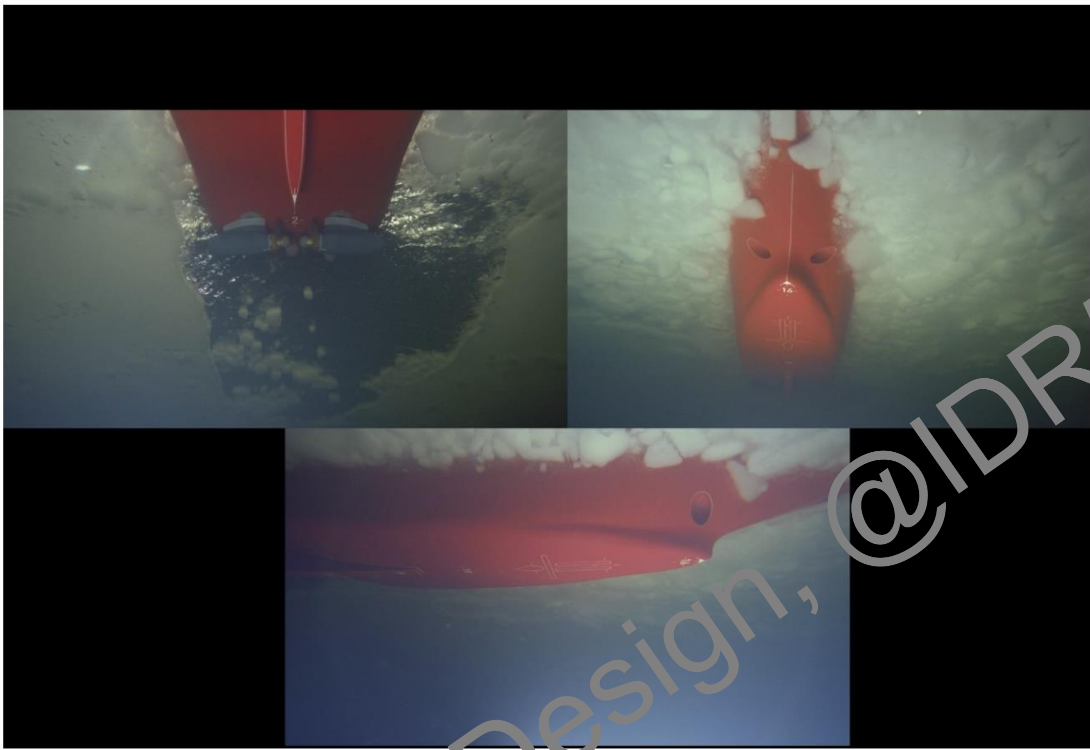

Figure 41 Test run no. 38010R underwater ice observations 1 (85 degree thruster angle)

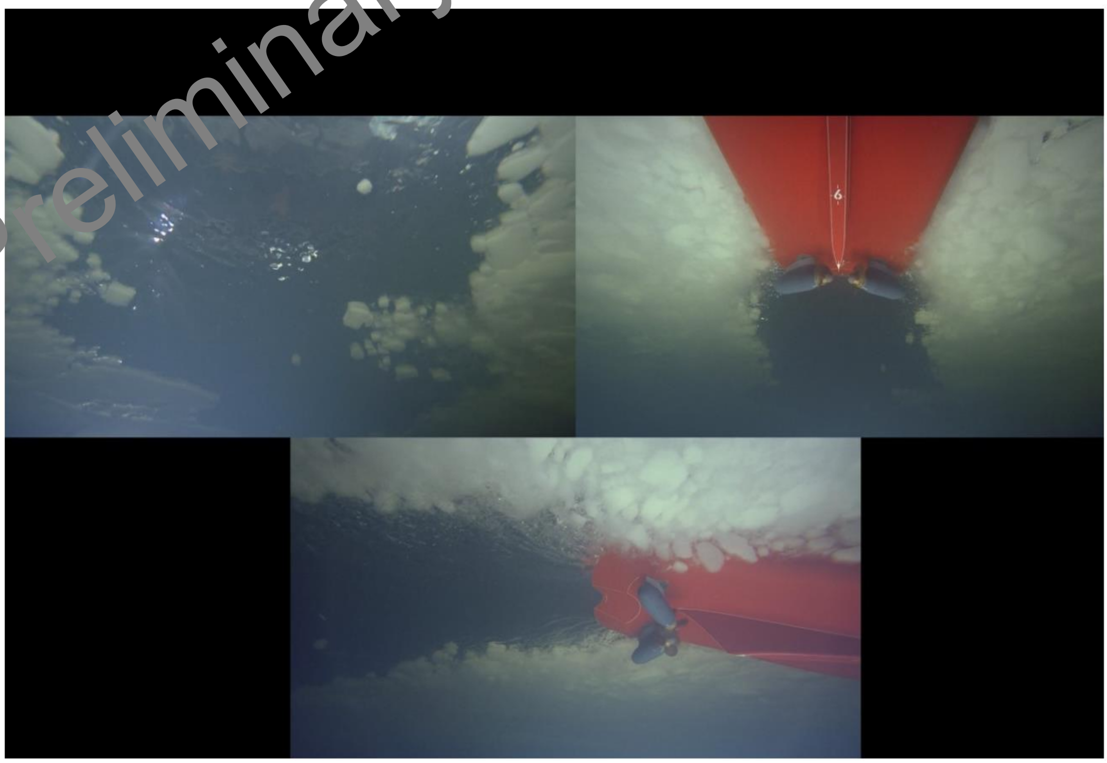

Figure 42 Test run no. 38010R underwater ice observations 2 (60 degree thruster angle)

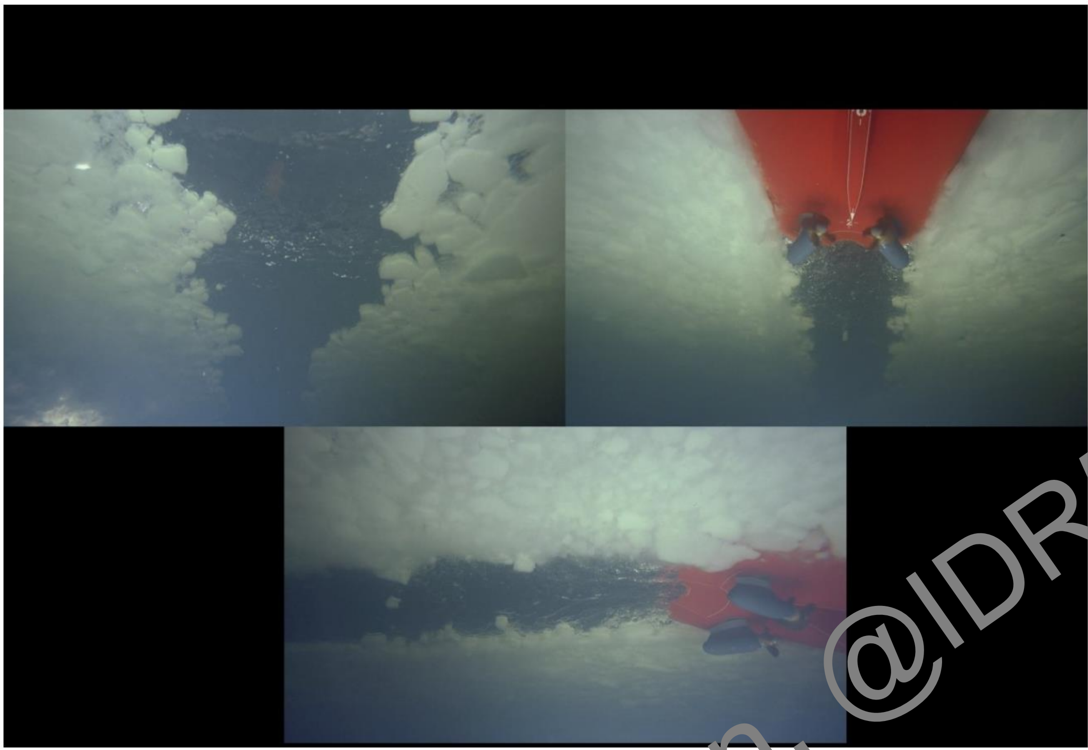

Figure 43 Test run no. 38010R underwater ice observations 3 (30 degree thruster angle)

6 Test Results

6.1 Test run no. 11010R, Towed Propulsion Test Ahead in Level Ice, 6 knots

Level Ice Test
Draft forward/aft : 0.406m/0.406m
Tank water density : 1005.5kg/m³

Corrected intervals data

Sub interval	V [m/s]	FN [-]	n_mean [1/s]	Q_tot [Nm]	PD_tot [W]	T_tot [N]	FP [N]	dFP/dT_tot [-]	RIT [N]
LI_1	0.6250	0.0945	14.1992	8.2210	733.4370	221.5780	39.0819	-1.0053	261.8265
LI_2	0.6250	0.0945	8.8987	3.8791	216.8796	63.7983	208.6000	-1.0053	272.7342
LI_3	0.6251	0.0945	11.8968	6.7563	505.0150	147.8573	119.6320	-1.0053	268.2678
LI_4	0.6250	0.0945	3.9007	1.1502	28.1942	-14.1275	274.6030	-1.0053	260.4012

RIT_mean = 265.807 N

Target values

H_ice [mm]	SIGF_ice [kPa]	FID [-]
56.1844	28.7073	0.0550

Ice feature : Level ice

Correction for deviations between actual and target test conditions

Test No.	H_ice [mm]	SIG_F [kPa]	FID [-]	FN_HI [-]	F1 (HI)	F2 (SIGF)	F3 (FID)	T' [illegible]	FP' [N]	dFP'/dT' [-]	RIT' [N]
LI_1	60.3000	32	0.1100	0.8420	0.9211	0.9647	[illegible]	[illegible]	27.3792	-1.0053	183.4249
LI_2	60.3000	32	0.1100	0.8420	0.9211	0.9647	[illegible]	44.6945	146.1368	-1.0053	191.0665
LI_3	60.3000	32	0.1100	0.8421	0.9211	[illegible]	[illegible]	103.5832	83.8097	-1.0053	187.9381
LI_4	60.3000	32	0.1100	0.8420	0.9211	[illegible]	[illegible]	-9.8971	192.3758	-1.0053	182.4266
Mean :	60.3000	32	0.1100		[illegible]	0.9647	0.7885				

RIT'_mean = 186.214 N

Approximation order for PD vs T : 2

Final model scale results

V [m/s]	RIT'_mean [N]	dFP'/dT' [-]	t' [-]	T'_sp [N]	PD'_sp [W]	ETAD' [-]
0.6250	[illegible]	-1.0053	-0.0053	185.2391	616.6468	0.1887

Self propulsion point

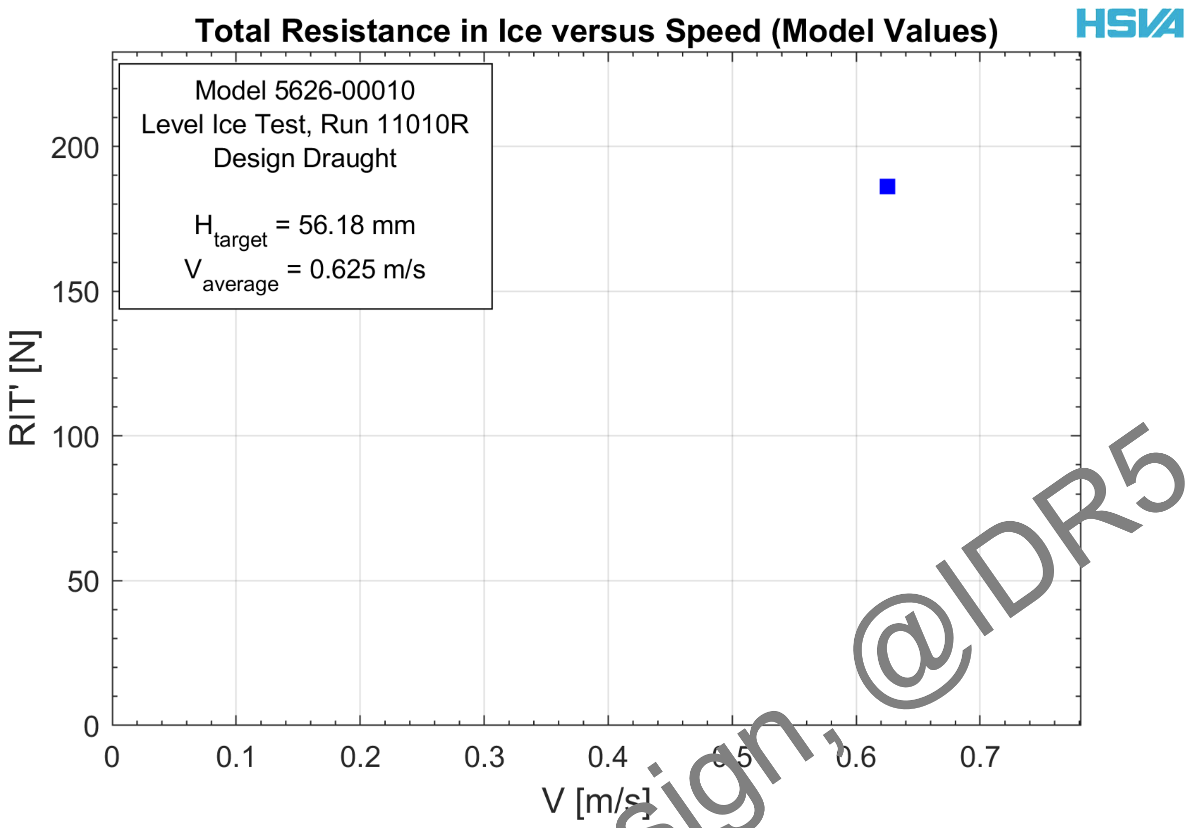

Figure 44 Total resistance ahead in 1.37m level ice, 6knots, model scale

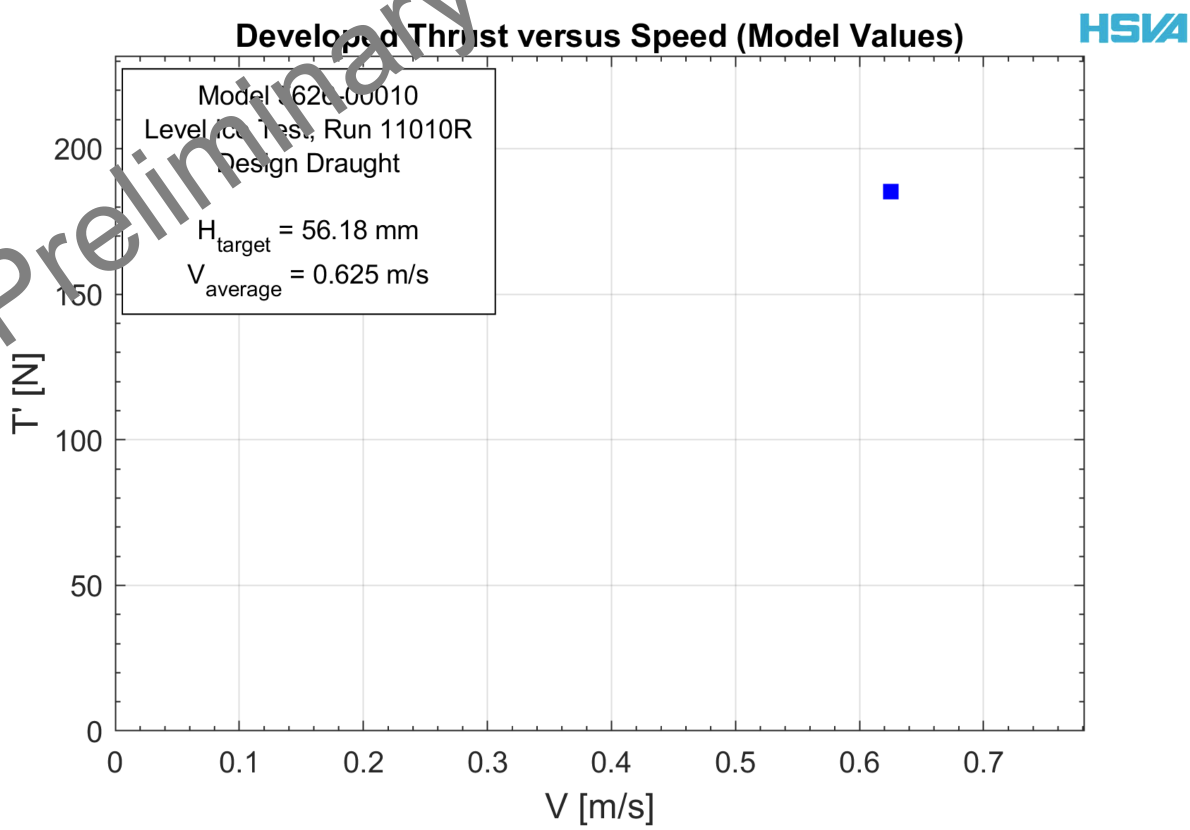

Figure 45 Total thrust ahead in 1.37m level ice, 6knots, model scale

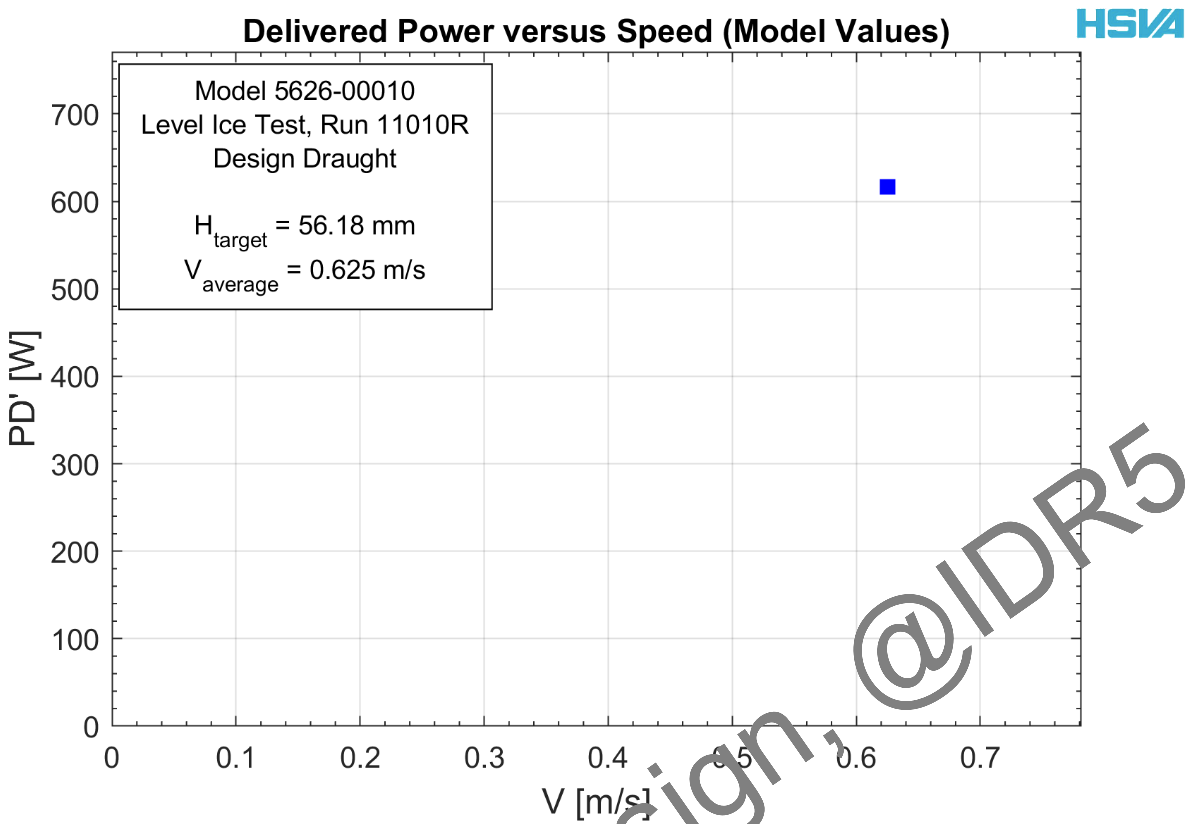

Figure 46 Delivered power ahead in 1.37m level ice, 6knots, model scale

Model : 5626-00010
Sh[illegible] Length L_pp : [illegible]
Propellers : HSVA No. 2288/89
S[illegible]op. diameters (1->2) : 4.877m/4.877m
Level Ice Test
[illegible]ea water density : 1024.9kg/m³
Draft forward/aft : 9.906m/9.90[illegible]m

Full scale values (from c[illegible]ecte[illegible] intervals data)

Sub interval	V [[illegible]]	[illegible]N [[illegible]]	n_mean [1/min]	Q_tot [kNm]	PD_tot [kW]	T_tot [kN]	FP [kN]	dFP/dT_tot [-]	RIT [kN]	FD [kN]
LI_1	5.[illegible]93	0.0945	172.5286	2962.47	53522.84	3274.54	577.56	-1.0053	3869.35	40.27
[illegible]	5.999[illegible]	0.0945	108.1242	1397.84	15826.87	942.83	3082.75	-1.0053	4030.54	40.27
LI_[illegible]	5.9998	0.0945	144.5536	2434.66	36853.66	2185.08	1767.96	-1.0053	3964.54	40.27
[illegible]_4	5.9992	0.0945	47.3958	414.46	2057.48	-208.78	4058.16	-1.0053	3848.28	40.27

RIT_mean = 3928.18 kN

Target full scale values

H_ice [m]	SIGF_ice [kPa]	FID [-]
1.3700	700	0.0550

k_FD_corr coefficient: 1
KQ correction (Rn) for PD: 0.96
Shaft efficiency: 0.99

i - correction :
RIT'_mean at Fn=0.05 2236.39 kN

Correction for deviations between actual and target test conditions, and for scale effects

Sub interval	H_ice [m]	SIG_F [kPa]	FID [-]	F1 (HI) [-]	F2 (SIGF) [-]	F3 (FID) [-]	T' [kN]	FP' [kN]	RIT' [kN]	i [-]	FP'' [kN]	dFP''/dT' [-]	RIT'' [kN]	PD'' [kW]
LI_1	1.4704	780.29	0.1100	0.9211	0.9647	0.7885	2294.01	404.62	2710.71	-0.1190	98.22	-1.0053	2404.30	51381.93
LI_2	1.4704	780.29	0.1100	0.9211	0.9647	0.7885	660.51	2159.65	2823.63	-0.1190	1853.25	-1.0053	2517.23	15193.80
LI_3	1.4704	780.29	0.1100	0.9211	0.9647	0.7885	1530.78	1238.56	2777.40	-0.1190	932.16	-1.0053	2471.00	35379.52
LI_4	1.4704	780.29	0.1100	0.9211	0.9647	0.7885	-146.26	2842.98	2695.95	-0.1190	2536.58	-1.0053	2389.55	1975.18
Mean :	1.4704	780.29	0.1100	0.9211	0.9647	0.7885								

RIT'_mean = 2751.92 kN

RIT''_mean = 2445.52 kN

Final full scale results

V [kts]	RIT''_mean [kN]	dFP''/dT' [-]	t'' [-]	T''_sp [kN]	PD''_sp [kW]	ETAD'' [-]
6.00	2445.52	-1.0053	-0.0053	2432.72	38284.44	0.1971

Self propulsion point

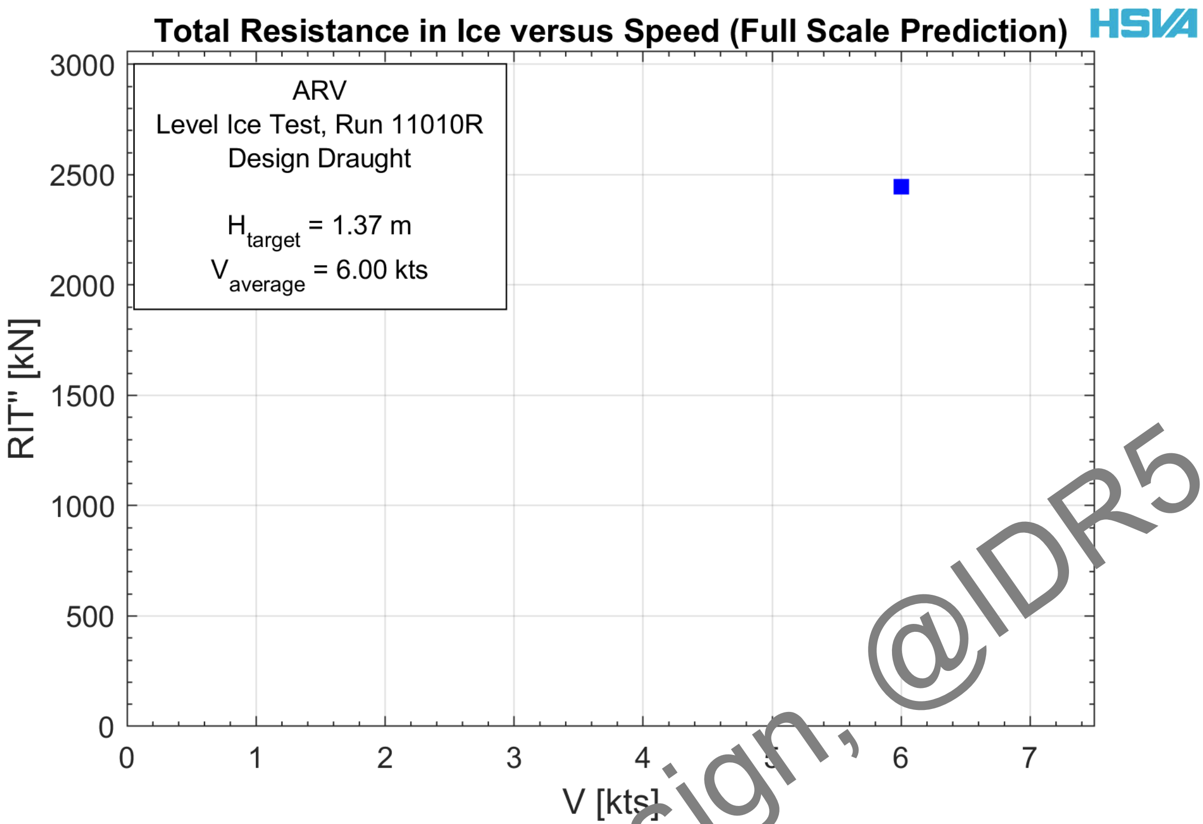

Figure 47 Total resistance ahead in 1.37m level ice, 6knots, full scale

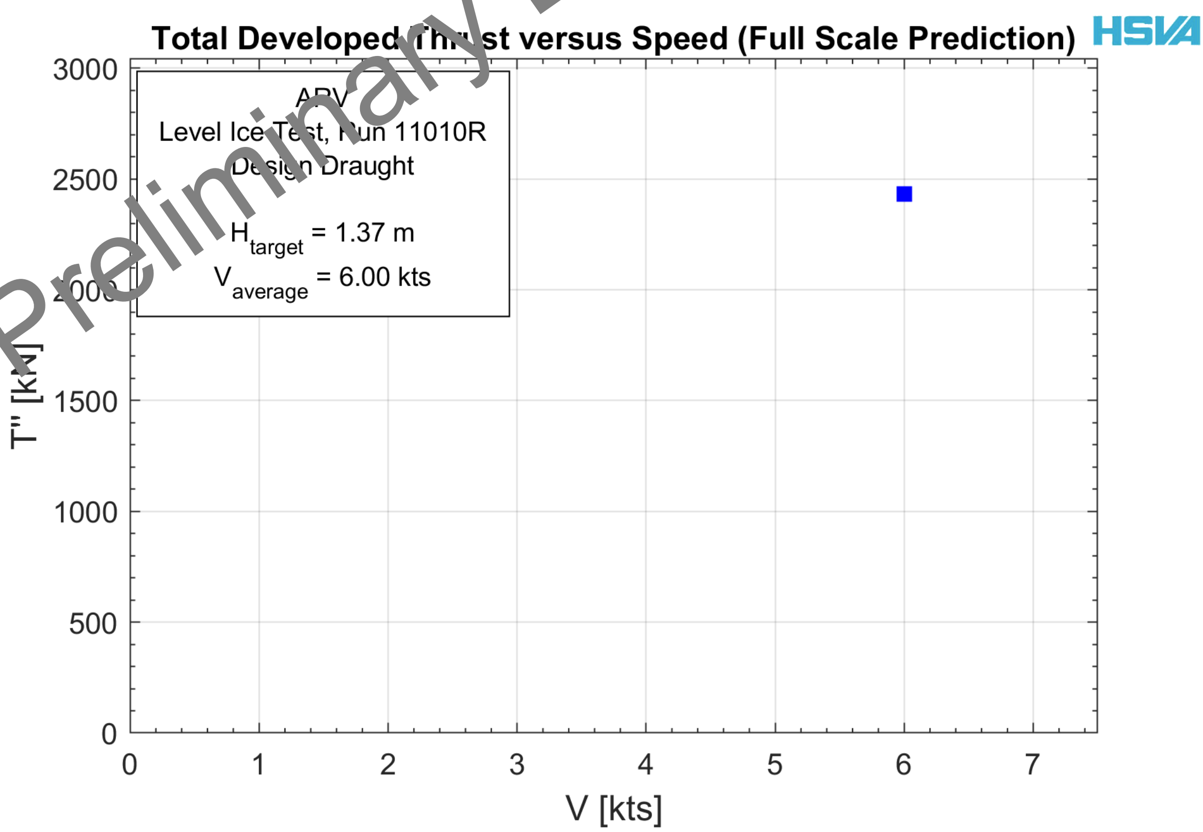

Figure 48 Total thrust ahead in 1.37m level ice, 6knots, full scale

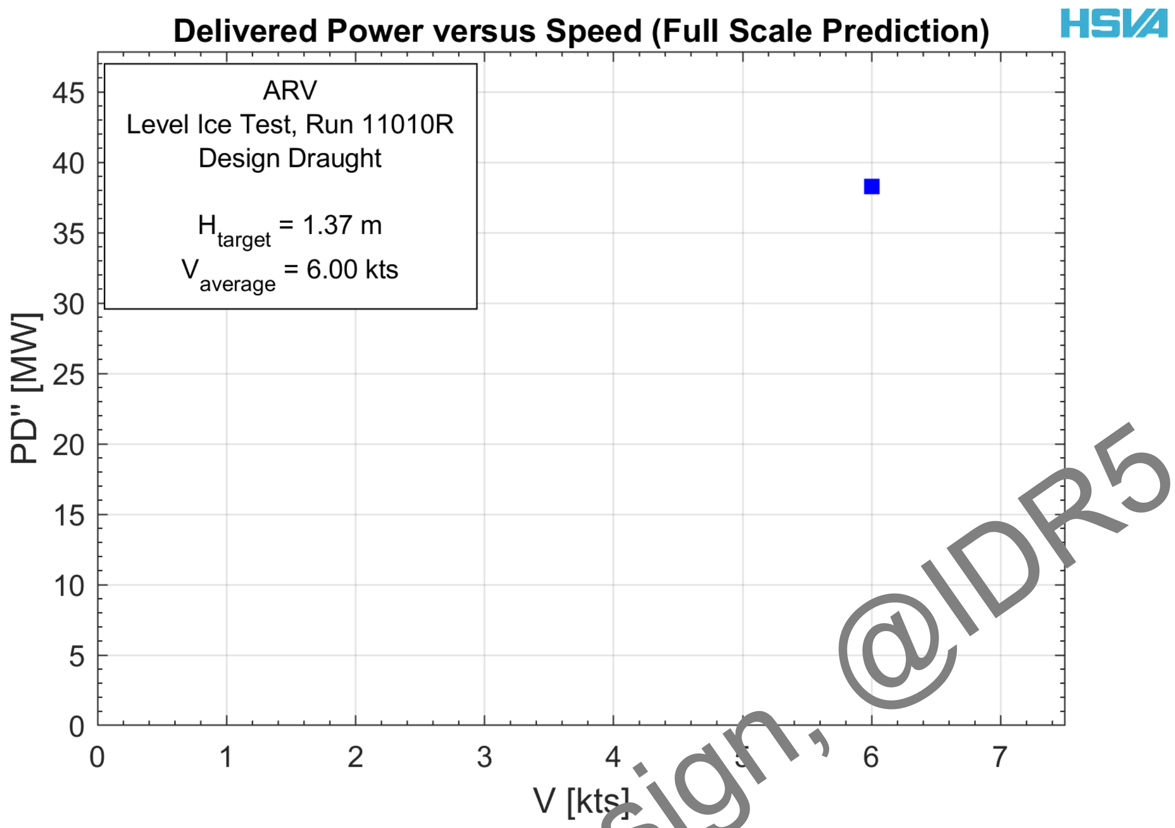

Figure 49 Delivered power ahead in 1.37m level ice, 6knots, full scale

6.2 Test Run No. 12010R, Towed Propulsion Test Ahead in Level Ice, 3 knots

Level Ice Test

Tank water density : 1005.5kg/m³

Draft forward/aft : 0.406m/0.406m

Corrected intervals data

Sub interval	V [m/s]	FN [-]	n_mean [1/s]	Q_tot [Nm]	PD_tot [W]	T_tot [N]	FP [N]	dFP/dT_tot [-]	RIT [N]
LI2_1	0.3129	0.0473	11.4993	5.6849	410.7400	158.0267	34.5059	-0.9877	190.5876
LI2_2	0.3130	0.0473	7.0001	2.4350	107.0921	44.1407	146.9910	-0.9877	190.5884
LI2_3	0.3130	0.0473	9.4995	3.9115	233.4660	102.8329	90.7803	-0.9877	192.3476
LI2_4	0.3131	0.0473	2.6988	0.3520	5.9647	-8.7388	199.8300	-0.9877	191.1988

RIT_mean = 191.181 N

Target values

H_ice [mm]	SIGF_ice [kPa]	FID [-]
56.1844	28.7073	0.0550

Ice feature : Level ice

Correction for deviations between actual and target test conditions

Test No.	H_ice [mm]	SIG_F [kPa]	FID [-]	FN_HI [-]	F1 (HI)	F2 (SIGF)	F3 (FID)	T' [N]	FP' [N]	dFP'/dT' [-]	RIT' [N]
LI2_1	62.4000	32	0.1100	0.4216	0.8696	0.9566	0.7885	103.6557	22.[illegible]	-0.9877	125.0150
LI2_2	62.4000	32	0.1100	0.4217	0.8696	0.9566	0.7885	2[illegible].9537	96.4173	-0.9877	125.0150
LI2_3	62.4000	32	0.1100	0.4217	0.8696	0.9566	[illegible]	67.4[illegible]24	59.5466	-0.9877	126.1696
LI2_4	62.4000	32	0.1100	0.4218	0.8696	0.9567	[illegible]7885	-5.7322	131.0778	-0.9877	125.4161

Mean : 62.4000 | 32 | 0.1100   [illegible] | 0.9566 | 0.7885

RIT'_mean = 125.404 N

Approximation order for PD vs T : 2

Final model scale results

V [m/s]	RIT'_mean [N]	dFP'/dT' [-]	[illegible] [-]	T'_sp [N]	PD'_sp [W]	ETAD' [-]
0.3130	125.4040	-[illegible]9877	0.0123	126.9649	311.0902	0.1262

Self propulsion point

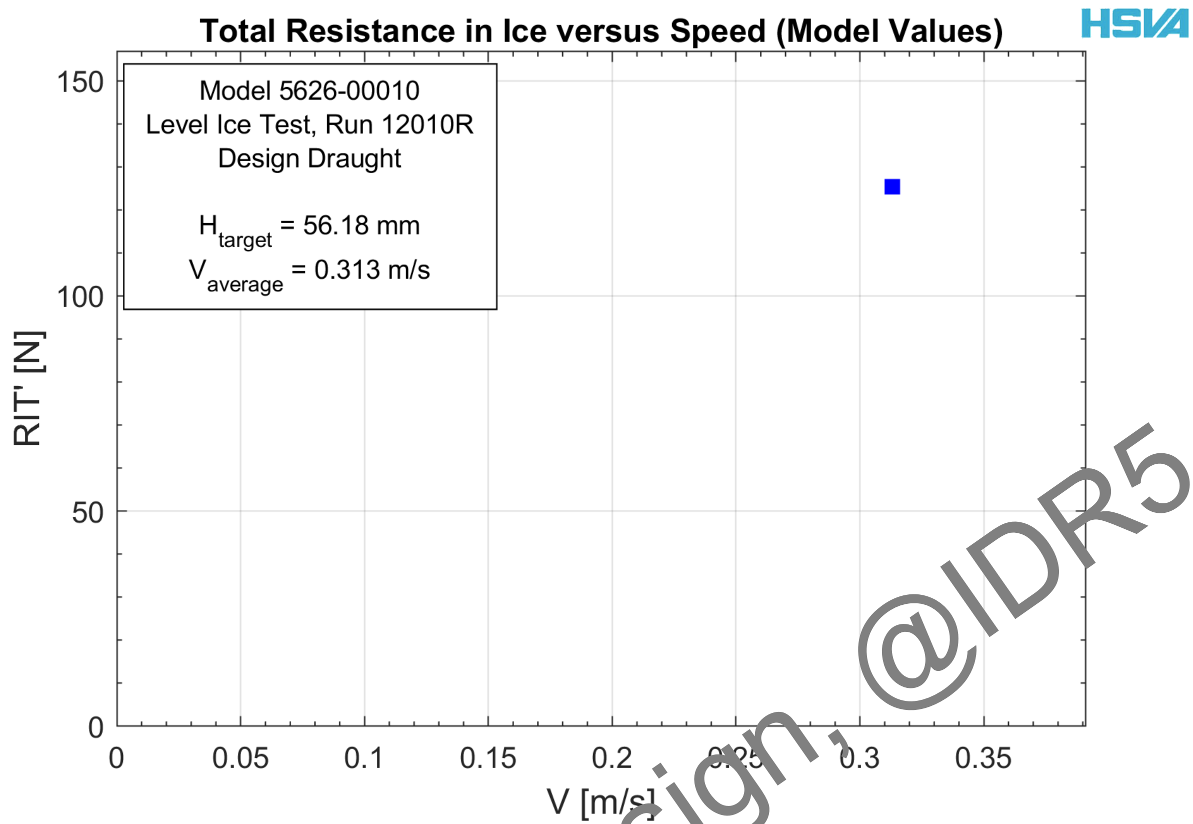

Figure 50 Total resistance ahead in 1.37m level ice, 3knots, model scale

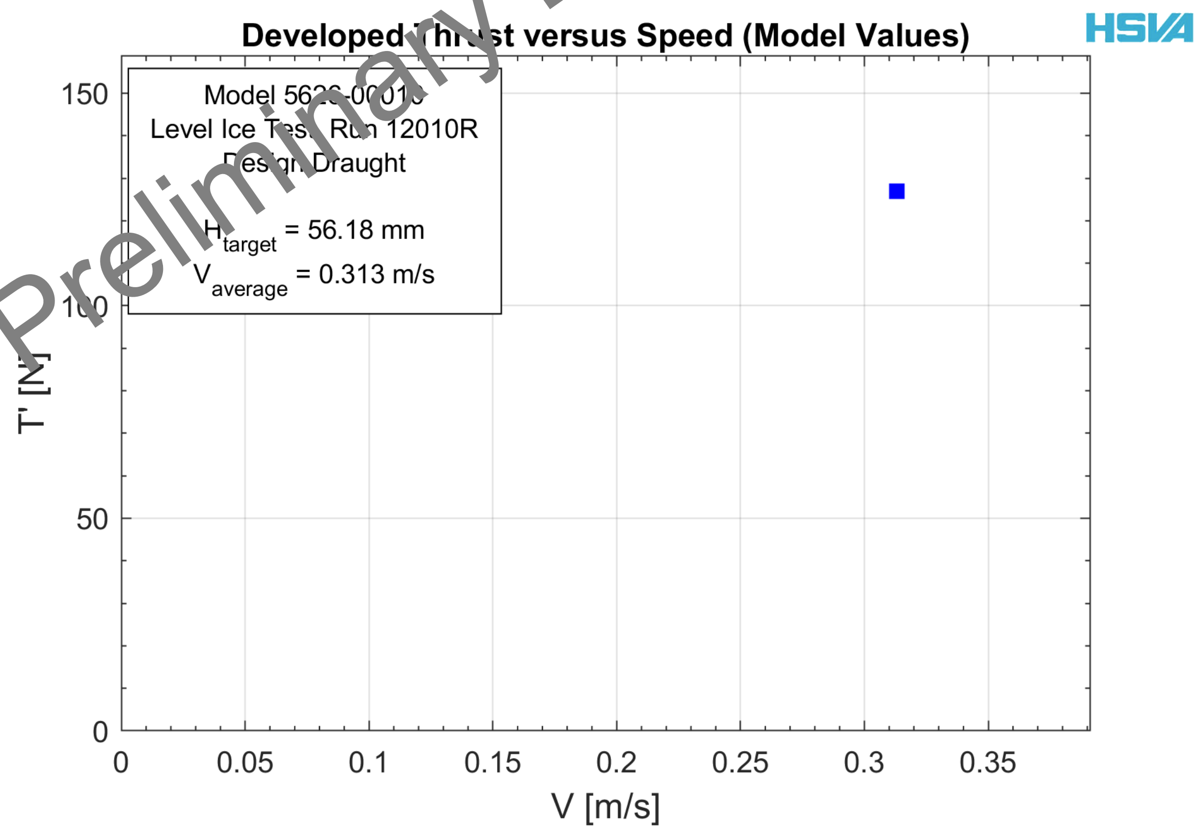

Figure 51 Total thrust ahead in 1.37m level ice, 3knots, model scale

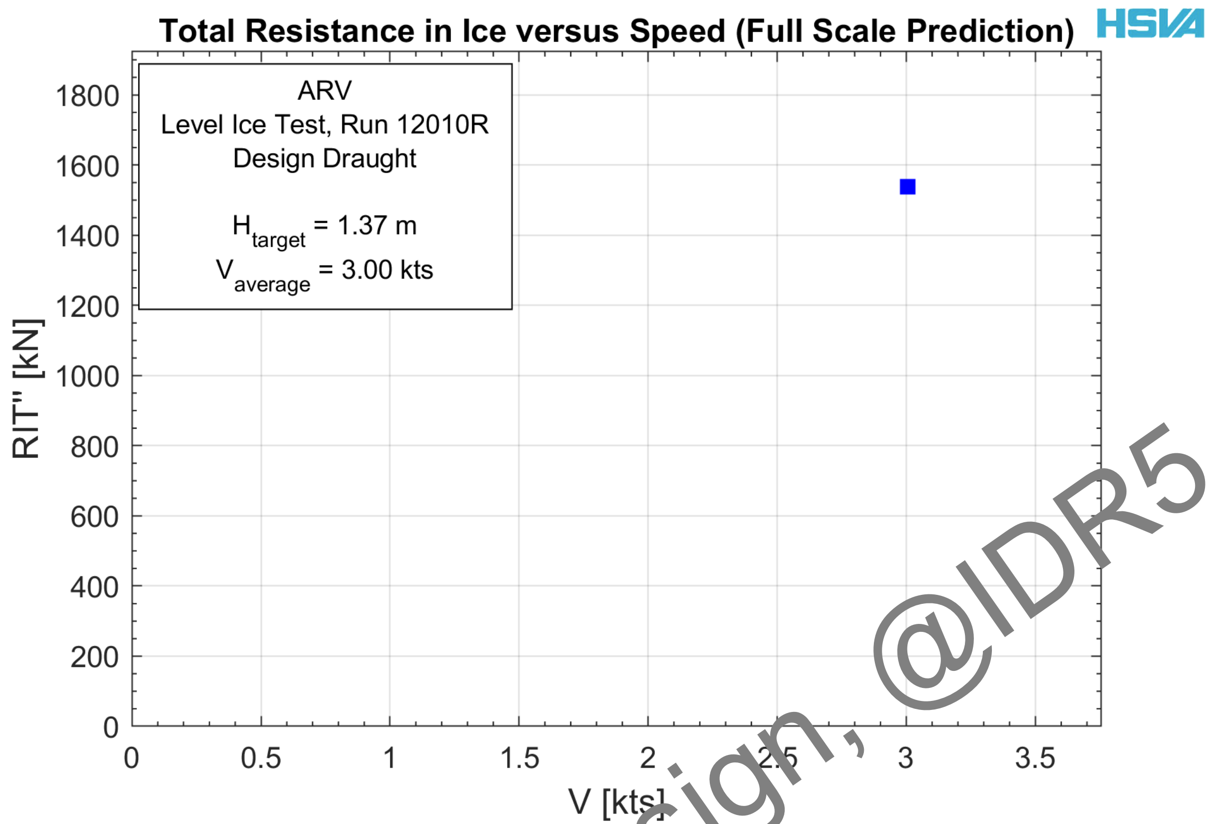

Figure 52 Delivered power ahead in 1.37m level ice, 3knots, model scale

Full scale values (from corrected intervals data)

Sub interval	V [kts]	FN [-]	n_mean [1/min]	Q_tot [kNm]	PD_to[illegible] [kW]	T_[illegible]t [kN]	[illegible]P [kN]	dFP/dT_tot [-]	RIT [kN]	FD [kN]
LI2_1	3.0039	0.0473	139.7231	2048.5[illegible]	[illegible]973[illegible]1	2335.36	509.94	-0.9877	2816.56	12.10
LI2_2	3.0043	0.0473	85.0560	877[illegible]	7[illegible]15.09	652.32	2172.27	-0.9877	2816.57	12.10
LI2_3	3.0045	0.0473	115.4253	1[illegible]9.53	17037.27	1519.69	1341.58	-0.9877	2842.57	12.10
LI2_4	3.0054	0.0473	32.79[illegible]6	12[illegible]3	435.28	-129.14	2953.14	-0.9877	2825.59	12.10

RIT_mean = 2825.32 kN

Target full scale valu[illegible]

H_ice [illegible]	SI[illegible]F_ic[illegible] [k[illegible]]	FID [-]
1.[illegible]00	700	0.0550

k_FD_corr coefficient: 1

KQ correction (Rn) for PD: 0.96

Shaft efficiency: 0.99

i - correction :

RIT'_mean at Fn=0.05 2236.39 kN

Cor[illegible]tion for deviations between actual and target test conditions, and for scale effects

Sub interval	H_ice [m]	SIG_F [kPa]	FID [-]	F1 (HI) [-]	F2 (SIGF) [-]	F3 (FID) [-]	T' [kN]	FP' [kN]	RIT' [kN]	i [-]	FP'' [kN]	dFP''/dT' [-]	RIT'' [kN]	PD'' [kW]
LI2_1	1.5216	780.29	0.1100	0.8696	0.9566	0.7885	1531.85	334.49	1847.51	-0.1353	19.73	-0.9877	1532.75	28774.95
LI2_2	1.5216	780.29	0.1100	0.8696	0.9566	0.7885	427.89	1424.88	1847.51	-0.1353	1110.12	-0.9877	1532.75	7502.48
LI2_3	1.5216	780.29	0.1100	0.8696	0.9566	0.7885	996.83	880.00	1864.57	-0.1353	565.24	-0.9877	1549.81	16355.78
LI2_4	1.5216	780.29	0.1100	0.8696	0.9567	0.7885	-84.71	1937.10	1853.43	-0.1353	1622.35	-0.9877	1538.68	417.86
Mean :	1.5216	780.29	0.1100	0.8696	0.9566	0.7885								

RIT'_mean = 1853.25 kN

RIT''_mean = 1538.50 kN

Final full scale results

V [kts]	RIT''_mean [kN]	dFP''/dT' [-]	t'' [-]	T''_sp [kN]	PD''_sp [kW]	ETAD'' [-]
3.00	1538.50	-0.9877	0.0123	1557.65	17392.84	0.1367

Self propulsion point

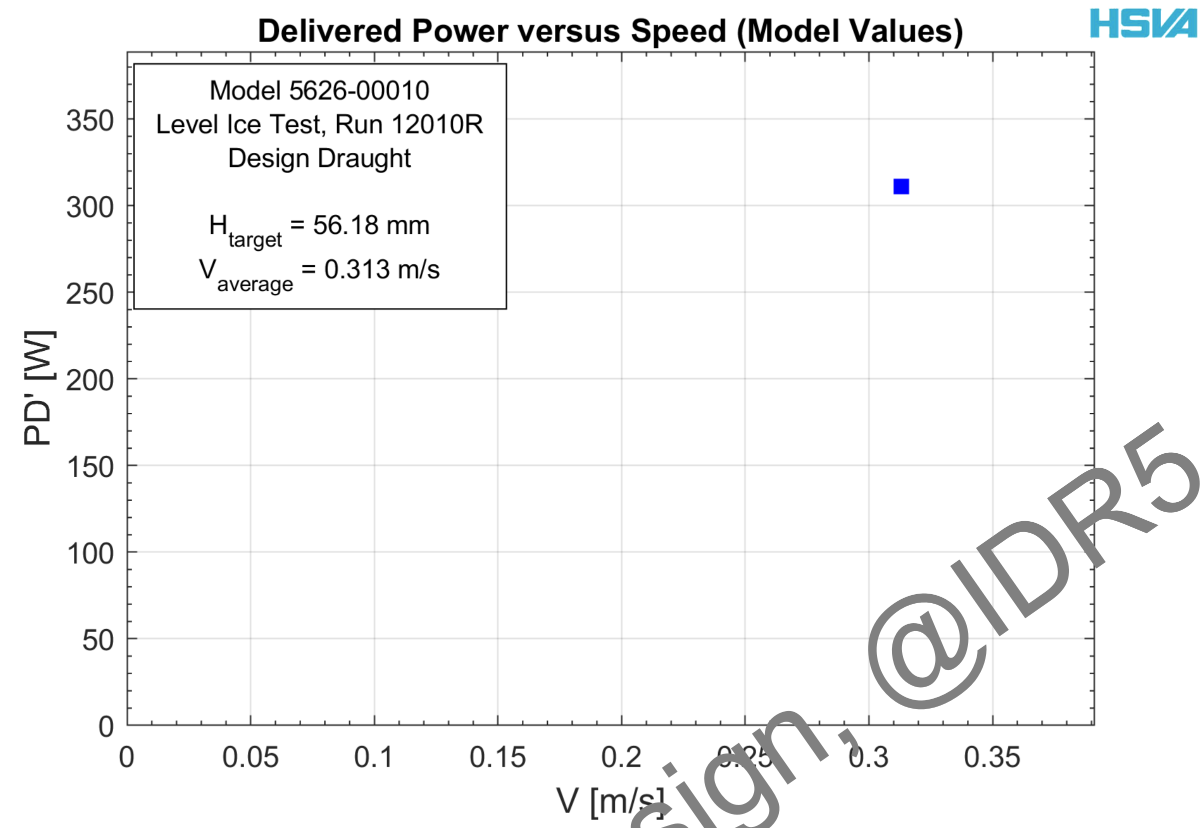

Figure 53 Total resistance ahead in 1.37m level ice, 3knots, full scale

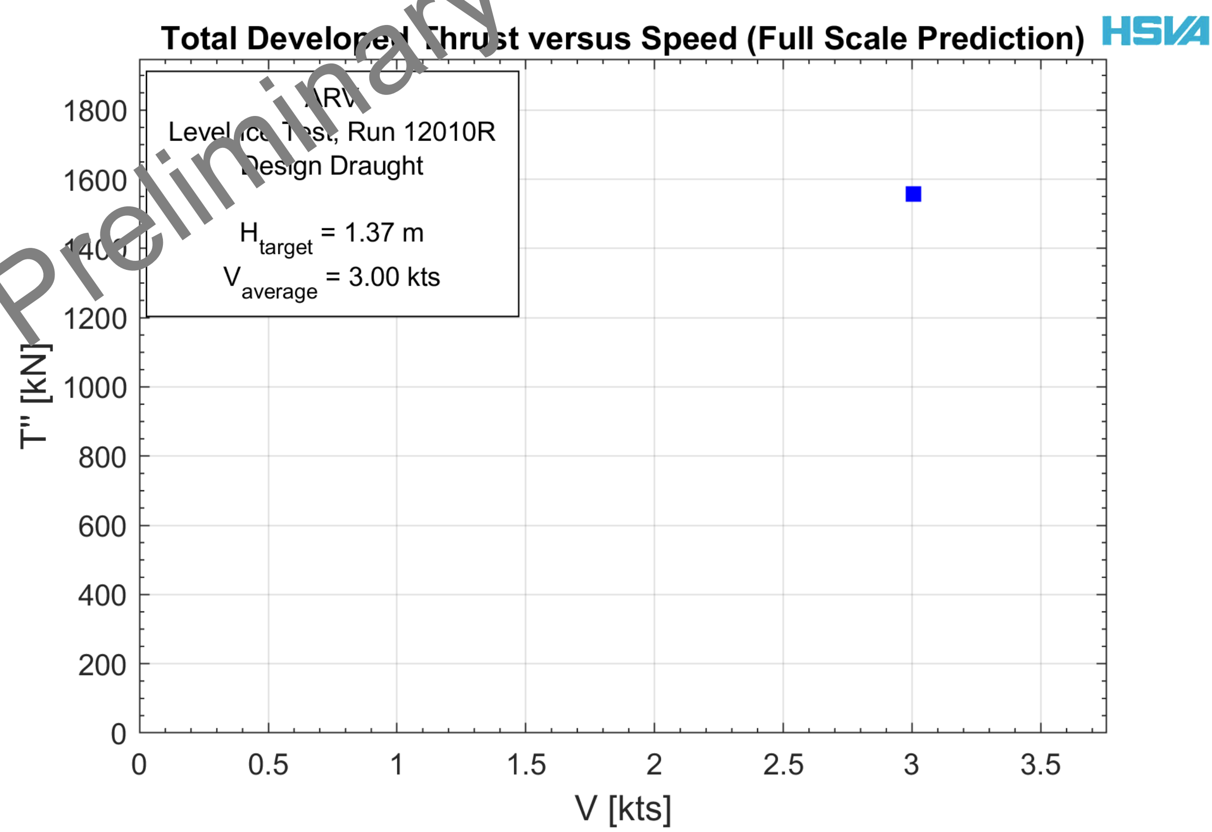

Figure 54 Total thrust ahead in 1.37m level ice, 3knots, full scale

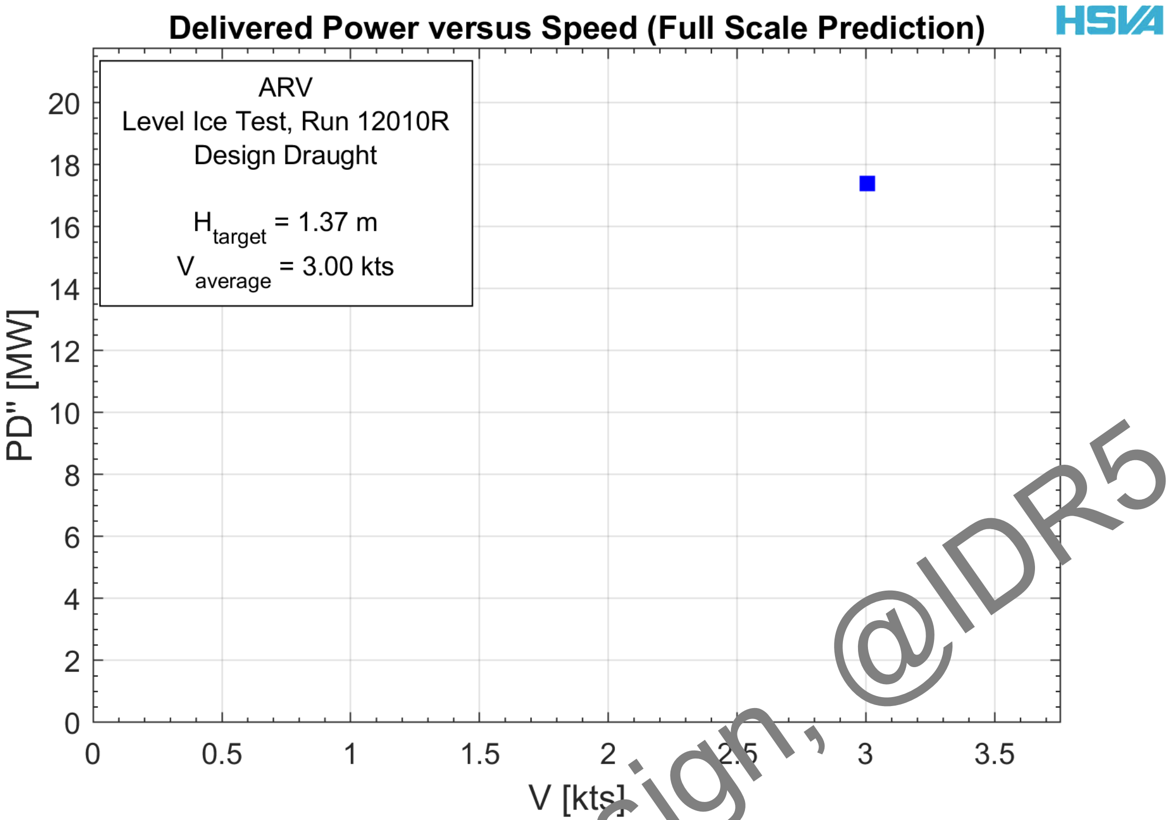

Figure 55 Delivered power ahead in 1.37m level ice, 3knots, full scale

6.3 Test Run No. 13011R Towed Propulsion Test Astern in Level Ice, 3 knots

Corrected intervals data ?

Sub interval	V [m/s]	FN [-]	n_mean [1/s]	Q_tot [Nm]	PD_tot [W]	T_tot [N]	FP [N]	dFP/dT_tot [-]	RIT [N]
LI_1	0.3100	0.0426	12.2000	5.2000	398.6900	131.3932	33	-1.1991	190.5536
LI_2	0.3100	0.0426	7.3000	1.7200	78.9200	-37.7935	236.0600	-1.1991	190.7419
LI_3	0.3100	0.0426	10.1000	3.4700	220.5500	41.6059	137.6400	-1.1991	187.5296
LI_4	0.3100	0.0426	10.1000	3.4700	220.5900	41.7359	137.5100	-1.1991	187.5555

Curve fit ? ☑ ☑ ☑ ☑

RIT_mean = 189.095 N

Target values

H_ice [mm]	SIGF_ice [kPa]	FID [-]
56.1844	28.7073	0.0550

Ice feature : Level ice

Correction for deviations between actual and target test conditions ?

Test No.	H_ice [mm]	SIG_F [kPa]	FID [-]	FN_HI [-]	F1 (HI)	F2 (SIGF)	F3 (FID)	T' [N]	FP' [N]	dFP'/dT' [-]	RIT' [N]
LI_1	59.8000	34	0.1100	0.4176	0.9202	0.9320	0.7885	88.8475	22.3145	-1.1991	128.8516
LI_2	59.8000	34	0.1100	0.4176	0.9202	0.9320	0.7885	-25.5558	159.6228	-1.1991	128.9789
LI_3	59.8000	34	0.1100	0.4176	0.9202	0.9320	0.7885	28.1337	93.0716	-1.1991	[illegible]
LI_4	59.8000	34	0.1100	0.4176	0.9202	0.9320	0.7885	28.2216	92.9837	[illegible]	[illegible]
Mean :	59.8000	34	0.1100		0.9202	0.9320	0.7885				

RIT'_mean = 127.865 N

Approximation order for PD vs T : 2 Check ☑ Zero PD at origin

Final model scale results ?

V [m/s]	RIT'_mean [N]	dFP'/dT' [-]	t' [-]	T'_sp [N]	PD'_sp [W]	ETAD' [-]
0.3100	127.8654	-1.1991	-0.1991	106.6344	[illegible]	[illegible]

Self propulsion point

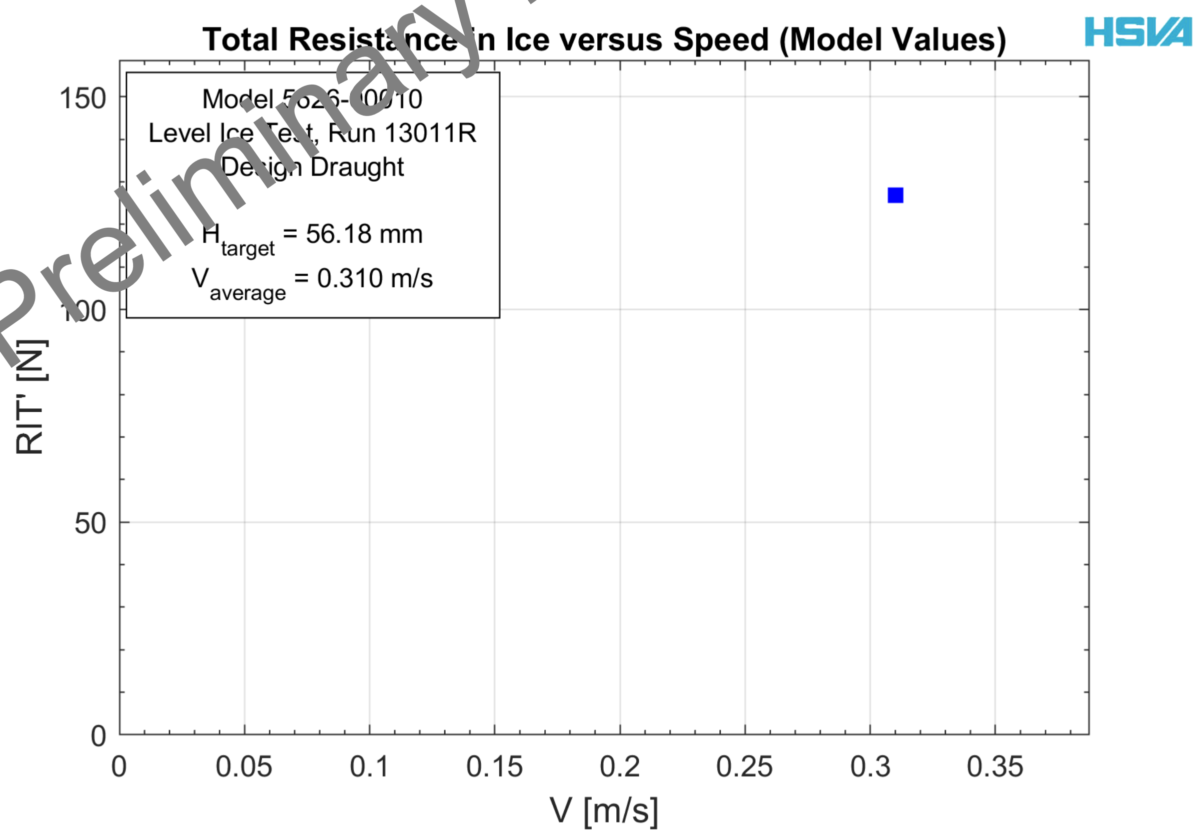

Figure 56 Total resistance astern in 1.37m level ice, 3knots, moderl scale

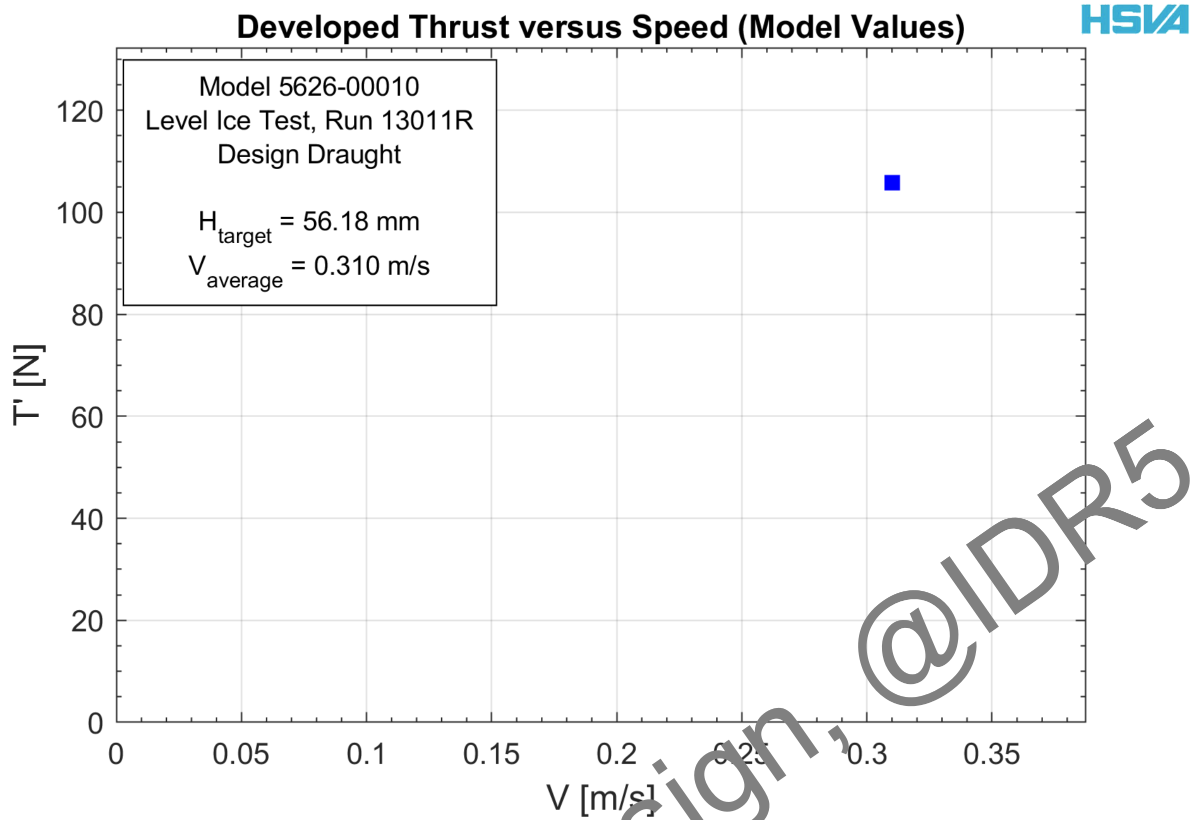

Figure 57 Total thrust astern in 1.37m level ice, 3knots, model scale

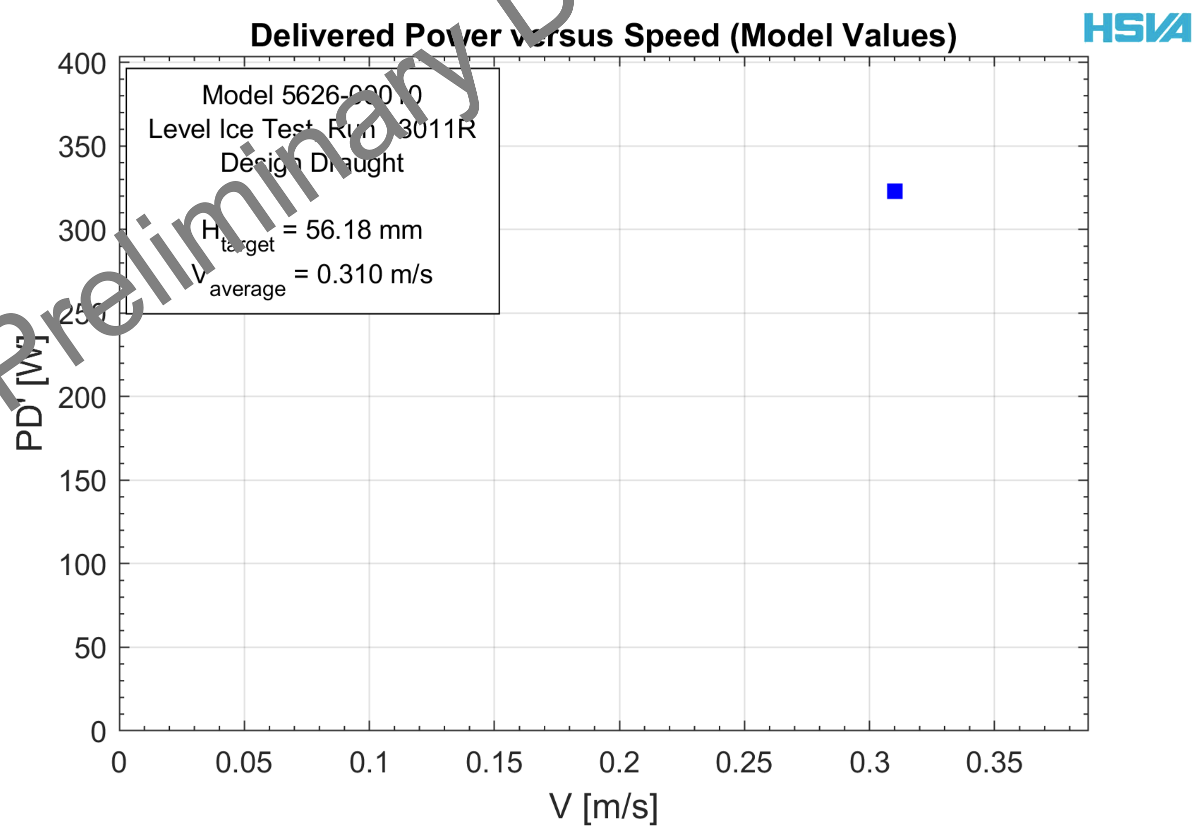

Figure 58 Delivered power astern in 1.37m level ice, 3knots, model scale

Full scale values (from corrected intervals data) ?

Sub interval	V [kts]	FN [-]	n_mean [1/min]	Q_tot [kNm]	PD_tot [kW]	T_tot [kN]	FP [kN]	dFP/dT_tot [-]	RIT [kN]	FD [kN]
LI_1	2.9756	0.0426	148.2377	1873.84	29094.55	1941.76	487.68	-1.1991	2816.05	11.90
LI_2	2.9756	0.0426	88.6996	619.81	5759.22	-558.52	3488.56	-1.1991	2818.84	11.90
LI_3	2.9756	0.0426	122.7214	1250.43	16094.72	614.86	2034.08	-1.1991	2771.36	11.90
LI_4	2.9756	0.0426	122.7214	1250.43	16097.64	616.78	2032.16	-1.1991	2771.75	11.90

RIT_mean = 2794.50 kN

Target full scale values

H_ice [m]	SIGF_ice [kPa]	FID [-]
1.3700	700	0.0550

k_FD_corr coefficient: 1
KQ correction (Rn) for PD: 0.96
Shaft efficiency: 0.99
Update

i - correction :
RIT'_mean at Fn=0.05 : 2236.39 kN

Correction for deviations between actual and target test conditions, and for scale effect ?

Sub interval	H_ice [m]	SIG_F [kPa]	FID [-]	F1 (HI) [-]	F2 (SIGF) [-]	F3 (FID) [-]	T' [kN]	FP' [kN]	RIT' [kN]	i [-]	FP'' [kN]	dFP''/dT' [-]	RIT'' [kN]	PD'' [kW]
LI_1	1.4582	829.06	0.1100	0.9202	0.9320	0.7885	1313.01	329.77	1904.20	-0.1151	60.44	-1.1991	[illegible]	27930.77
LI_2	1.4582	829.06	0.1100	0.9202	0.9320	0.7885	-377.67	2358.95	1906.09	-0.1151	2089.62	[illegible]	1636.75	5528.85
LI_3	1.4582	829.06	0.1100	0.9202	0.9320	0.7885	415.77	1375.44	1873.99	-0.1151	1106.11	[illegible]	1604.65	15450.93
LI_4	1.4582	829.06	0.1100	0.9202	0.9320	0.7885	417.07	1374.14	1874.24	-0.1151	[illegible]	[illegible]	1604.91	15453.73

Mean : 1.4582 | 829.06 | 0.1100 | 0.9202 | 0.9320 | 0.7885

RIT'_mean = 1889.63 kN
RIT''_mean = 1620.30 kN

Final full scale results ?

V [kts]	RIT''_mean [kN]	dFP''/dT' [-]	t'' [-]	T''_sp [kN]	PD''_sp [kW]	ETAD'' [-]
2.98	1620.30	-1.1991	-0.1991	1351.26	18634.16	0.1331

Self propulsion point

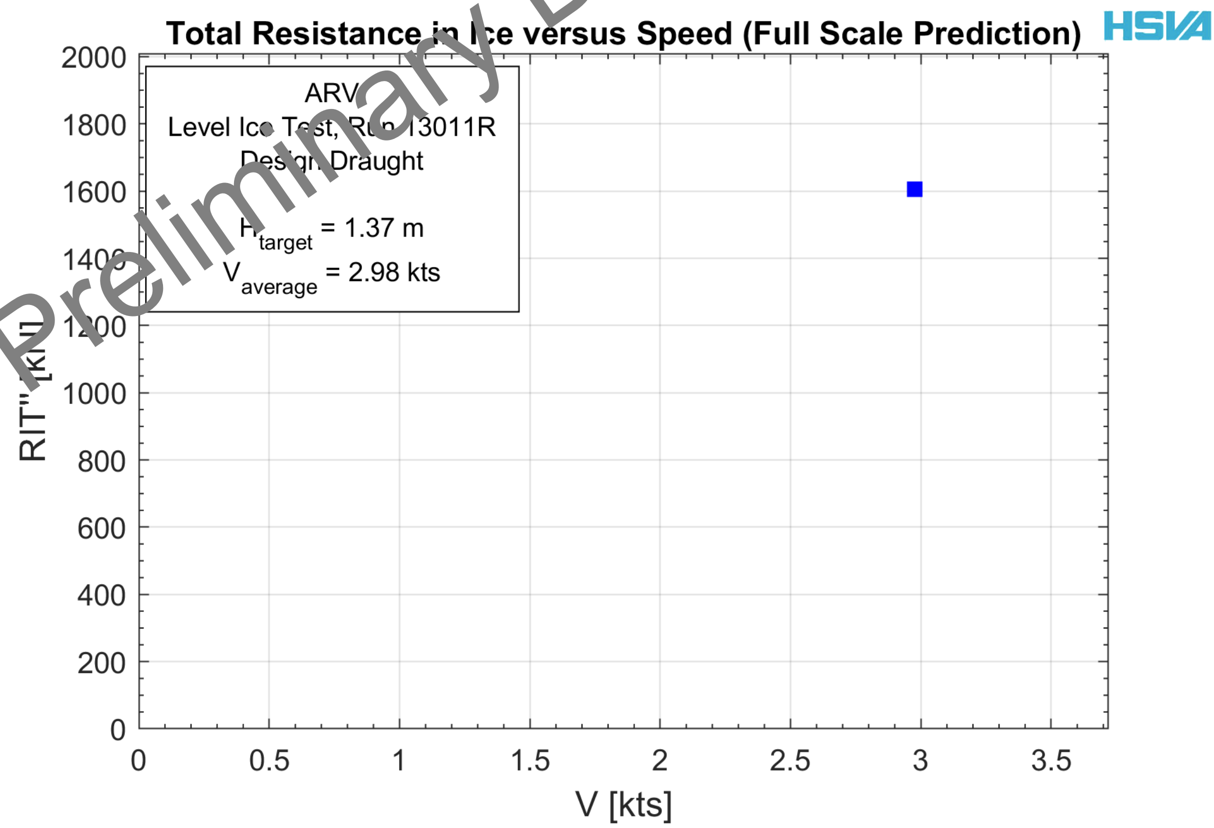

Figure 59 Total resistance astern in 1.37m level ice, 3knots, full scale

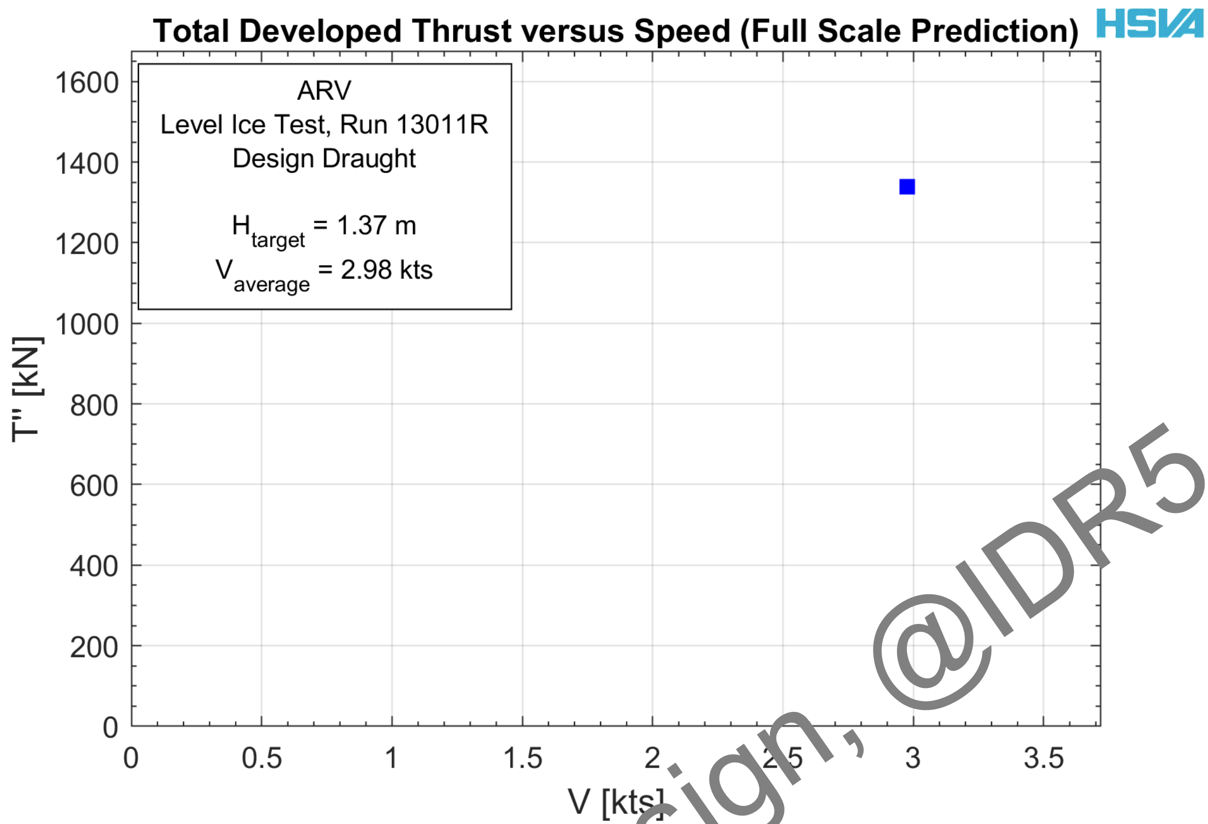

Figure 60 Total thrust astern in 1.37m level ice, 3knots, full scale

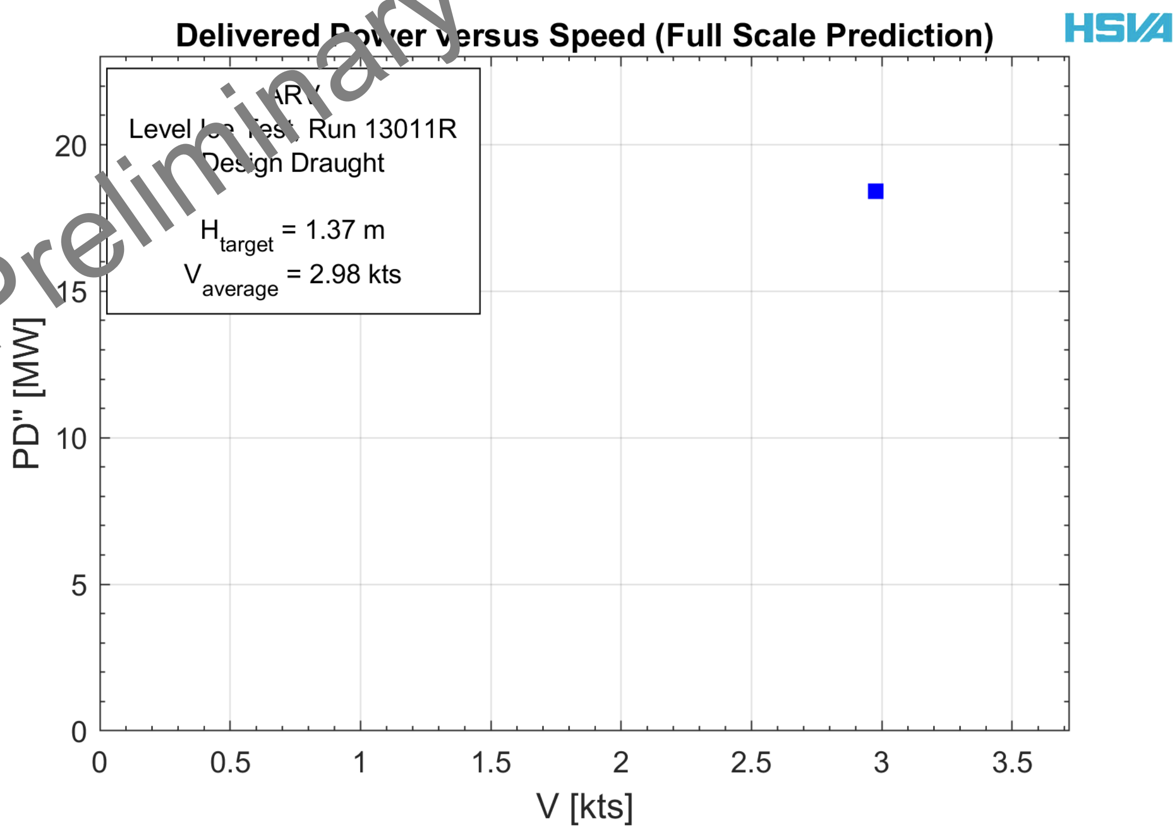

Figure 61 Delivered power astern in 1.37m level ice, 3knots, full scale

6.4 Summary of Free Running Test Results

Table 7 Results of free running tests in 1.37m level ice

		FS correction			Transfer to power correction			MS		FS corrected values		
Description	PD_act	i_corr	ΔR	F4	F1*F2*F3*F4	b	(F1*F2*F3*F4)^b	PD'	PD''	PB''	% PBmax	Speed
	[MW]	[-]	[kN]	[-]	[-]	[-]	[-]	[W]	[MW]	[MW]	[%]	[kts]
Ice condition 2 - Hi = 1.37m level ice + 0.305m snow												
Run 14011R	43.44	-0.202	-332.64	0.7921	0.5524	1.341	0.45134	382.5	19.61	19.61	103.19	3.17
Run 15011R	54.65	-0.225	-371.14	0.7680	0.4969	1.326	0.39544	437.7	21.61	21.61	113.74	3.46
Ice condition 2 - Hi = 1.37m level ice + 0.305m snow												
Run 21010R	34.33	-0.194	-320.32	0.7843	0.5821	1.407	0.46714	322.2	16.04	16.04	84.40	1.82
Run 23010R	40.64	-0.209	-344.96	0.7829	0.5617	1.364	0.45531	368.7	18.50	18.50	97.38	2.69
Run 24111R	26.62	-0.203	-334.18	0.7696	0.5583	1.421	0.43684	240.8	11.63	11.63	61.21	1.54
Run 25011R	39.23	-0.228	-375.76	0.7429	0.4773	1.416	0.35088	299.3	13.77	13.77	72.46	1.63
Run 26010R	40.64	-0.209	-344.96	0.8004	0.5772	1.308	0.48747	378.3	19.81	19.81	104.26	3.84

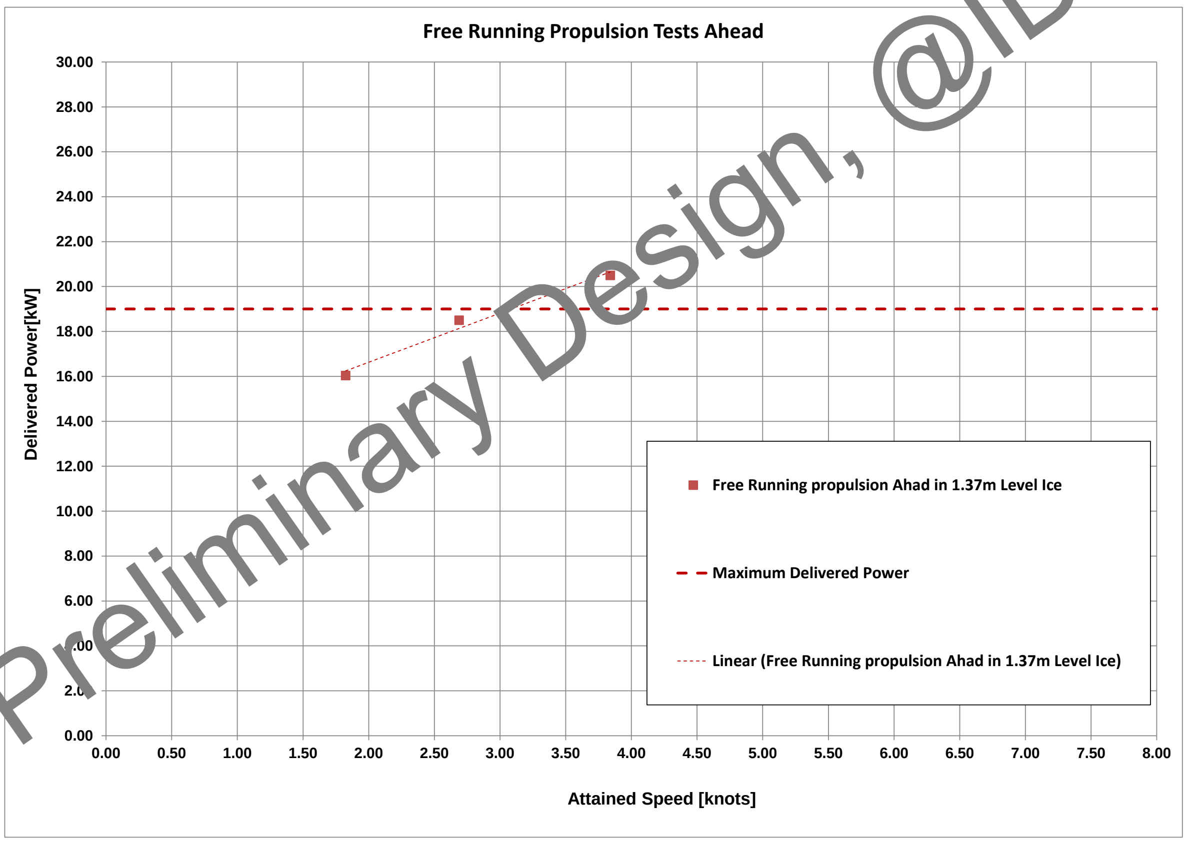

Figure 62 Summary of free running test results ahead

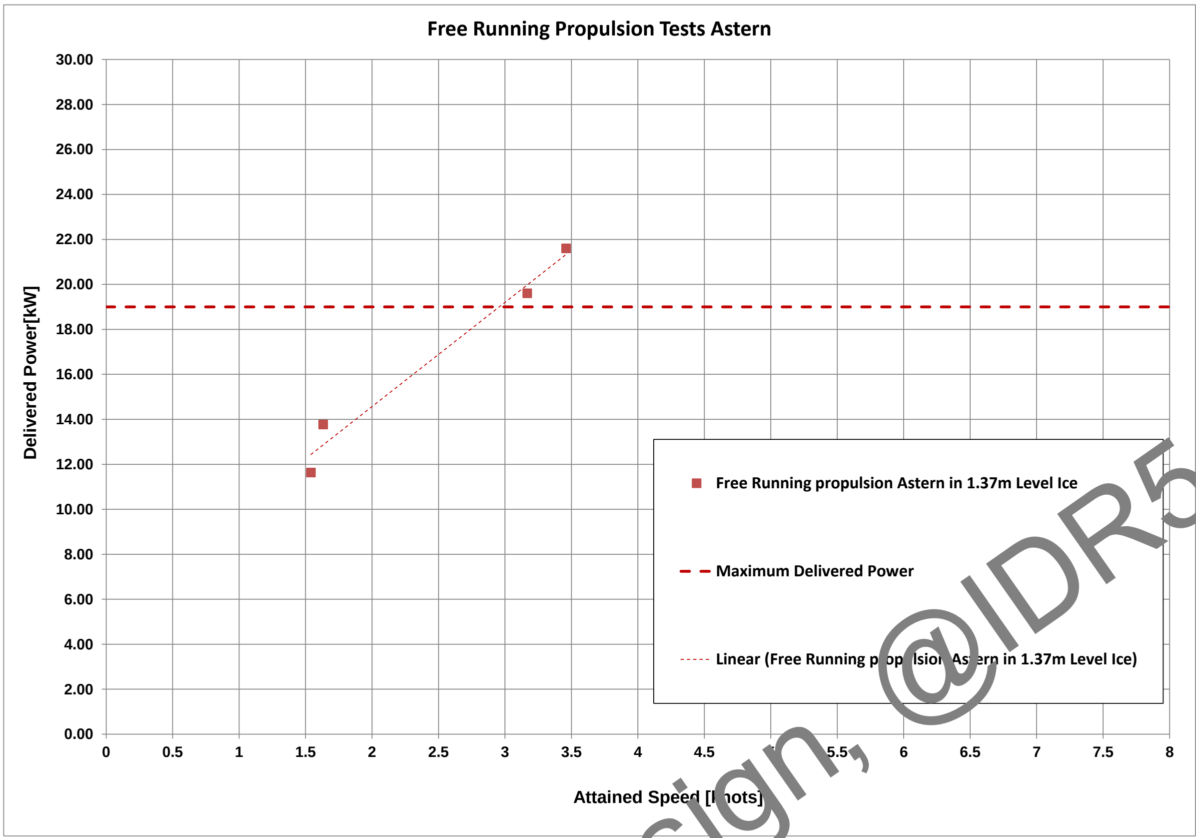

Figure 63 Summary of free running test results astern

The detailed results of the free running propulsion tests are presented in the following sections.

6.5 Test Run No. 14011R Free Running Test Astern in 1.37m Level Ice, 70% Power

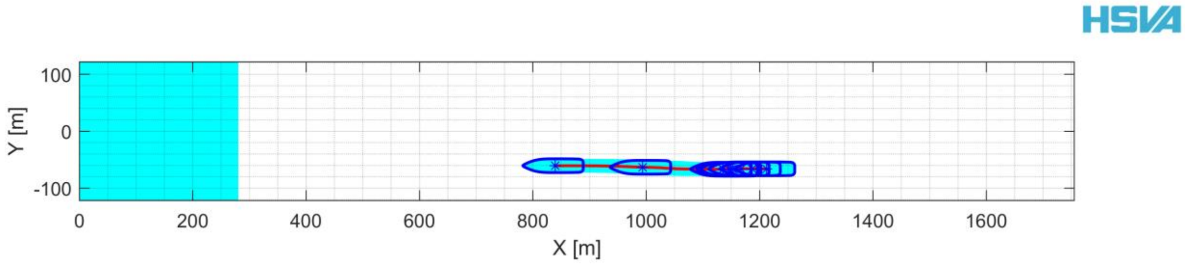

Figure 64 Test run 14011R track plot

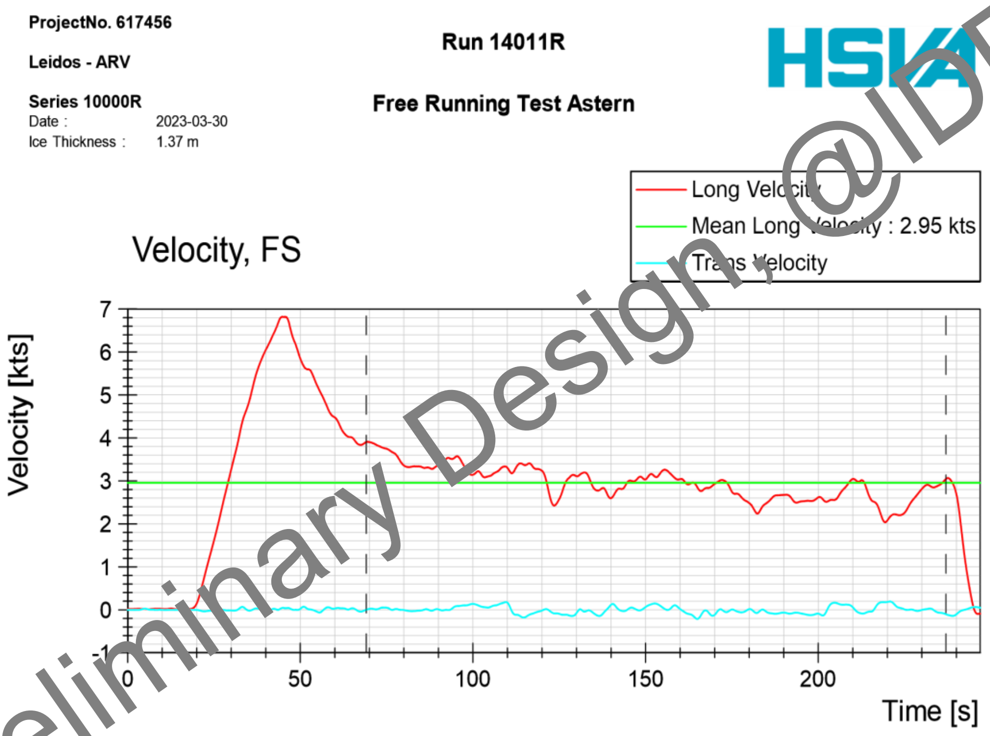

Figure 65 Test run no. 14011R, free running test astern, velocity

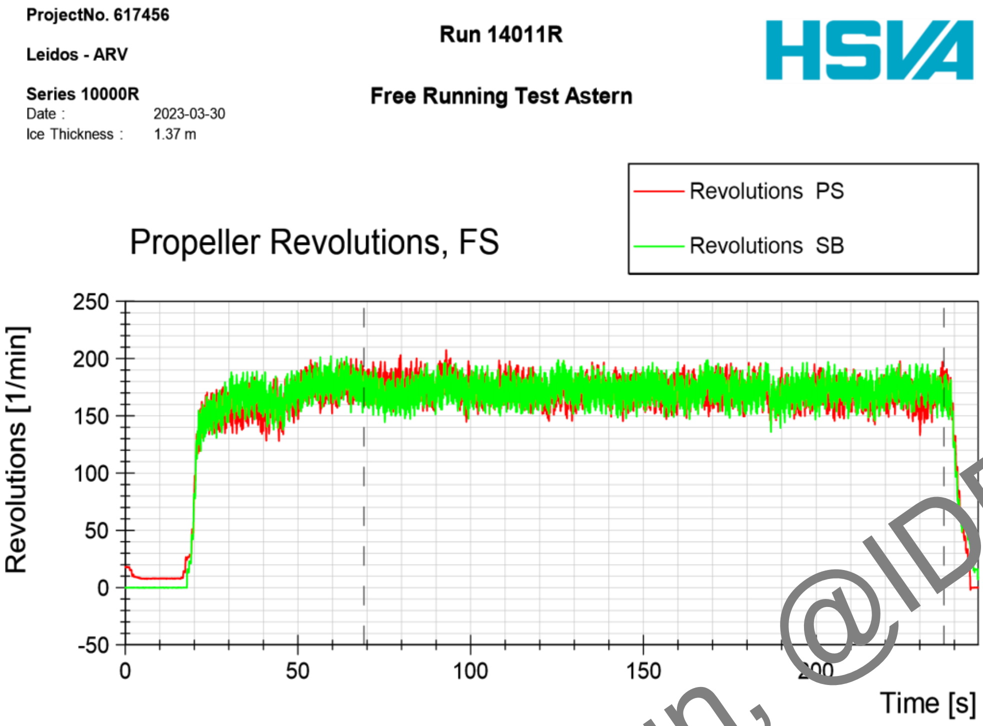

Figure 66 Test run no. 14011R, free running test astern, propeller revolution

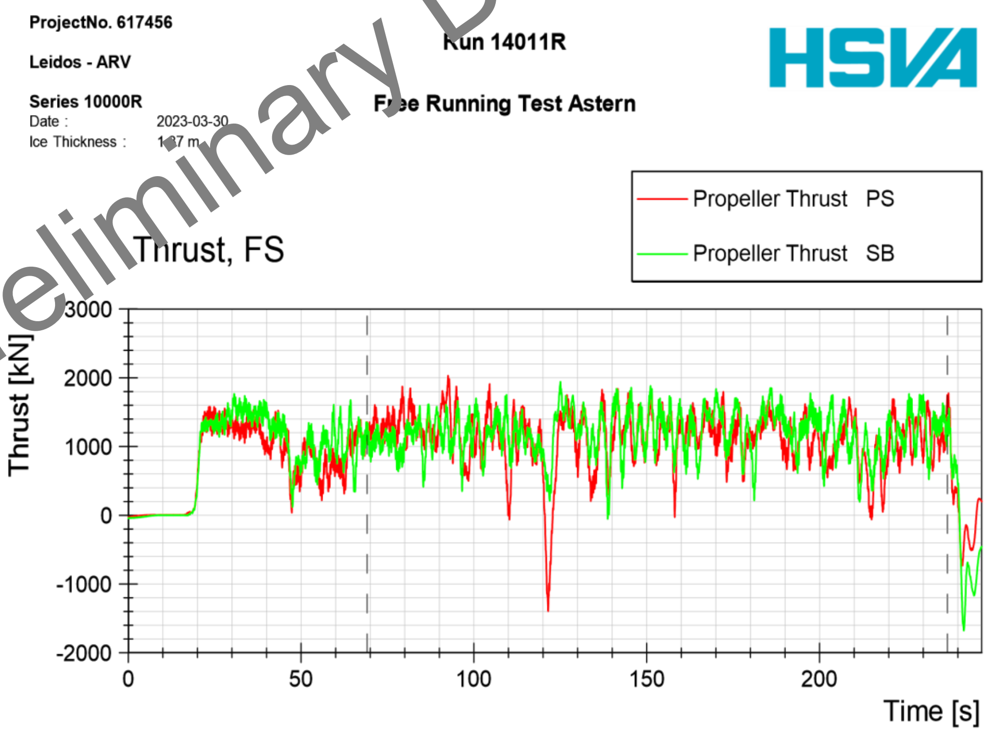

Figure 67 Test run no. 14011R, free running test astern, thrust

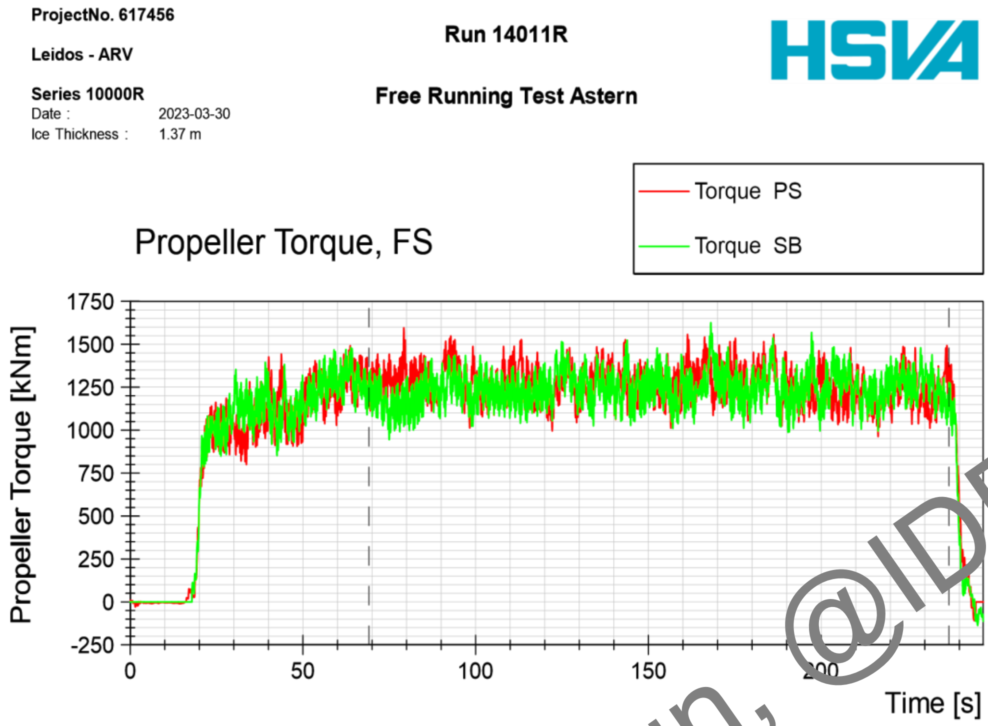

Figure 68 Test run no. 14011R, free running test astern, torque

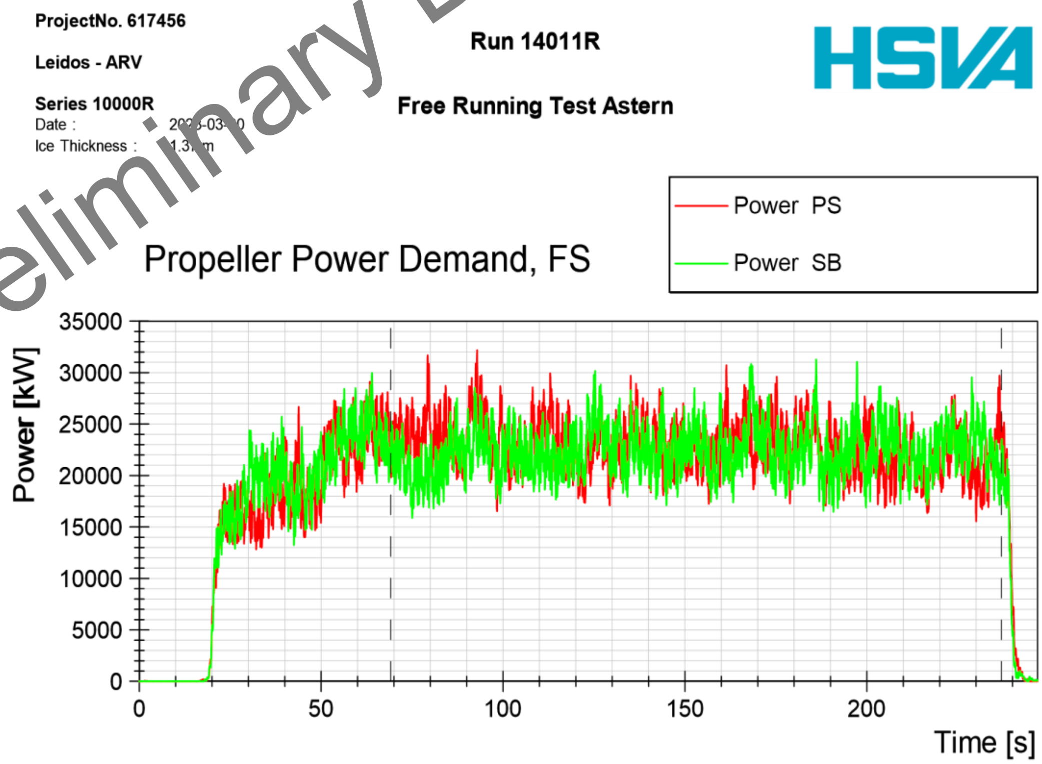

Figure 69 Test run no. 14011R, free running test astern, power

6.6 Test Run No. 15011R Free Running Test Astern in 1.37m Level Ice, 100% Power

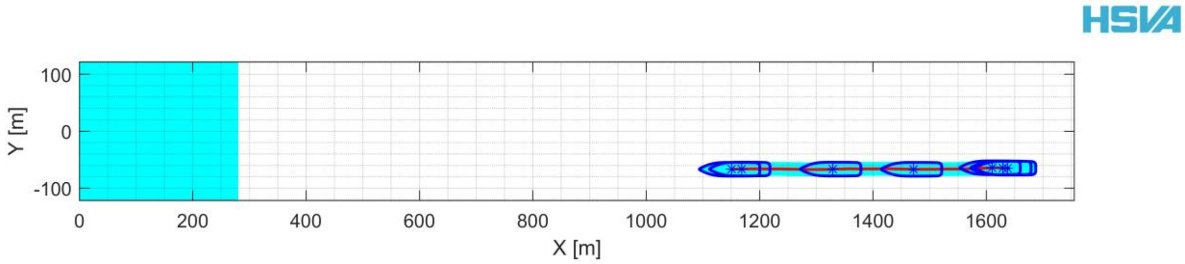

Figure 70 Test run no. 15011R track plot

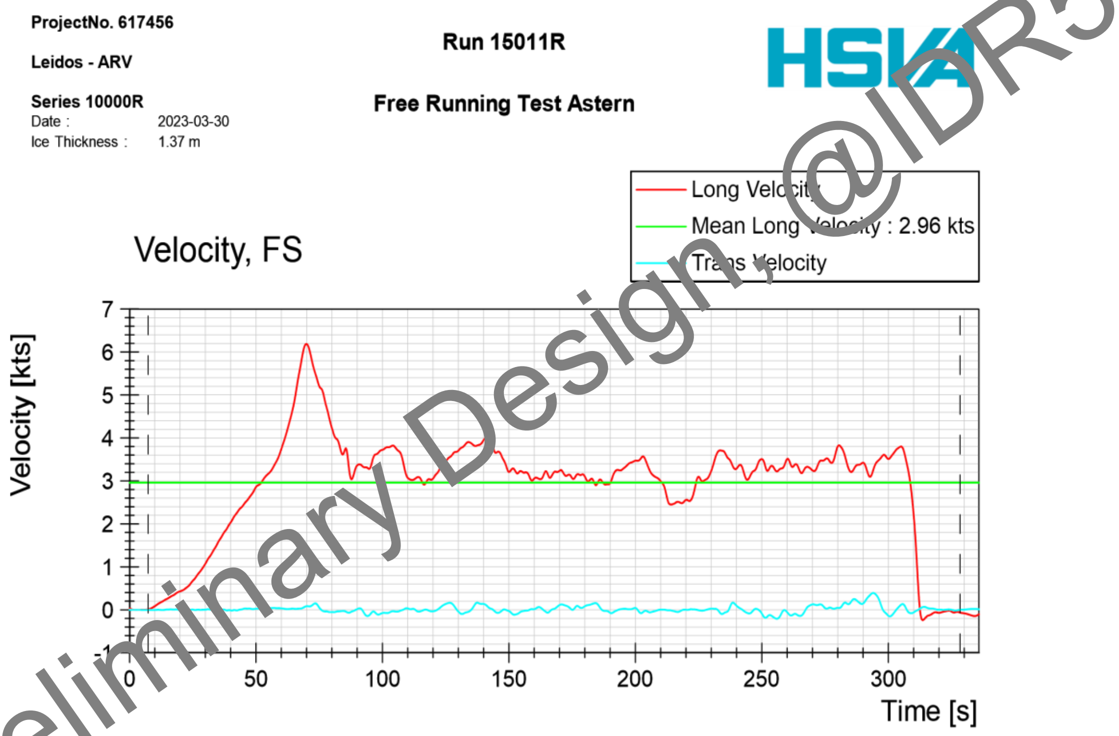

Figure 71 Test run no. 15011R, free running test astern, velocity

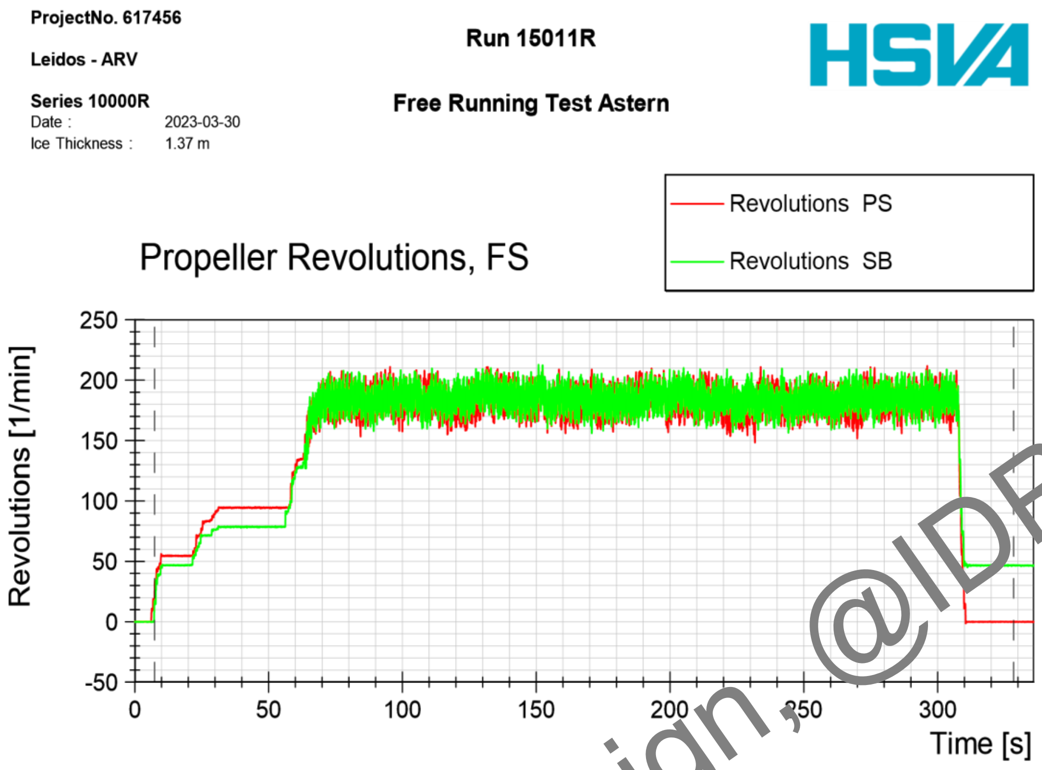

Figure 72 Test run no. 15011R, free running test astern, propeller revolution

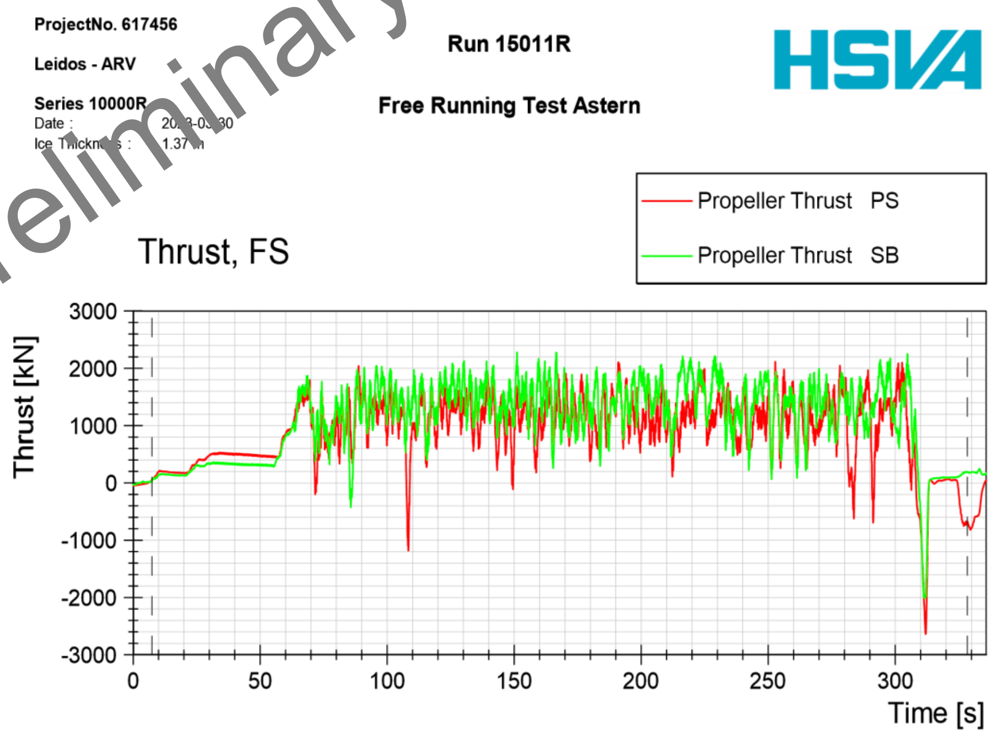

Figure 73 Test run no. 15011R, free running test astern, thrust

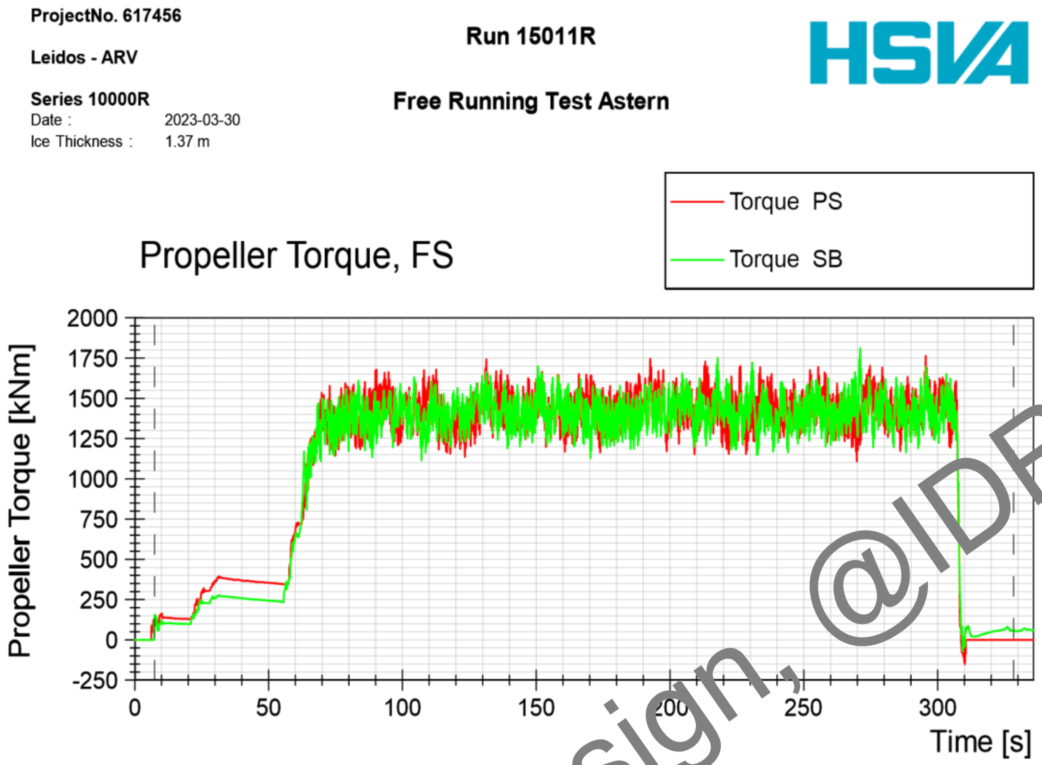

Figure 74 Test run no. 15011R, free running test astern, torque

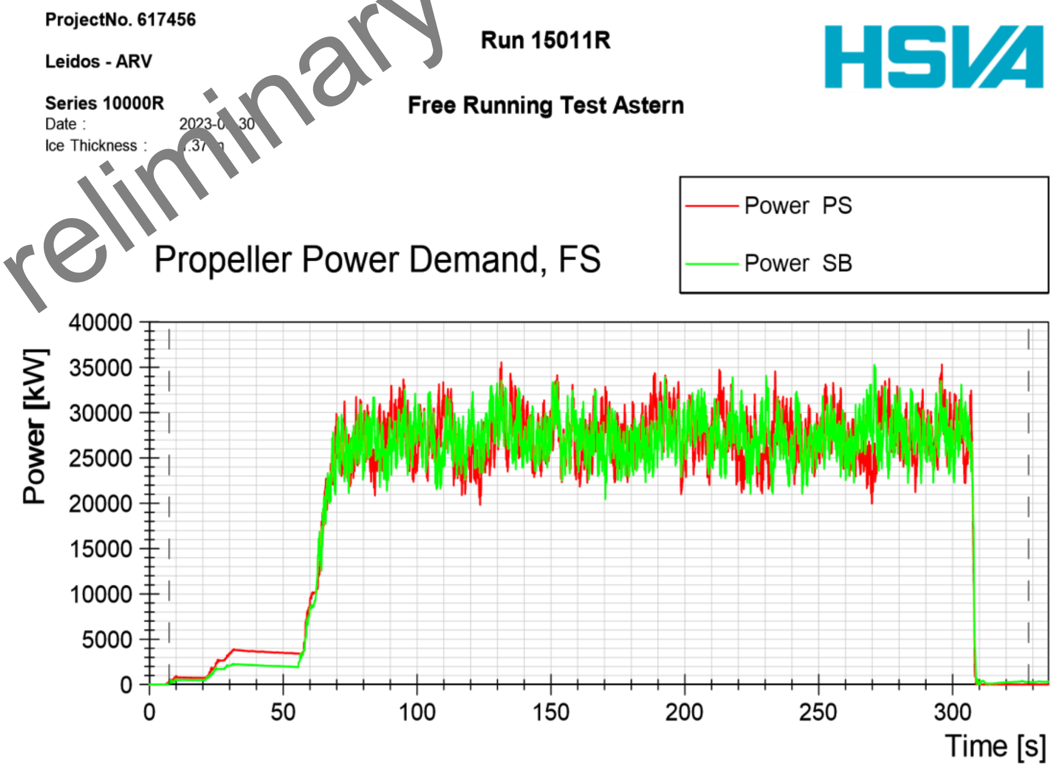

Figure 75 Test run no. 15011R, free running test astern, power

6.7 Test Run No. 21010R Free Running Test Ahead in 1.37m Level Ice, 40% Power

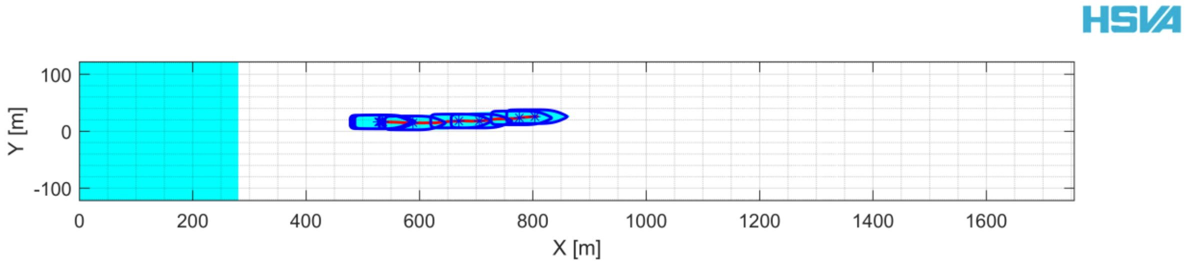

Figure 76 Test run no. 21010R track plot

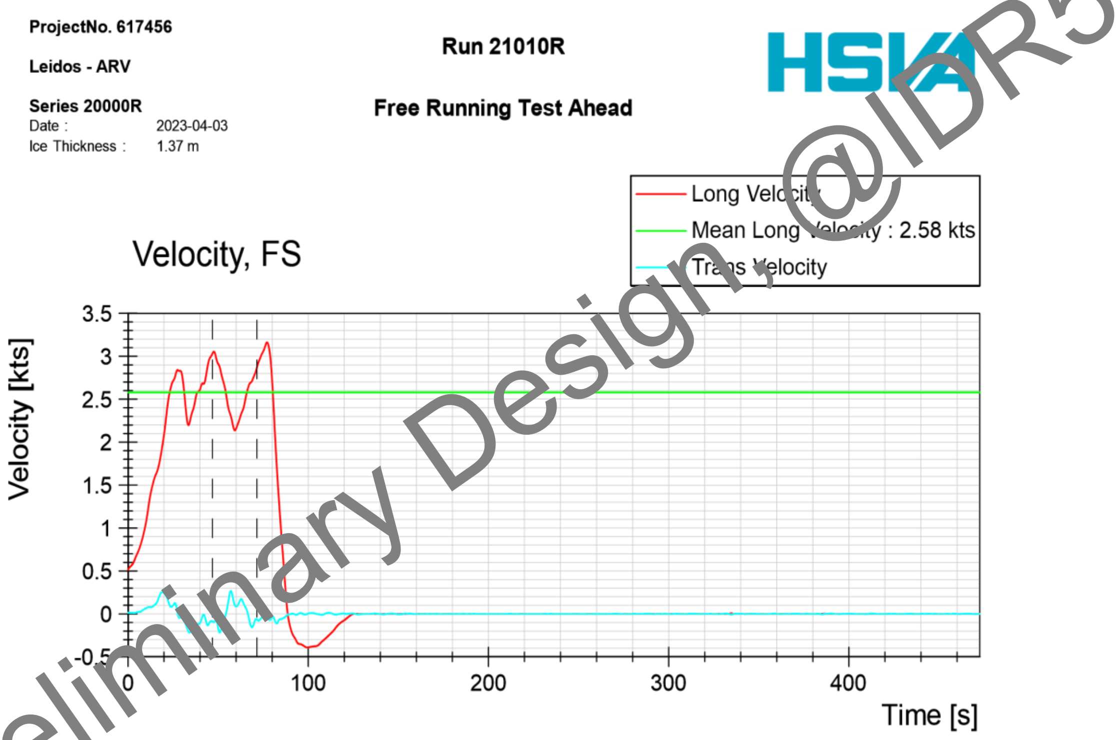

Figure 77 Test run no. 21010R, free running test astern, velocity

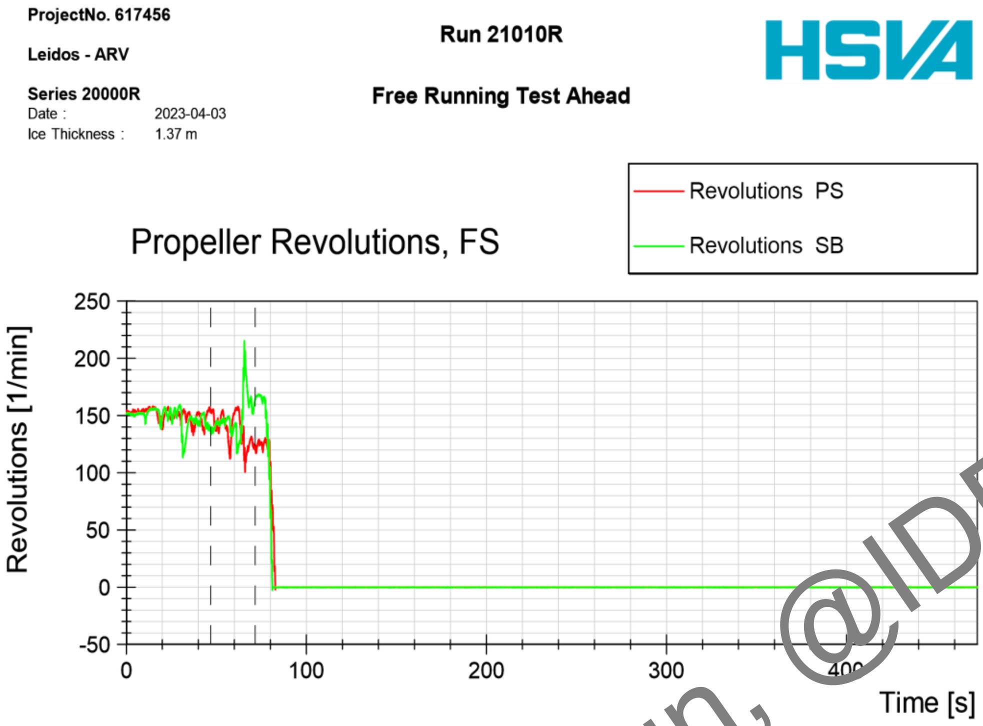

Figure 78 Test run no. 21010R, free running test astern, propeller revolution

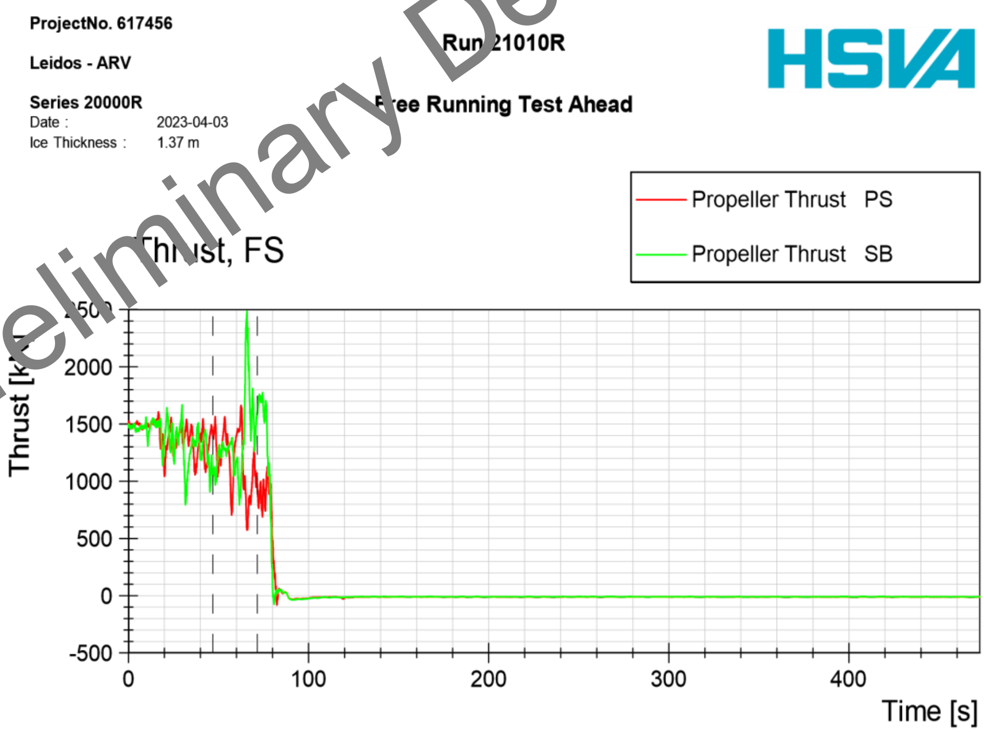

Figure 79 Test run no. 21010R, free running test astern, thrust

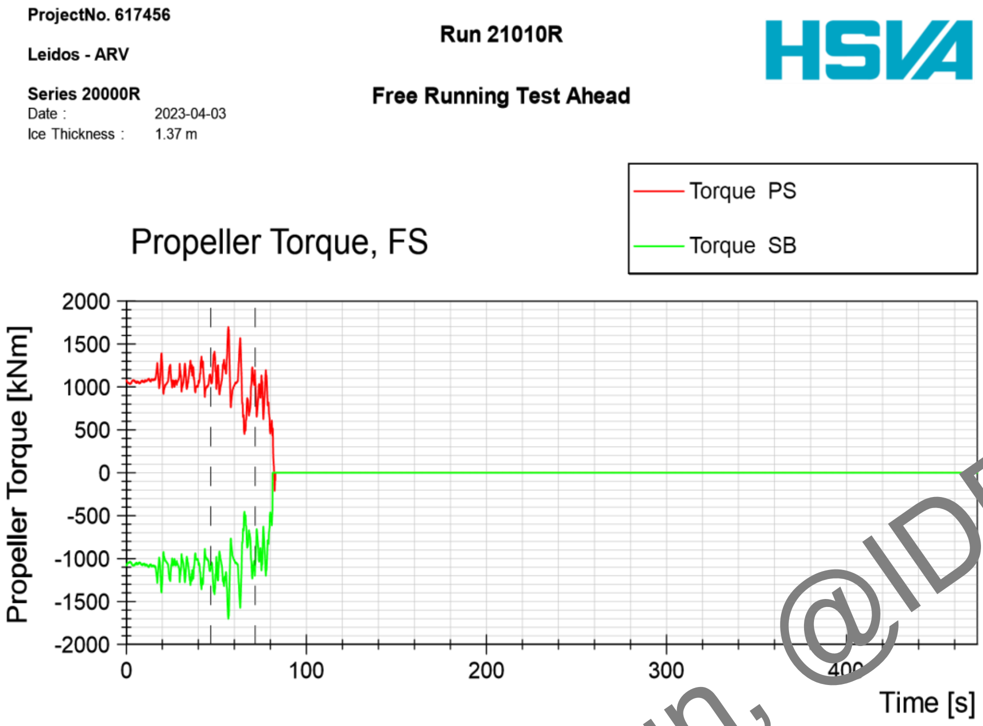

Figure 80 Test run no. 21010R, free running test astern, torque

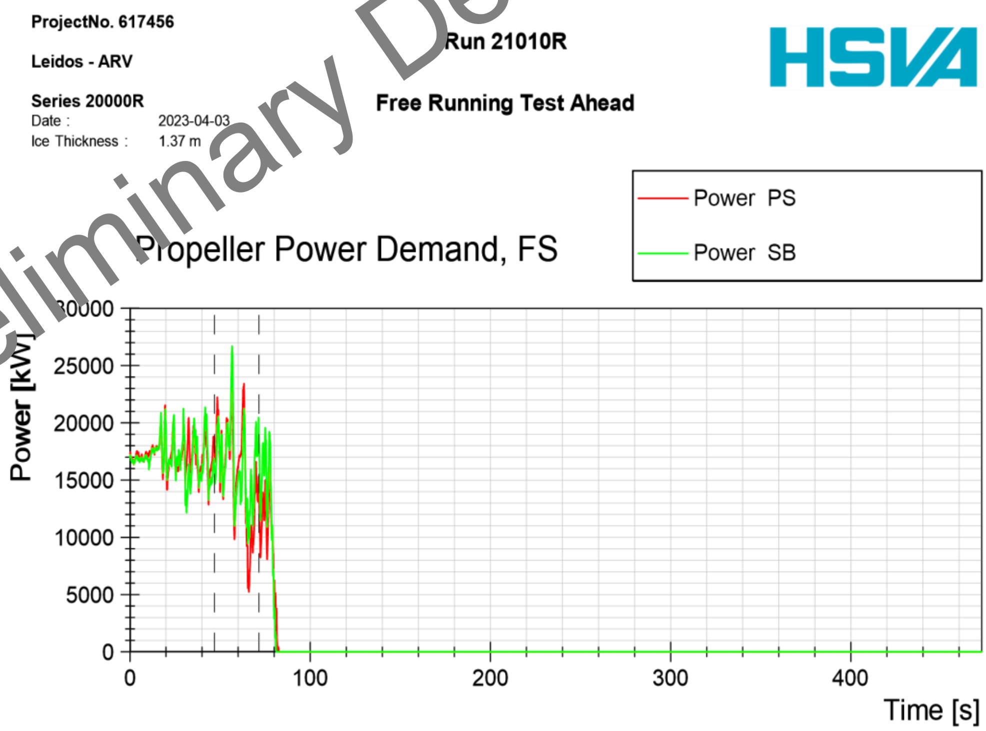

Figure 81 Test run no. 21010R, free running test astern, power

6.8 Test Run No. 23010R Free Running Test Ahead in 1.37m Level Ice, 70% Power

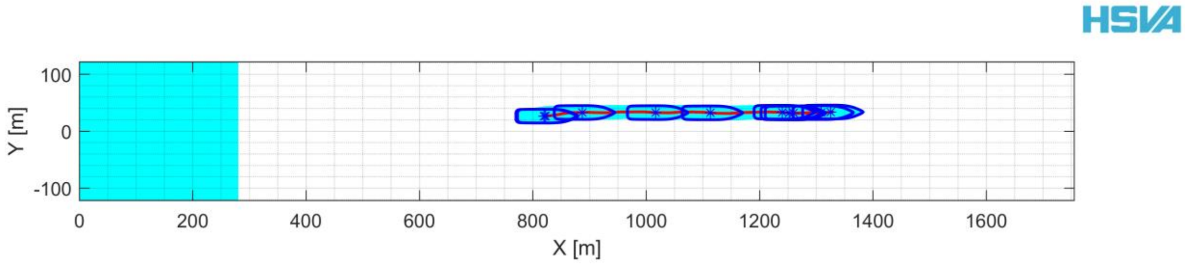

Figure 82 Test run no. 23010R track plot

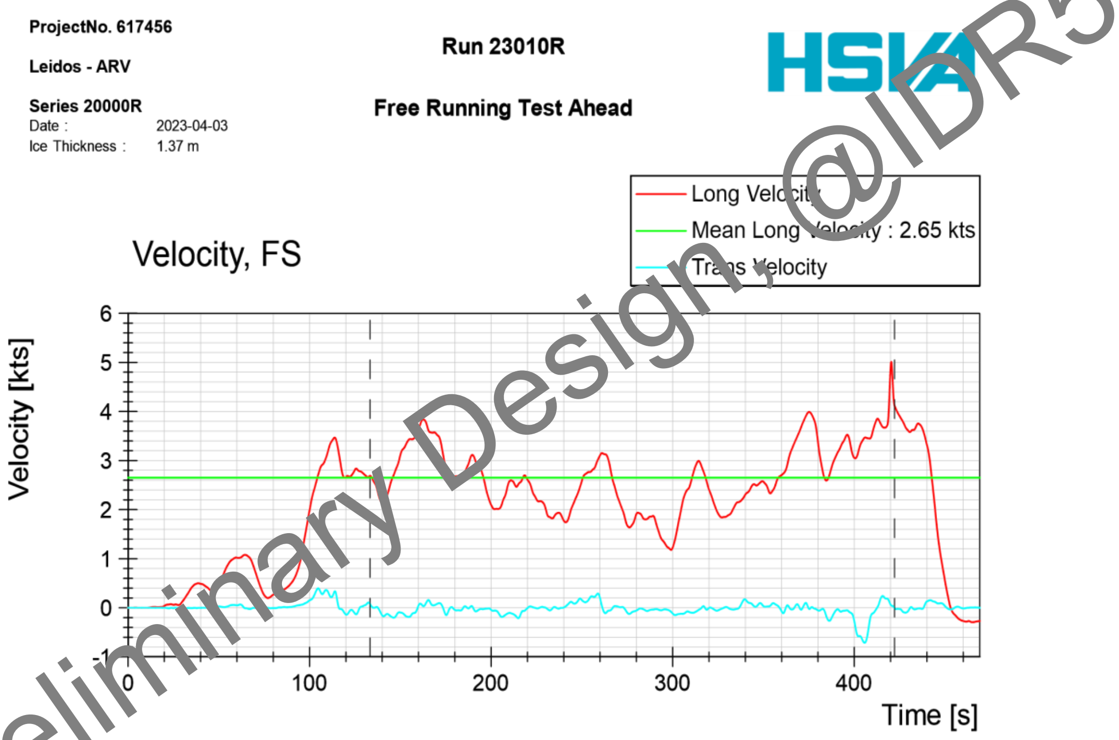

Figure 83 Test run no. 23010R, free running test astern, velocity

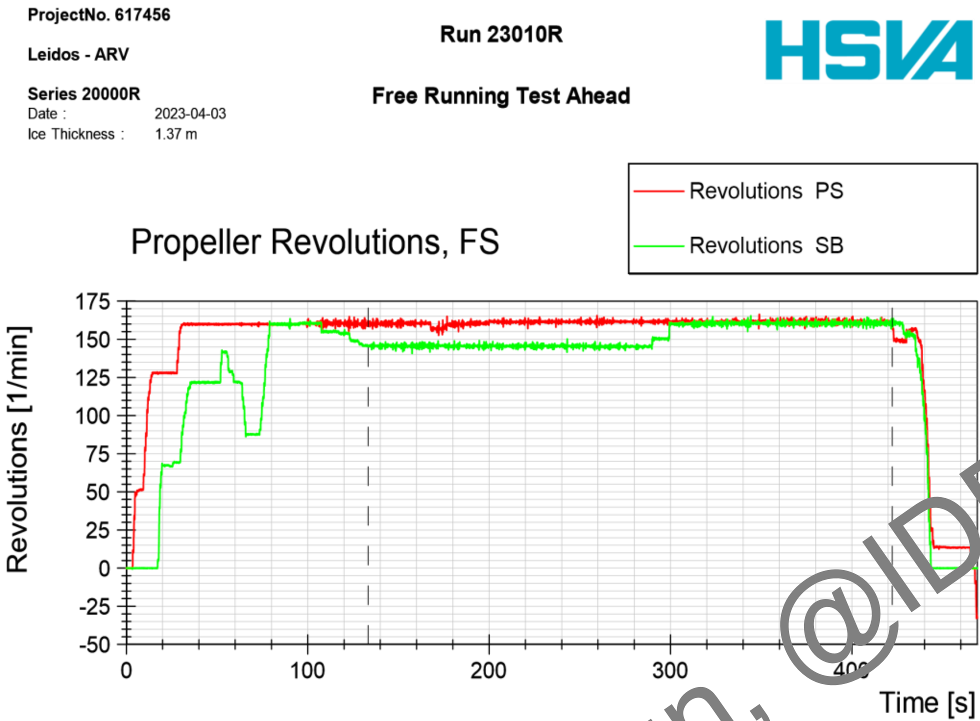

Figure 84 Test run no. 23010R, free running test astern, propeller revolution

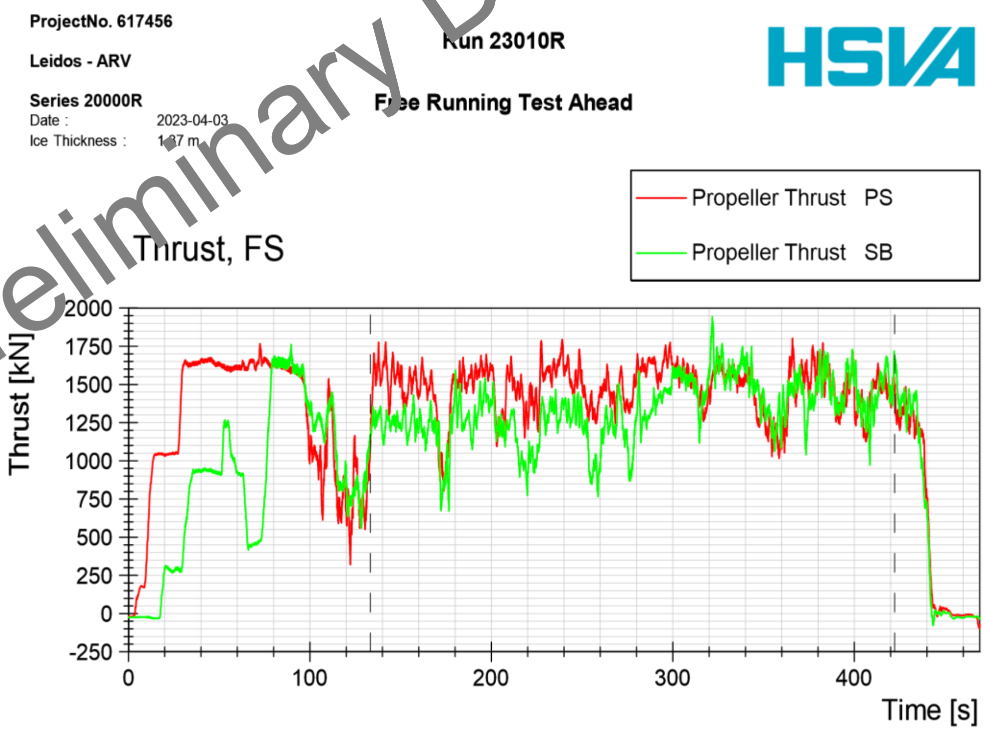

Figure 85 Test run no. 23010R, free running test astern, thrust

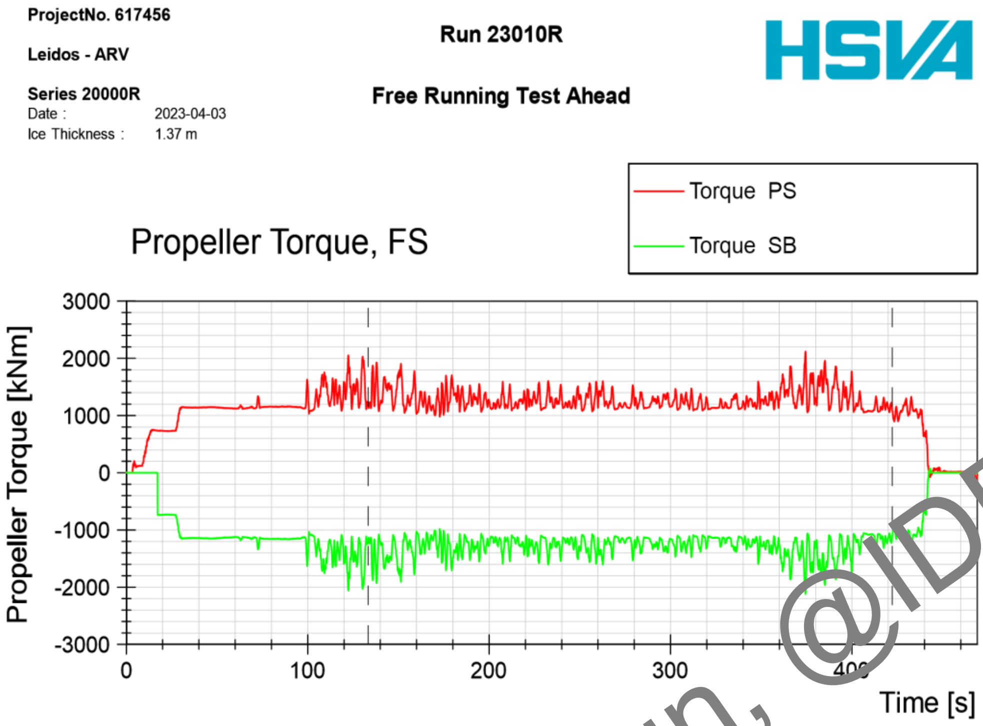

Figure 86 Test run no. 23010R, free running test astern, torque

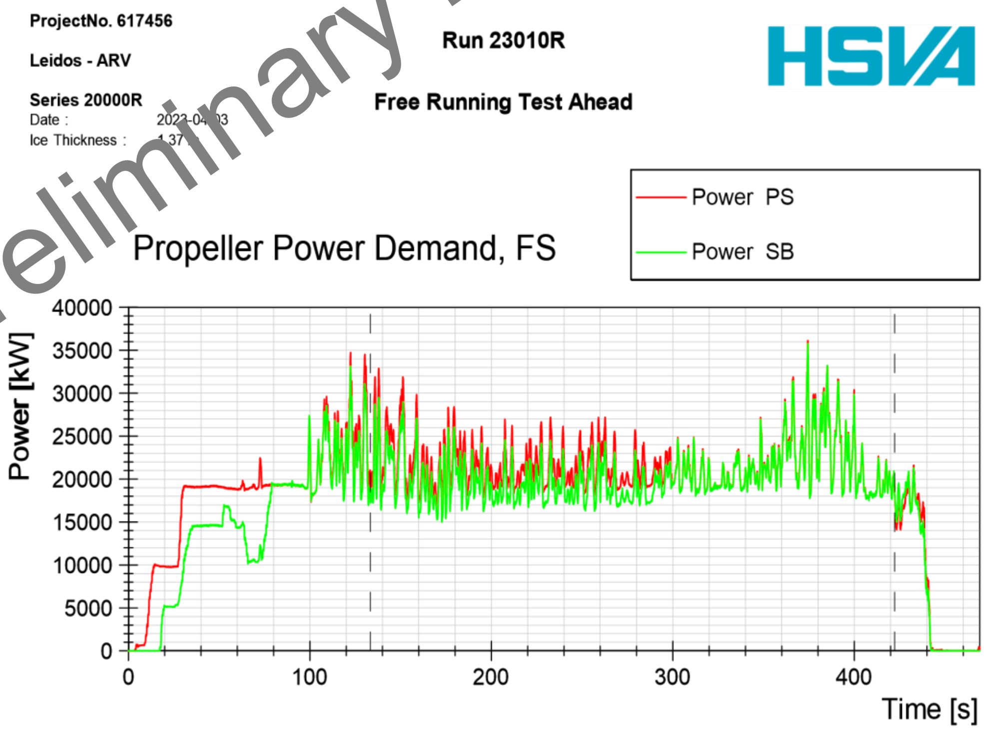

Figure 87 Test run no. 23010R, free running test astern, power

6.9 Test Run No. 24011R Free Running Test Ahead in 1.37m Level Ice, 100% Power

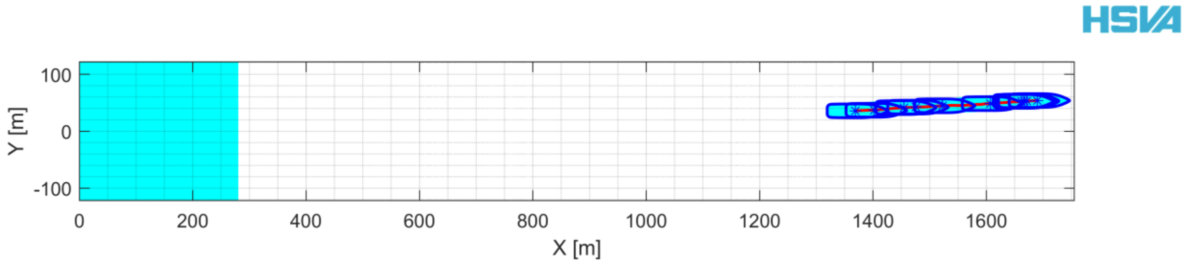

Figure 88 Test run no. 24011R track plot

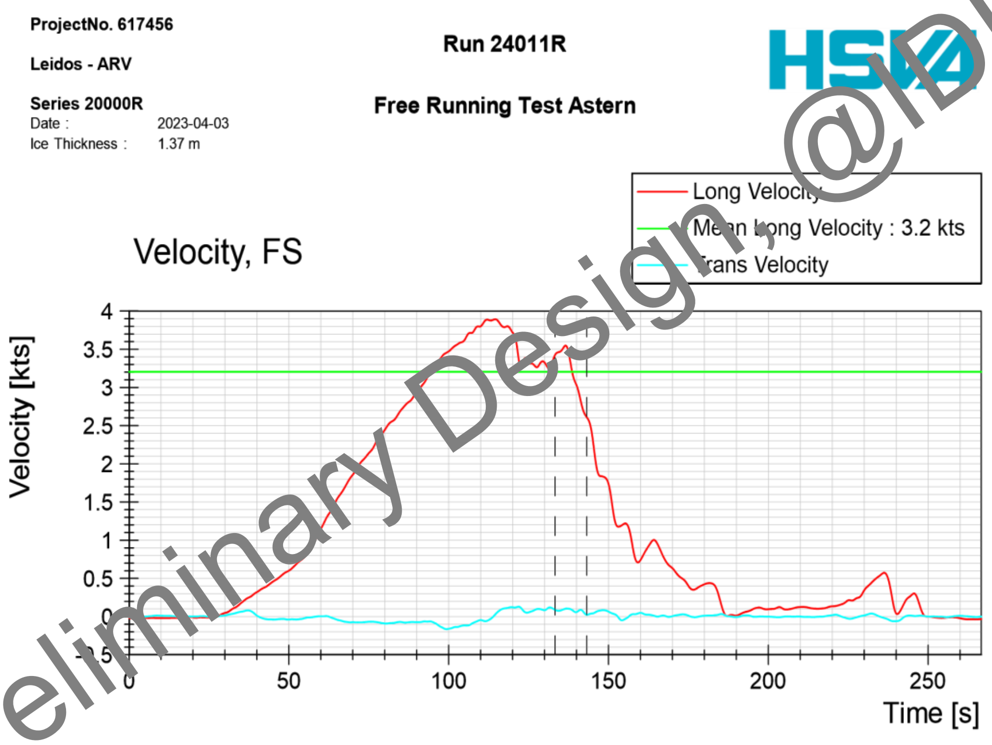

Figure 89 Test run no. 24011R, free running test astern, velocity

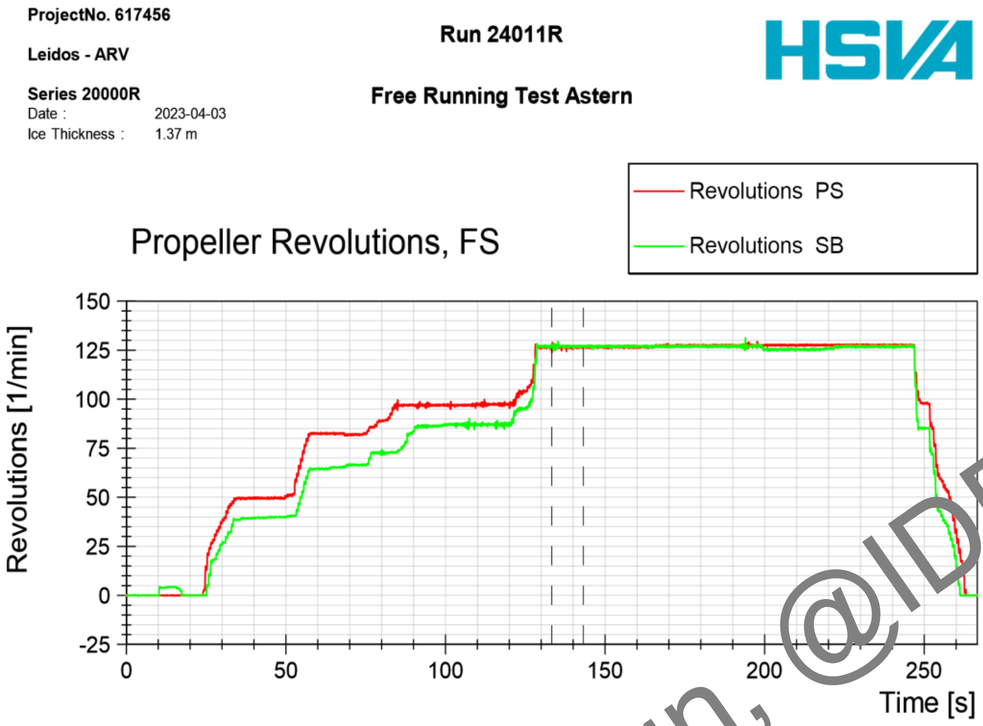

Figure 90 Test run no. 24011R, free running test astern, propeller revolution

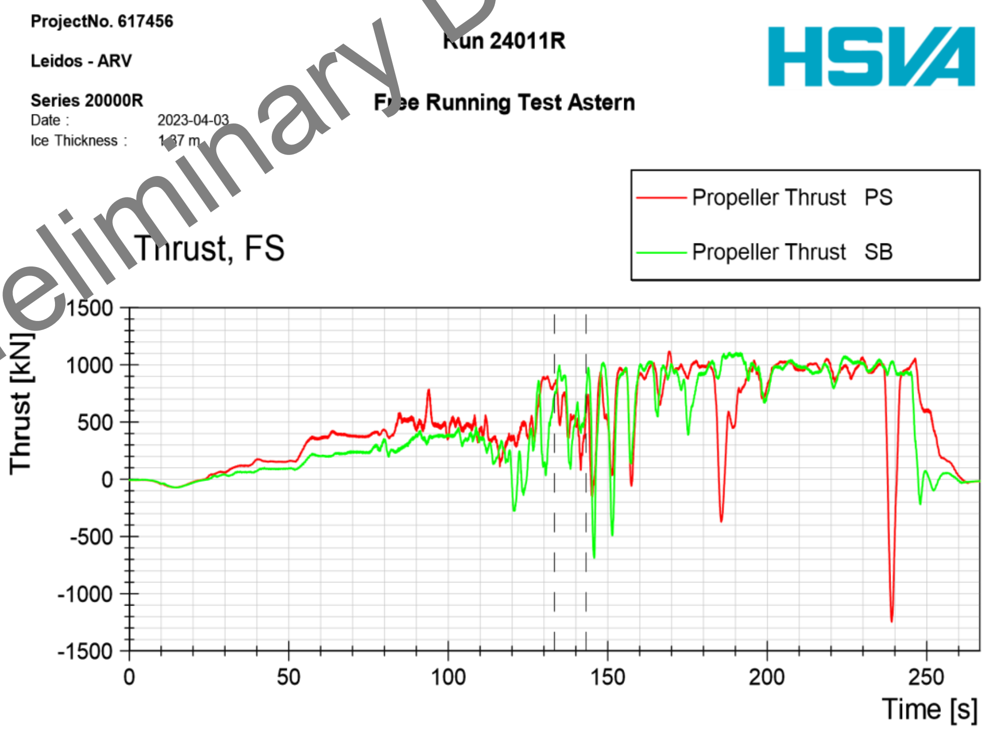

Figure 91 Test run no. 24011R, free running test astern, thrust

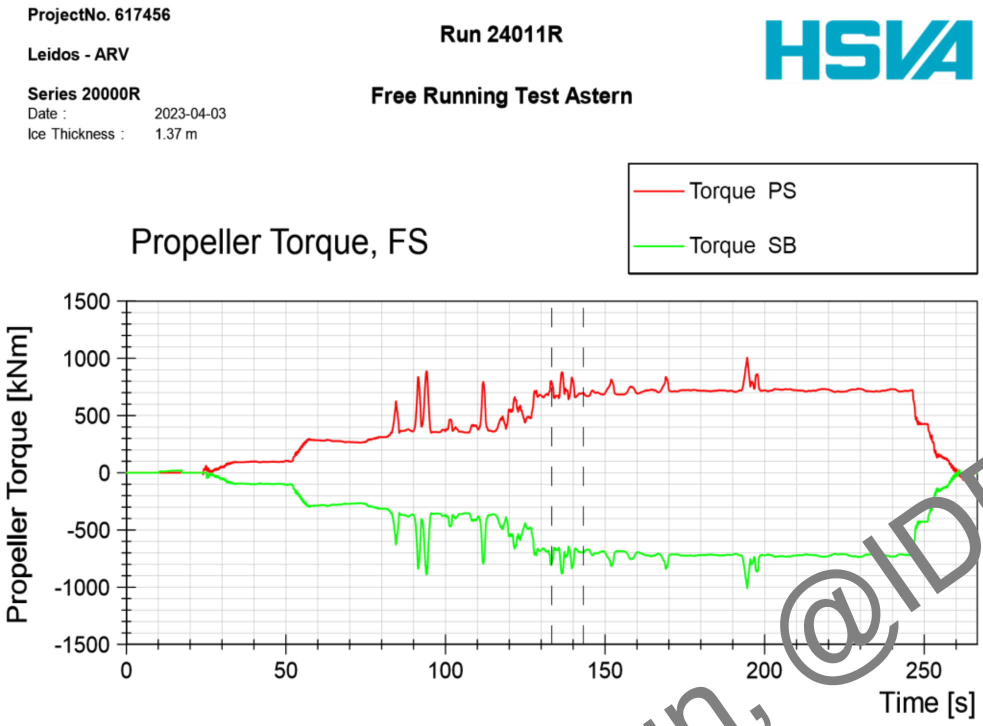

Figure 92 Test run no. 24011R, free running test astern, torque

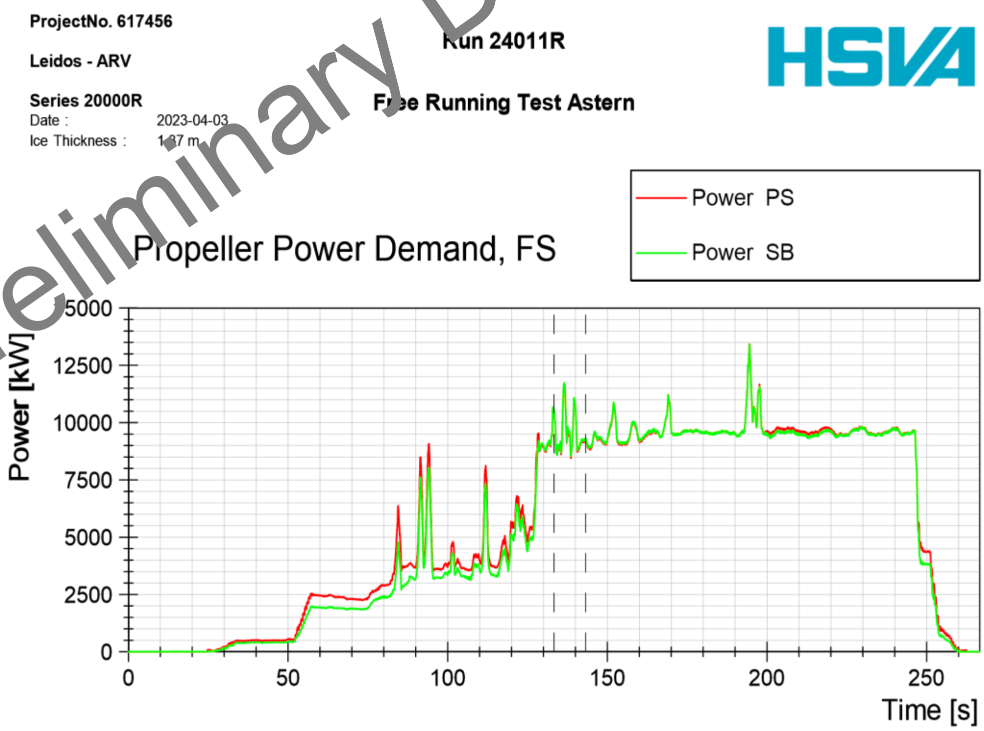

Figure 93 Test run no. 24011R, free running test astern, power

6.10 Test Run No. 24111R Free Running Test Astern in 1.37m Level Ice, 100% Power

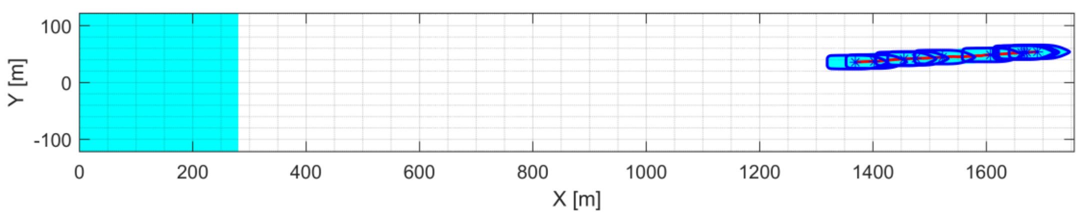

Figure 94 Test run no. 24111R track plot

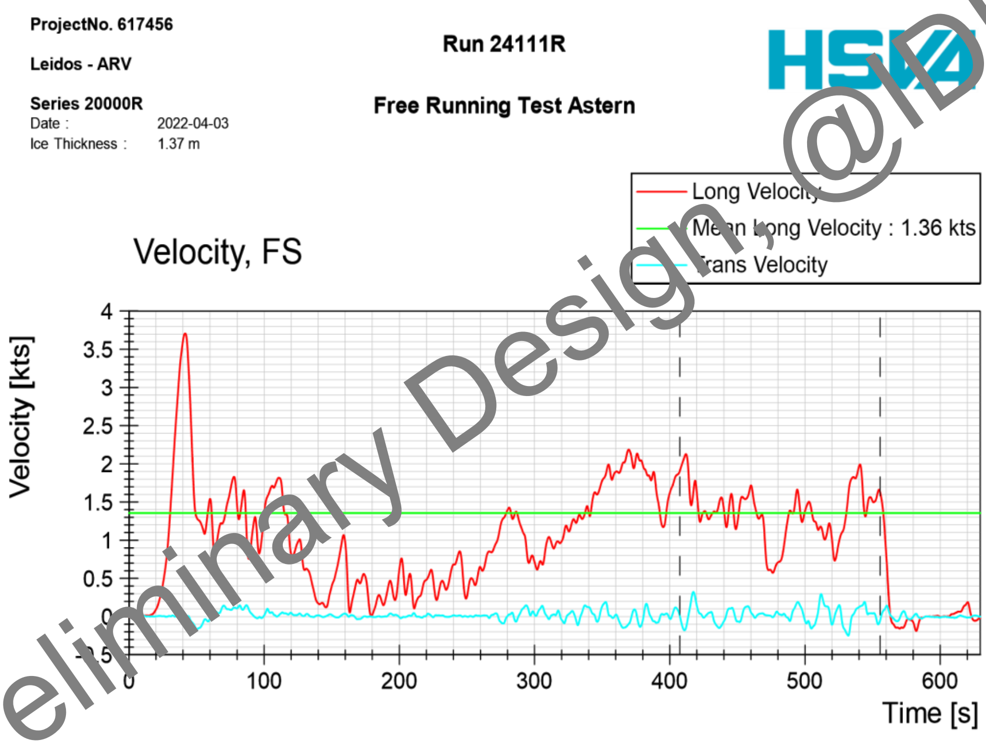

Figure 95 Test run no. 24111R, free running test astern, velocity

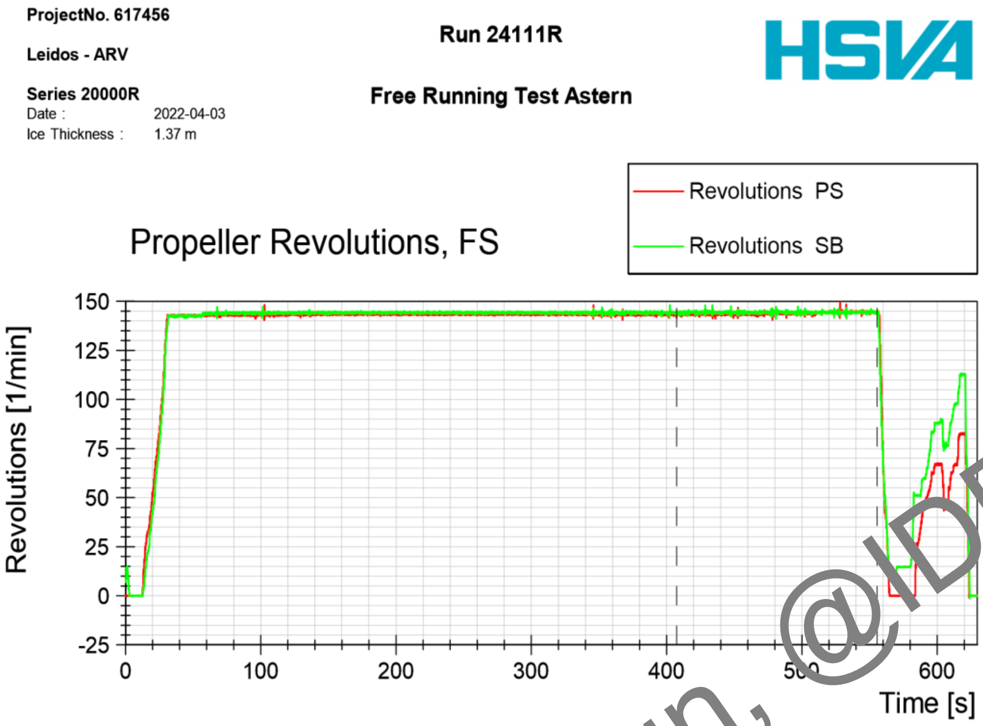

Figure 96 Test run no. 24111R, free running test astern, propeller revolution

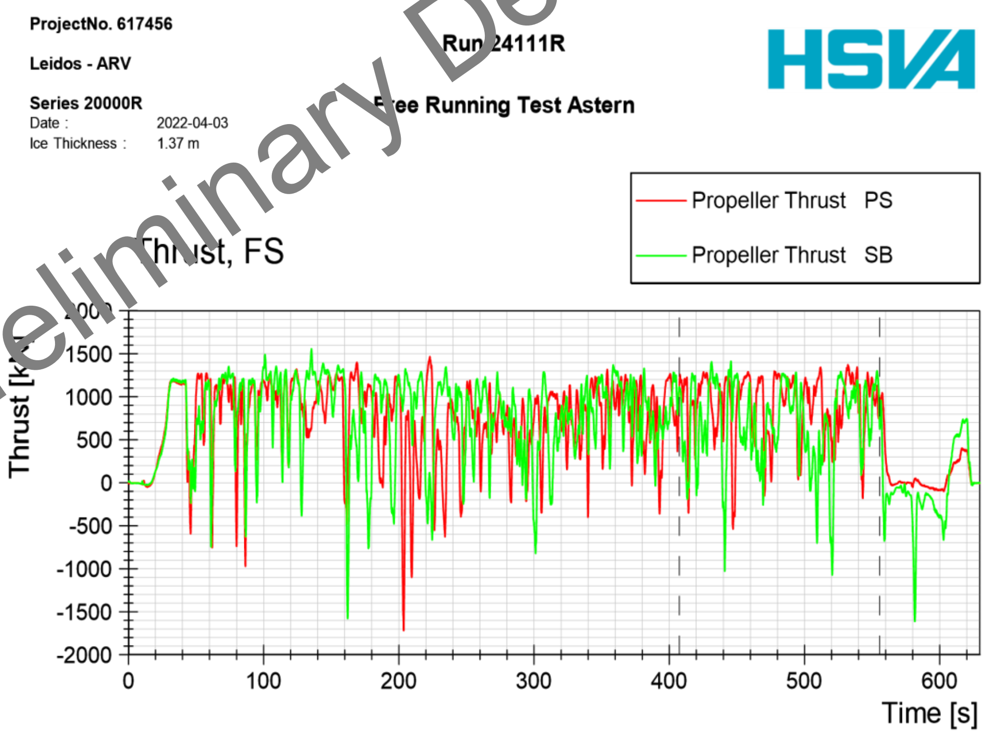

Figure 97 Test run no. 24111R, free running test astern, thrust

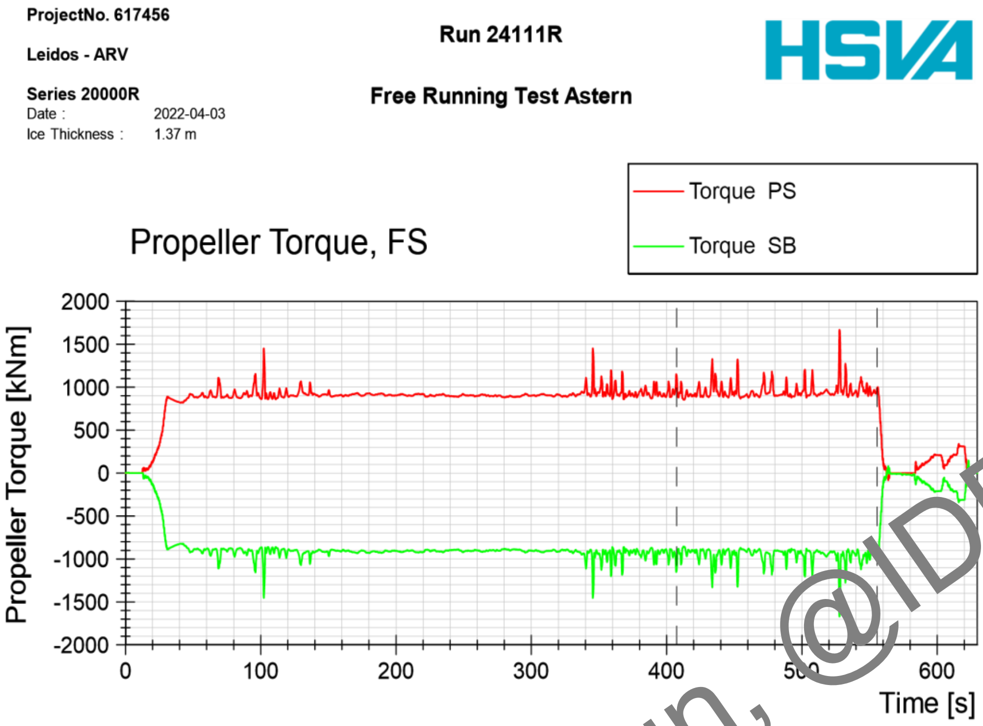

Figure 98 Test run no. 24111R, free running test astern, torque

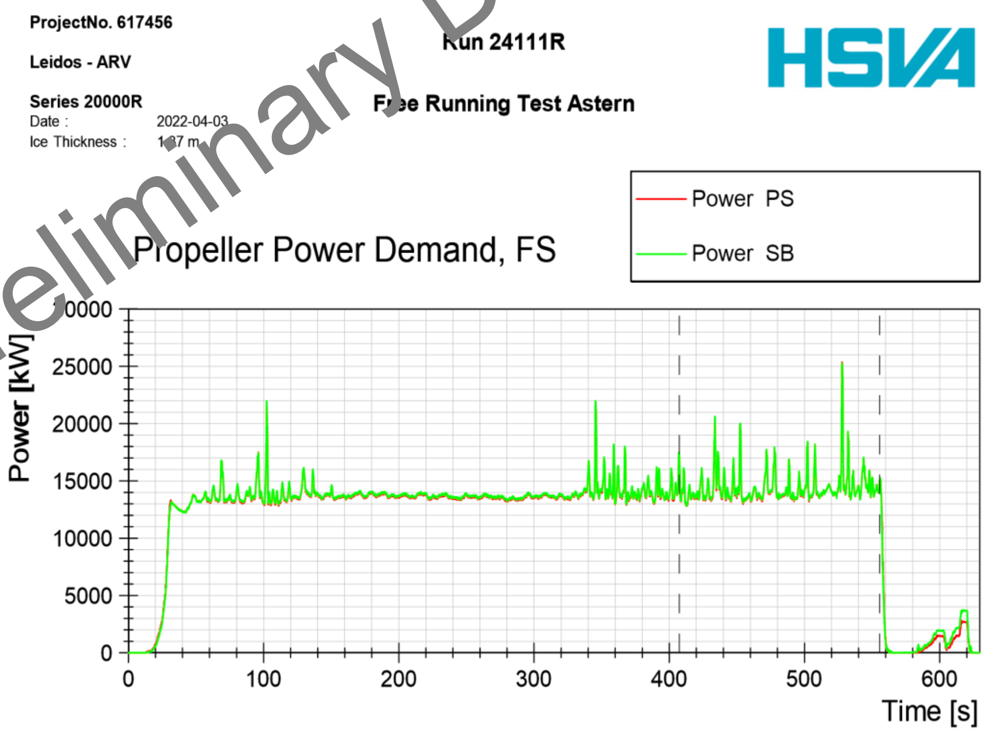

Figure 99 Test run no. 24111R, free running test astern, power

6.11 Test Run No. 25011R Break Out Test Astern in 1.37m Level Ice

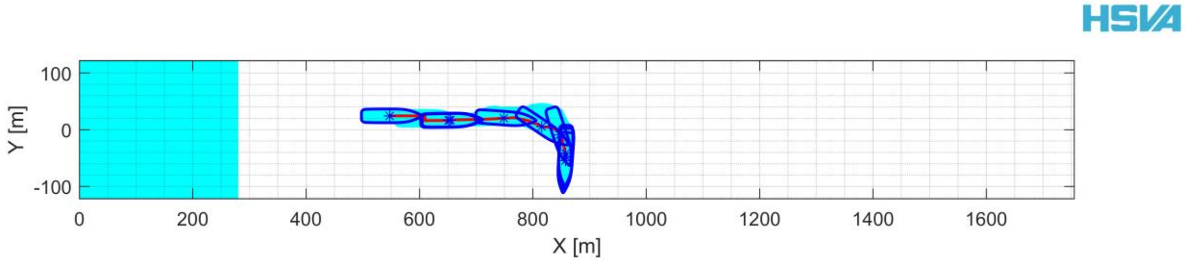

Figure 100 Test run no. 25010R track plot

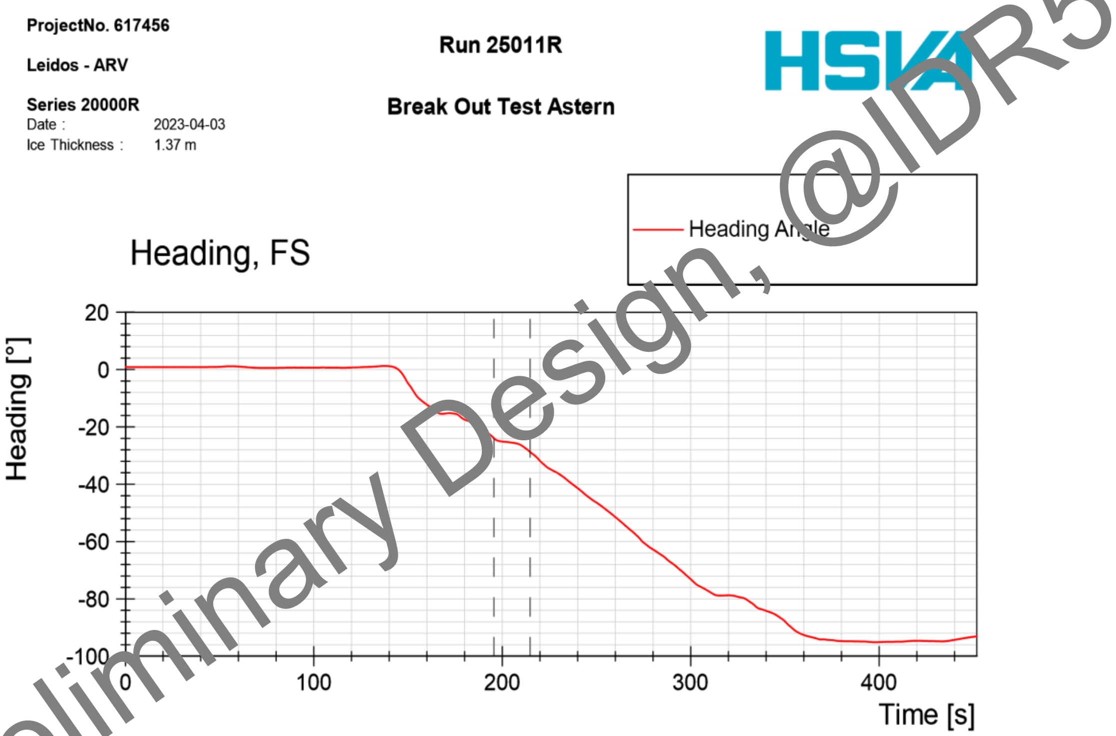

Figure 101 Test run no. 25011R, free running test astern, heading

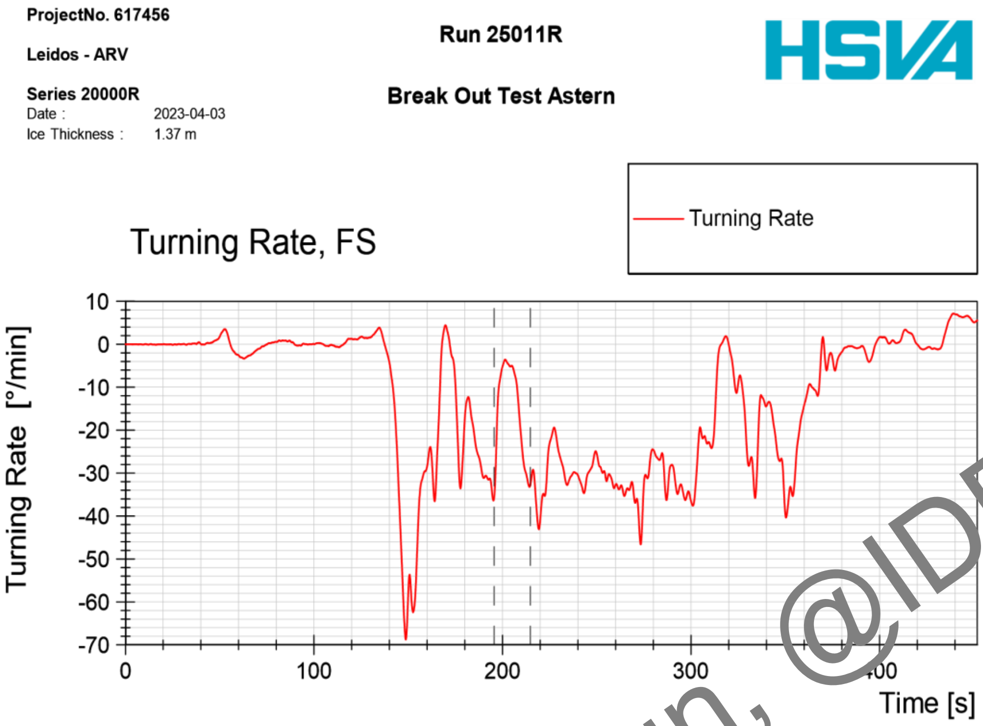

Figure 102 Test run no. 25011R, free running test astern, turning rate

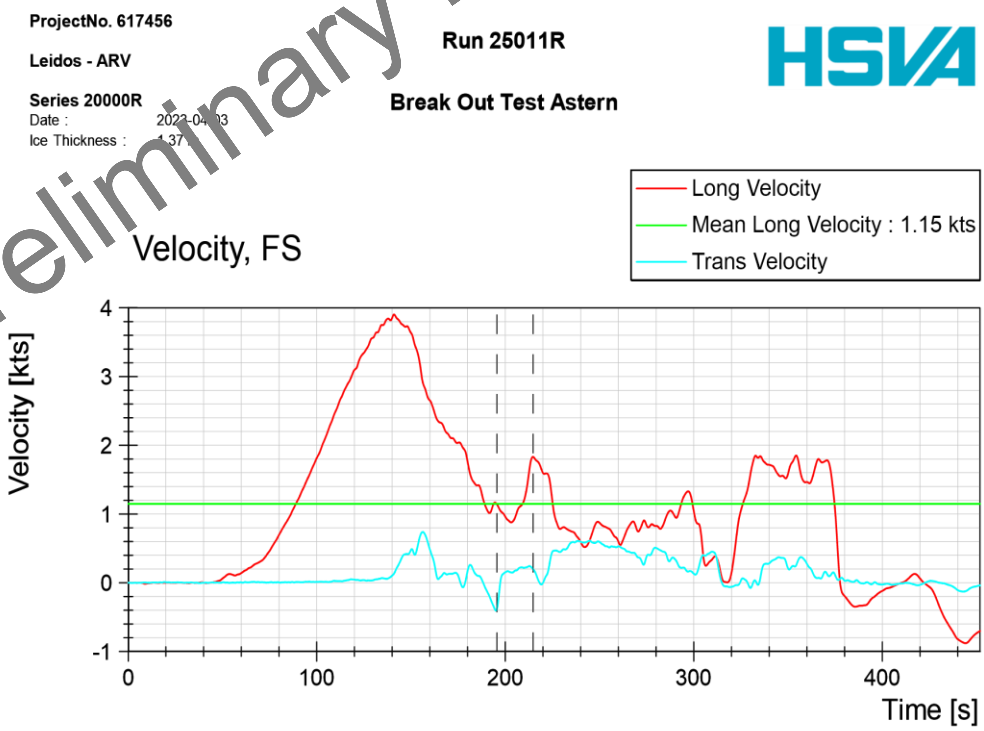

Figure 103 Test run no. 25011R, free running test astern, velocity

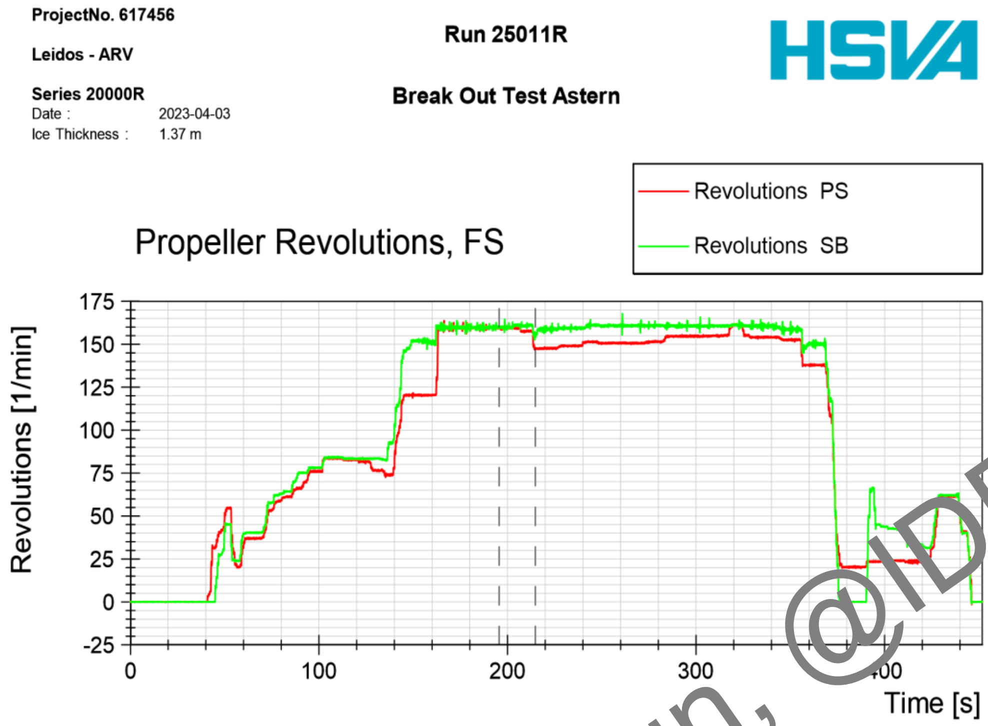

Figure 104 Test run no. 25011R, free running test astern, propeller revolution

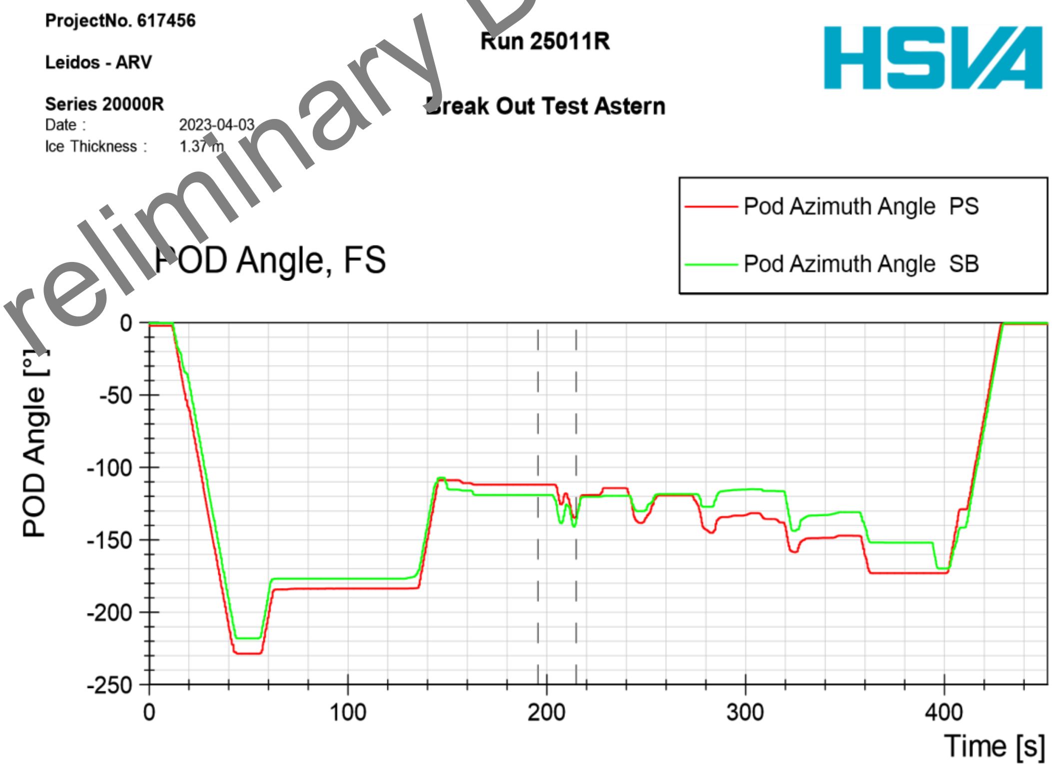

Figure 105 Test run no. 25011R, free running test astern, POD angle

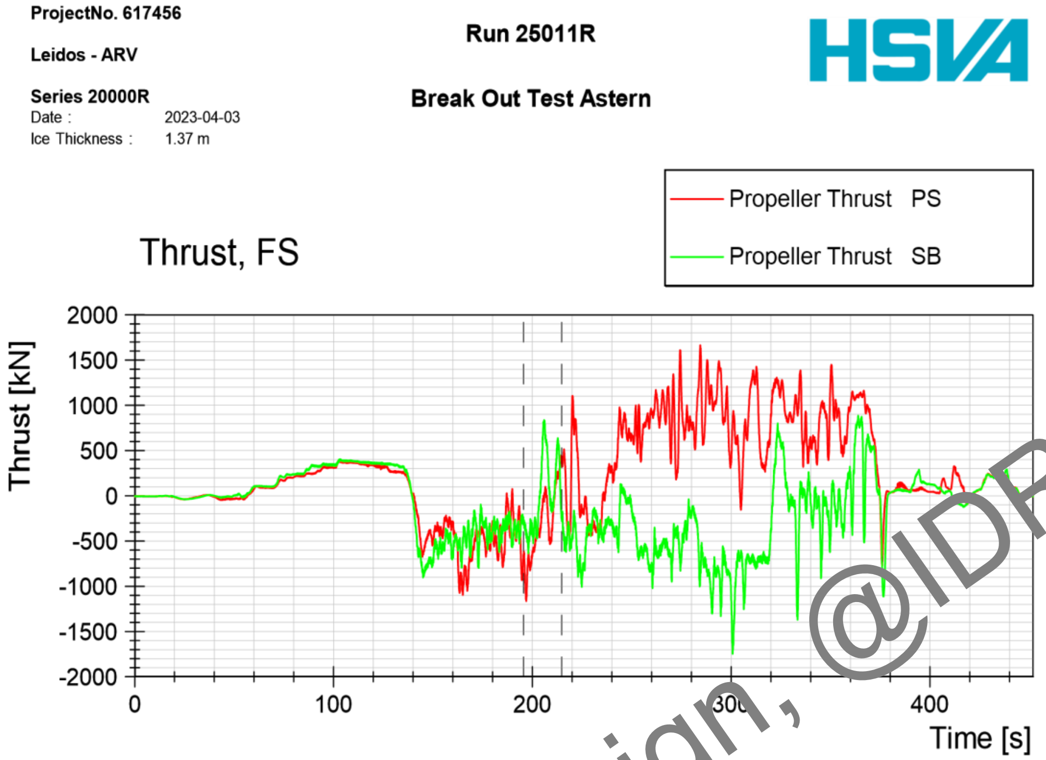

Figure 106 Test run no. 25011R, free running test astern, thrust

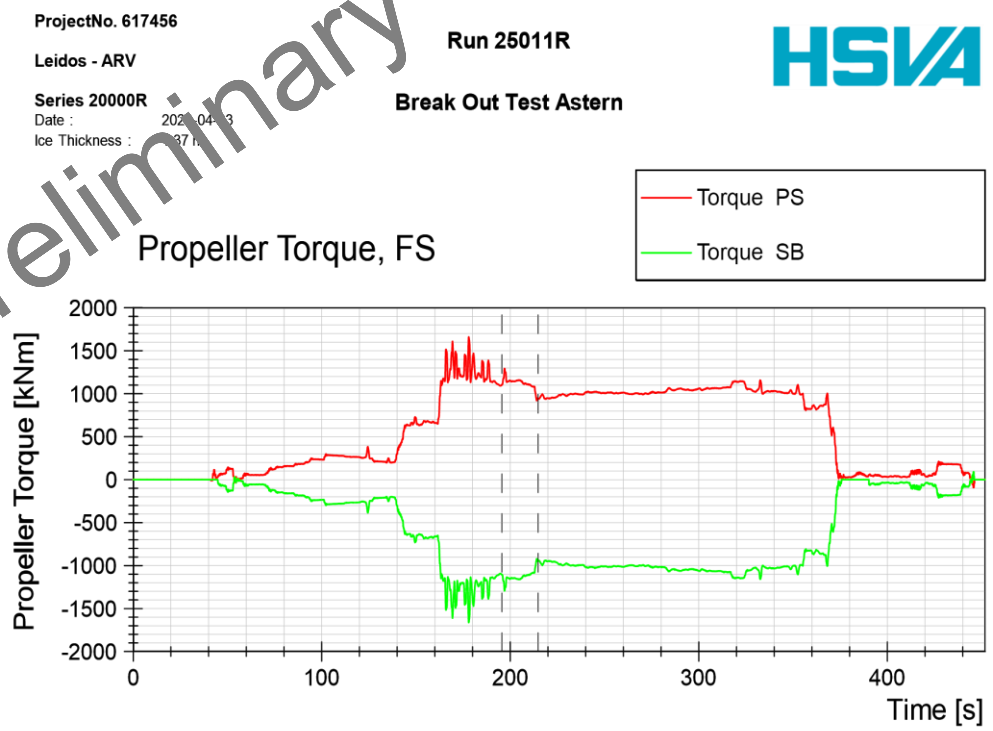

Figure 107 Test run no. 25011R, free running test astern, torque

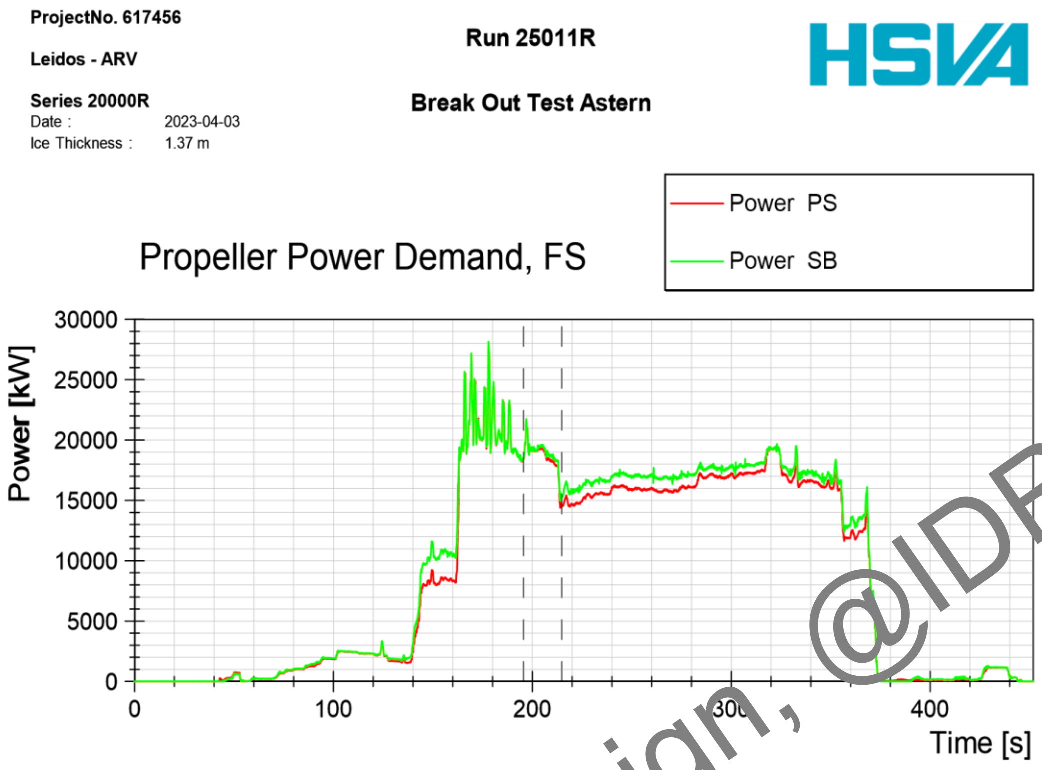

Figure 108 Test run no. 25011R, free running test astern, power

6.12 Test Run No. 26010R Break Out Test Ahead in 1.37m Level Ice

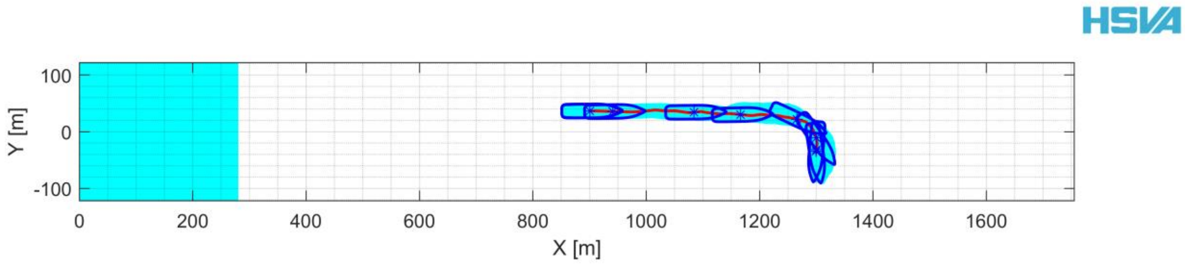

Figure 109 Test run no. 26010 track plot

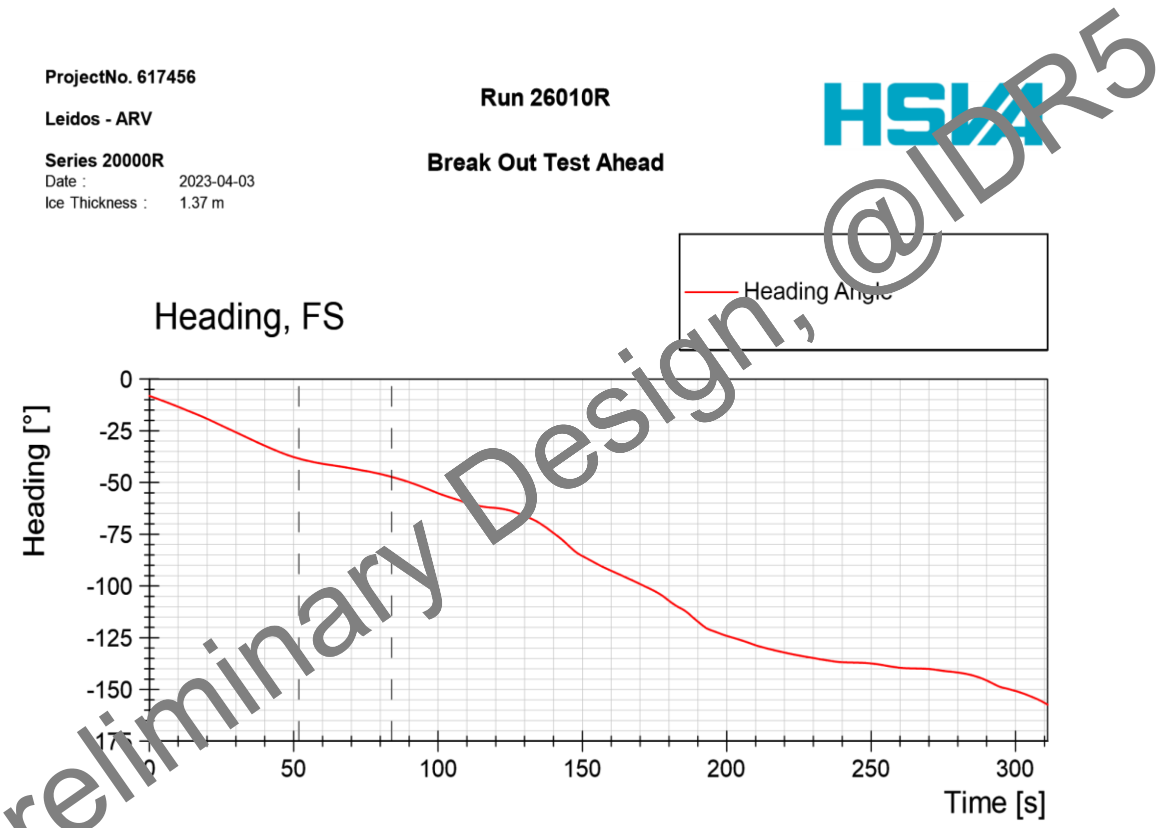

Figure 110 Test run no. 26010R, free running test ahead, heading

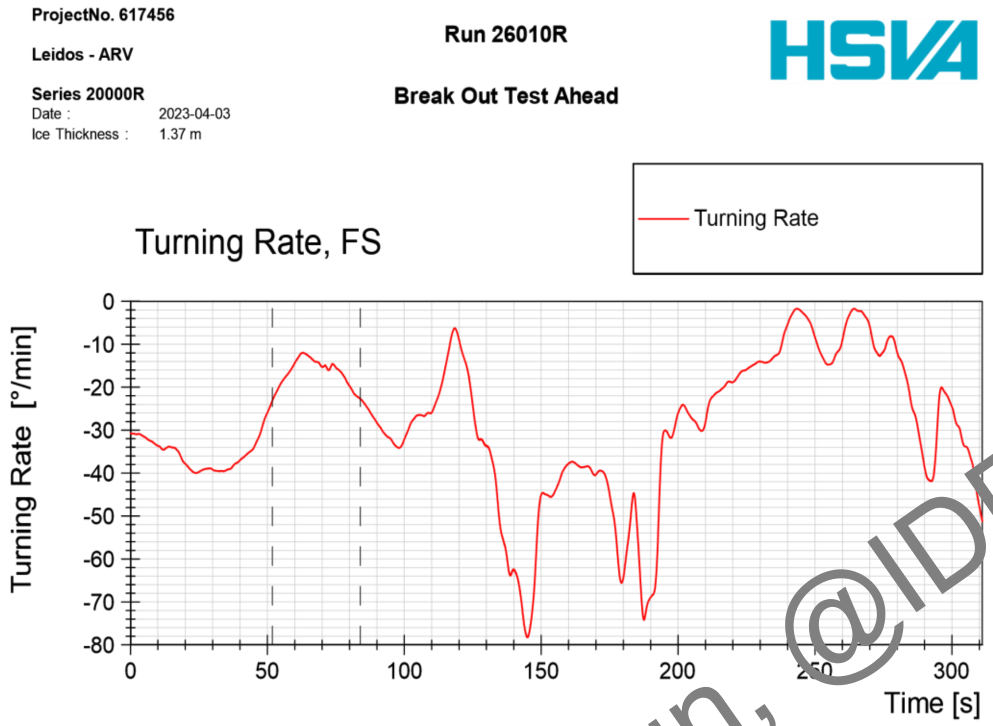

Figure 111 Test run no. 26010R, free running test ahead, turning rate

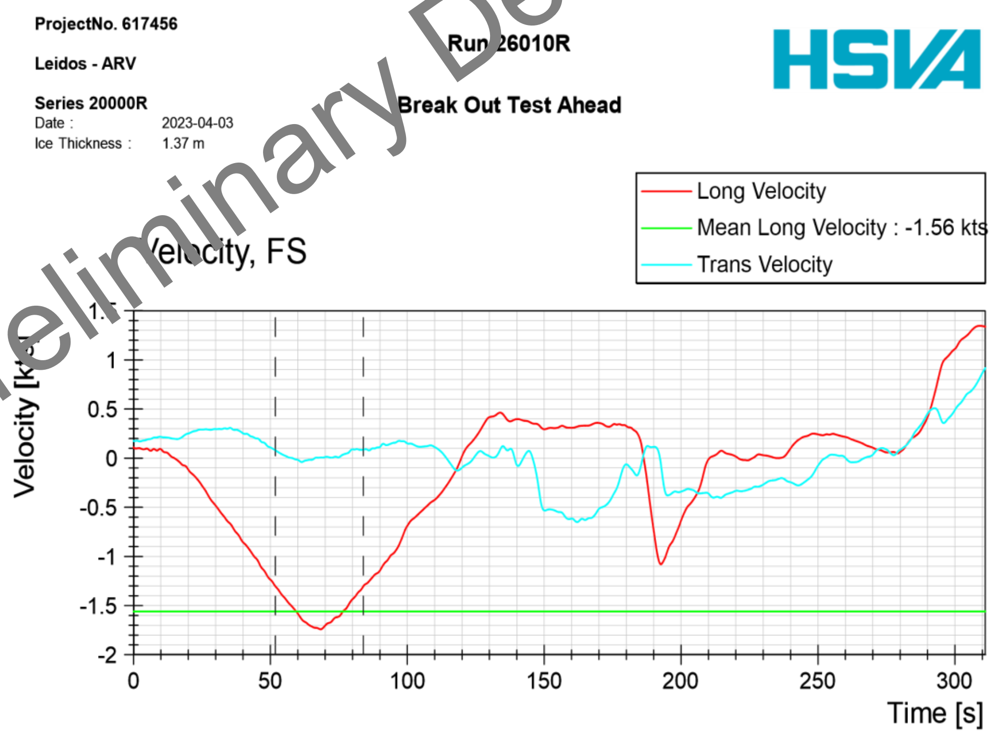

Figure 112 Test run no. 26010R, free running test ahead, velocity

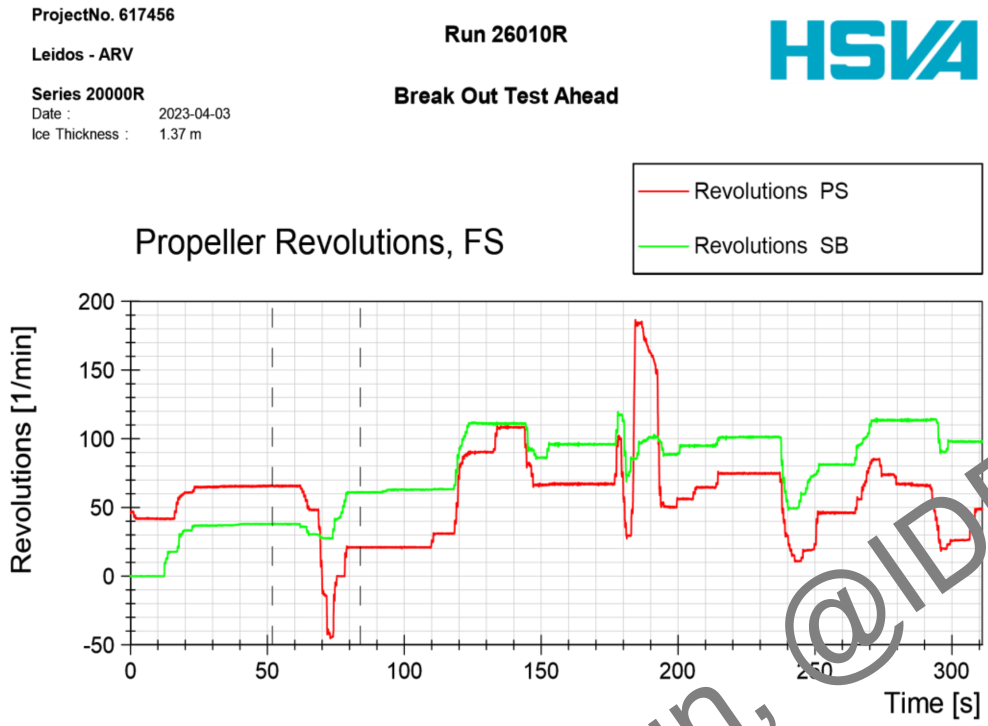

Figure 113 Test run no. 26010R, free running test ahead, propeller revolution

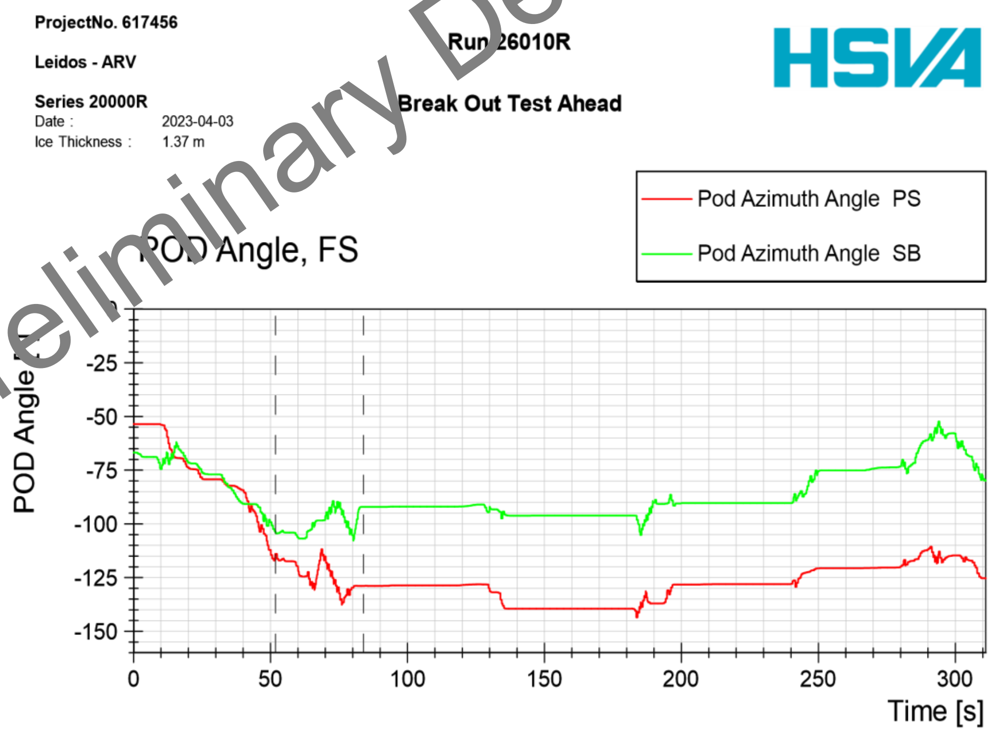

Figure 114 Test run no. 26010R, free running test ahead, POD angle

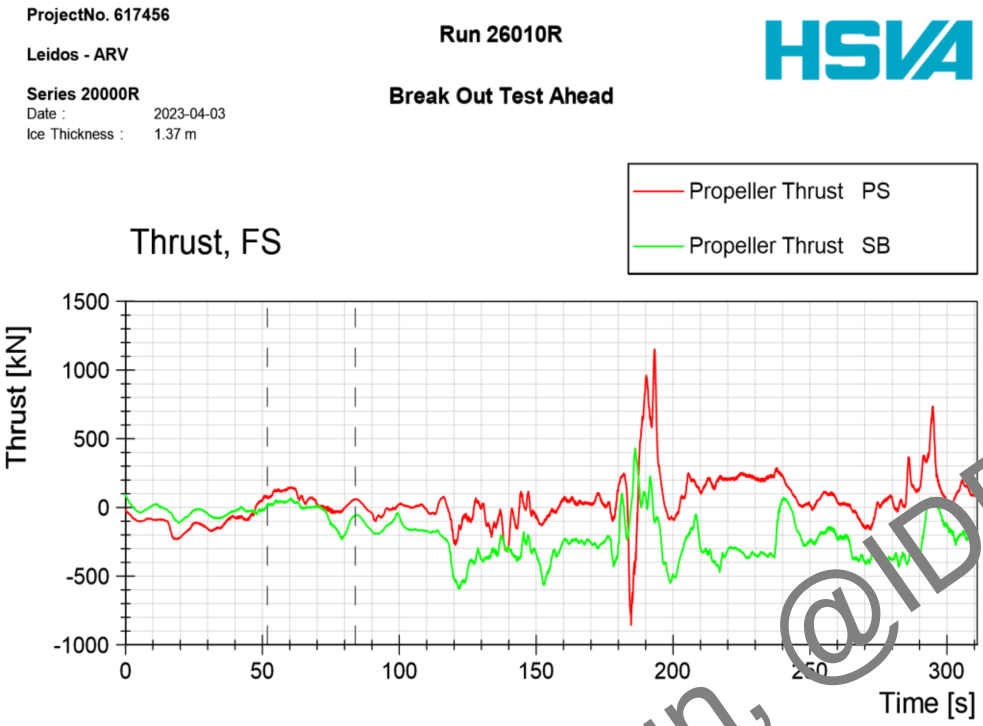

Figure 115 Test run no. 26010R, free running test ahead, thrust

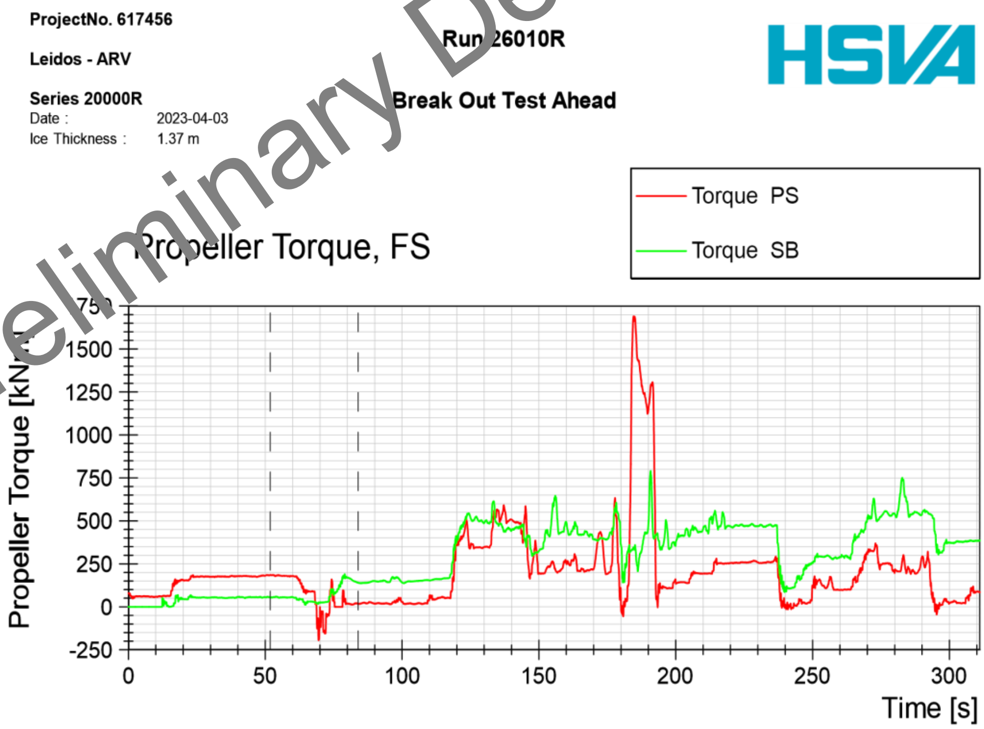

Figure 116 Test run no. 26010R, free running test ahead, torque

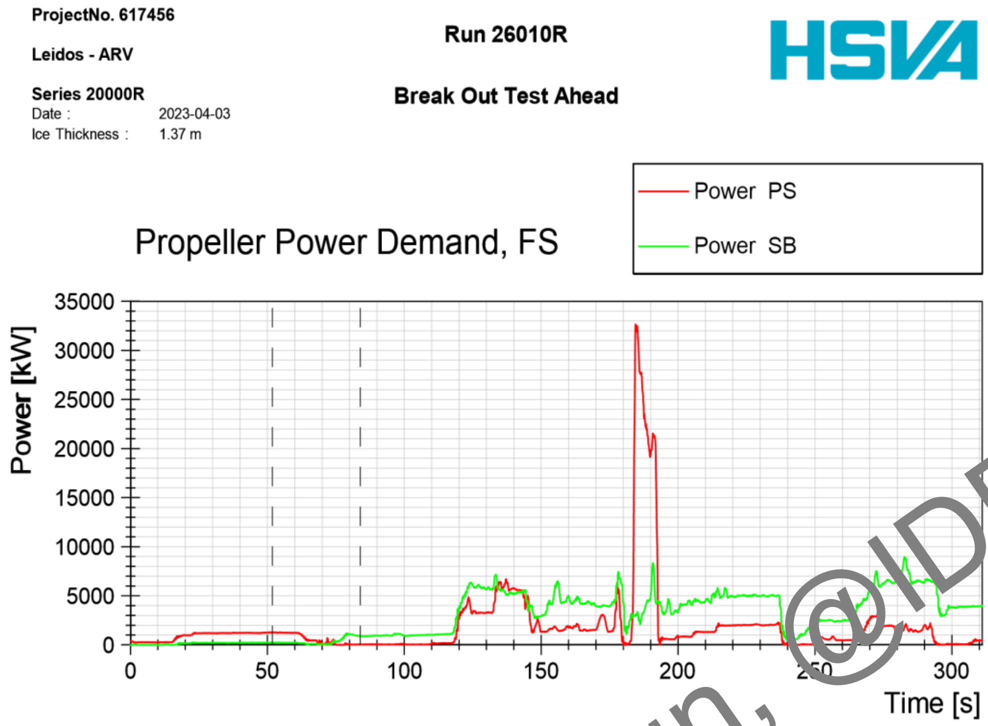

Figure 117 Test run no. 26010R, free running test ahead, power

6.13 Test Run No. 31010R Free Running Test Ahead in 1.0m Level Ice, 100% Power

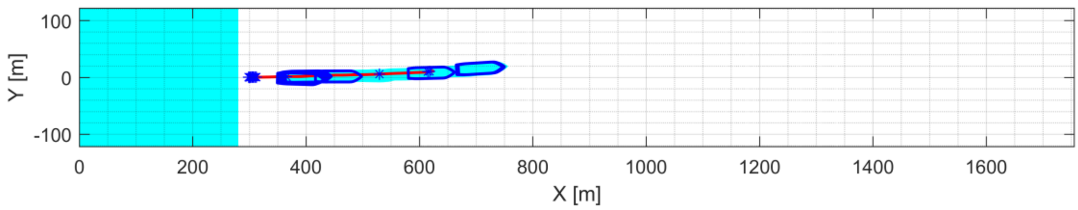

Figure 118 Test run no. 31010R

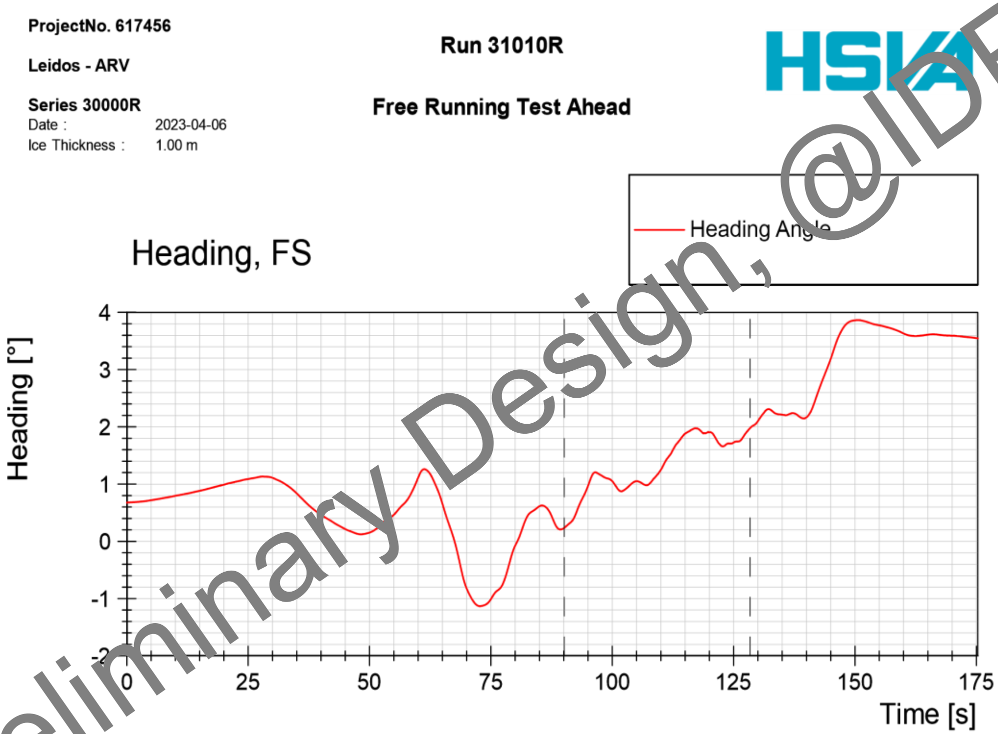

Figure 119 Test run no. 31010R, free running test ahead, heading

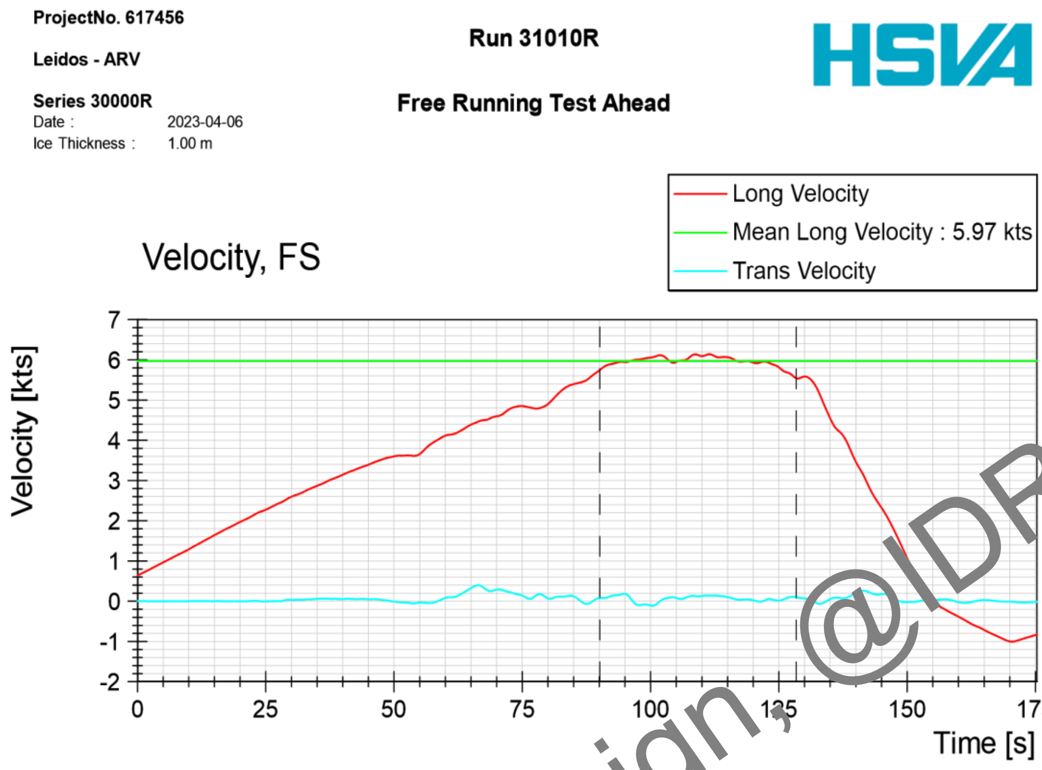

Figure 120 Test run no. 31010R, free running test ahead, velocity

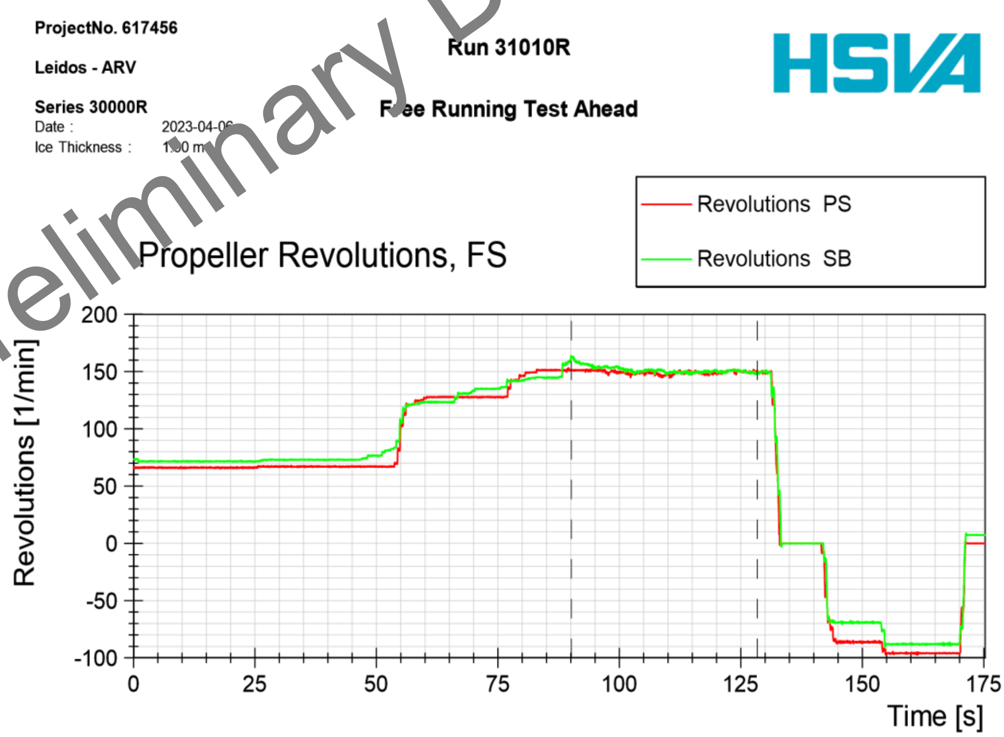

Figure 121 Test run no. 31010R, free running test ahead, propeller revolution

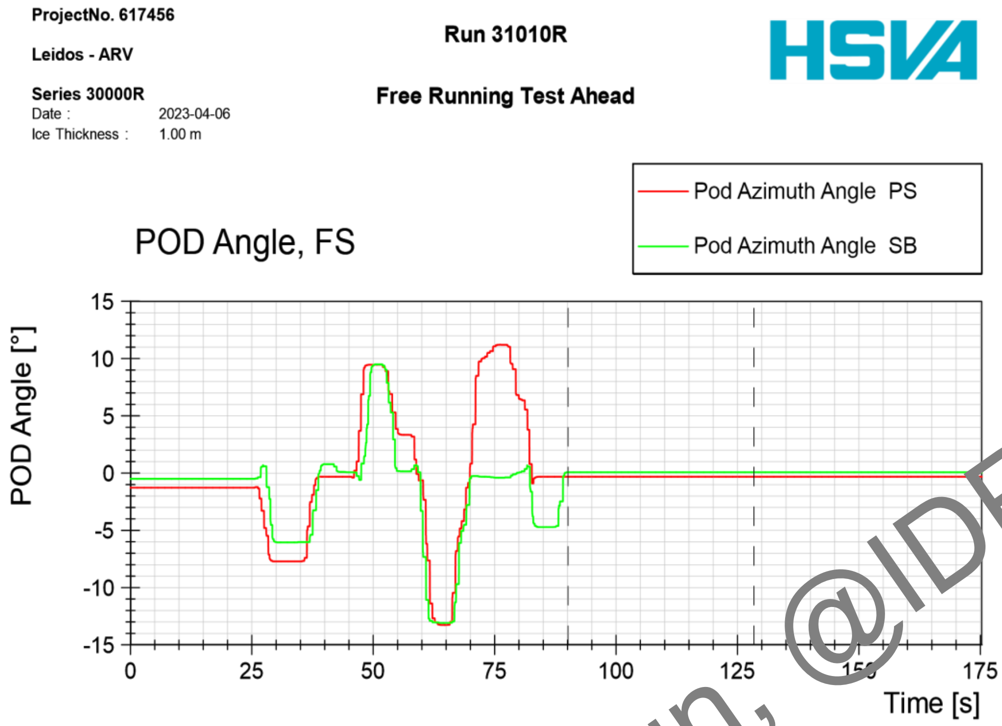

Figure 122 Test run no. 31010R, free running test ahead, POD angle

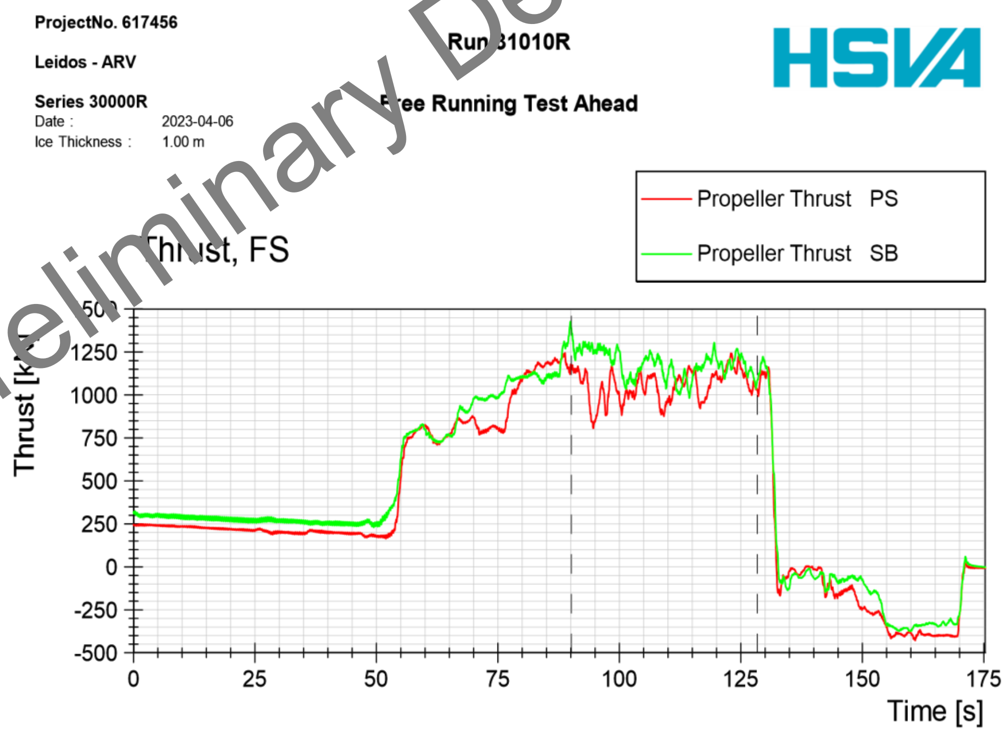

Figure 123 Test run no. 31010R, free running test ahead, thrust

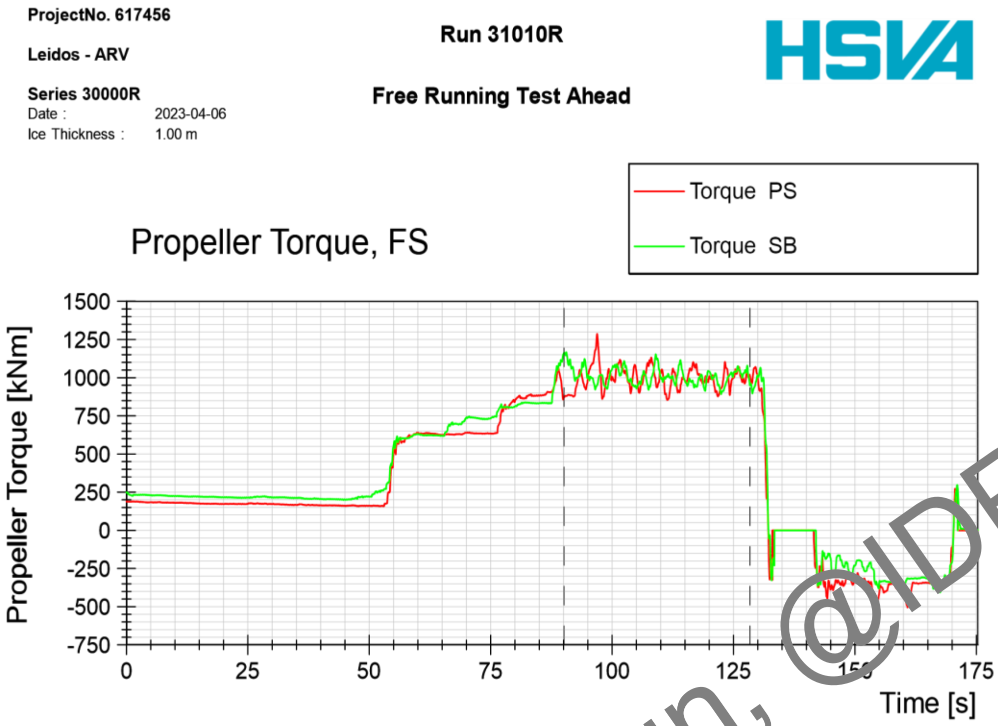

Figure 124 Test run no. 31010R, free running test ahead, torque

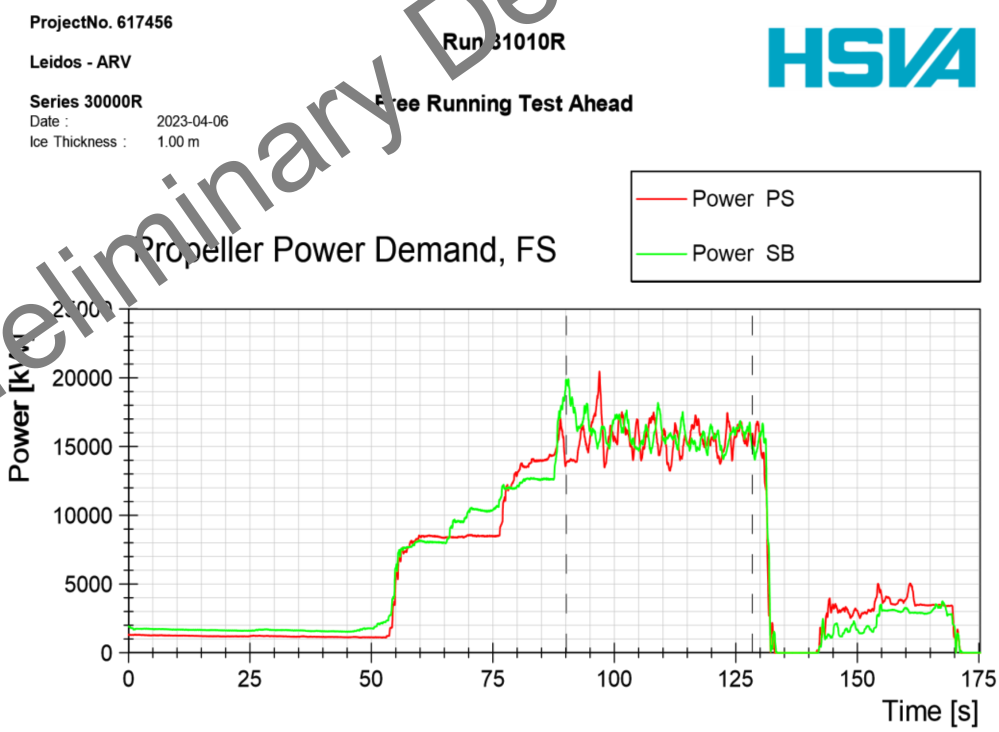

Figure 125 Test run no. 31010R, free running test ahead, power

6.14 Test Run No. 32010R Channel Clearing Test Ahead in 1.00m Level Ice, 60 Degree Pod Angle Inward

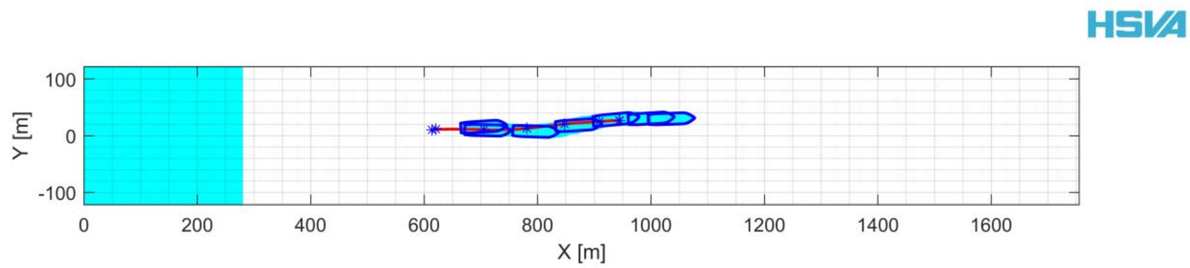

Figure 126 Test run no. 32010R track plot

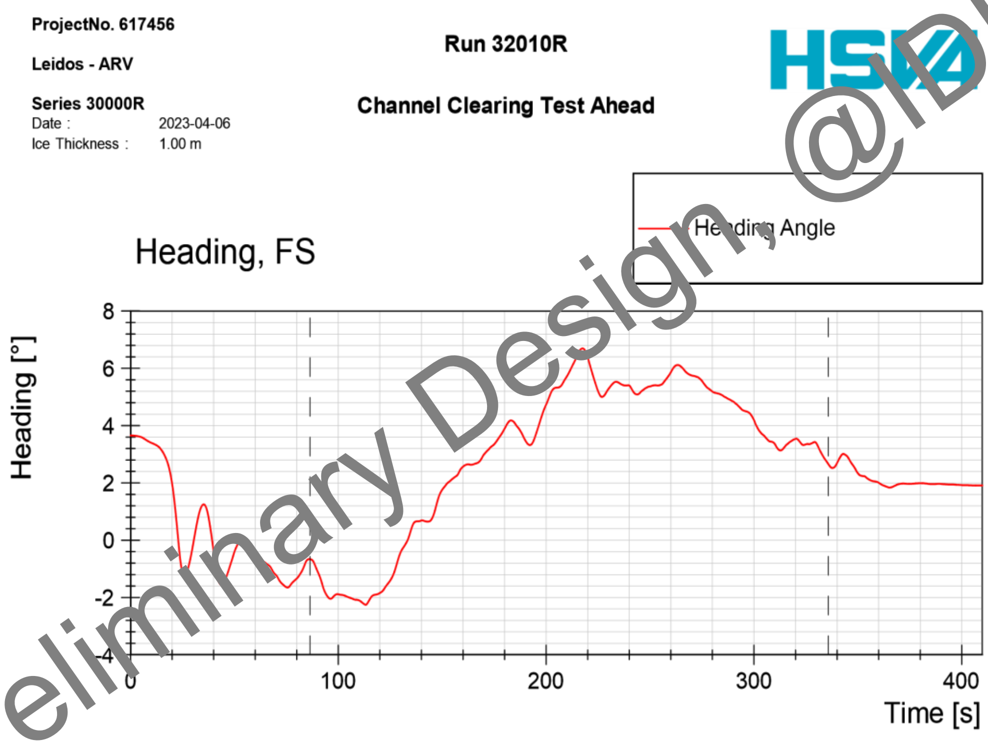

Figure 127 Test run no. 32010R, channel clearing test ahead, heading

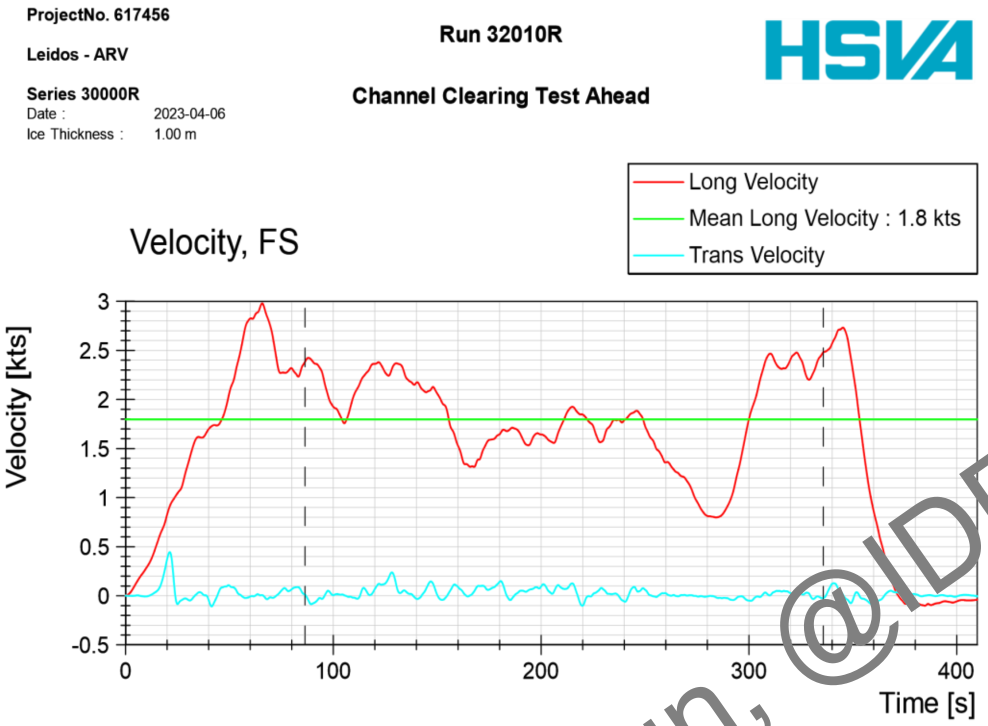

Figure 128 Test run no. 32010R, channel clearing test ahead, velocity

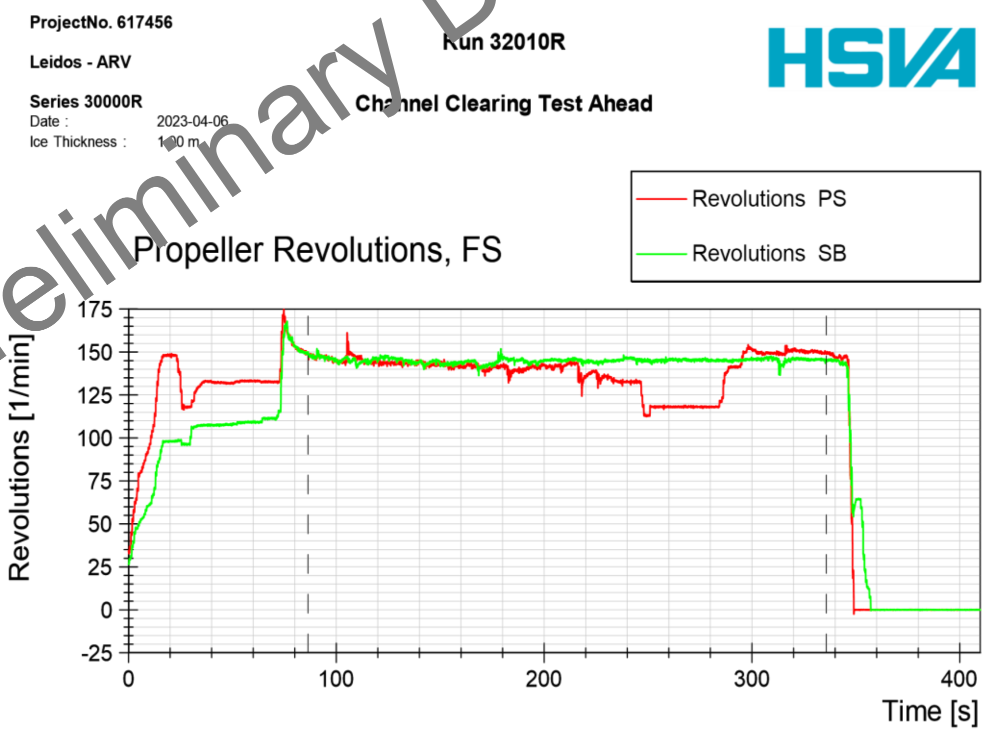

Figure 129 Test run no. 32010R, channel clearing test ahead, propeller revolution

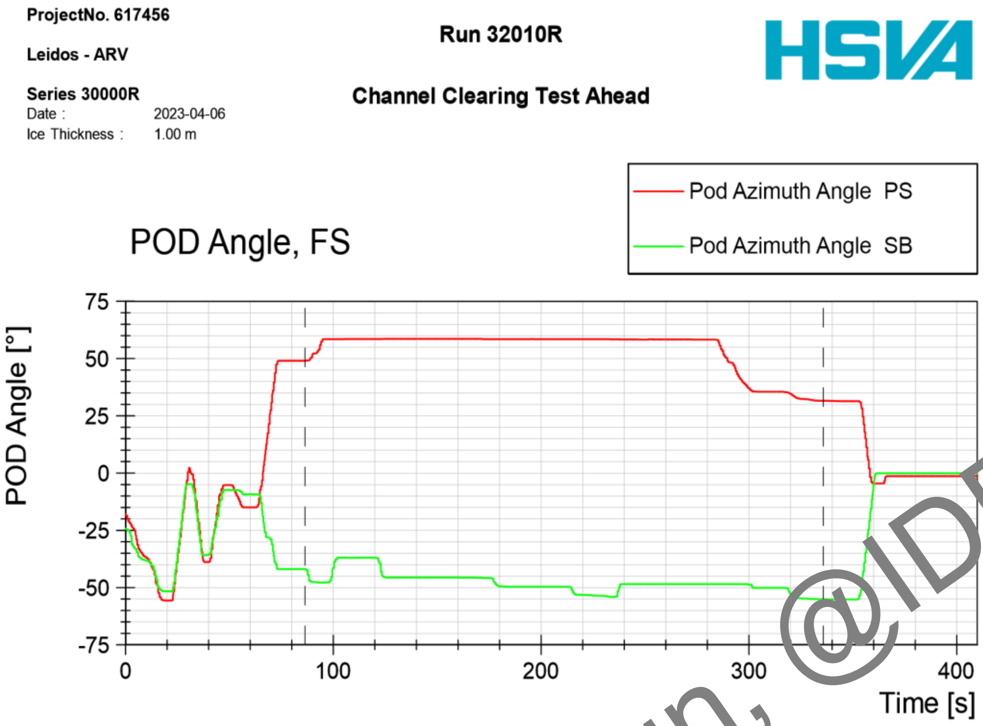

Figure 130 Test run no. 32010R, channel clearing test ahead, POD angle

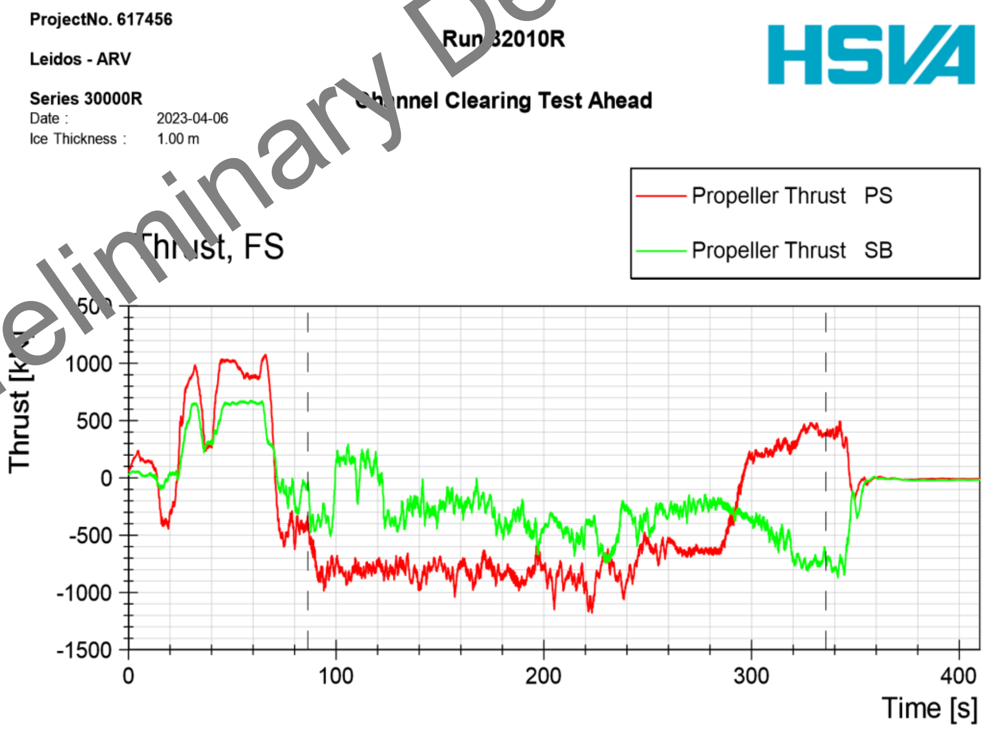

Figure 131 Test run no. 32010R, channel clearing test ahead, thrust

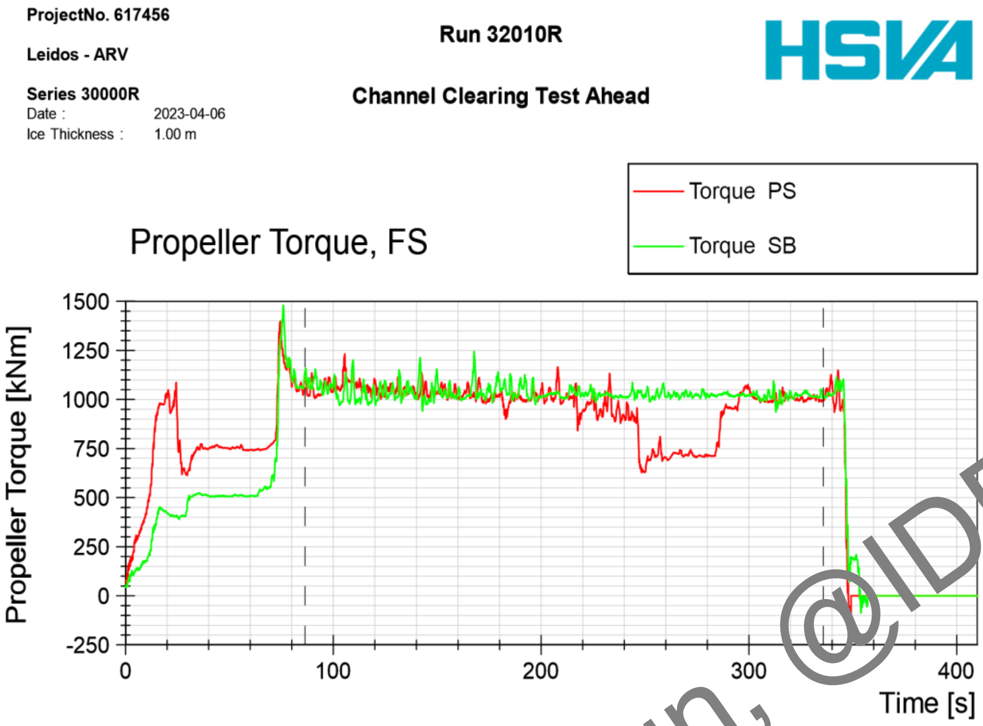

Figure 132 Test run no. 32010R, channel clearing test ahead, torque

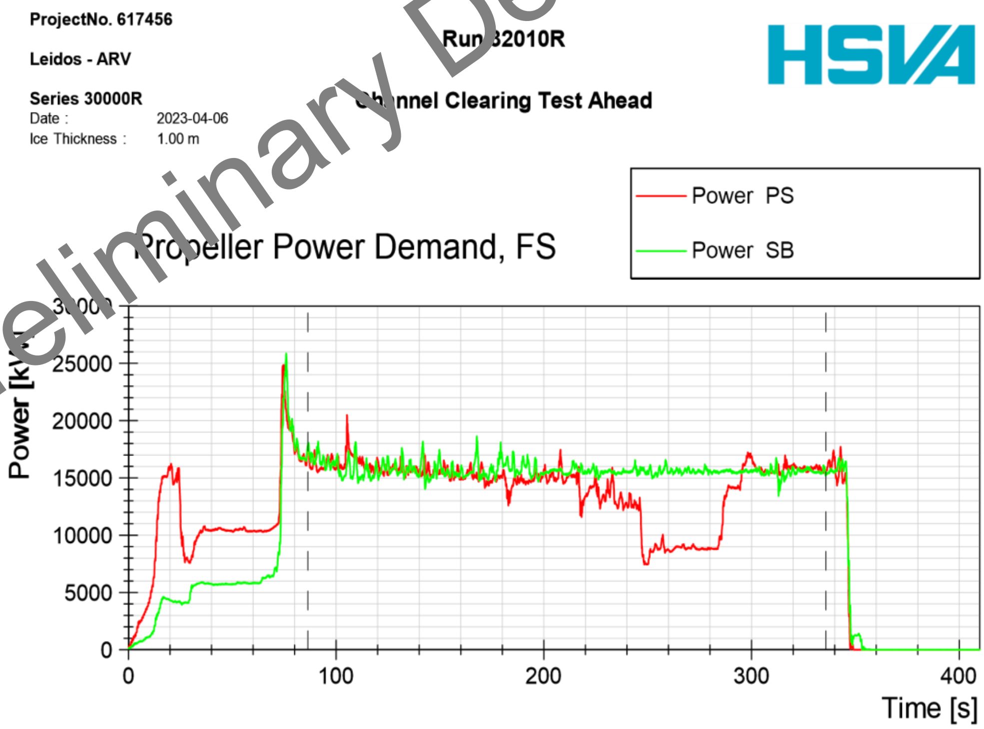

Figure 133 Test run no. 32010R, channel clearing test ahead, power

6.15 Test Run No. 33010R Channel Clearing Test Ahead in 1.00m Level Ice, 60 Degree Pod Angle Outward

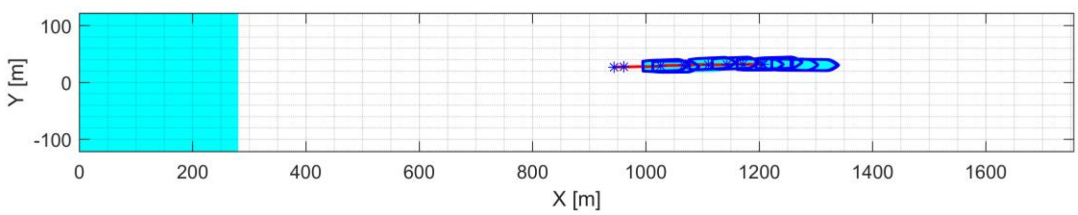

Figure 134 Test run no. 33010R track plot

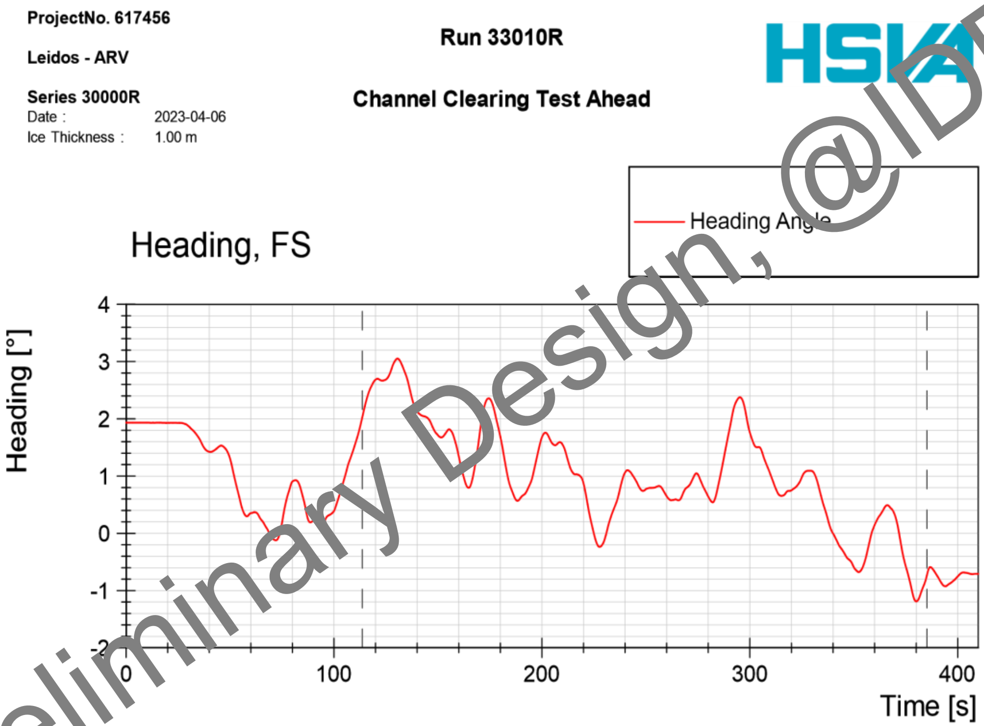

Figure 135 Test run no. 33010R, channel clearing test ahead, heading

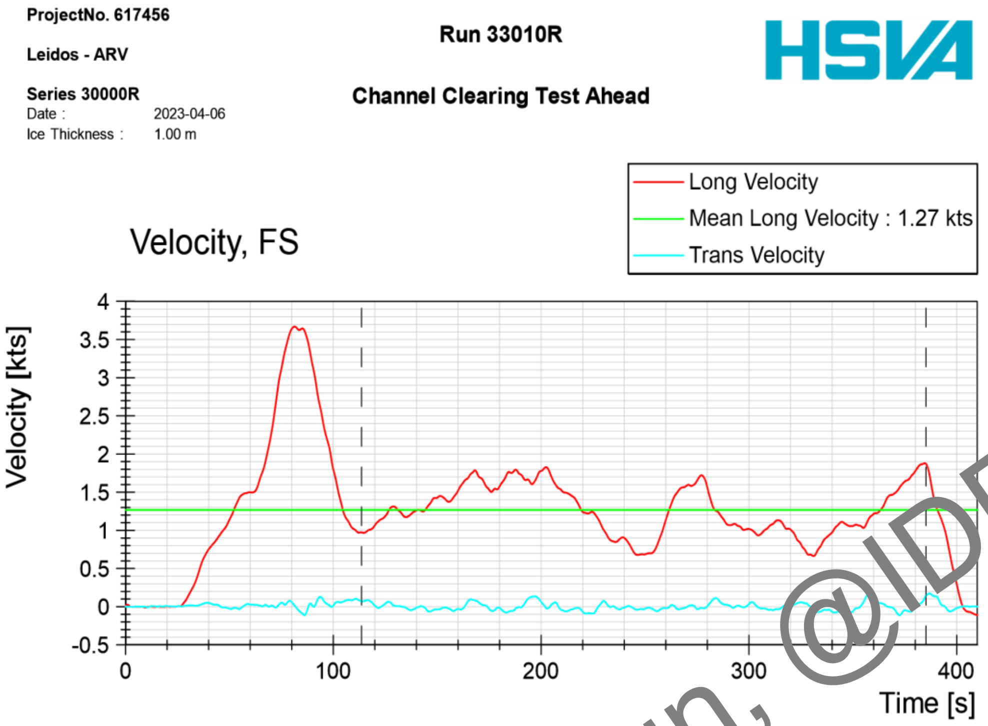

Figure 136 Test run no. 33010R, channel clearing test ahead, velocity

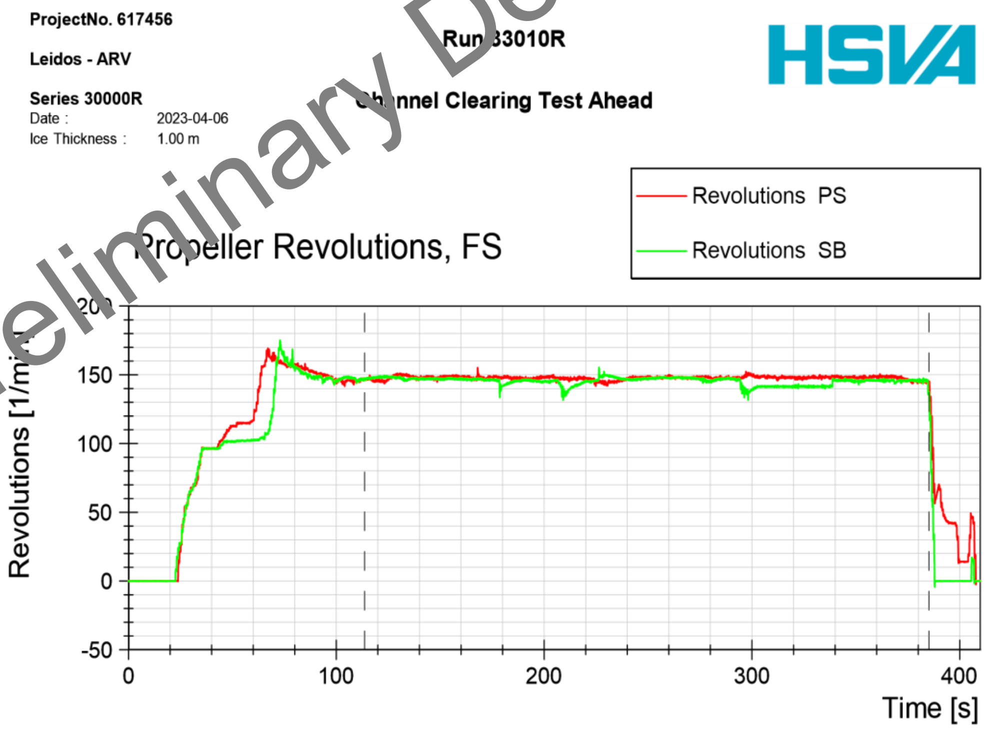

Figure 137 Test run no. 33010R, channel clearing test ahead, propeller revolution

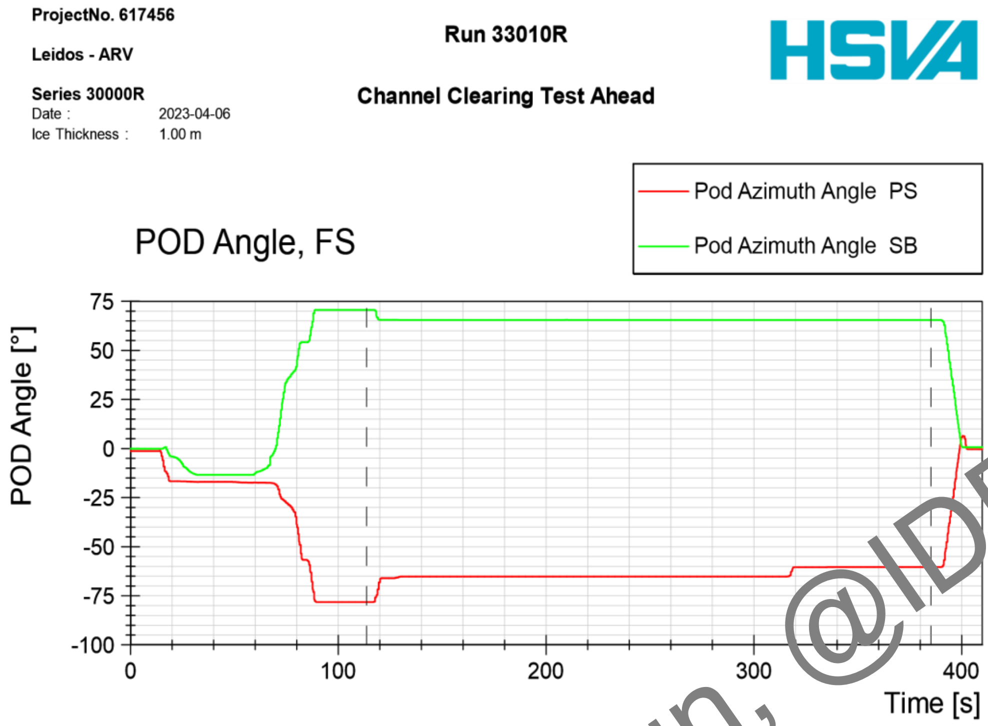

Figure 138 Test run no. 33010R, channel clearing test ahead, POD angle

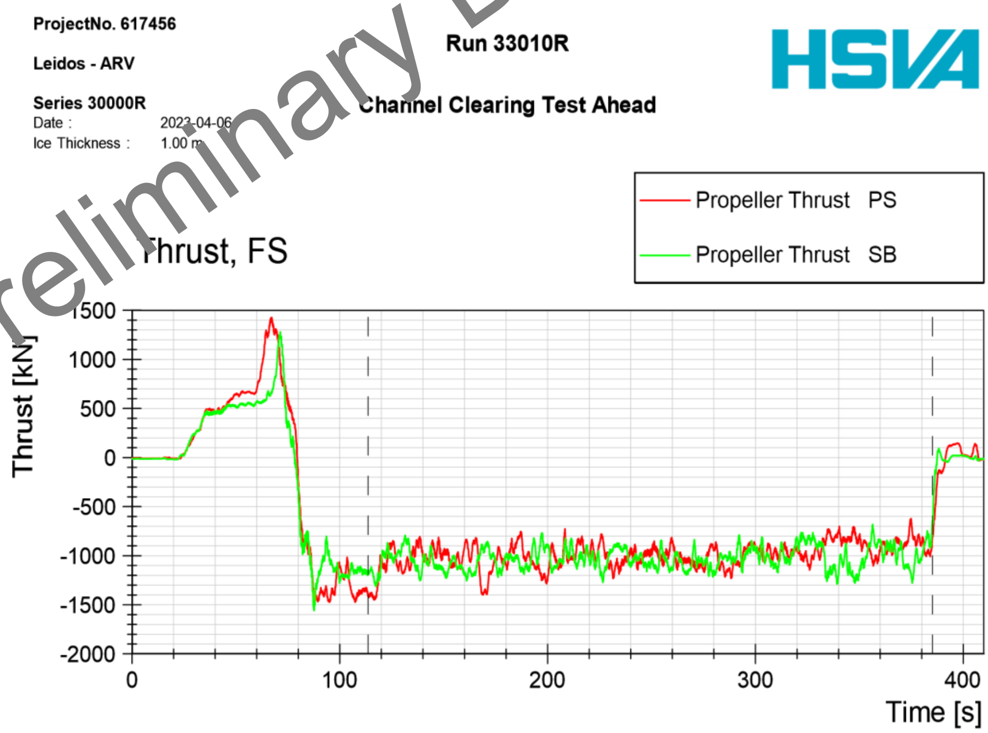

Figure 139 Test run no. 33010R, channel clearing test ahead, thrust

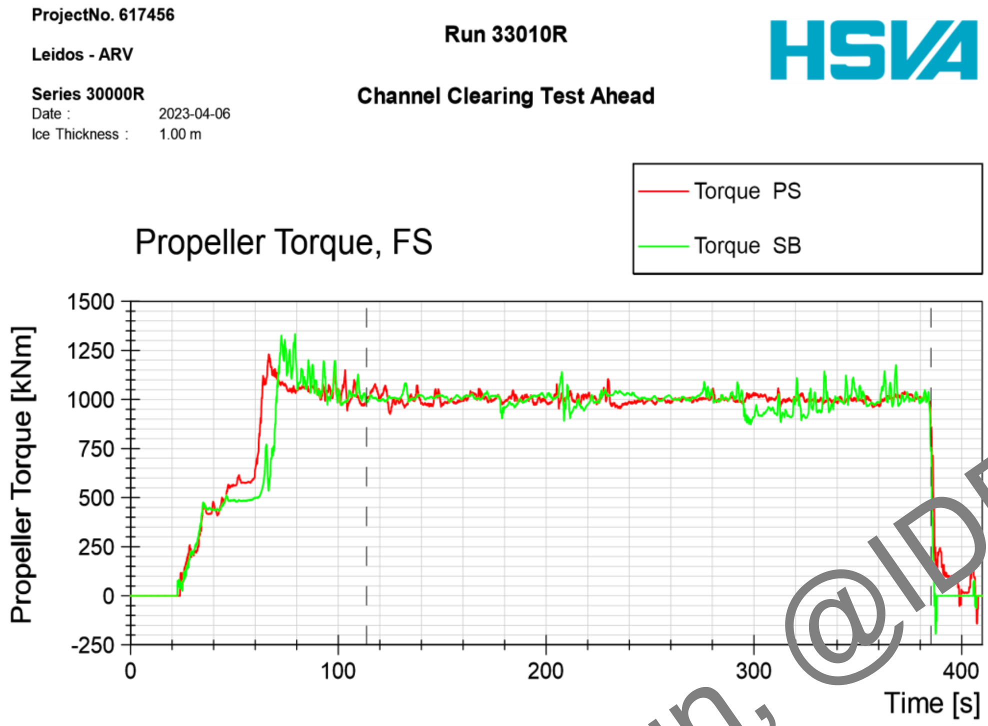

Figure 140 Test run no. 33010R, channel clearing test ahead, torque

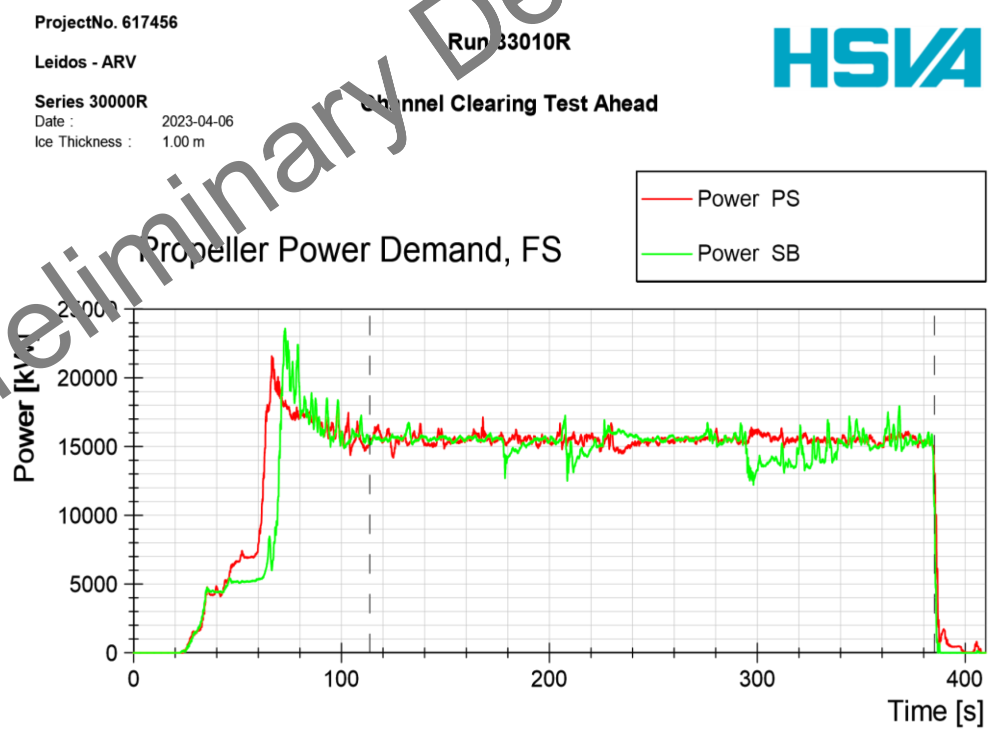

Figure 141 Test run no. 33010R, channel clearing test ahead, power

6.16 Test Run No. 34010R Channel Clearing Test Ahead in 1.00m Level Ice, Alternating Pod Angle

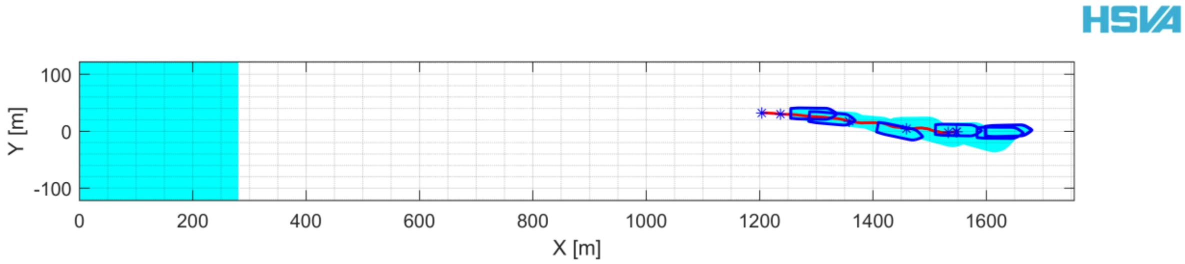

Figure 142 Test run no. 34010R track plot

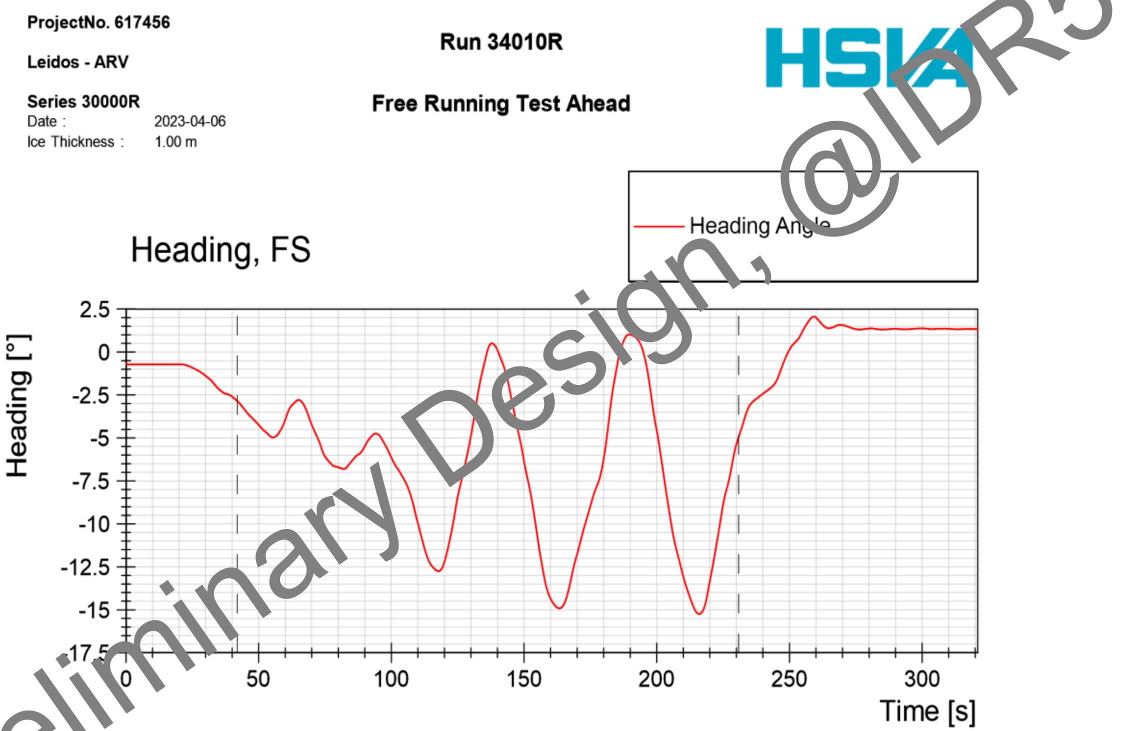

Figure 143 Test run no. 34010R, free running test ahead, heading

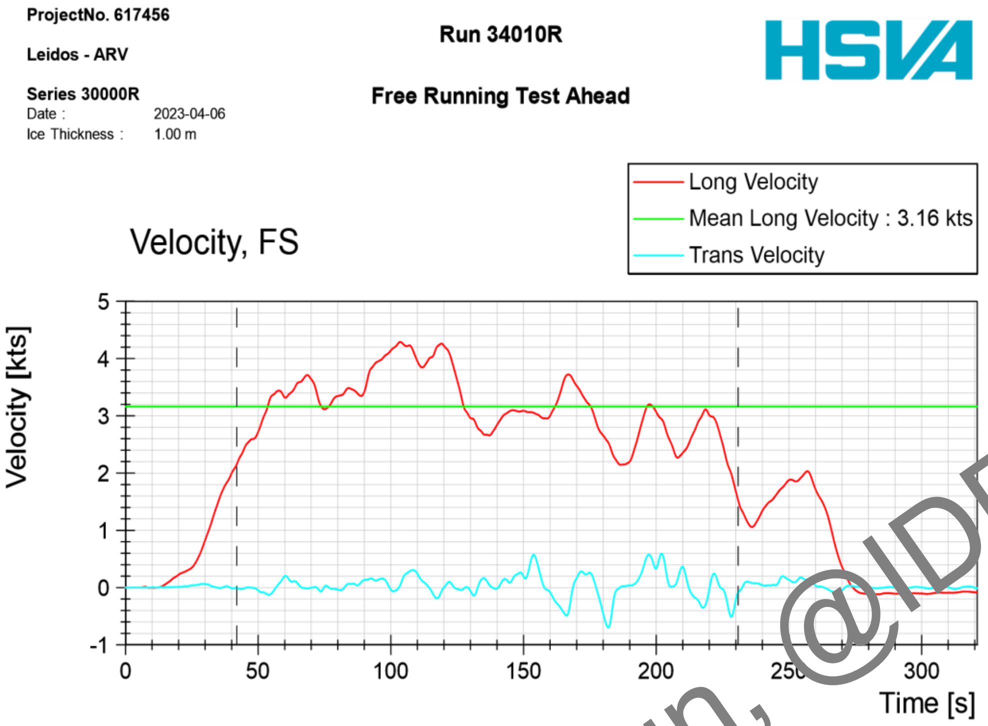

Figure 144 Test run no. 34010R, free running test ahead, velocity

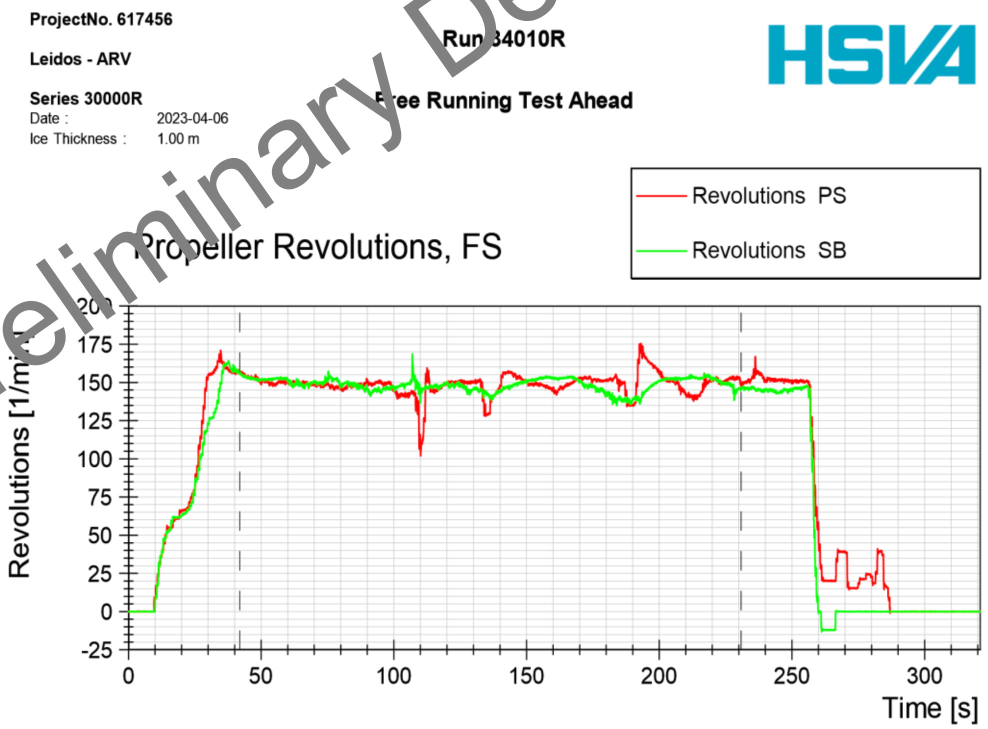

Figure 145 Test run no. 34010R, free running test ahead, propeller revolution

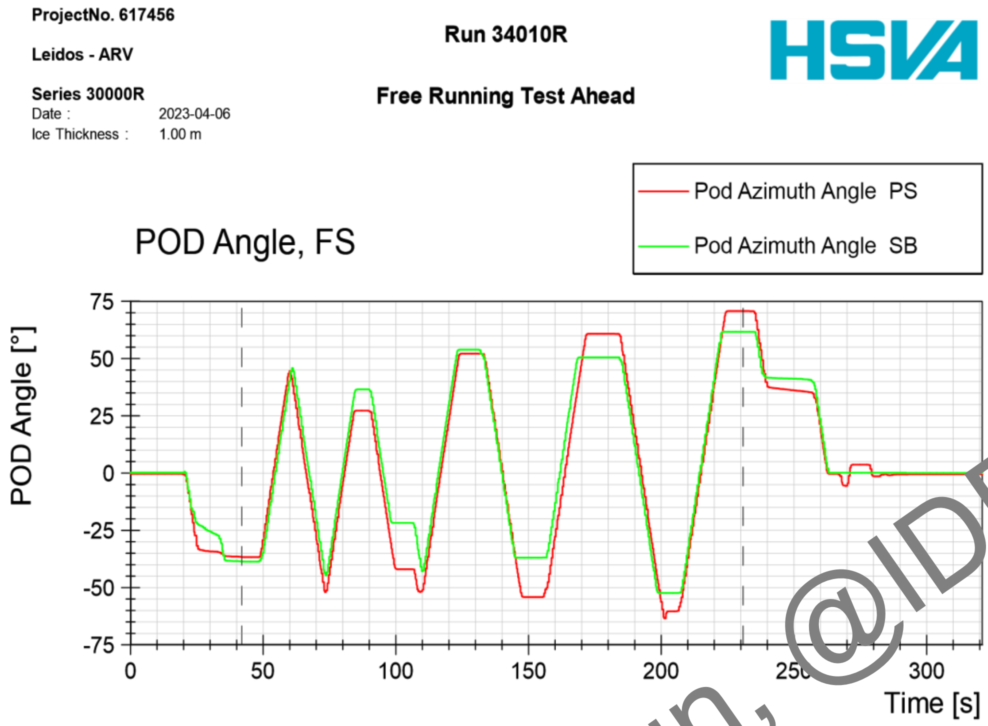

Figure 146 Test run no. 34010R, free running test ahead, POD angle

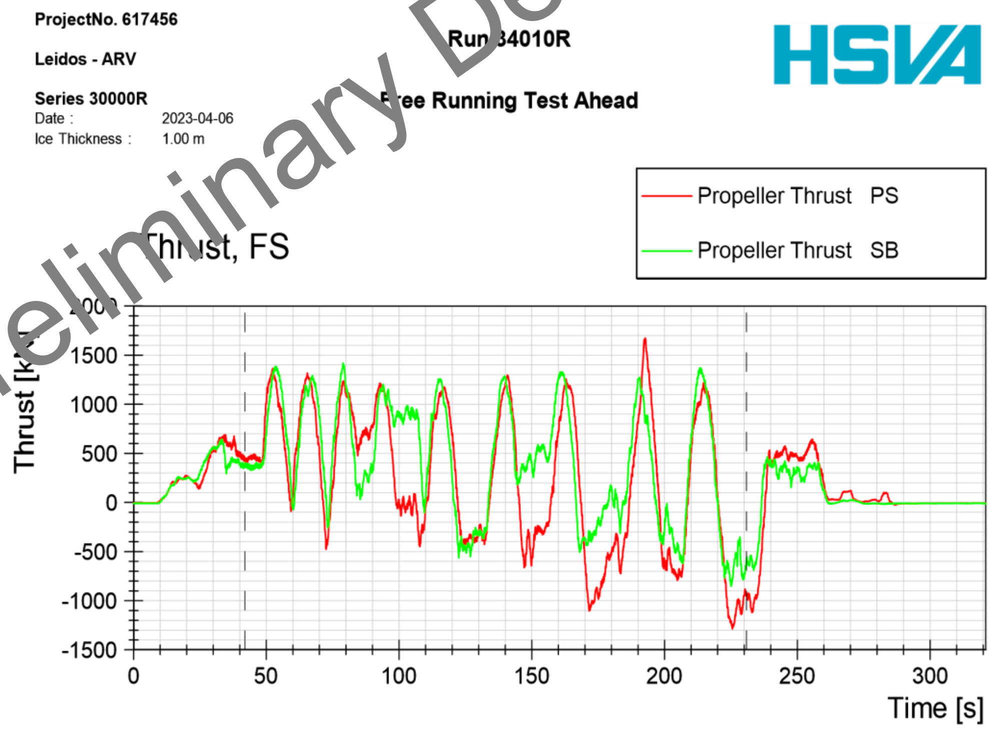

Figure 147 Test run no. 34010R, free running test ahead, thrust

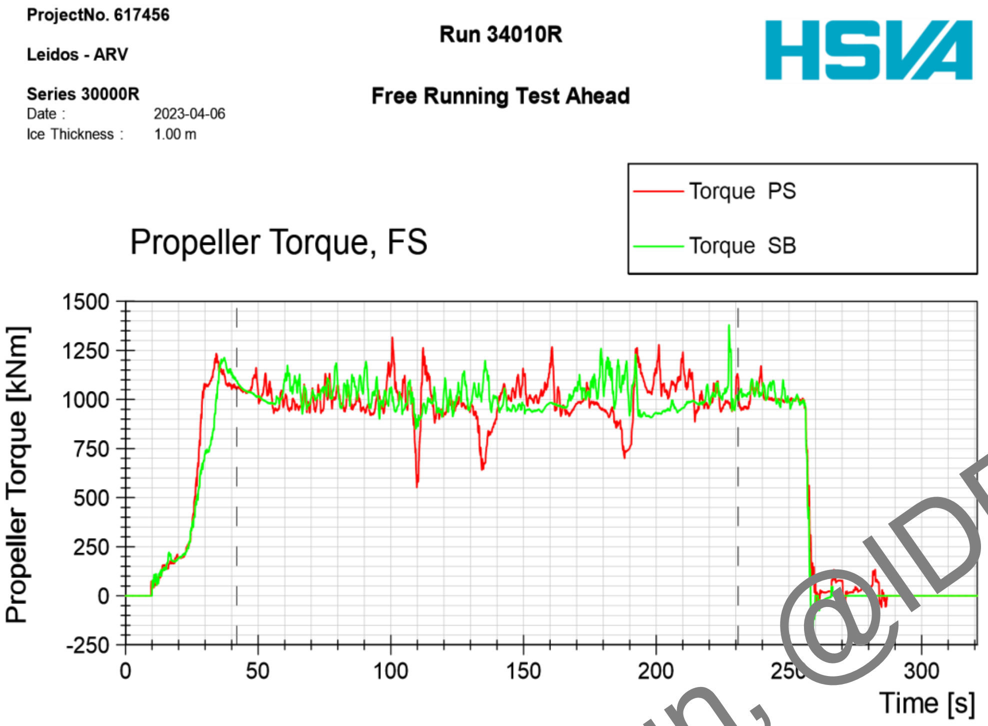

Figure 148 Test run no. 34010R, free running test ahead, torque

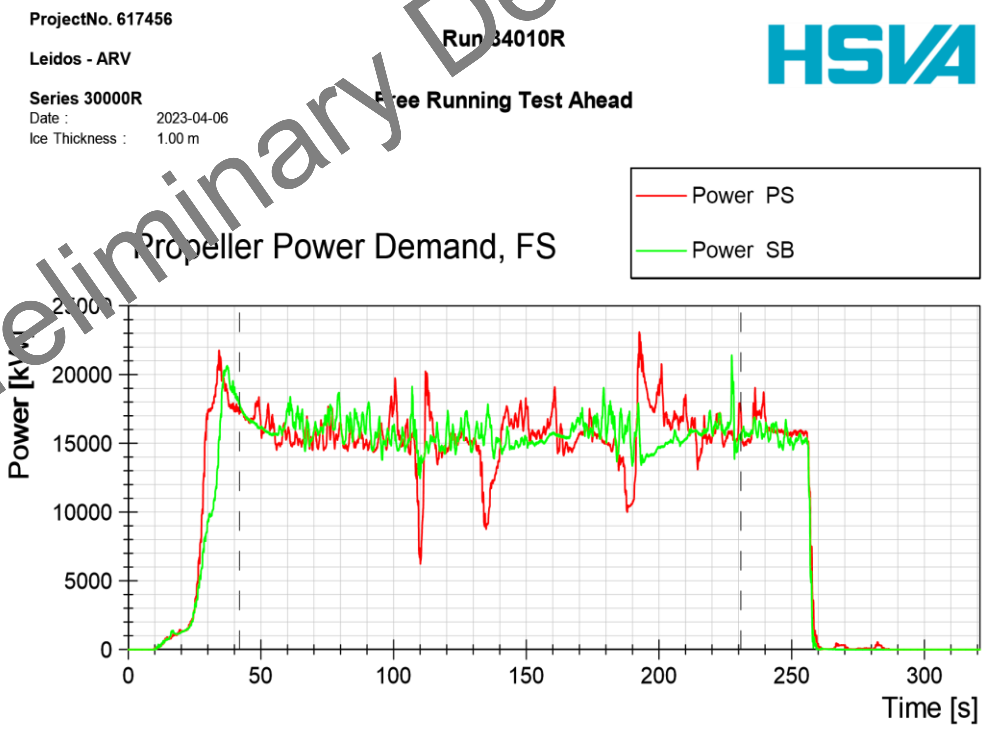

Figure 149 Test run no. 34010R, free running test ahead, power

6.17 Test Run No. 35010R Side Step Test in 1.0m Level Ice

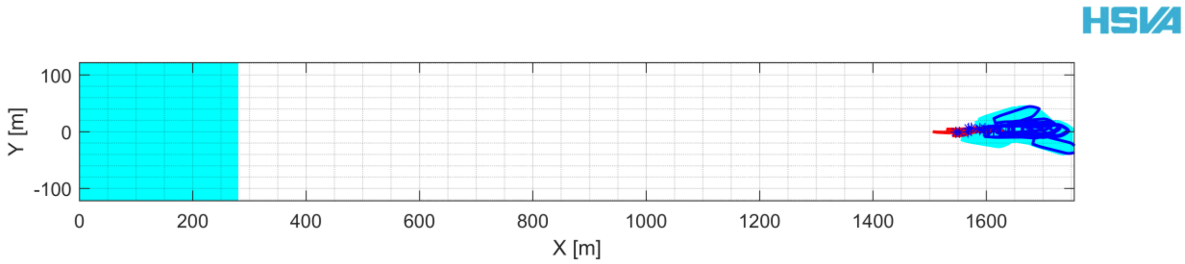

Figure 150 Test run no. 35010R track plot

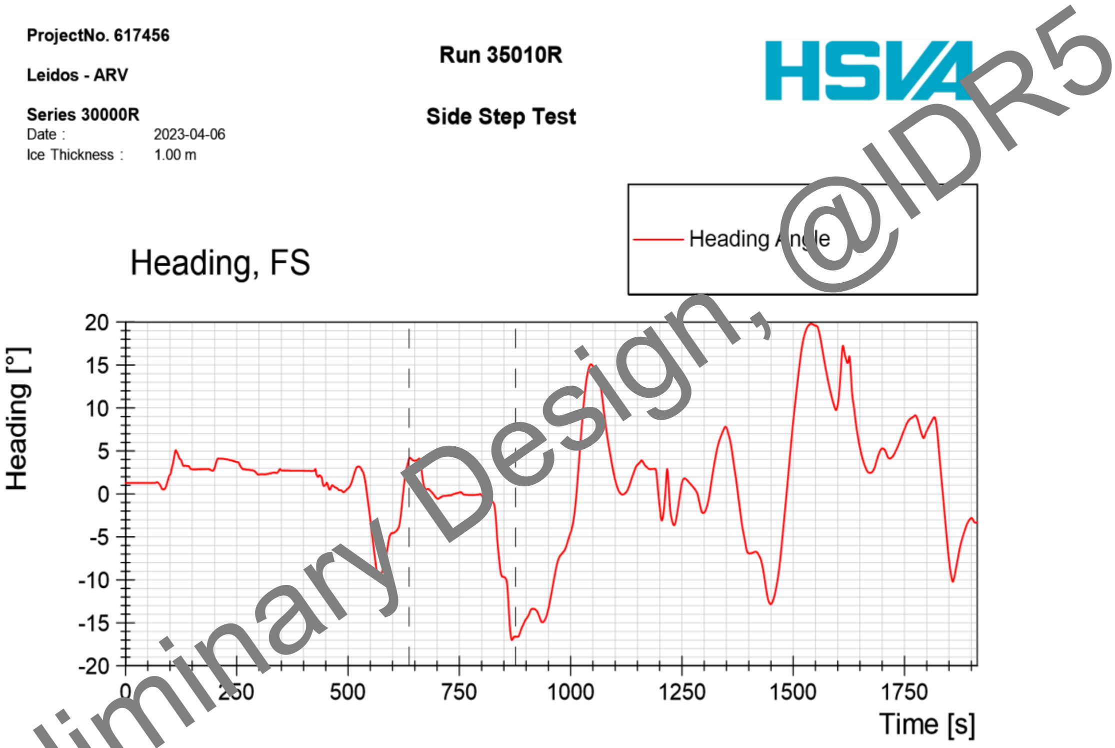

Figure 151 Test run no. 35010R, free running test ahead, heading

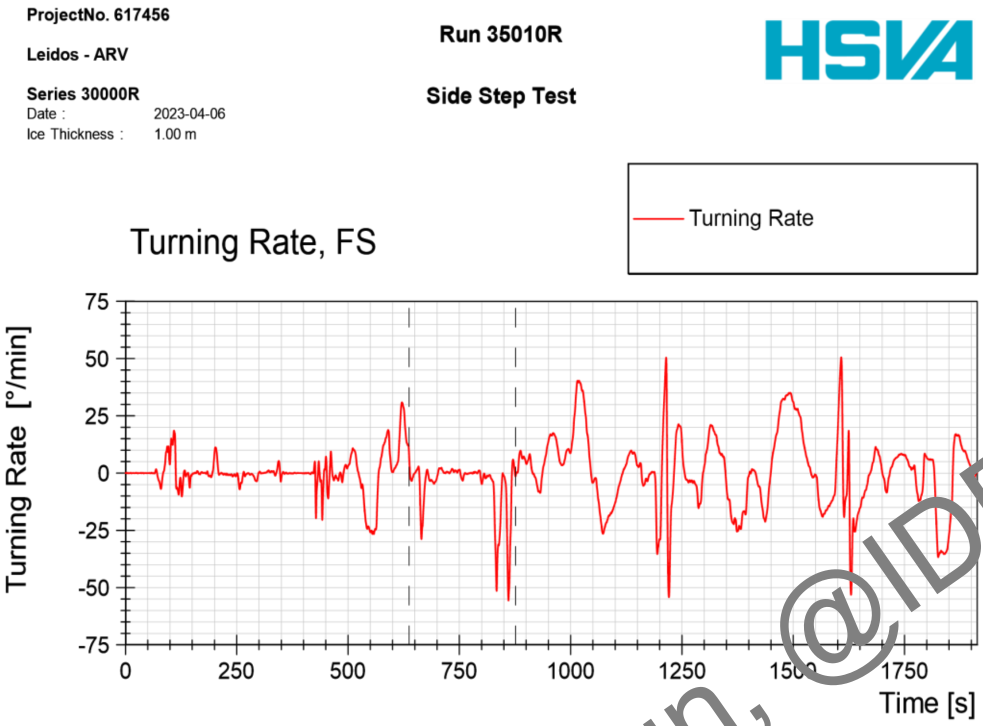

Figure 152 Test run no. 35010R, free running test ahead, turning rate

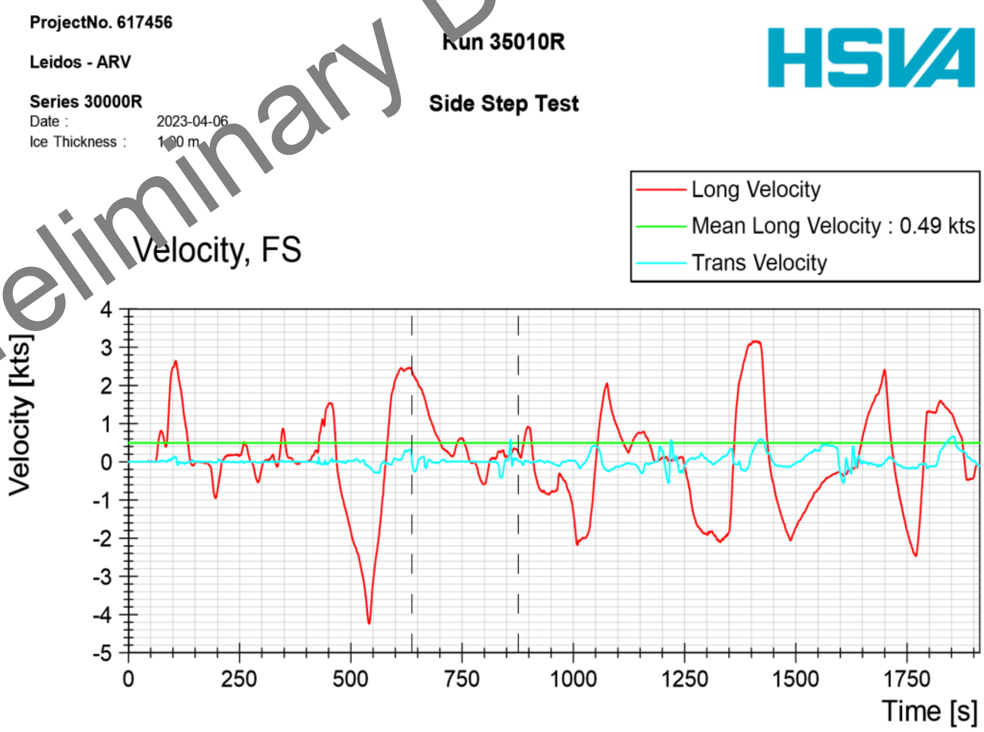

Figure 153 Test run no. 35010R, free running test ahead, velocity

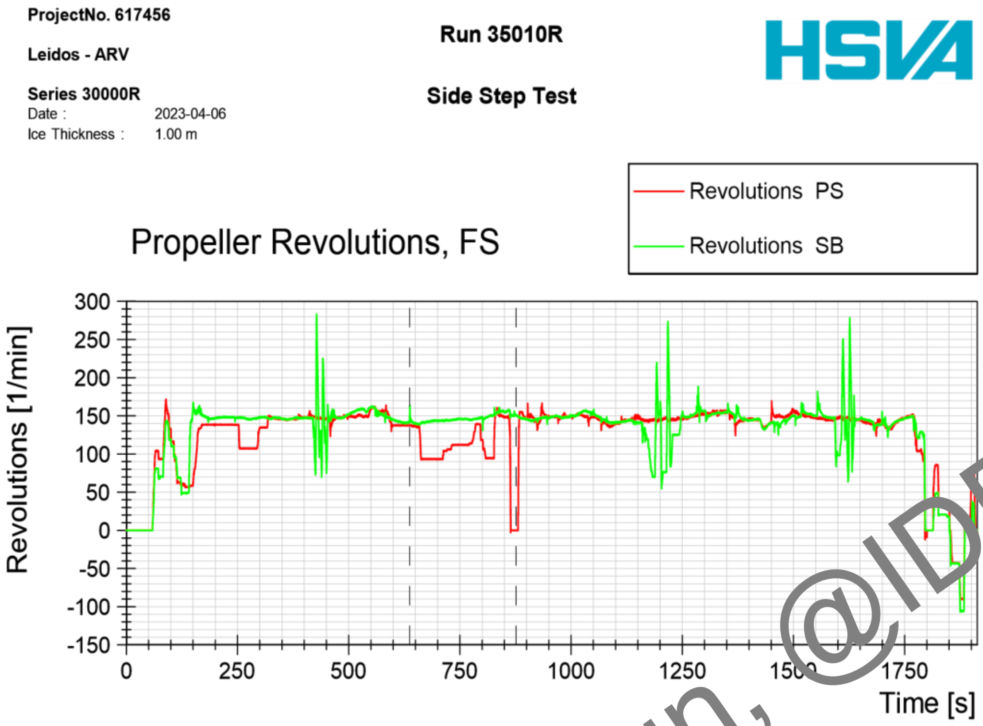

Figure 154 Test run no. 35010R, free running test ahead, propeller revolution

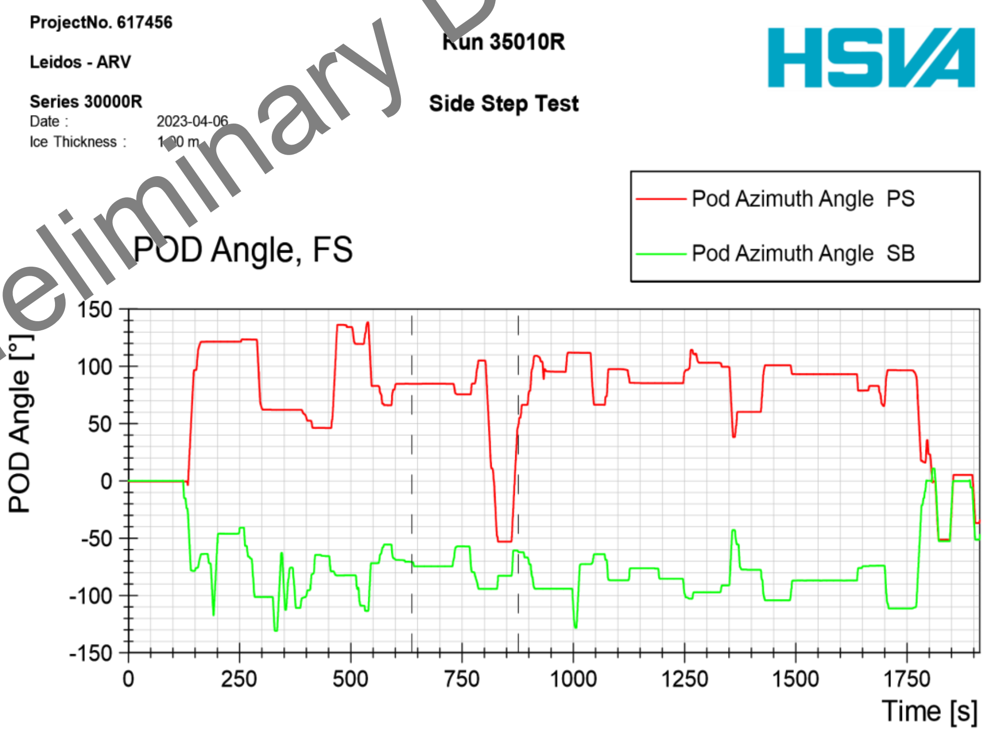

Figure 155 Test run no. 35010R, free running test ahead, POD angle

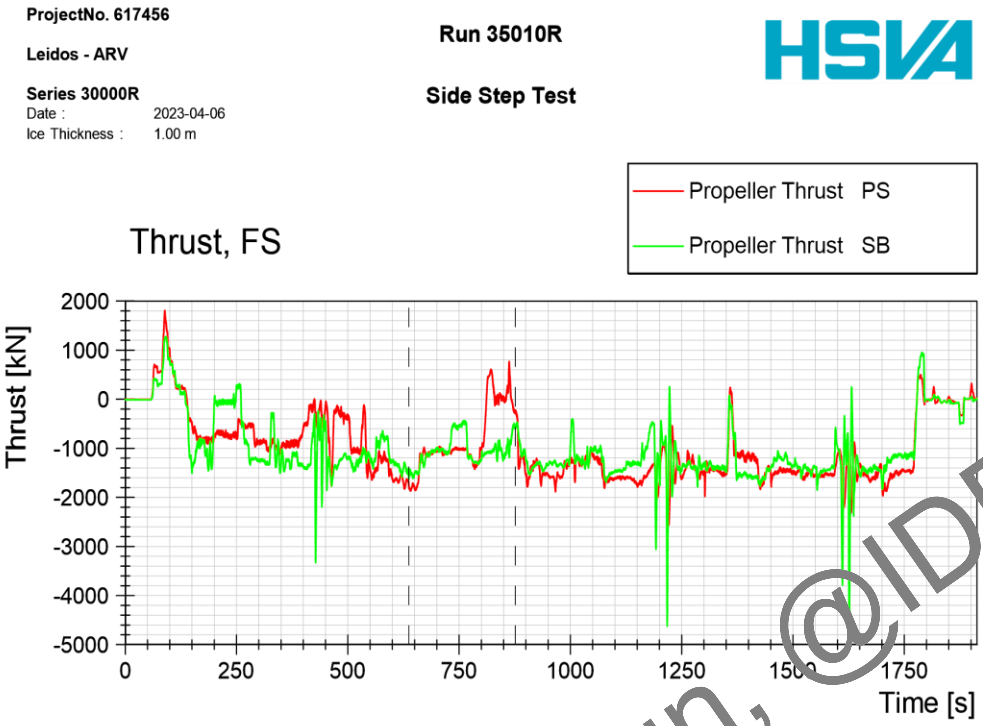

Figure 156 Test run no. 35010R, free running test ahead, thrust

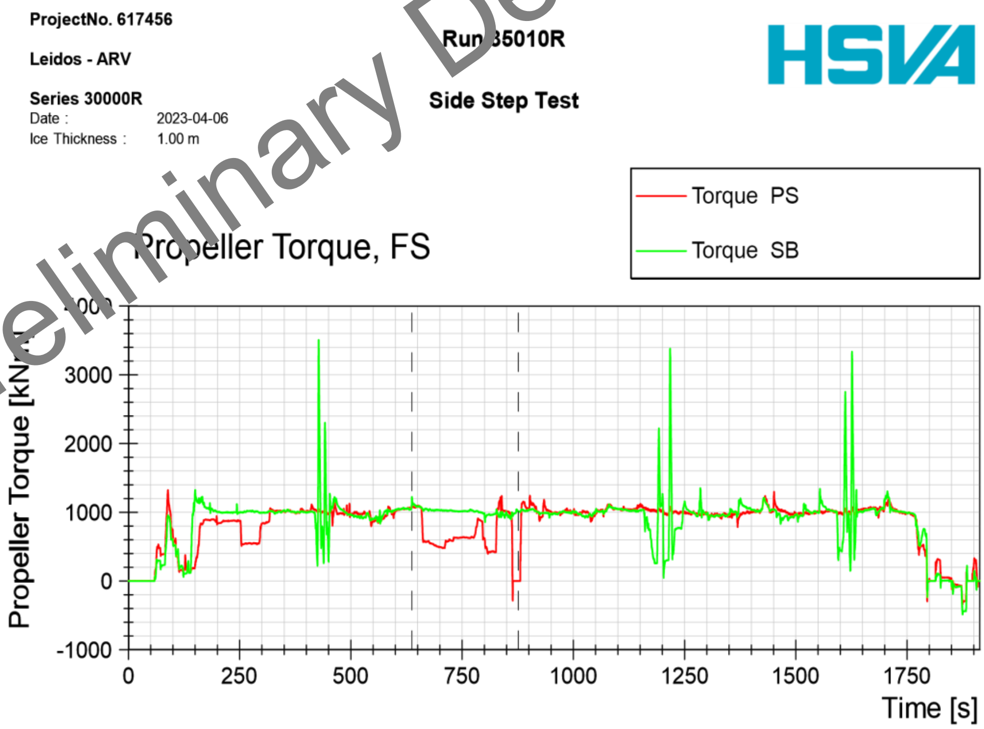

Figure 157 Test run no. 35010R, free running test ahead, torque

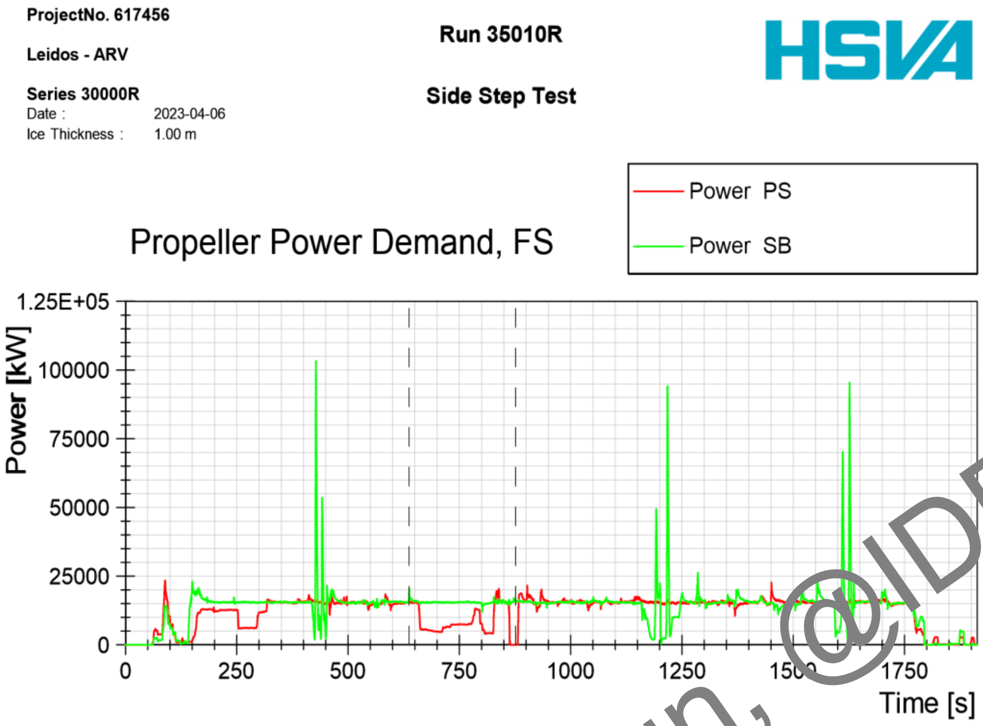

Figure 158 Test run no. 35010R, free running test ahead, power

6.18 Test Run No. 36010R Channel Clearing Test Ahead in 1.0m Level Ice, 80 Degree Pod Angle Inward

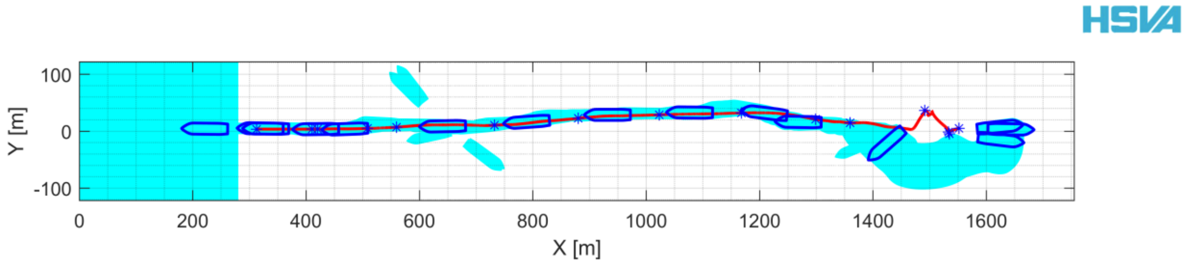

Figure 159 Test run no. 36010R track plot

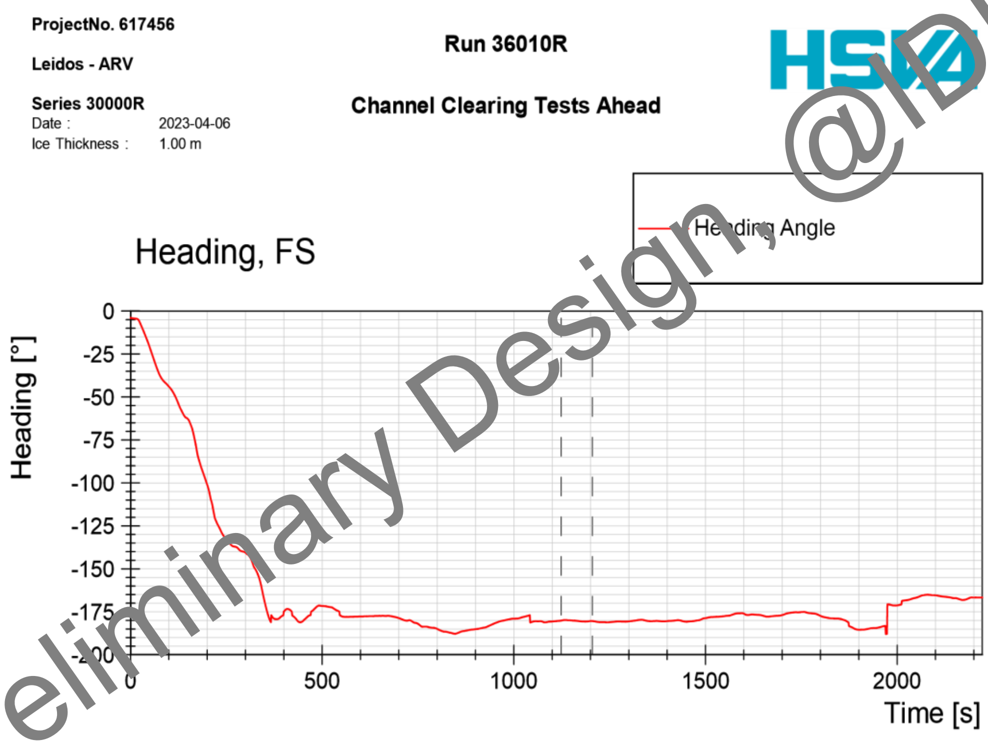

Figure 160 Test run no. 36010R, free running test ahead, heading

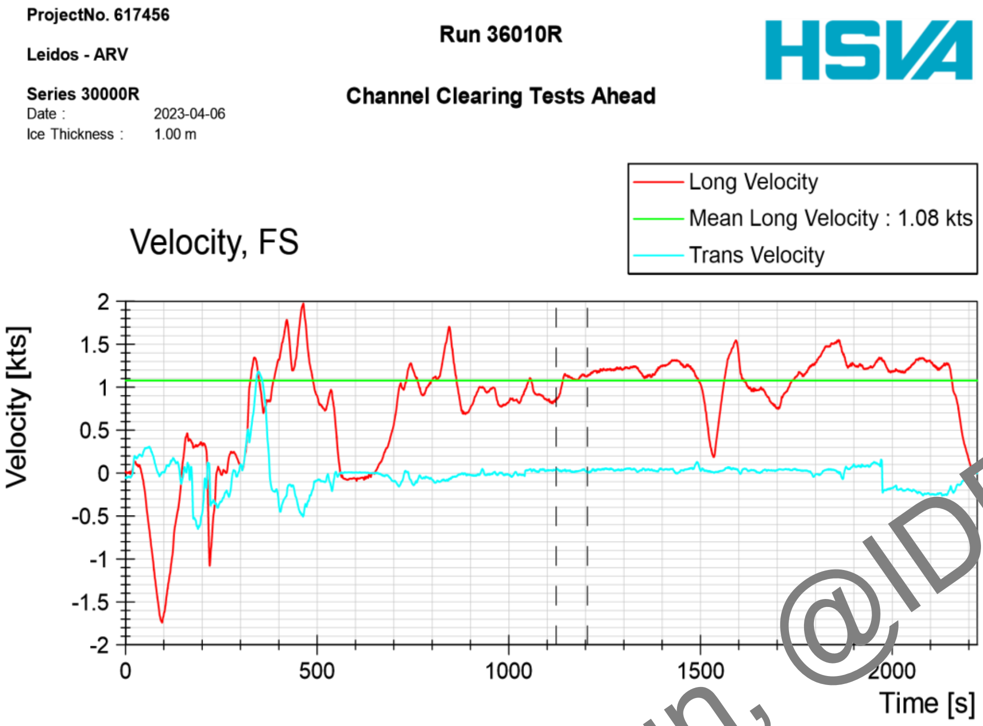

Figure 161 Test run no. 36010R, free running test ahead, velocity

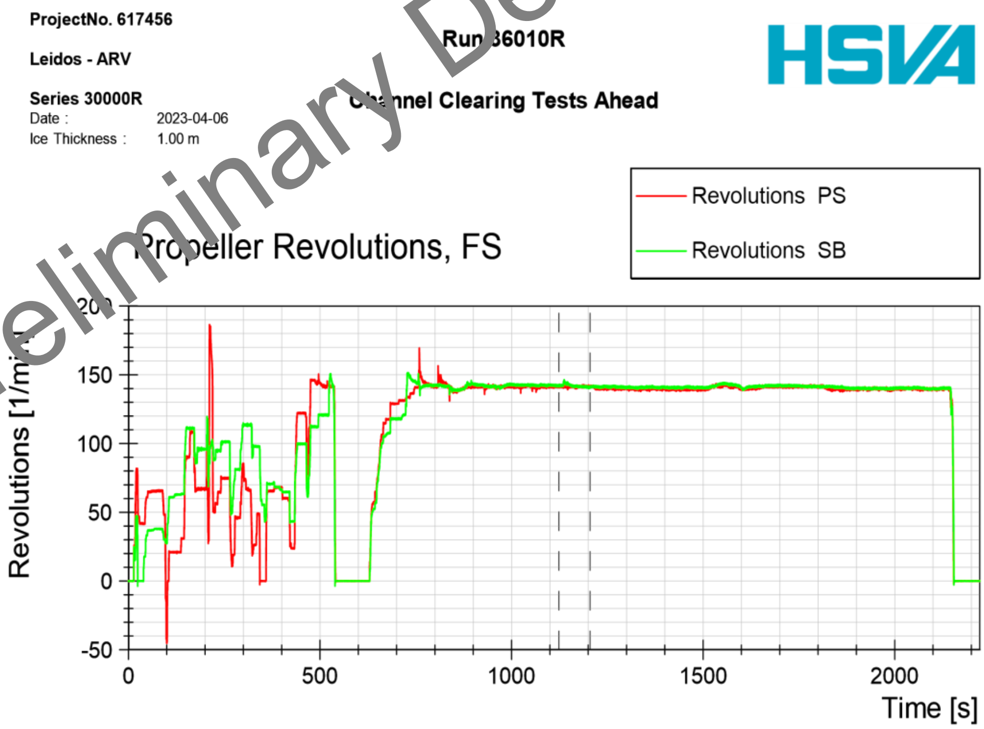

Figure 162 Test run no. 36010R, free running test ahead, propeller revolution

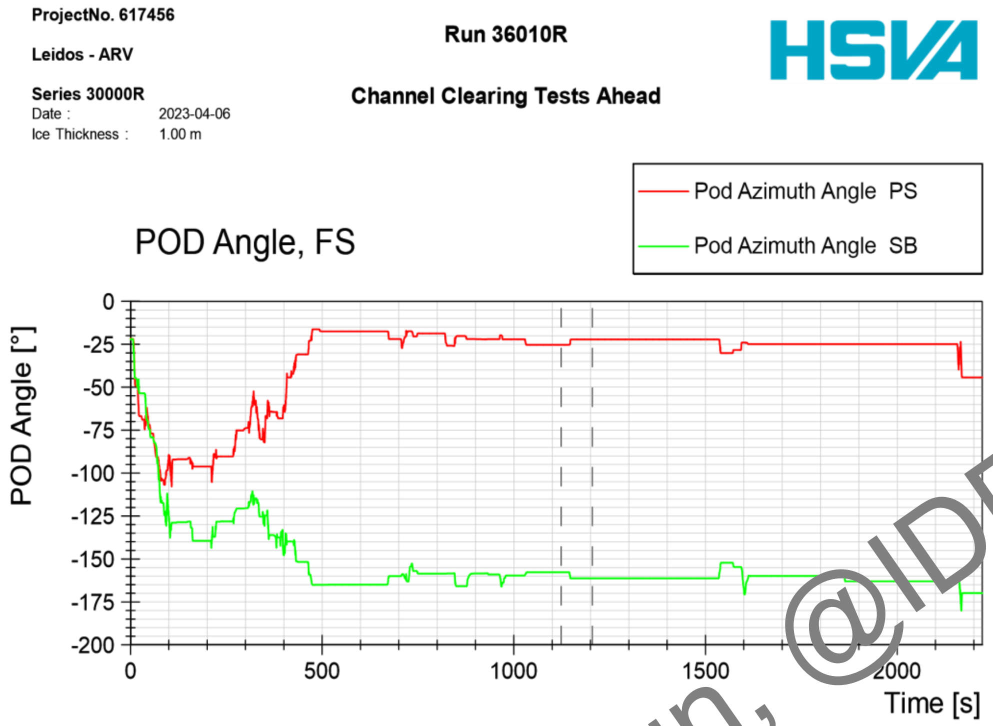

Figure 163 Test run no. 36010R, free running test ahead, POD angle

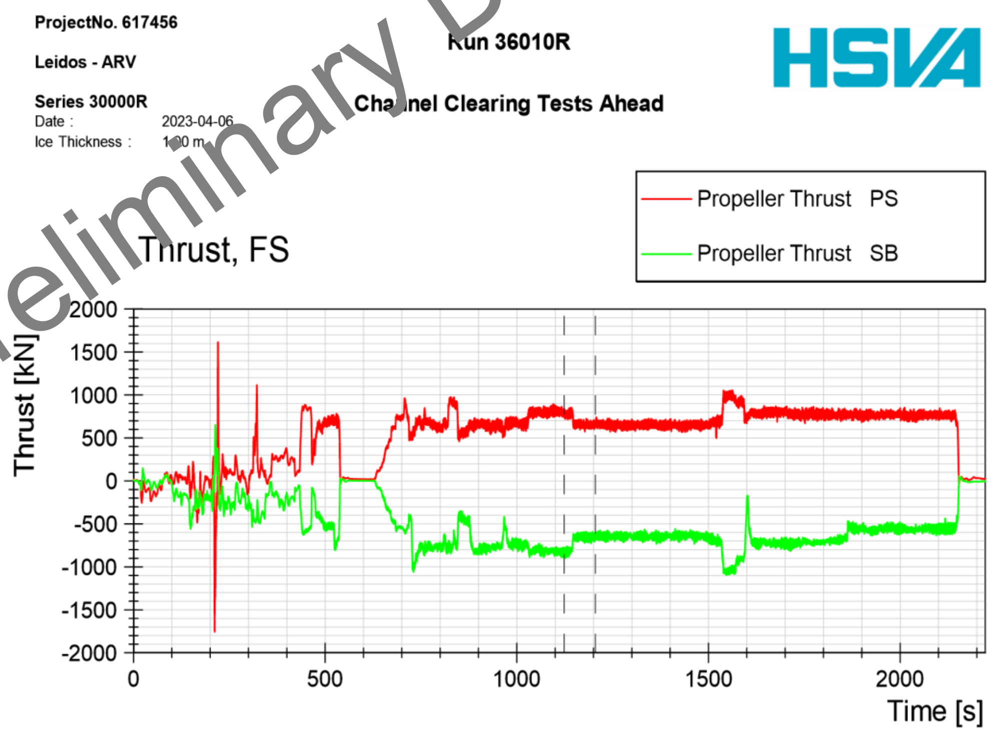

Figure 164 Test run no. 36010R, free running test ahead, thrust

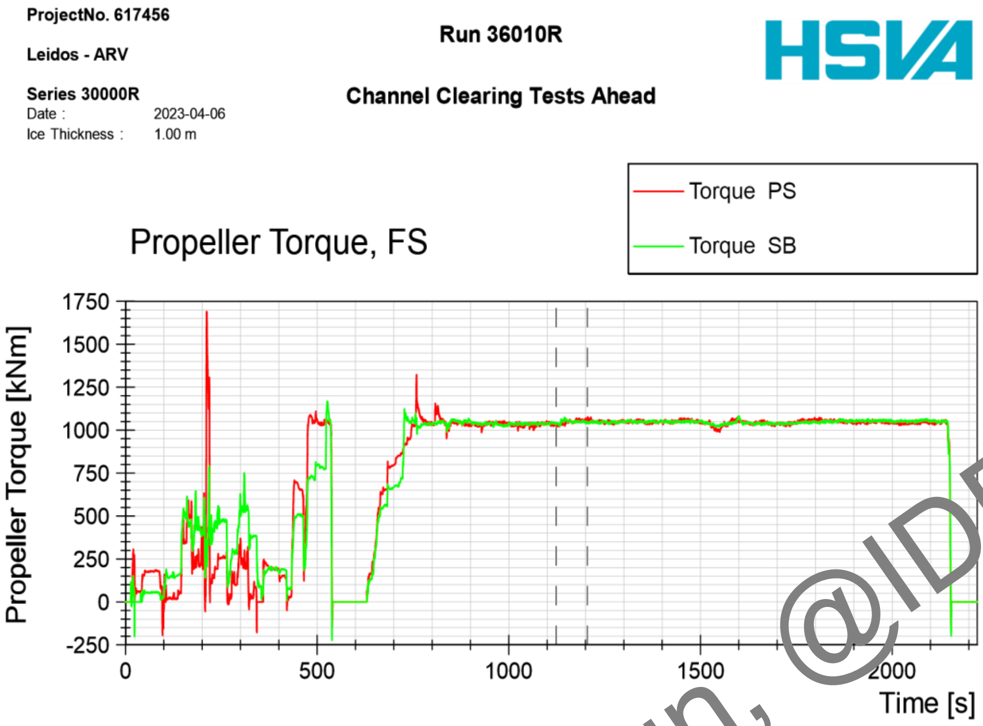

Figure 165 Test run no. 36010R, free running test ahead, torque

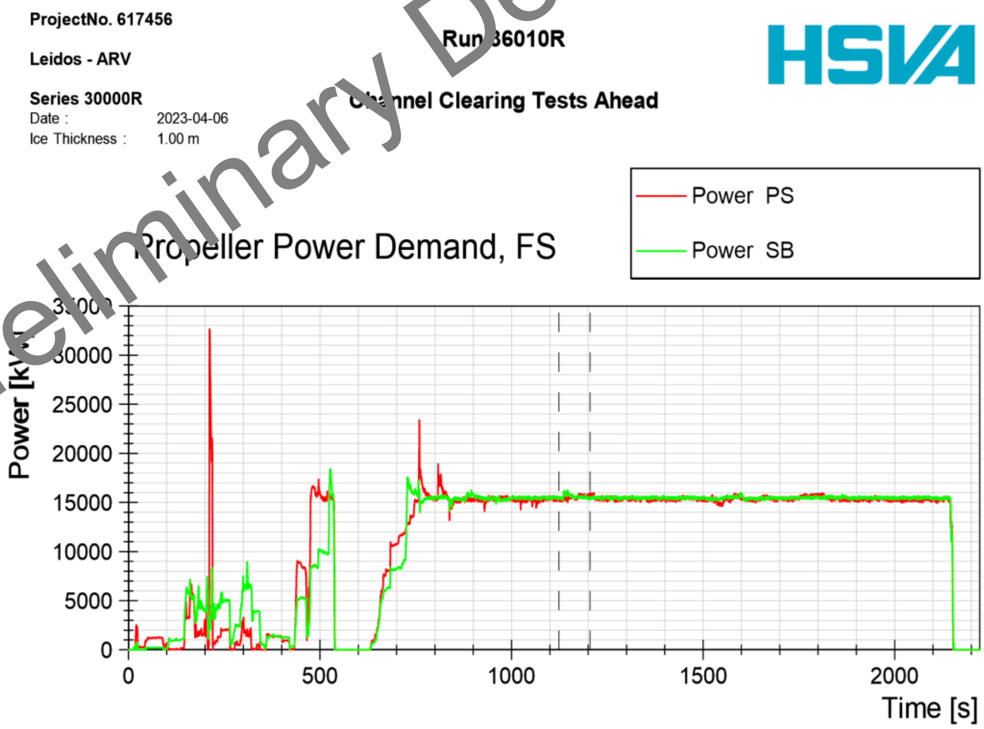

Figure 166 Test run no. 36010R, free running test ahead, power

6.19 Test Run No. 37011R Creation of Brash Ice Field

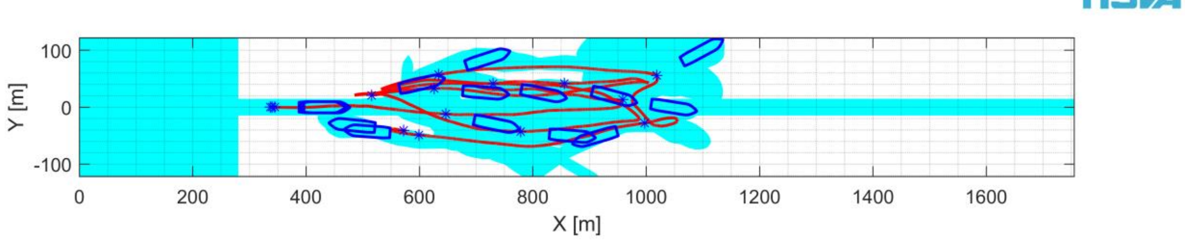

Figure 167 Test run no. 37011R

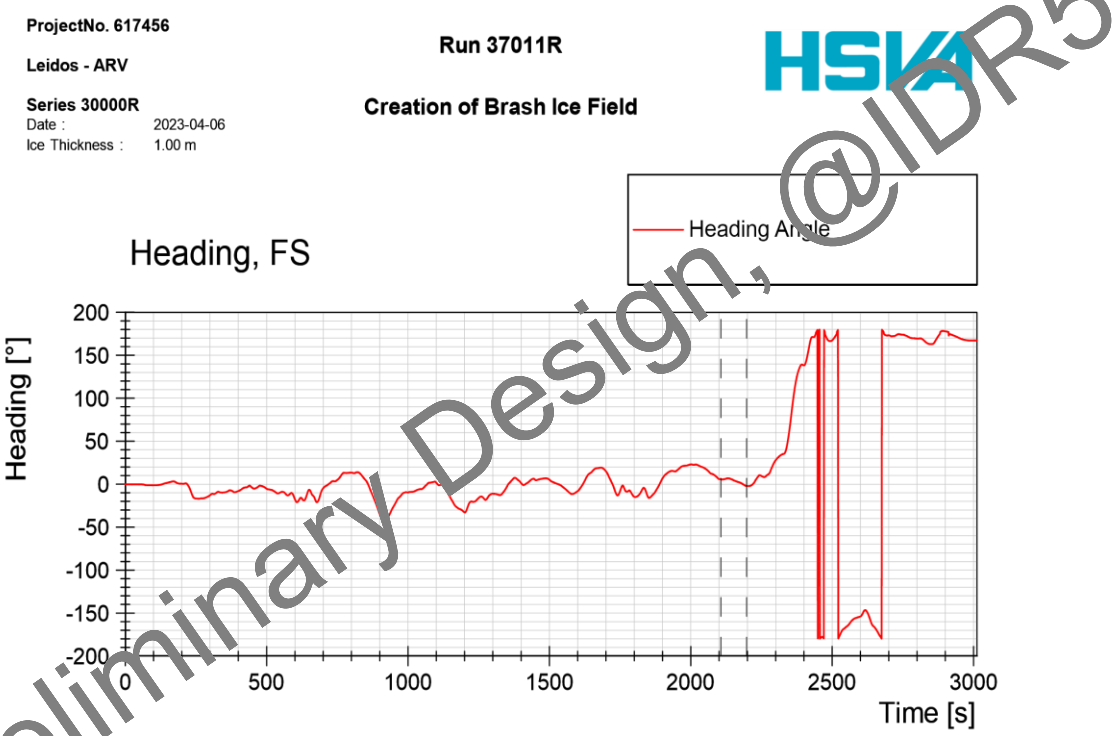

Figure 168 Test run no. 36010R, free running test ahead, heading

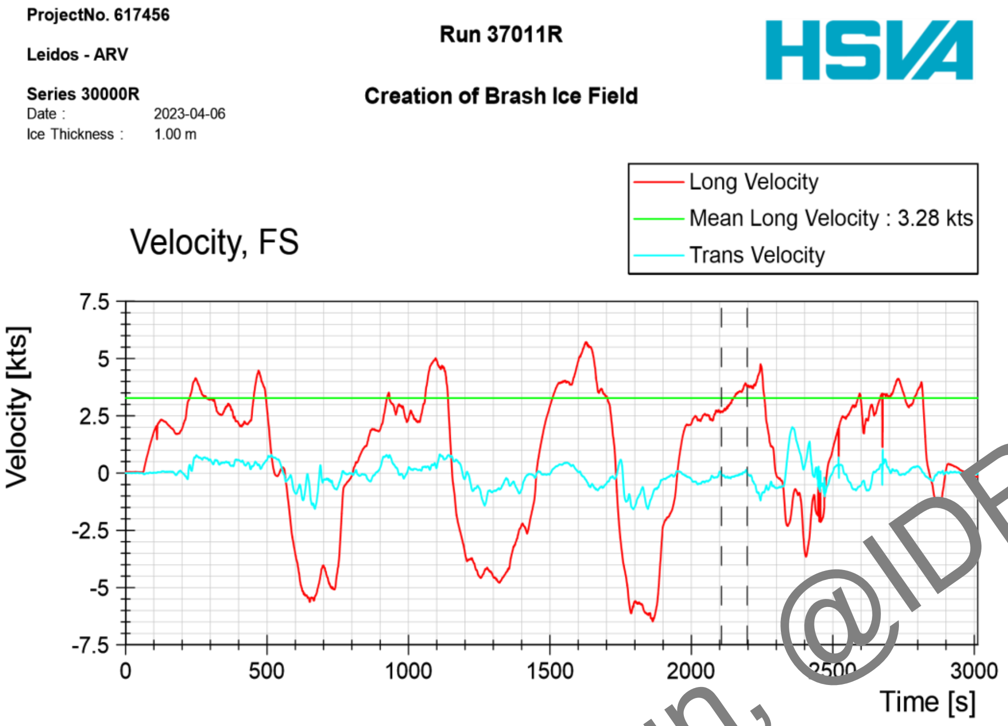

Figure 169 Test run no. 36010R, free running test ahead, velocity

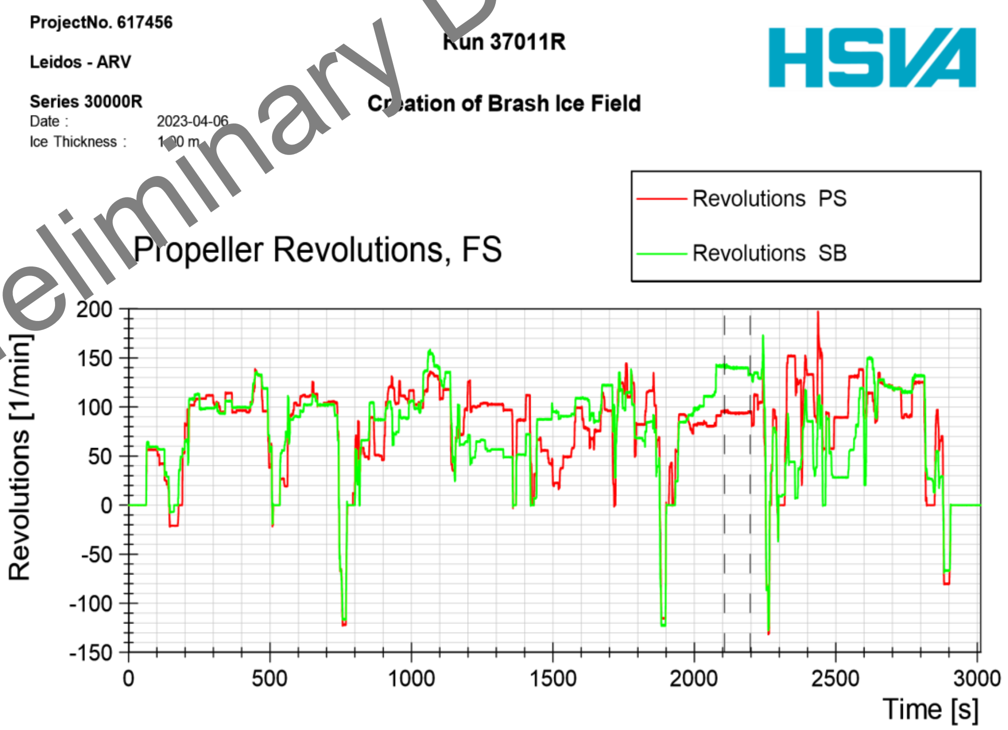

Figure 170 Test run no. 36010R, free running test ahead, propeller revolution

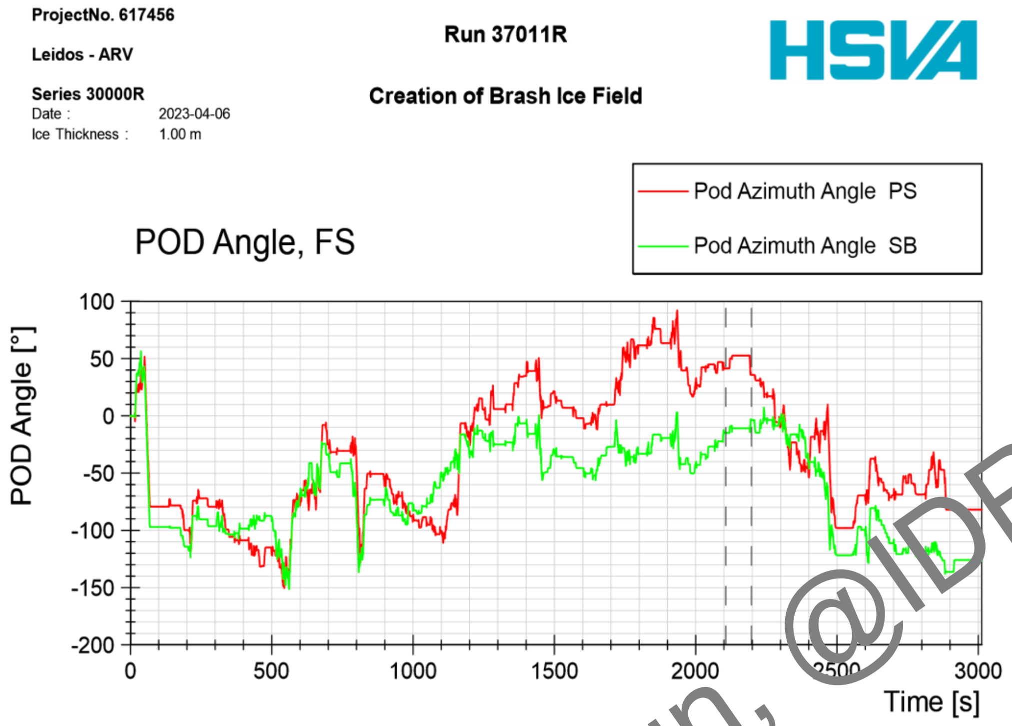

Figure 171 Test run no. 36010R, free running test ahead, POD angle

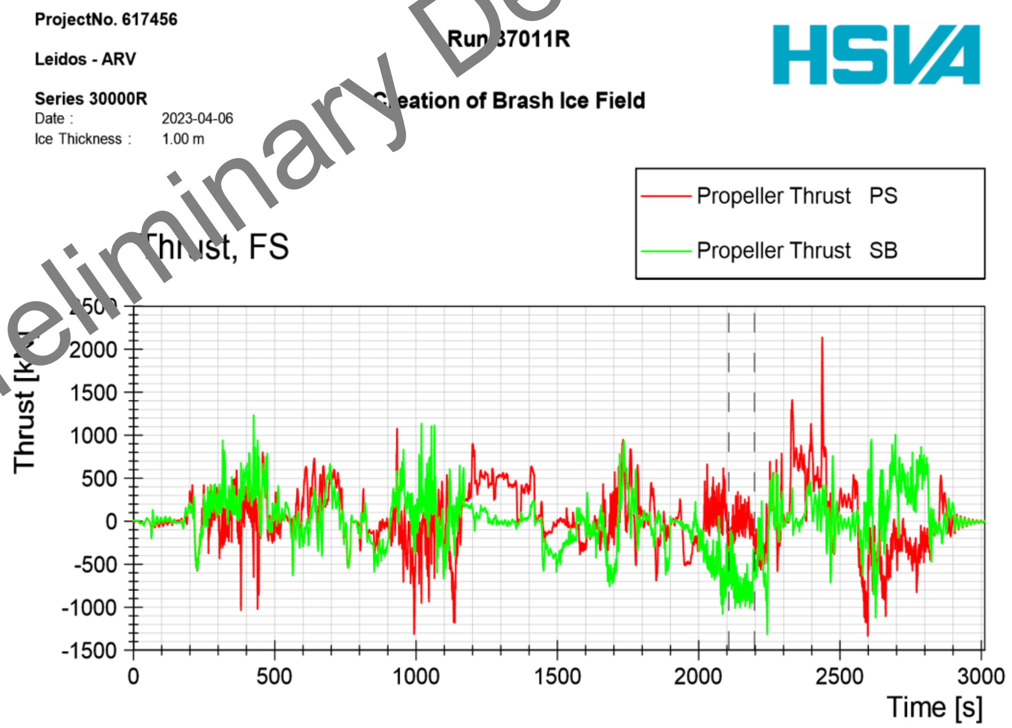

Figure 172 Test run no. 36010R, free running test ahead, thrust

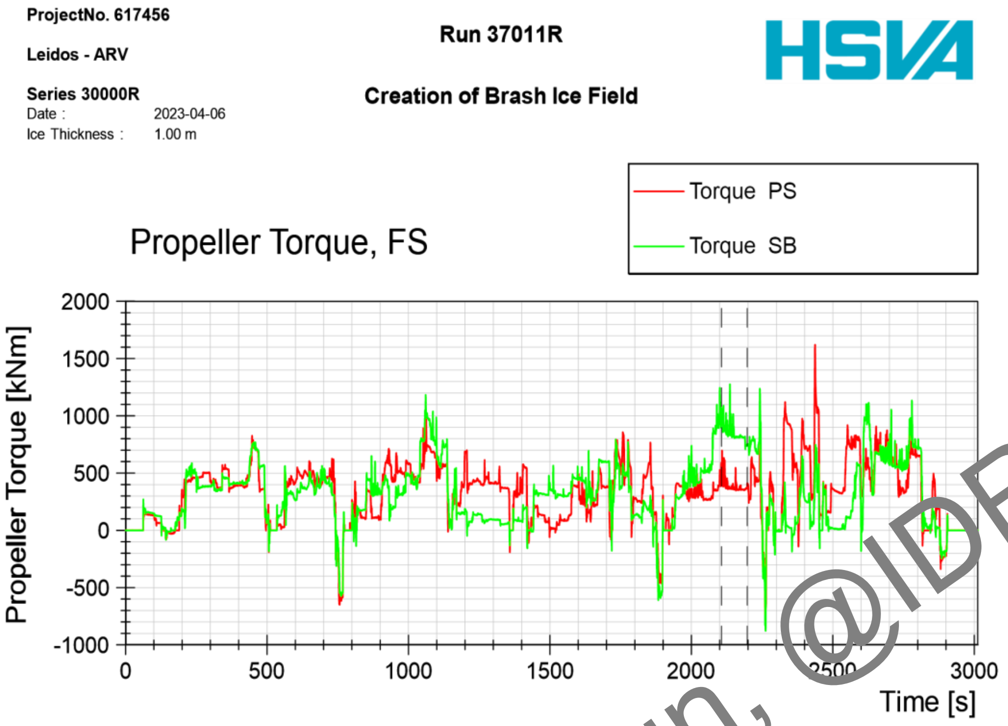

Figure 173 Test run no. 36010R, free running test ahead, torque

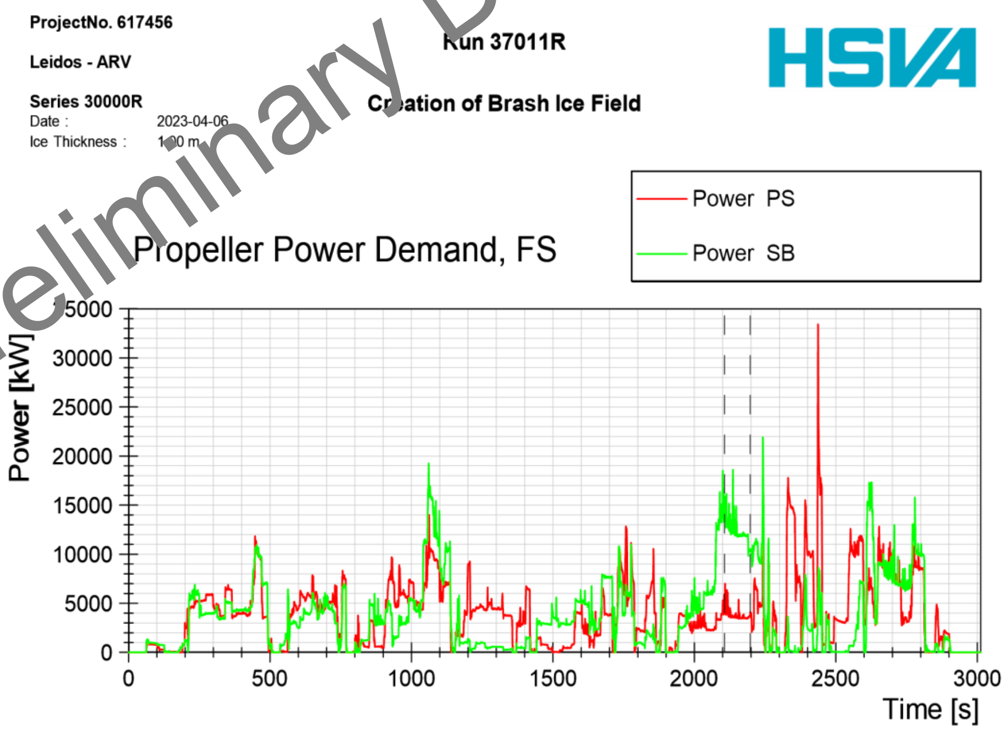

Figure 174 Test run no. 36010R, free running test ahead, power

6.20 Test Run No. 38010R Brash Ice Clearing Test, 85, 60, 30 Degree POD Angle

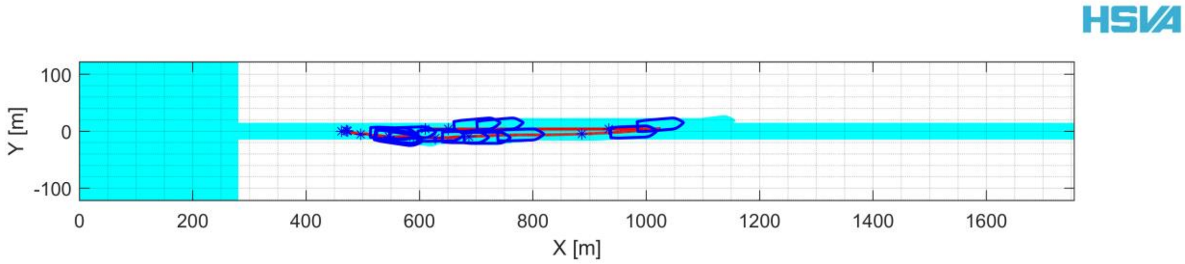

Figure 175 Test run no. 38010R track plot

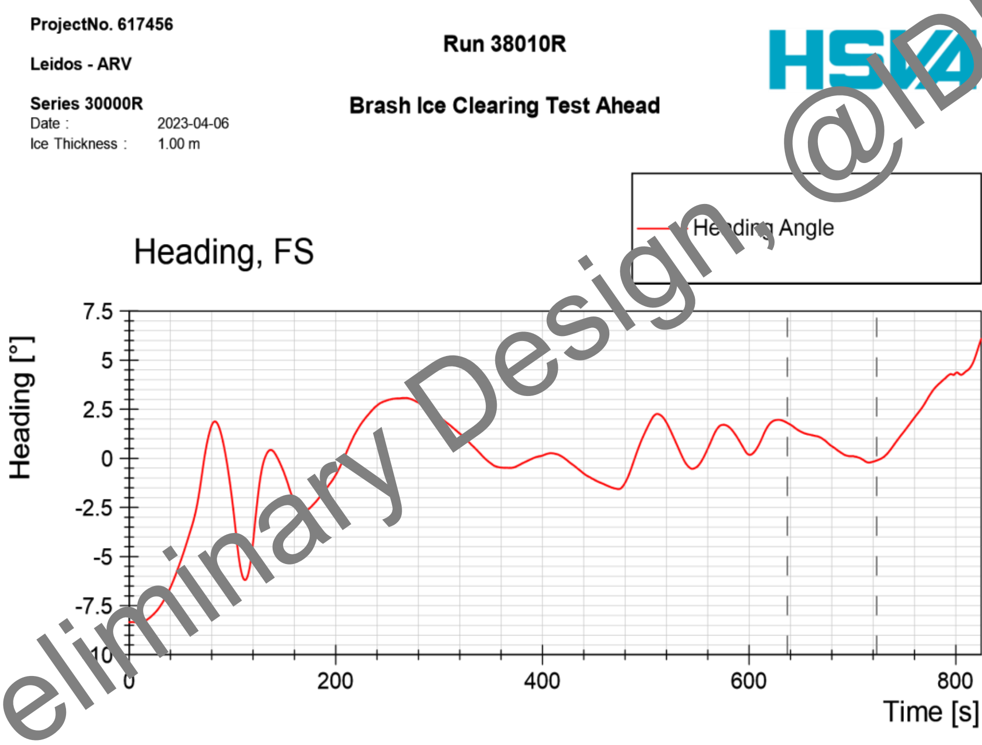

Figure 176 Test run no. 38010R, free running test ahead, heading

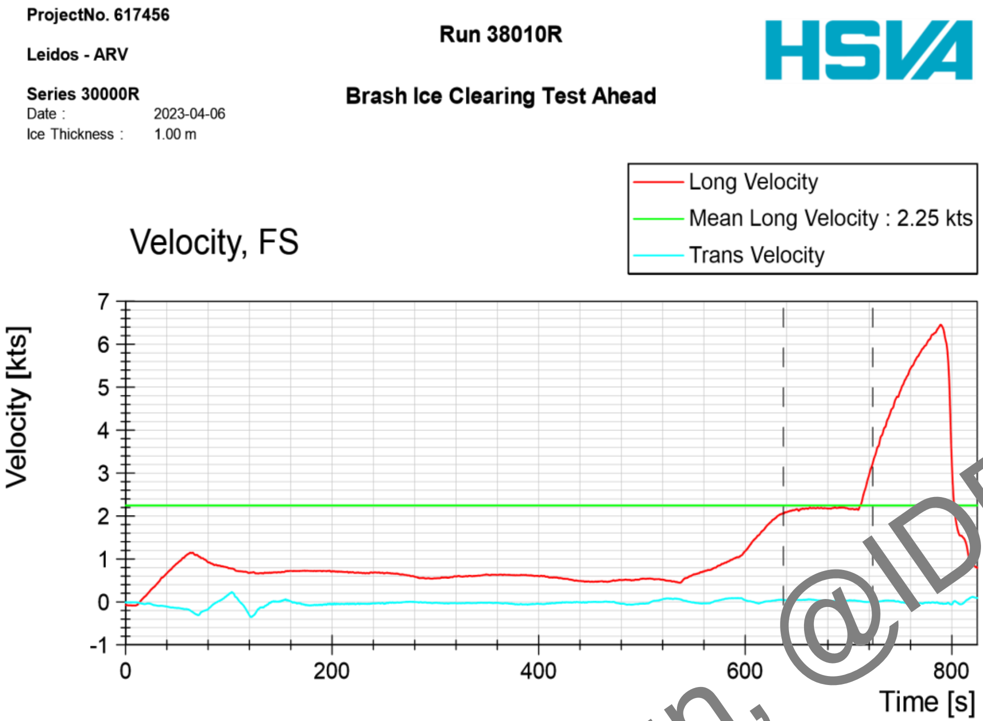

Figure 177 Test run no. 36010R, free running test ahead, velocity

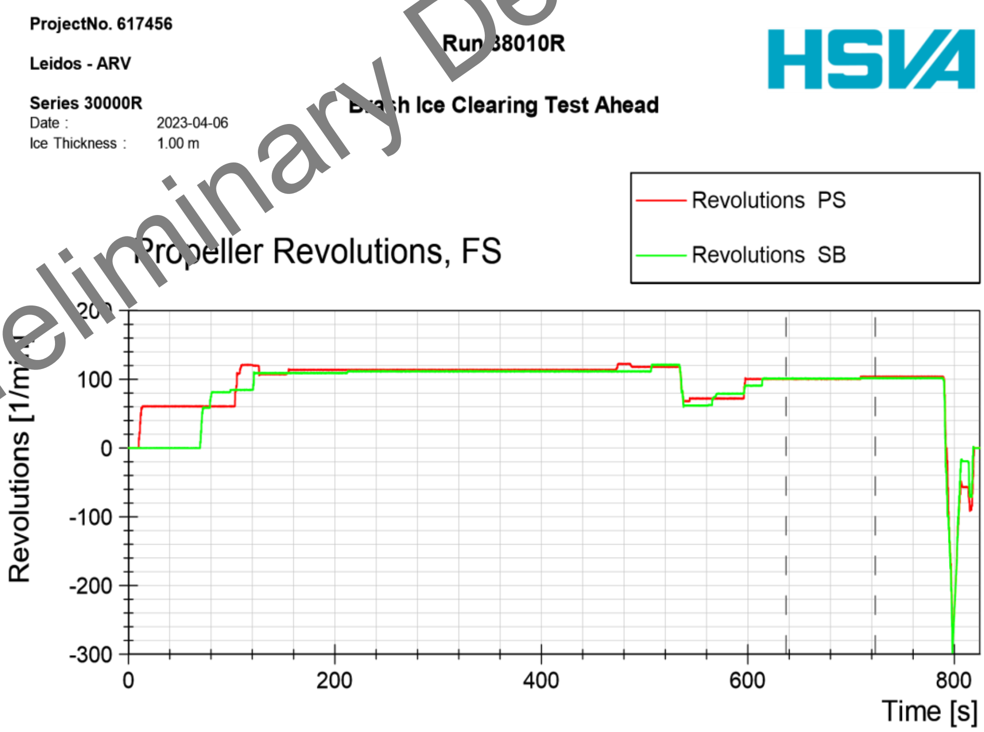

Figure 178 Test run no. 36010R, free running test ahead, propeller revolution

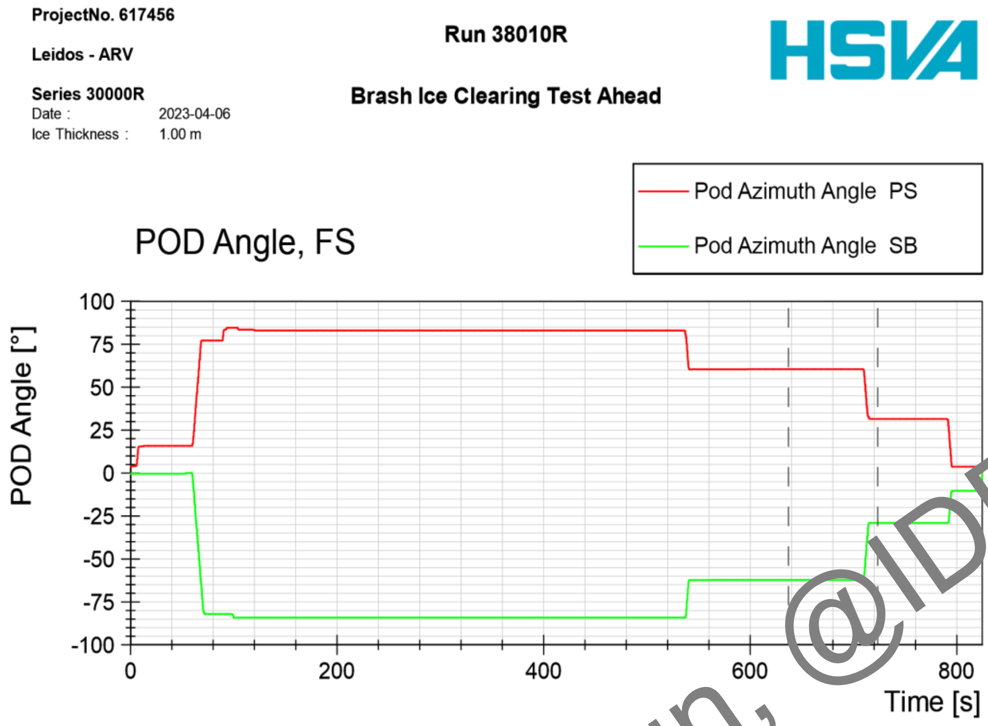

Figure 179 Test run no. 36010R, free running test ahead, POD angle

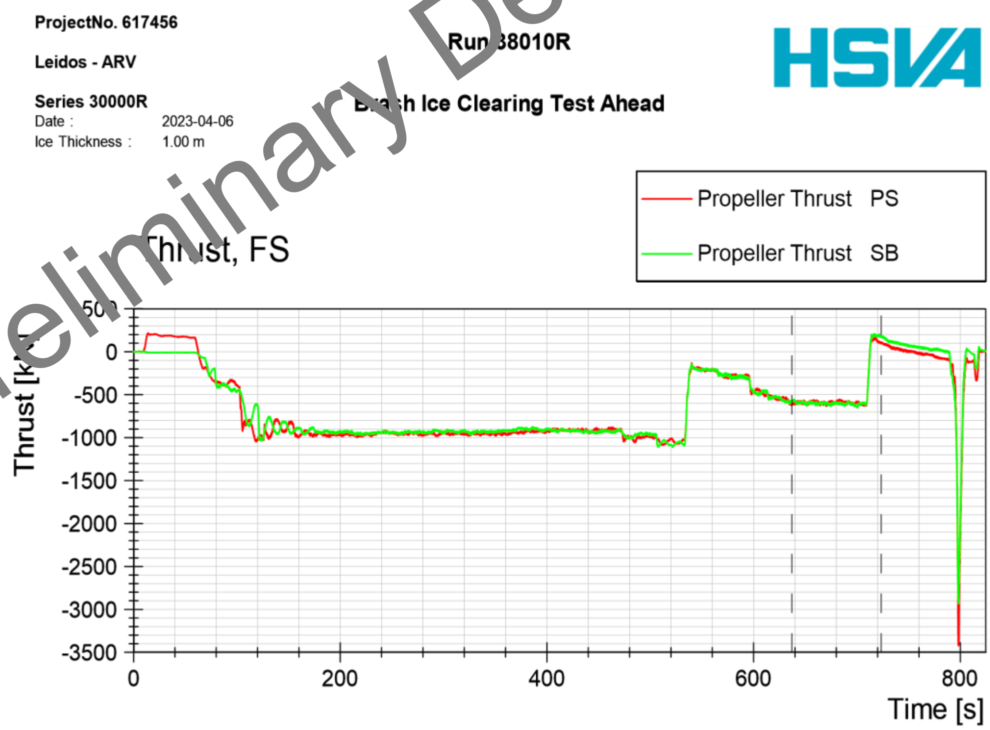

Figure 180 Test run no. 36010R, free running test ahead, thrust

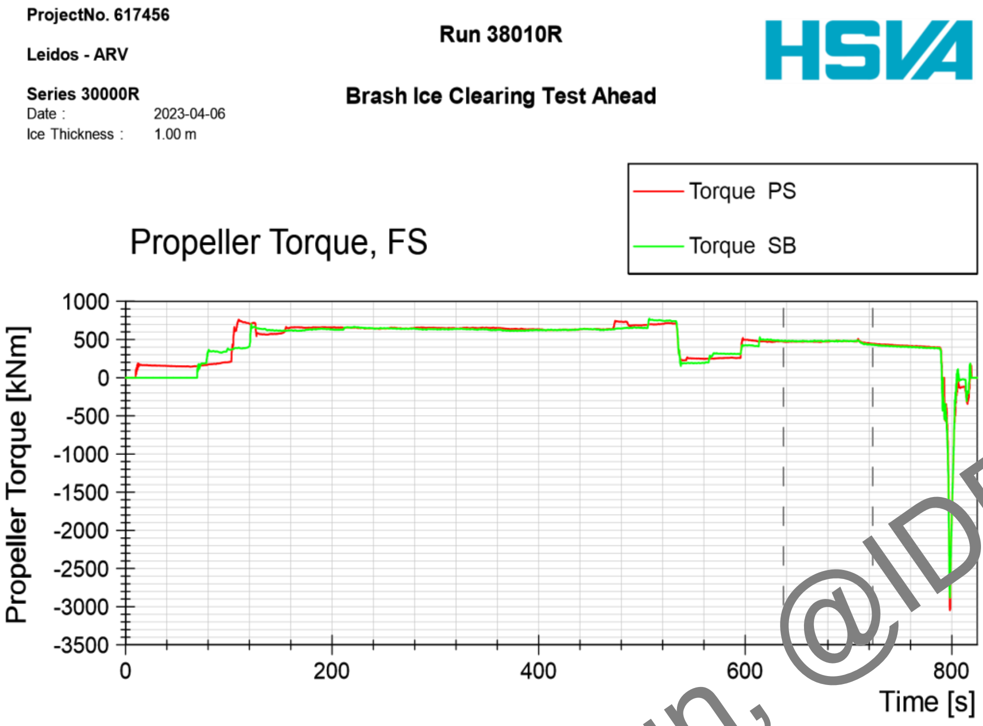

Figure 181 Test run no. 36010R, free running test ahead, torque

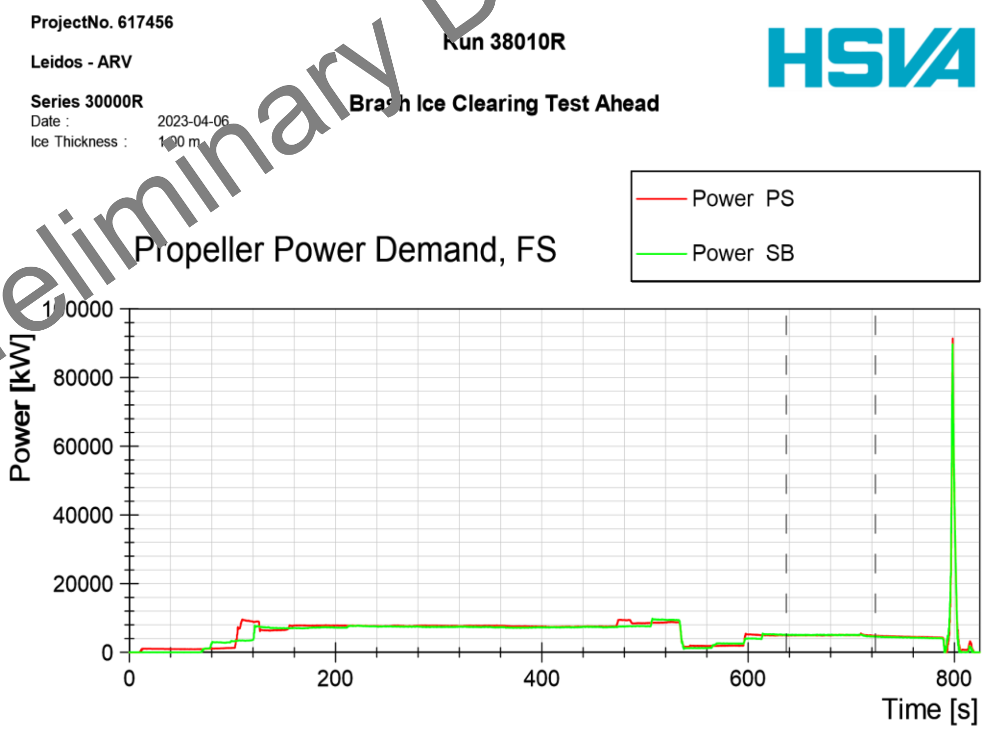

Figure 182 Test run no. 36010R, free running test ahead, power

6.21 Propeller-Ice Interaction

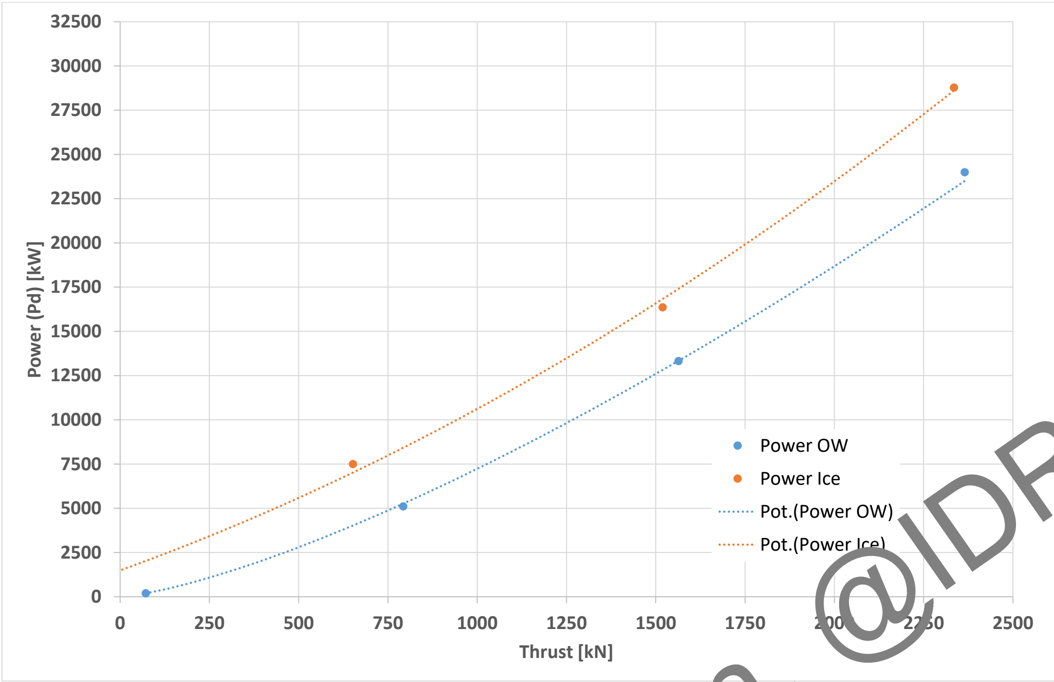

Figure 183 Comparison of power vs. thrust curve in towed propulsion test and ice free overload test

7 Summary and Conclusions

- According to the model test prediction the model will achieve a speed of 3knots ahead in level ice 1.37m (snow cover 0.305m) at power of 17392kW
- According to the model test prediction the model will achieve a speed of 3knots astern in level ice 1.37m (snow cover 0.305m) at power of 18416kW
- The propeller-ice interaction of HSVA model 5626 turned out to be less than for HSVA model 5601
- The design is capable to break out from previous broken channel and leave the channel completely in level ice with thickness of 1.37m
- The break out astern can be accomplished within a bit more than one ship length
- The break out ahead requires 2-3 ship length to pre-widen the channel
- The design is able to clear the broken channel in the wake of the vessel by operating the thrusters at an angle
- The design is able to clear a wider brash ice field while proceeding at slow speed
- The design is bale to clear brash ice in the wake of the vessel while running at moderate speed

Table 8 Comparison ice performance data hull variant 11 and hull variant 6 in 1.37m level ice

Speed		Hull variant 11	Hull variant 6
ahead	power @ 3knots kW	17393	19358
astern	power @ 3knots kW	18416	18156